AD-A016 969

EFFECT OF LARGE NEARSHORE STRUCTURES ON WAVE MOTION IN THE VICINITY OF THE STRUCTURE AND ADJACENT COAST

Volker W. Harms, et al

California University

Prepared for:

Coastal Engineering Research Center

January 1974

EFFECT OF LARGE NEARSHORE STRUCTURES ON WAVE MOTION IN THE VICINITY OF THE STRUCTURE AND ADJACENT COAST

by

Volker W. Harms
Ho Tak Sun
R. L. Wiegel
Manssour A. Kian

HYDRAULIC ENGINEERING LABORATORY
COLLEGE OF ENGINEERING

UNIVERSITY OF CALIFORNIA
BERKELEY

January 1974

Reproduced by
NATIONAL TECHNICAL
INFORMATION SERVICE
U S Department of Commerce
Springfield VA 22151

SECURITY CLASSIFICATION OF THIS PAGE (When Data Entered)

REPORT DOCUMENTATION PAGE

READ INSTRUCTIONS BEFORE COMPLETING FORM

1. REPORT NUMBER: HEL 1-22	2. GOVT ACCESSION NO.
3. RECIPIENT'S CATALOG NUMBER	
4. TITLE (and Subtitle): EFFECT OF LARGE NEARSHORE STRUCTURES ON WAVE MOTION IN THE VICINITY OF THE STRUCTURE AND ADJACENT COAST	5. TYPE OF REPORT & PERIOD COVERED: Technical Report
	6. PERFORMING ORG. REPORT NUMBER: HEL 1-22
7. AUTHOR(s): Volker W. Harms, R.L. Wiegel, Ho Tak Sun, Manssour A. Kian	8. CONTRACT OR GRANT NUMBER(s): DACW72-72-C-0030
9. PERFORMING ORGANIZATION NAME AND ADDRESS: University of California, Berkeley, Hydraulic Engineering Laboratory, Berkeley, California 94720	10. PROGRAM ELEMENT, PROJECT, TASK AREA & WORK UNIT NUMBERS
11. CONTROLLING OFFICE NAME AND ADDRESS: Department of the Army, Coastal Engineering Research Center, Kingman Building, Fort Belvoir, VA 22060	12. REPORT DATE: January 1974
	13. NUMBER OF PAGES: 154
14. MONITORING AGENCY NAME & ADDRESS (if different from Controlling Office)	15. SECURITY CLASS. (of this report): UNCLASSIFIED
	15a. DECLASSIFICATION/DOWNGRADING SCHEDULE

16. DISTRIBUTION STATEMENT (of this Report)

Approved for public release; distribution unlimited

17. DISTRIBUTION STATEMENT (of the abstract entered in Block 20, if different from Report)

18. SUPPLEMENTARY NOTES

19. KEY WORDS (Continue on reverse side if necessary and identify by block number)

Waves
Wave Diffraction
Offshore structures

20. ABSTRACT (Continue on reverse side if necessary and identify by block number)

This report deals with the diffraction of water waves by large impermeable offshore structures. It presents the first phase of a laboratory study of the diffraction of uniform periodic waves by rigid, impervious, vertical-wall offshore structures. The laboratory tests were evaluated in view of an extension of existing diffraction theory using an available, modified computer program (Fan, Cumming, and Wiegel, 1967). In addition, some studies were made of the effect of wave energy absorbing material placed on the seaward side of laboratory breakwater models. (Continued)

DD FORM 1 JAN 73 1473 EDITION OF 1 NOV 65 IS OBSOLETE

UNCLASSIFIED

SECURITY CLASSIFICATION OF THIS PAGE (When Data Entered)

20. Abstract (Continued)

Problems encountered in trying to obtain uniform waves in a wide hydraulic model basin are described, together with modifications to the equipment to improve laboratory wave characteristics. An approximate method, permitting use of theory of wave diffraction by a semi-infinite breakwater oriented at any angle with the incident waves to predict diffraction effects of a detached breakwater. This theory compared favorably with data obtained in the hydraulic model study. Laboratory data are presented for a variety of cases.

It was found for the semi-infinite breakwater that for small values of y/L (e.g., near the breakwater in its lee) the approximate diffraction theory predicted the measured values reasonably well. For large values of y/L (e.g., $y/L > 10$) the theoretical diffraction coefficients were larger than the measured values in the region of $-1 < s/L < -4$, and smaller than the measured values in the lee (shadow region) of the breakwater. The difference between theory and measurements increased with increasing distance from the breakwater (increasing y/L).

University of California
Hydraulic Engineering Laboratory
Wave Research Projects

Technical Report HEL 1-22

The work reported herein was done under Contract DACW 72-72-C-0030 with the Coastal Engineering Research Center, Corps of Engineers, U. S. Army.

EFFECT OF LARGE NEARSHORE STRUCTURES ON WAVE MOTION IN THE VICINITY OF THE STRUCTURE AND ADJACENT COAST

by

Volker W. Harms
Ho Tak Sun
R. L. Wiegel
Manssour A. Kian

Berkeley, California
January 1974

TABLE OF CONTENTS

LIST OF FIGURES

LIST OF SYMBOLS

a	Coordinates (a,-a) of foci of homofocal ellipse
b	Separation constant, dimensionless
d	Water depth, feet
D	Distance from offshore structure to shore, feet
F	Function, Helmholtz Eq., Eq. 1
H	Wave height, feet
k	Wave number, $2\pi/L$
K'	Diffraction coefficient, dimensionless
L	Wave length, feet
T	Wave period, second
X	Horizontal coordinate, along the wave crest-line; X = 0 at the center of the breakwater
Y	Horizontal coordinate, in the direction of wave progress; Y = 0 at the center of the breakwater
X'	Horizontal coordinate, in direction of breakwater, X' = 0 at breakwater tip, feet
Y'	Horizontal coordinate, in direction normal to breakwater, Y' = 0 at breakwater tip
α	Phase angle, diffracted wave, degrees (unless specified as radians)
θ	Angle measured counterclockwise from breakwater
θ_o	Angle of incident wave, measured counterclockwise from breakwater
λ	Length of breakwater (or diameter), feet
ξ	Coordinate in elliptical coordinate system
ϕ	Coordinate in elliptical coordinate system
ψ_1	A function, part of F
ψ_2	A function, part of F

I. INTRODUCTION

A number of large offshore structures are being considered at the present time, and some have been constructed already. These include offshore airports, nuclear power plants, bulk terminals, oil drilling islands and oil storage structures, island ports (Tasco Migliardi and Pezza, 1973), and even offshore cities.* The floating nuclear power plant surrounded by a breakwater (approximately 1800 ft by 1800 ft), that is being designed for a location nearly 3 miles offshore Little Egg Inlet, New Jersey, is an example of such new concepts (Ashworth, 1973). Coastal engineers are actively engaged in most of these activities.

A large structure, if not too far from shore, might be responsible for a major change in the transport and in the deposition or erosion of sand along the shore. The detached breakwaters offshore Santa Monica, California (Johnson, 1957) and Winthrop Beach, Massachusetts (U.S. Army Coastal Engineering Research Center, 1966, p. 239) are examples of structures that have affected the shoreline. On the other hand, Rincon Island, California (Blume and Keith, 1959) is an example of a man-made island that does not appear from a casual glance to have had much effect on the shoreline. These are simply qualitative observations. The coastal engineer would like to be able to predict, quantitatively, the effects of size, geometry, wave energy absorbing capability, distance from shore, etc., of the structure on the shore processes.

In some cases these structures would be placed on rather fine sediments that would be in equilibrium with the waves and currents in the

---

*See references at end of this report

absence of the structure. What will be the effect of the structure on these sediments? Where will scour occur, where will accretion occur, and in what amounts? There has been appreciable scour under some offshore oil platforms in the Gulf of Mexico (Posey, 1971). Again, the coastal engineer has only a qualitative knowledge of these phenomena.

In order to be able to understand and predict what will happen to the sediments, it is necessary to develop a quantitative knowledge of the effect of the structure on the wave pattern around the structure and between the structure and the shore. Further, the effect of diffraction on the 3-dimensional characteristics of this wave motion and the wave-induced currents will be major factors in the deposition or erosion of the sediment.

A great amount of research will be necessary (theoretical, hydraulic model, and prototype studies) before the coastal engineer will be able to perform the job he should do in a manner that will satisfy his professional standards. One portion of the research that is needed is on the problem of the diffraction of water waves by large impermeable offshore structures. This report presents the first phase of a laboratory study, combined with existing diffraction theory which has been extended together with a computer program (Fan, Cumming and Wiegel, 1967) which has been modified, of the diffraction of uniform periodic waves by rigid impervious vertical wall offshore structures. In addition, some studies were made of the effect of wave energy absorbing material placed on the seaward side of some of the models.

II. PAST RESEARCH

Consider a wave system interrupted by an impervious structure such as a breakwater. The portion of the waves incident to the structure will be reflected, break, or both, whereas the portion moving past the tip of the structure will be the source of a flow of energy in the direction essentially along the wave crest and into the region in the lee of the structure. The "end" of the wave will act somewhat as a potential source and the wave in the lee of the breakwater will spread out in approximately a circular arc with the amplitude decreasing along this arc. The same phenomenon will also occur in the reflected portion of the wave. This complicates the physical picture considerably, as part of the wave energy associated with the "radial" wave being generated from the "end" of the reflected wave will move into the lee region. The two sets of waves, cylindrical and radial, reinforce and cancel each other in such a manner as to cause an irregular wave height in this region. This physical phenomenon is known as diffraction.

Mathematical solutions have been obtained for semi-infinite breakwaters, for gaps in breakwaters, for detached breakwaters, and for vertical circular cylinders, to various degrees of approximation (see Wiegel, 1964 for a discussion of some of these solutions and for a presentation of the results of the experimental studies that have been made).

The most important finding that results from a review of the papers on hydraulic laboratory studies of wave diffraction is that the work was done for regions in the lee of breakwaters, extending to only a few wave lengths from the breakwaters (Putnam and Arthur, 1948; Blue and Johnson, 1949; Carr and Stelzriede, 1952). The reason for this is that coastal engineers have in the past been interested primarily in the shelter afforded to ships and

small craft by breakwaters, that is in the usefulness of the harbor area created by breakwaters. The problem being studied and reported on herein is thus an extension of the previous work to a large number of wave lengths from the breakwater (or other structure). Most of the work on large diameter circular cylinders has been in conjunction with the pressure distribution on the cylinder rather than on the scattering of the waves, even though the work is on the diffraction problem (MacCamy and Fuchs, 1954; Chakrabarti, 1972).

Many theoretical studies have been made of diffraction problems in naval hydrodynamics, but these are beyond the scope of this report.

The diffraction of plane waves by an isolated thin rigid impervious vertical breakwater has been studied by several authors (Fan, Cumming and Wiegel, 1967; Hönl, Maur and Westpfahl, 1961; Johnson, 1953; Montefusco, 1968; Morse and Rubinstein, 1938; Penny and Price, 1952; Silvester and Lim, 1968; U.S. Army Coastal Engineering Research Center, 1966; Wada, 1965). Generally an Elliptic Cylinder Coordinate System is used as the one most convenient to describe positions in the horizontal plane (Fig. 1). A velocity potenti is assume to exist; this leads to a function $F(\xi, \emptyset)$ which describes the wave height at each point in the plane. This function must satisfy Helmholtz Equation

$$\nabla^2 F + k^2 F = 0 \qquad (1)$$

By the separation of variables method, letting $F(\xi,\emptyset) = \psi_1 \xi \cdot \psi_2(\emptyset)$ this may be reduced to the two ordinary differential equations

$$\frac{d^2 \psi_1}{d \xi^2} + \left\{ a^2 k^2 \cosh^2 \xi - b \right\} \psi_1 = 0$$

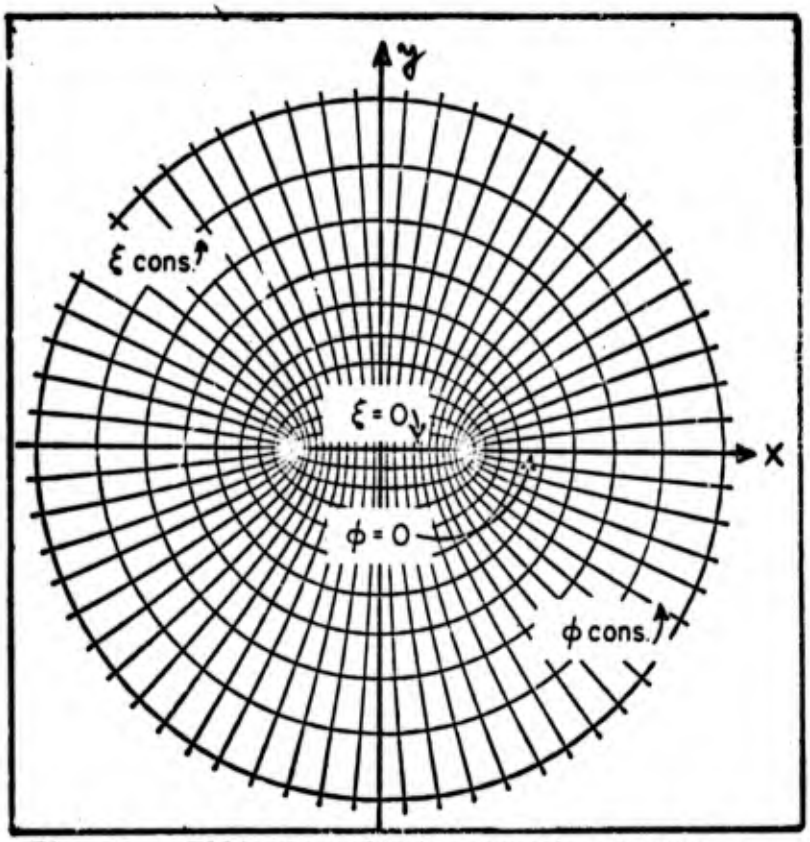

Fig. 1 . Elliptic cylinder coordinant system (from Carr and Stelzriede, 1952)

$$\frac{d^2 \psi_1}{d \phi^2} \left\{ a^2 k^2 \cos^2 \phi - b \right\} \psi_2 = 0 \qquad (2)$$

which are known as the Mathieu Equations. The solution of these equations constitutes the solution to the problem.

It is known that the diffraction behavior about the tips of a detached breakwater many wavelengths long is essentially like that of a semi-infinite breakwater; i.e., one tip is not aware of the existence of the other. In this case one can use the detailed knowledge of the diffraction characteristics for a semi-infinite breakwater to predict the behavior for an isolated one. As the length of the isolated breakwater is reduced, a point is reached where the wave diffracting around one tip will influence the wave being diffracted by the other tip, and the behavior can no longer be considered to be the sum of two independent phenomena associated with each tip.

In the mathematical treatment of the problem as done by Wada (1965) one can separate the solution conveniently into a "non-interaction term" and an "interaction term." The "non-interaction" represents that part of the solution which would be obtained if one simply superimposed the diffracted waves produced by each tip, treating each tip as though it belonged to a semi-infinite breakwater. This part of the solution thus adds the effects of two semi-infinite tips, and the "interaction term" is a measure of how reasonable such an addition is. For a detached breakwater of length 10L one would expect to find that the "interaction term" is quite small, whereas for a breakwater one wavelength long the term would become significant. In the literature (Penney and Price, 1952; Wada, 1965) it is assumed that the deletion of the "interaction term" is valid for breakwaters of at least 5 or 10 wavelengths in length.

It has been observed that the waves emitted by the tips and progressing into the shadow zone of the breakwater had very nearly circular fronts, like those predicted by Sommerfeld (1896) for electromagnetic waves and Penney and Price (1952) for gravity waves diffracted by a semi-infinite breakwater. As will be described in a later section of this report, it has been found that the wave pattern as predicted by Sommerfeld's solution for the semi-infinite breakwater is also valid for each tip of the isolated breakwater down to a breakwater length of only 1.6L. It will be shown that the phase relationship between the two wave-trains coming around the two breakwater tips can be adequately calculated for each point shoreward of the breakwater by simply applying the semi-infinite theory at each tip.

It is of interest to note the distribution of energy near the tip, as obtained for the diffraction of electromagnetic waves by a screen (Hönl, Maue and Westpfahl, 1961). This is indicated in Fig. 2, with the lines of constant phase and constant diffraction coefficient shown in Figs. 2b and 2c.

After the work described herein was completed, and the initial report submitted, a short discussion was discovered in the ASCE Journal of the Waterways, Harbors and Coastal Engineering Division (Goda and Yoshimura, 1973) in which similar conclusions were reached. The laboratory results reported by them were, however, for a small and intermediate distance from the detached breakwater, rather than for large distances.

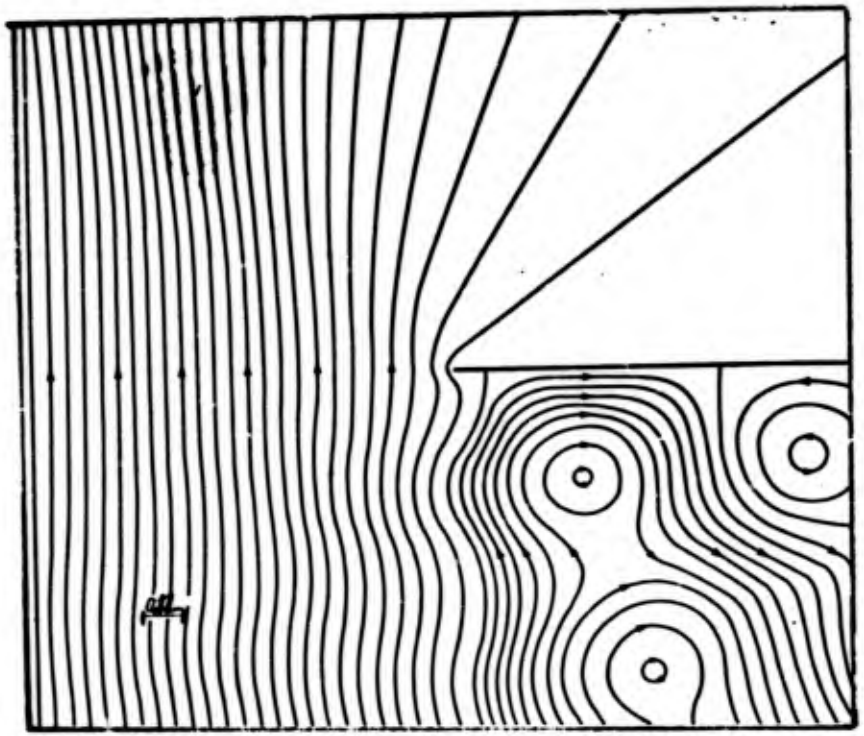

a. Lines of constant energy

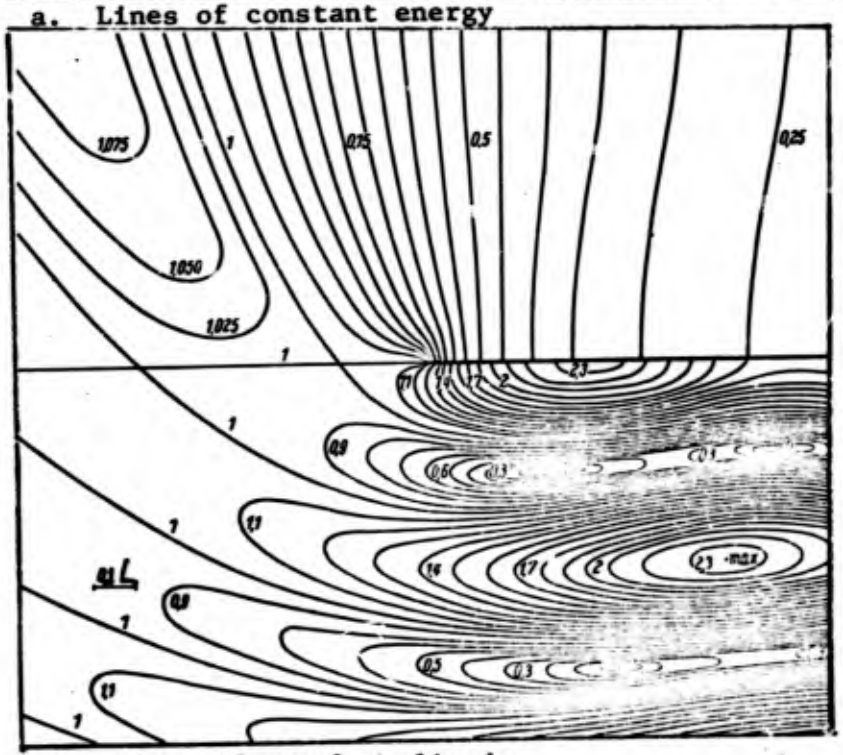

c. Lines of equal amplitude

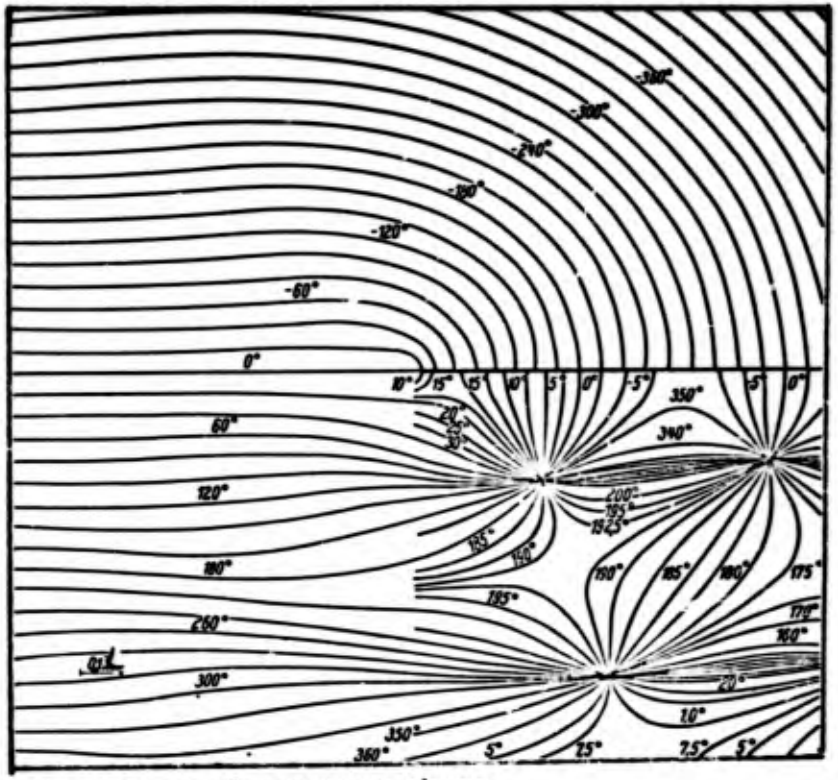

b. Lines of constant phase

⟷ Scale
0.1L

Fig.2 . Lines of constant energy, constant phase, and equal amplitude, electromagnetic waves, 90 degree incident wave angle (i.e., normal to structure).
Reproduced from Hönl, Maue, and Westpfahl (who credit Braunbek and Laukien).

III. PRESENT STUDY

A. Introduction

The main purposes of the present study are to determine diffraction effects at reasonably large distances in the lee of offshore structures, comparing hydraulic laboratory observations with theory, and to determine the effects on wave diffraction of the shapes of offshore structures together with their wave energy absorbing characteristics. In addition, a reasonably simple superposition method for calculating diffracted wave characteristics in the lee of offshore structures is developed, and predictions using it compared with observations.

In planning the tests, the size of proposed prototype structures was kept in mind, together with the sizes of waves that the structures would be subjected to. For example, the nuclear power plant structure proposed for offshore New Jersey would have a distance offshore to structure length ratio of D/λ = 3 miles x 5,280/1800 ≈ 9. It would be subjected to waves of periods from 6 to 15 seconds (roughly) in water 40 feet deep. The range of wave lengths in this water depth, L, would be from 170 to 520 feet (deep water wave lengths of from 185 to 1150 feet), so that the range of λ/L would be from 11 to 3-1/2. The distance offshore, measured in wave lengths (the lengths at the structure) would range from 95 to 30.

B. Ripple Tank Studies

1. Purpose

Owing to the expense involved in performing tests in a large model basin, the first work done was to devise and make a series of tests in a small facility, the Ripple Tank (3.7 ft wide by 20 ft long by 0.4 ft deep).

This was a "model study" of a model study. Based upon these tests, the arrangements for the larger scale tests in the Model Basin (64 ft wide by 148 ft long by 2-1/2 ft deep) were planned. However, the results of the ripple tank study served for more than just a preliminary study, and some of the results are given herein.

2. Experimental Arrangements and Techniques

The name "ripple tank" is misleading. The waves used in the tests were of sufficient length that they were "gravity waves," and not the "surface tension" waves that might be suggested by the name "ripple." The ripple tank has a glass bottom in one section, with a light source under the tank which permits still photographs, motion pictures, and observations to be made of the wave patterns "projected" onto an overhead screen. This permits a number of types of observations to be made which cannot be done in the case of studies made in the model basin. A sketch of a section of the apparatus is shown in Fig. 3. The actual wave generator used was of a different type than is shown in the sketch.

Measurements of the wave heights were made at a large number of locations for the types of obstacles shown in Fig. 4, all of which had vertical walls. Parallel wire resistance type gages were used to measure the water surface time history at a number of locations in the tank. An oscillating flap type wave generator was at one end of the tank and a wave energy absorbing beach was at the other end.

3. Results

a. Diffraction coefficients. The waves in the tank were not uniform across the width of the tank (transverse direction) but varied about ± 10% to 15% from the mean value. In addition, they decreased in amplitude

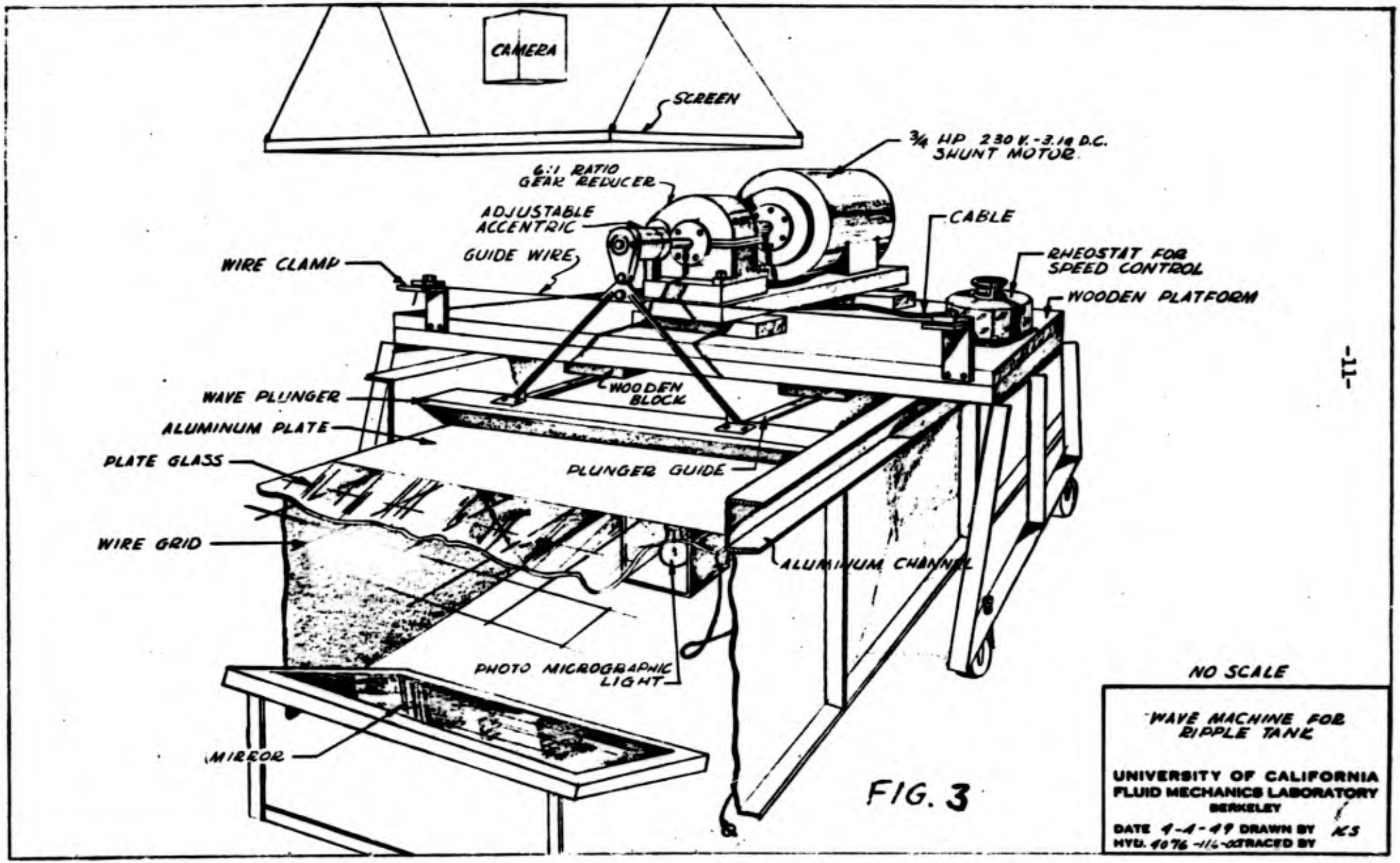

FIG. 3

NO SCALE

WAVE MACHINE FOR RIPPLE TANK

UNIVERSITY OF CALIFORNIA
FLUID MECHANICS LABORATORY
BERKELEY

DATE 4-4-49 DRAWN BY KS
HYD. 4076-114-0 TRACED BY

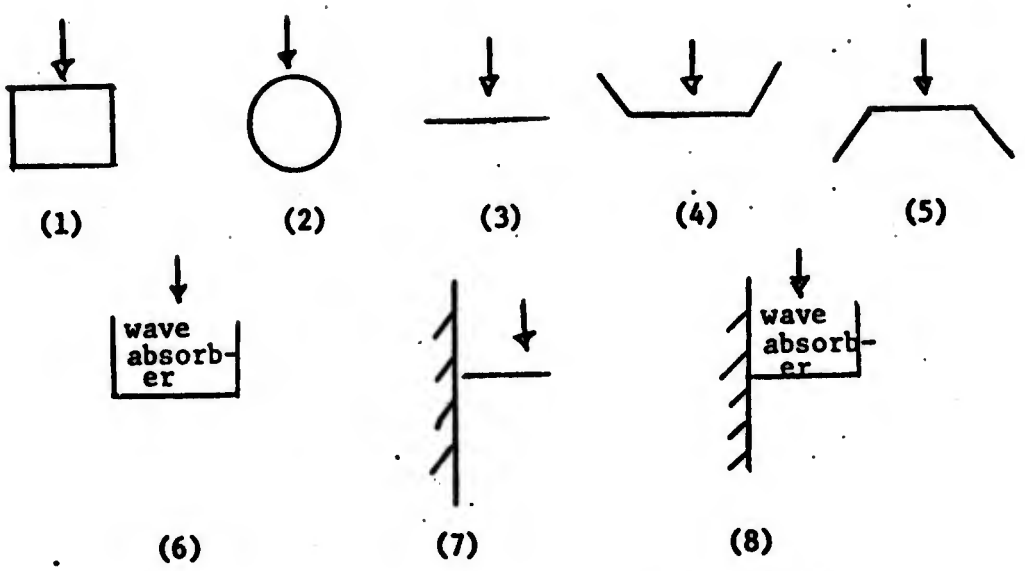

Fig. 4. Shapes Studied in the Ripple Tank

as they traveled down the tank (longitudinal direction) owing to the rather rapid energy dissipation that is inherent for short waves in shallow water.* It was found that some combinations of wave period, wave amplitude and water depth resulted in more uniform waves than other combinations. Results of two runs are presented in Figs. 4 and 5. Many measurements were made, using a 4-inch square grid, labeled 1, 2, ... 11 in the transverse direction (the tank was 44 inches wide) and A, B, ... O in the longitudinal direction (only a 5-foot-long test section was studied). The wave generator was started, and run for a short time and then stopped. The locations of the wave gages were changed, the water allowed to become still, and the wave generator started again. The average height of the 5th, 6th and 7th waves, measured by a rectilinear writing oscillograph, is the value shown in the figures.

Three sets of numbers are shown in each square. The middle number is the wave height measured in the square, called the incident wave height. After these measurements had been made, a 13-inch diameter vertical wall circular (in one case, and an 8-inch square in the second case) island was placed in the tank as shown by the dashed circle or square in the figures. The upper number shown in each square is the wave height at that location with the island in the tank, called the diffracted wave (perhaps scattered wave would be a better term) height. The lower number is the ratio of the diffracted to incident wave height, called the diffraction coefficient. Of course, no measurements were made of the diffracted (scattered) waves at

*Little decrease in wave height for the case shown in Fig. 4, as the water was nearly twice as deep as for the case shown in Fig. 5.

	1	2	3	4	5	6	7	8	9	10	11	Wave attenuation (avg.)	Ave. wave height in feet
A	.029 .029 1.0	.034 .028 1.21	.039 .032 1.22	.032 .034 .94	.019 .037 .51	.020 .035 .57	.020 .031 .64	.027 .028 .96	.040 .030 1.33	.042 .033 1.27	.032 .031 1.03	1.0	0.32
B	.033 .028 1.18	.027 .027 1.0	.028 .031 .90	.038 .027 1.41	.046 .033 1.40	.043 .031 1.39	.041 .030 1.37	.041 .027 1.52	.032 .028 1.14	.031 .032 .97	.037 .029 1.27	0.91	0.29
C	.036 .027 1.33	.025 .027 .93	.034 .030 1.13	.029 .029 1.0	.034 .031 1.10	.063 .029 2.2	.038 .028 1.36	.023 .027 .85	.036 .030 1.20	.030 .032 .94	.037 .029 1.27	0.91	0.29
D	.030 .028 1.07	.034 .026 1.31	.028 .030 .93	.036 .029 .90	.036 .029 1.24	- .031 -	.032 .030 1.07	.024 .027 .89	.028 .031 .90	.039 .033 1.18	.034 .029 1.17	0.91	0.29
E	.032 .026 1.23	.032 .026 1.23	.028 .029 .96	.029 .027 1.07	.036 .029 1.24	- .028 -	.029 .028 1.04	.028 .027 1.04	.029 .028 1.04	.035 .030 1.17	.034 .029 1.17	0.88	0.28
F	.035 .027 1.30	.019 .027 .70	.034 .029 1.17	.034 .028 1.21	.0125 .030 .42	.0106 .034 .31	.0097 .027 .36	.032 .028 1.14	.038 .029 1.31	.022 .029 .76	.038 .029 1.31	0.91	0.29
G	.031 .028 1.11	.031 .027 1.15	.035 .032 1.10	.035 .029 1.21	.15 .030 .50	.0154 .027 .57	.014 .030 .47	.031 .032 .97	.037 .031 1.19	.034 .029 .87	.033 .028 1.18	0.91	0.29
H	.026 .026 1.0	.039 .029 1.35	.035 .030 1.17	.027 .031 .87	.015 .027 .56	.024 .028 .86	.016 .030 .53	.025 .034 .73	.034 .031 1.10	.041 .029 1.41	.029 .029 1.0	0.91	0.29
I	.024 .027 .89	.042 .031 1.35	.036 .030 1.20	.026 .029 .90	.015 .025 .60	.028 .028 1.0	.019 .028 .68	.023 .033 .70	.036 .032 1.12	.042 .031 1.36	.028 .029 .97	0.91	0.29
J	.031 .028 1.11	.038 .029 1.31	.034 .030 1.13	.0168 .028 .60	.014 .028 .50	.025 .026 .96	.022 .029 .76	.018 .032 .56	.034 .032 1.06	.038 .031 1.22	.032 .028 1.14	0.91	0.29
K	.038 .028 1.5	.030 .029 1.03	.028 .030 .93	.020 .027 .74	.019 .028 .68	.019 .028 .68	.026 .031 .84	.023 .032 .72	.027 .031 .73	.032 .030 1.07	.037 .029 1.28	0.91	0.29
L	.042 .029 1.6	.025 .029 .86	.020 .028 .71	.022 .027 .81	.022 .028 .79	.020 .028 .72	.025 .030 .83	.026 .031 .84	.020 .028 .71	.023 .029 .79	.041 .027 1.52	0.91	0.29
M	.044 .029 1.52	.025 .027 .93	.016 .026 .61	.019 .027 .70	.020 .027 .74	.026 .029 .90	.026 .027 .96	.024 .033 .73	.017 .031 .55	.024 .030 .80	.043 .027 1.6	0.91	0.29
N	.043 .029 1.48	.027 .029 .93	.015 .027 .55	.014 .027 .52	.022 .027 .81	.030 .030 1.0	.025 .030 .83	.018 .031 .58	.019 .031 .61	.025 .030 .83	.041 .027 1.52	0.88	0.28

Fig. 5. Incident wave heights in ripple tank without structure present; diffracted ("scattered") wave heights, and diffraction coefficients, 8-inch (0.67 ft) square island. Water depth = 0.15 ft, wave period = 0.50 sec, wave length = 0.96 ft, d/L = 0.16, λ/L = 0.70

Notes:
1. The average height of 5th, 6th and 7th waves are given.
2. Top number in square is diffracted wave height, middle number is incident wave height, and bottom number is diffraction coefficient.

	1	2	3	4	5	6	7	8	9	10	11	Wave attenuation (avg.)	Avg. wave height in ft.
A	.019 .024 .79	.032 .021 1.52	.026 .020 1.3	.020 .024 .83	.023 .025 .92	.036 .025 1.44	.025 .022 1.14	.020 .023 .87	.026 .026 1.0	.033 .023 1.43	.023 .024 .96	1	.0234
B	.028 .020 1.4	.015 .021 .71	.023 .024 1.1	.034 .023 1.48	.020 .023 .87	.017 .024 .71	.017 .020 .85	.032 .022 1.46	.025 .022 1.13	.020 .024 .83	.028 .022 1.27	.94	.0220
C	.015 .021 .71	.031 .021 1.48	.020 .022 .91	.013 .022 .59	.032 .022 1.45	.032 .022 1.45	.032 .020 1.60	.014 .021 .67	.020 .022 .91	.032 .022 1.45	.018 .022 .82	.92	.0216
D	.023 .021 1.1	.018 .020 .99	.020 .021 .95	.026 .019 1.37	- .021 -	- .022 -	- .019 -	.026 .021 1.24	.021 .022 .95	.018 .021 .86	.025 .021 1.19	.89	.0207
E	.023 .021 1.1	.017 .021 .81	.021 .021 1.0	.024 .019 1.26	- .020 -	- .022 -	- .020 -	.024 .020 1.20	.022 .021 1.05	.020 .021 .95	.024 .021 1.14	.88	.0206
F	.021 .024 .87	.022 .022 1.0	.021 .020 1.05	.022 .019 1.16	.014 .020 .70	.014 .022 .64	.011 .021 .52	.022 .021 1.05	.022 .022 1.00	.023 .020 1.15	.021 .023 .91	.91	.0213
G	.021 .023 .91	.021 .022 .95	.024 .020 1.2	.019 .019 1.0	.0104 .019 .55	.016 .022 .73	.0104 .021 .50	.019 .023 .83	.025 .022 1.13	.022 .020 1.1	.021 .023 .91	.91	.0213
H	.016 .022 .73	.026 .021 1.24	.024 .019 1.26	.014 .019 .74	.010 .020 .50	.016 .021 .76	.0097 .019 .51	.013 .022 .59	.025 .022 1.13	.028 .020 1.4	.017 .021 .81	.88	.0201
I	.015 .020 .75	.026 .021 1.24	.023 .020 1.15	.012 .019 .63	.0122 .020 .61	.016 .021 .73	.0124 .021 .59	.013 .023 .57	.024 .023 1.04	.027 .020 1.35	.019 .019 1.0	.88	.0207
J	.020 .021 .95	.024 .020 1.2	.021 .019 1.1	.013 .019 .68	.0135 .020 .67	.013 .022 .59	.0143 .021 .68	.018 .022 .82	.021 .023 .91	.024 .021 1.14	.023 .020 1.15	.89	.0207
K	.026 .020 1.3	.017 .019 .89	.017 .019 .89	.016 .019 .84	.014 .020 .70	.013 .021 .62	.015 .021 .71	.020 .022 .91	.017 .022 .77	.017 .020 .85	.028 .020 1.40	.87	.0201
L	.028 .018 1.56	.014 .018 .78	.0122 .019 .64	.015 .019 .79	.014 .021 .67	.019 .021 .90	.016 .021 .76	.018 .022 .82	.0133 .022 .60	.013 .019 .68	.029 .018 1.61	.85	.0198
M	.027 .019 1.42	.017 .019 .94	.0116 .019 .61	.0108 .019 .57	.015 .020 .75	.024 .022 1.09	.016 .020 .80	.0132 .021 .63	.0128 .021 .61	.017 .019 .89	.027 .019 1.42	.84	.0197
N	.025 .019 1.32	.020 .019 1.05	.0116 .019 .61	.008 .019 .42	.016 .020 .80	.027 .022 .022	.016 .020 .80	.009 .021 .43	.0126 .021 .60	.020 .019 1.05	.025 .019 1.32	.85	.0198
O	.023 .019 1.21	.021 .018 1.17	.0116 .019 .61	.008 .019 .42	.016 .020 .80	.025 .021 1.19	.016 .020 .80	.010 .010 .50	.0126 .020 .63	.021 .019 1.1	.023 .018 1.33	.83	0194

Fig. 6. Incident wave heights in ripple tank without structure; diffracted ("scattered") wave heights, and diffraction coefficients, 13-inch (1.09 ft) circular island. Water depth = 0.083 ft, wave period = 0.62 sec, wave length = 0.93 ft, d/L = 0.089, $\lambda/L = 1.2$

Notes:
1. The average height of 5th, 6th and 7th waves are given.
2. Top number in square is diffracted wave height, middle number is incident wave height, and bottom number is diffraction coefficient.

the location of the structures after they had been installed. Several measurements were made immediately adjacent to the structures, however, and are shown in the figures.

Along the right-hand side of the figures are two columns of numbers. The second column is the simple arithmetic average of the incident wave heights (11 of them) in row A, B, etc. The first column is the ratio of the arithmetic average in each row to the value in row A. This ratio is called wave attenuation, and indicates the wave energy decrease as the wave travels down the tank.

Similar tests were made with a variety of structure geometries. The results are shown in Figs. 7-14.

One reason for making the tests in small scale was to check the effect of the reflection from the walls and wave generator of the waves scattered by the structure. Thus, two of the geometries (Types 3 and 7) were modified by placing "splitter walls" seaward of the structures, a wave energy absorbing beach being placed between the splitters. These modifications are shown as Types 6 and 8 in Fig. 4. If the reflections could be made to be quite small, then the wave generator could be run continuously and the many wave measurements that had to be made could be made in a shorter time. It appeared that this was possible. Compare Fig. 13 (no absorber, intermittent running) with Fig. 14 (absorber, continuous running); the results are reasonably close.

Although Type 7 (Fig. 13) is labeled a "semi-infinite" breakwater, it is far from that. Considering the tank wall to be a plane of symmetry, it is a "detached" breakwater with a value $\lambda/L = 2 \times 1.9 = 3.8$. Type 8 (Fig. 14), on the other hand, is an approximation to a semi-infinite breakwater

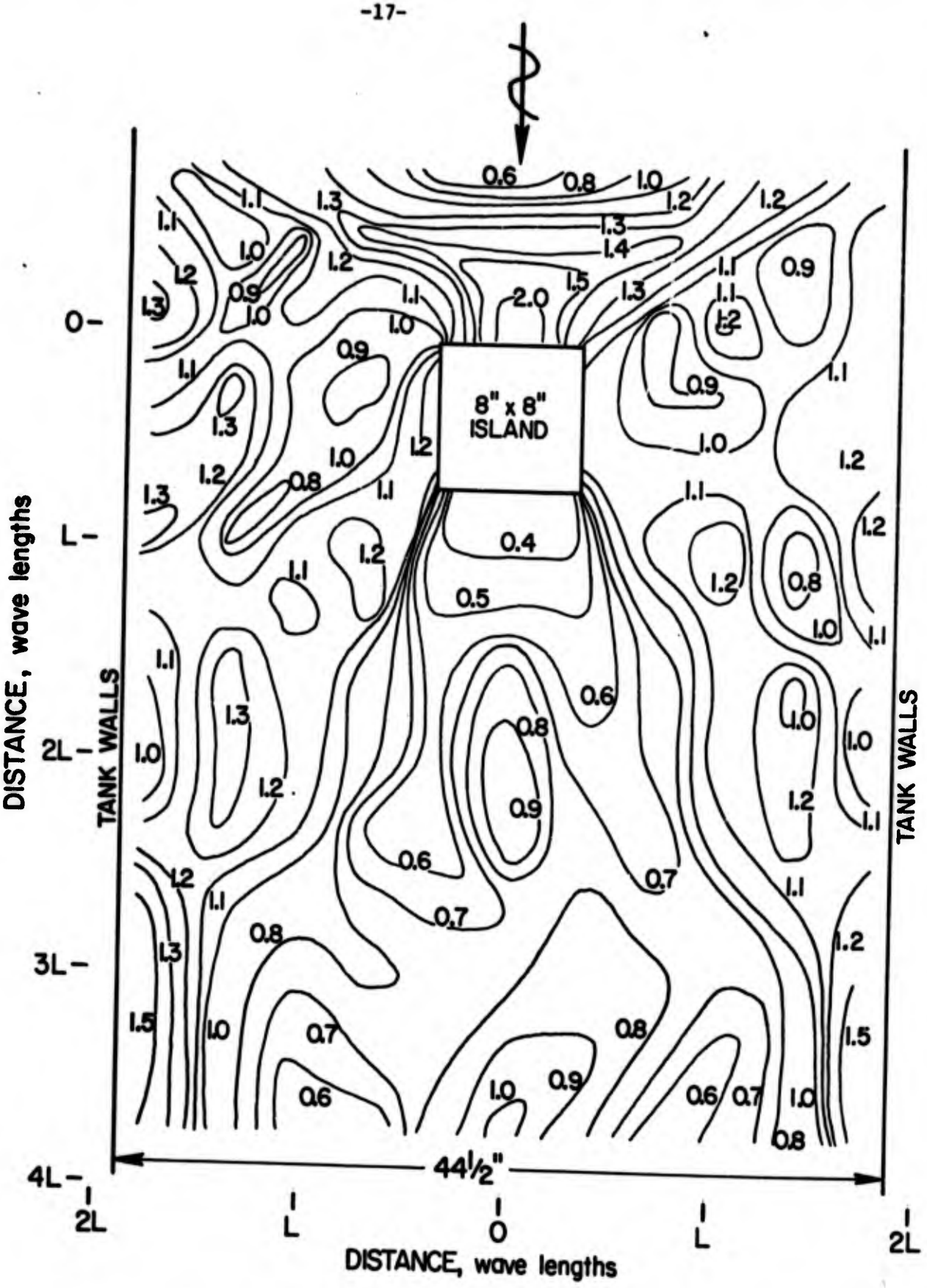

FIG. 7 WAVE DIFFRACTION COEFFICIENT CONTOURS, 8 inch (0.67 ft.) SQUARE ISLAND, RIPPLE TANK TEST.
d = 0.15 ft., T = 0.50 sec., L = 0.96 ft., d/L = 0.16, $\lambda/L = 0.70$

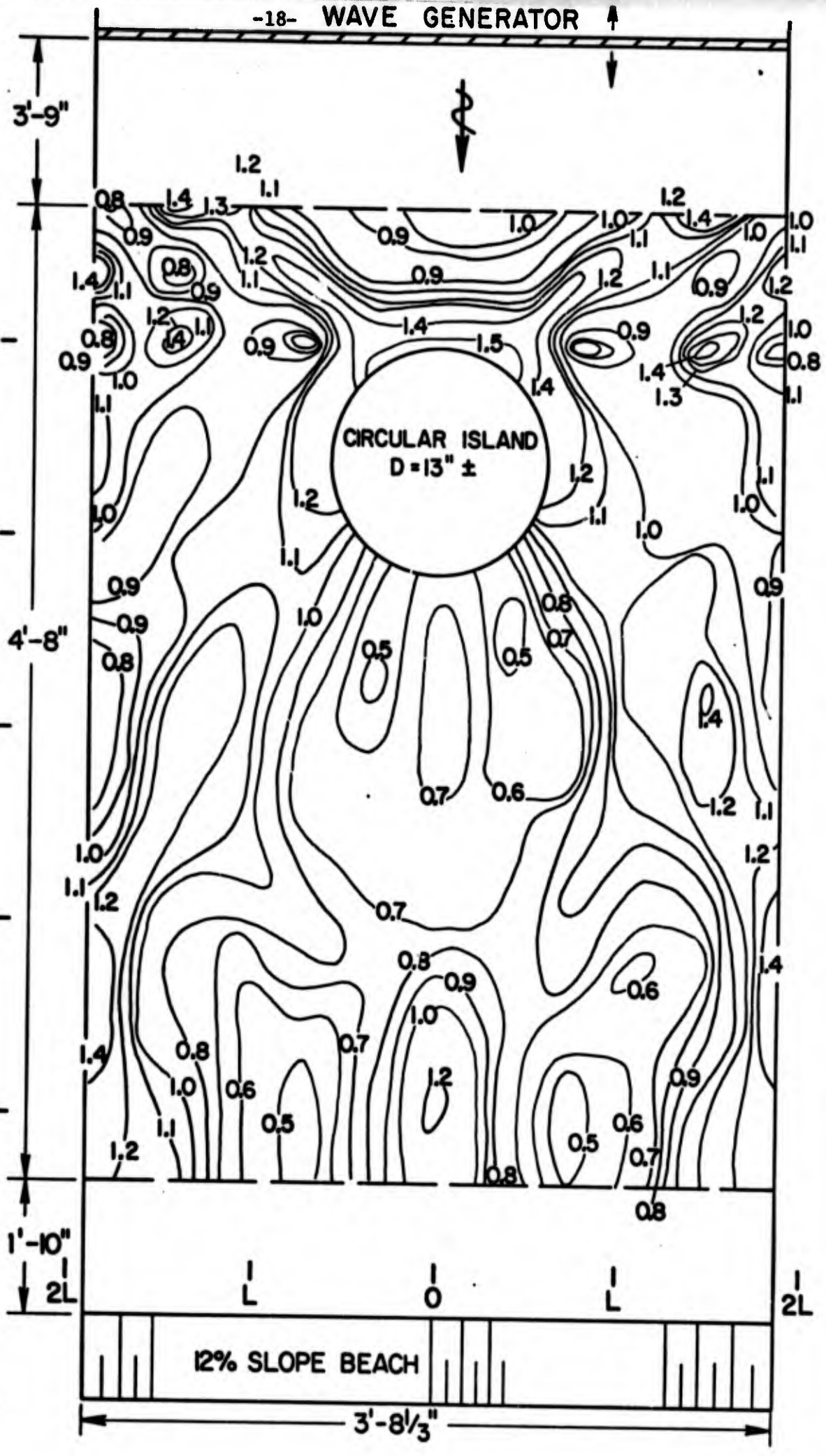

FIG. 8 WAVE DIFFRACTION COEFFICIENT CONTOURS, 13-inch (1.09 ft.) DIAMETER ISLAND, RIPPLE TANK TEST.
d = 0.083 ft., T = 0.62 sec., L = 0.93 ft., d/L = 0.089, λ/L = 1.2

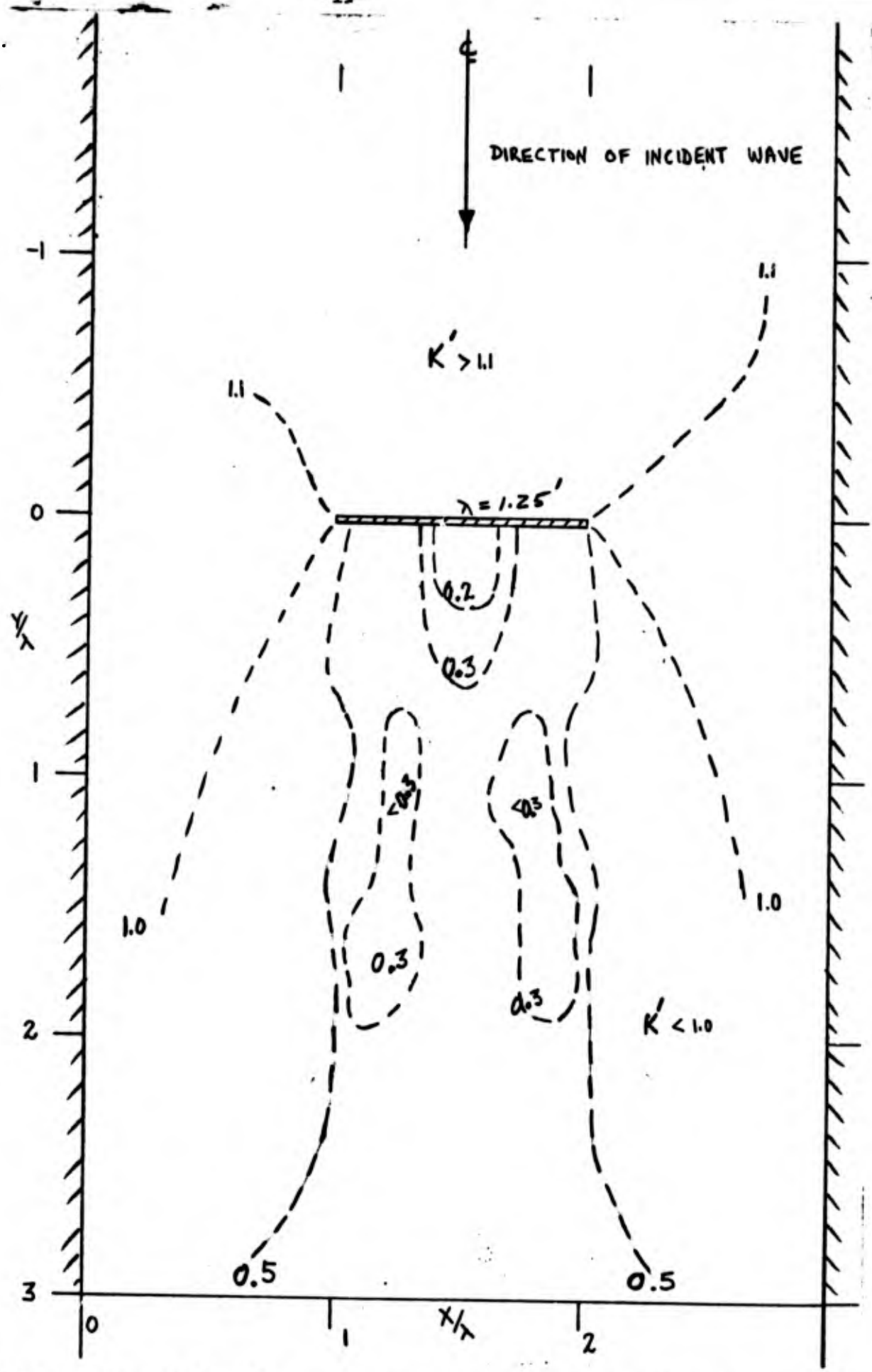

Fig. 9. Wave diffraction coefficient contours, 1.25 ft detached breakwater, ripple tank test. d = 0.13 ft, T = 0.39 sec, L = 0.66 ft, d/L = 0.20, λ/L = 1.9.

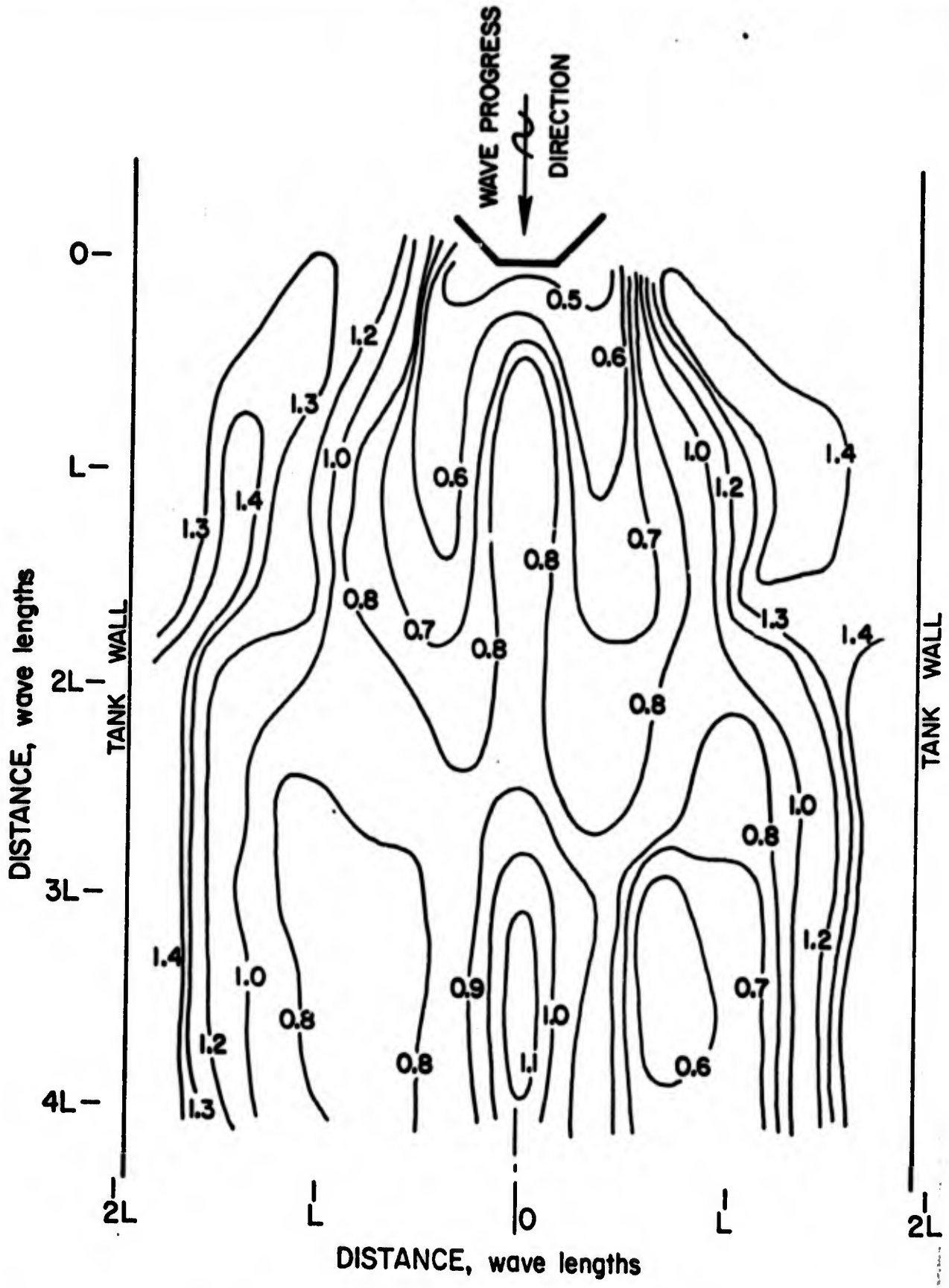

FIG. 10 WAVE DIFFRACTION COEFFICIENT CONTOURS, 8-inch (0.67 ft.) WINGED SEAWARD DETACHED BREAKWATER, RIPPLE TANK TEST. d=0.15 ft., T=0.50 sec., L=0.96 ft., d/L=0.16, λ/L=0.70

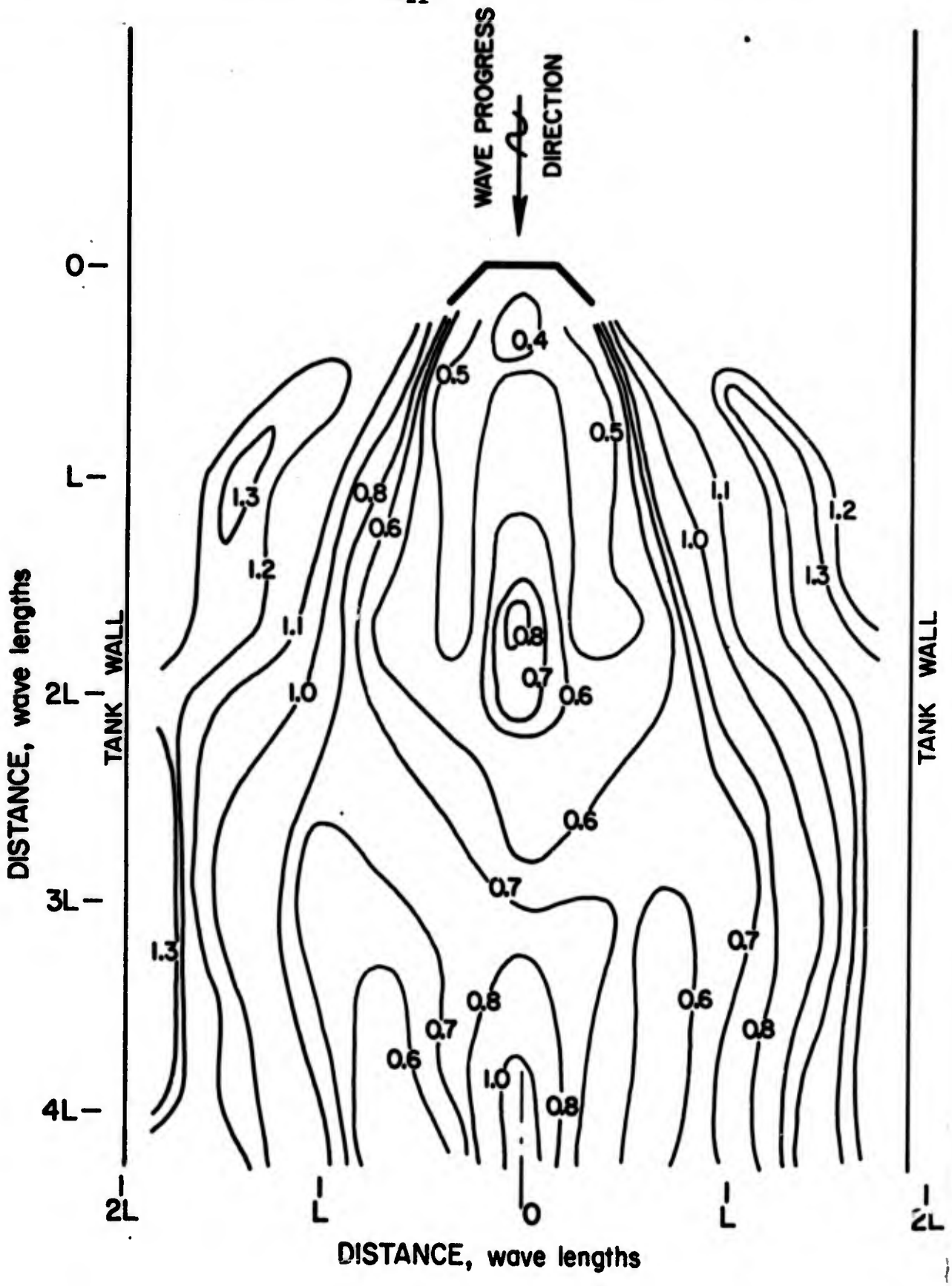

FIG. 11 WAVE DIFFRACTION COEFFICIENT CONTOURS, 8-inch (0.67 ft.) WINGED LEEWARD DETACHED BREAKWATER, RIPPLE TANK TEST. d=0.15 ft., T=0.50 sec., L=0.96 ft., d/L=0.16, $\lambda/L=0.70$

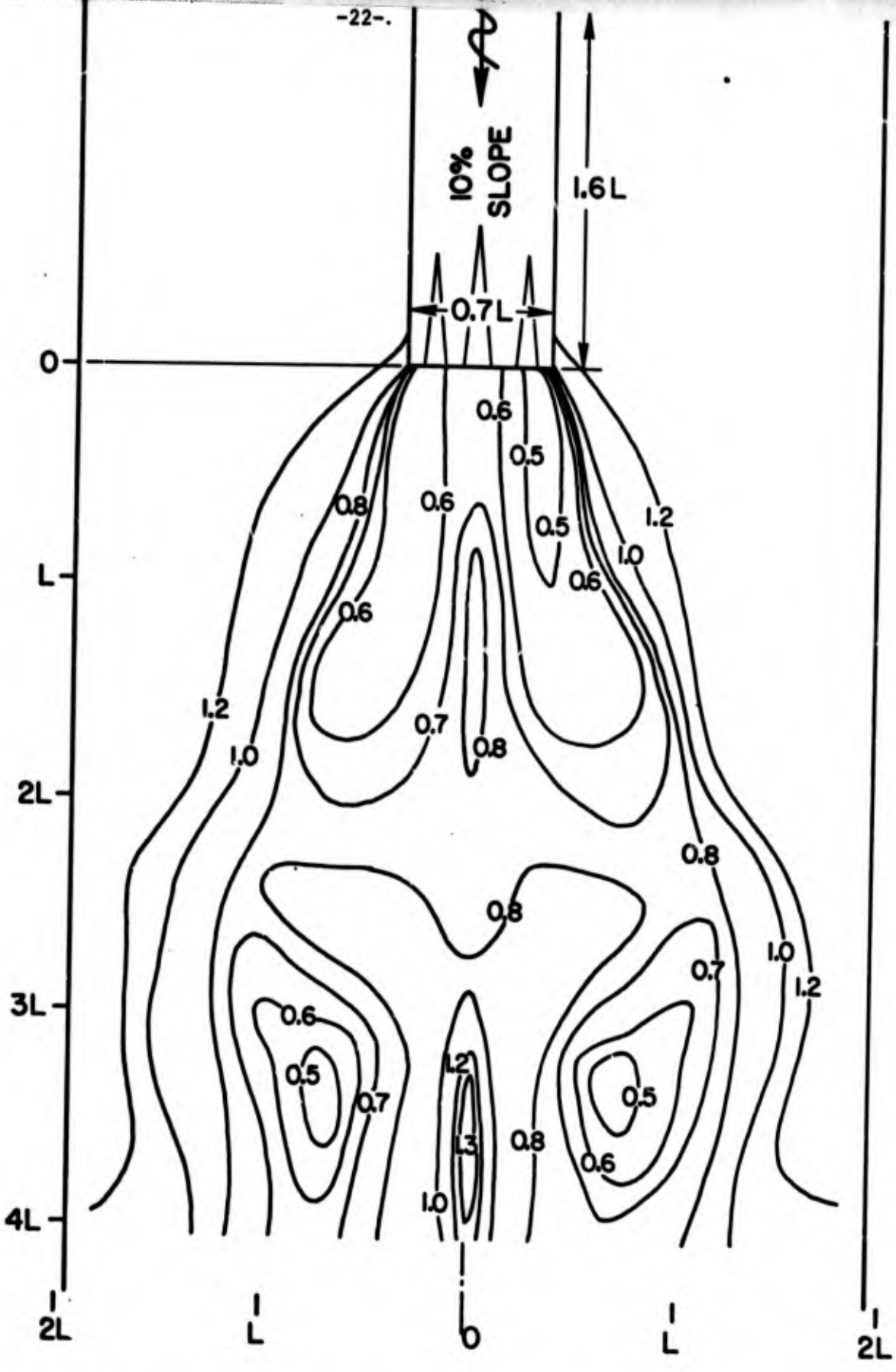

FIG. 12 WAVE DIFFRACTION COEFFICIENT CONTOURS, 8-inch (0.67 ft.) DETACHED BREAKWATER WITH WAVE ENERGY ABSORBERS ON SEAWARD SIDE, RIPPLE TANK TEST. d=0.15 ft., T=1.0 sec., L=0.96 ft., d/L=0.16, λ/L=0.70

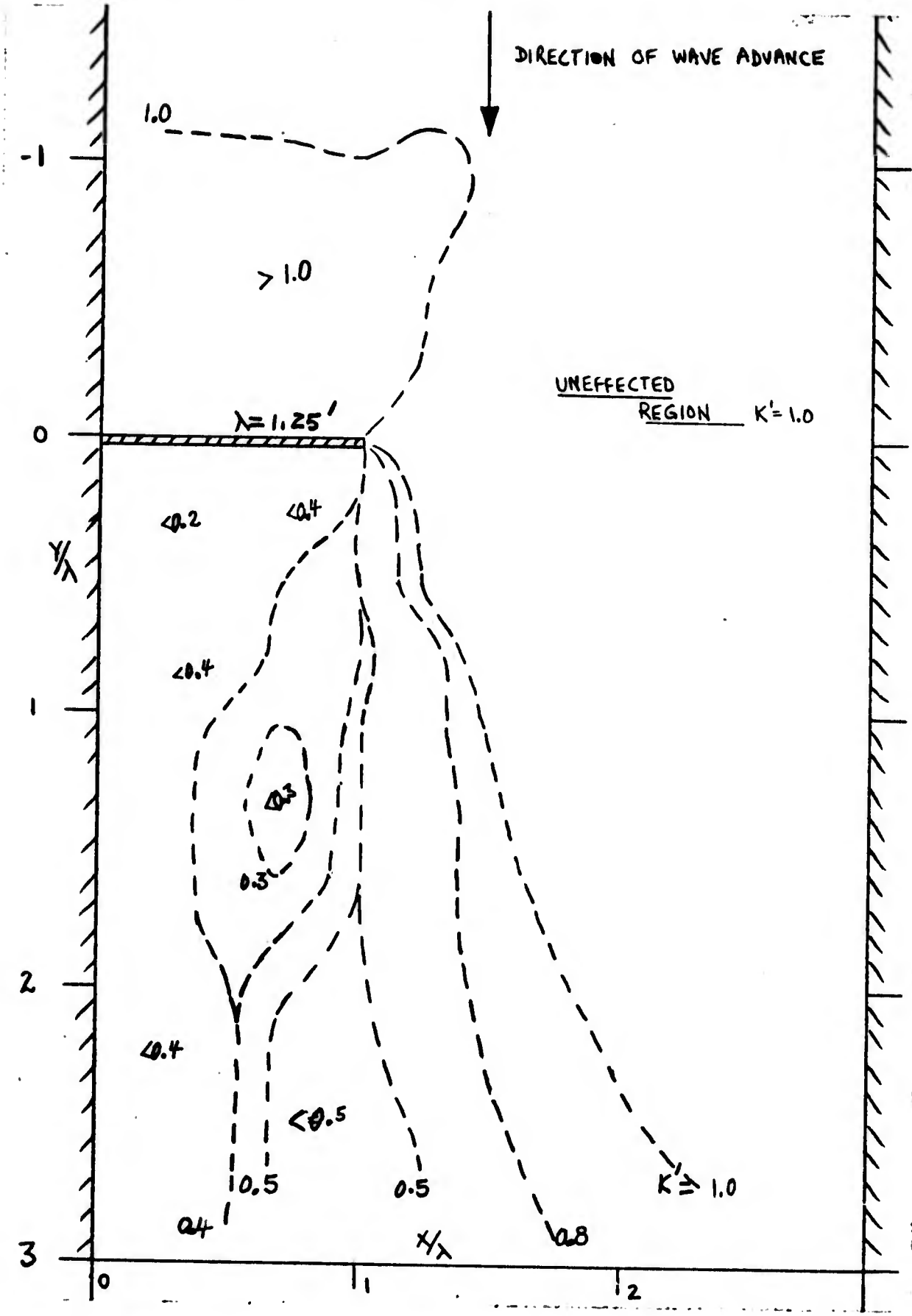

Fig. 13. Wave diffraction coefficient contours, 1.25 ft semi-infinite breakwater, ripple tank test. d = 0.14 ft, T = 0.40 sec, L = 0.70 ft, d/L = 0.20, λ/L = 1.9.

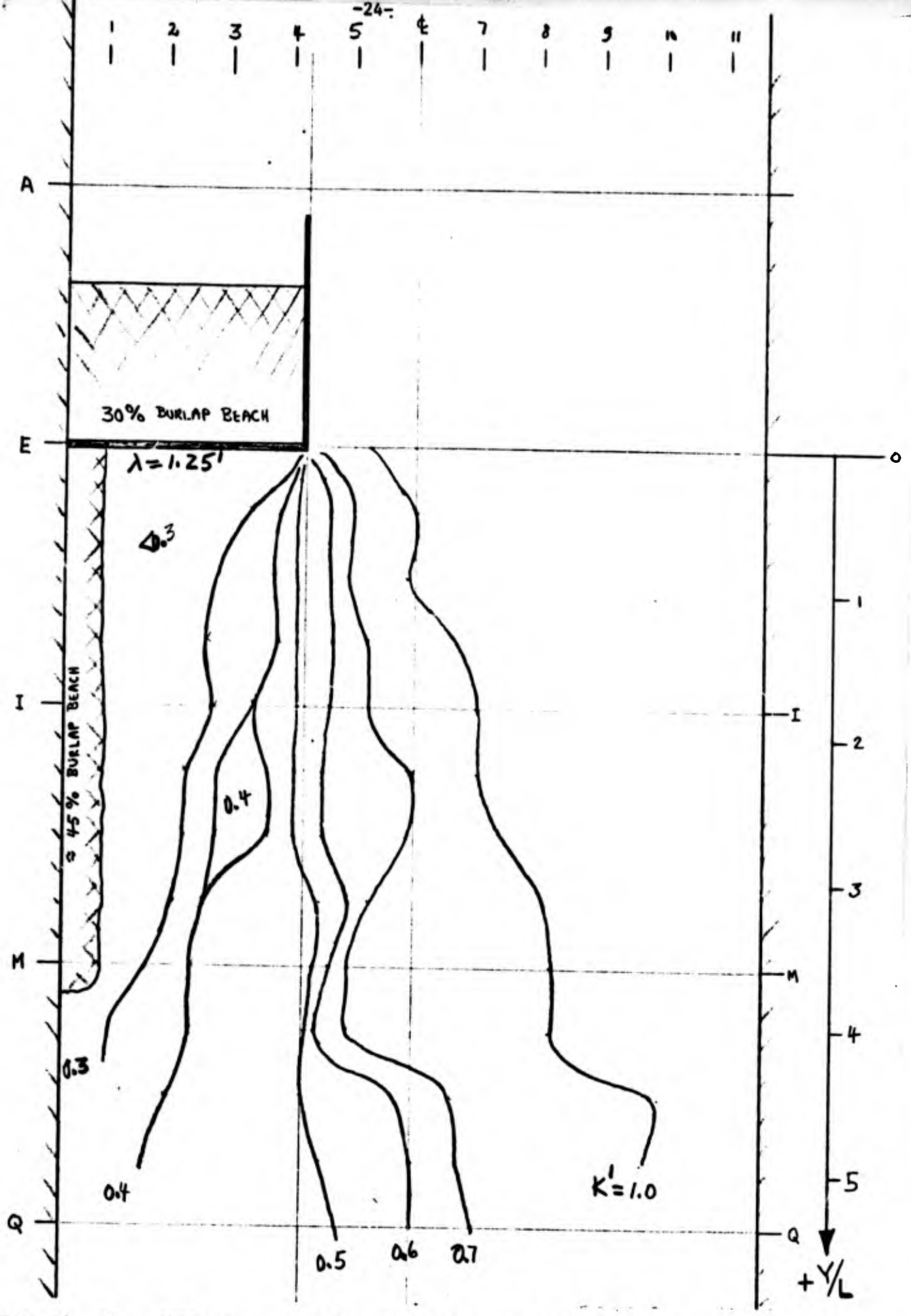

Fig. 14. Wave diffraction coefficient contours, 1.25 ft semi-infinite breakwater with wave energy absorber on seaward side, ripple tank test. d = 0.15 ft, T = 0.40 sec, L = 0.70 ft, d/L = 0.20, λ/L = 1.9.

owing to the wave energy absorbing material placed along the tank wall in the lee of the breakwater. Because of this, it appeared to be reasonable to compare the results of the test for the case shown in Fig. 14 with the theory for a semi-infinite breakwater and with the hydraulic laboratory tests reported in 1948 by Putnam and Arthur (1948). These results are shown in Fig. 15.

Owing to the reasonable agreement between the ripple tank data and previous studies described in the paragraph above, it is perhaps likely that other ripple tank data are valid in a quantitative as well as a qualitative sense. It is interesting to compare the results shown in Figs. 7, 10, 11 and 12. The values of λ/L and d/L are nearly the same for each case. There does not appear to be any gross difference in the diffraction coefficients in the lee of these four types of structures, except very close to the structure.

b. Sediment motion. In order to obtain some ideas about the direction of "diffraction currents" and the effects of these currents and other wave effects on bottom sediment, some tests were made using some find sand and some plastic pellets (specific gravity a little greater than one) on the bottom. The motions were observed, and examples of the results are shown in Figs. 16-18. These observations were made for the Type 3 structure (see also Fig. 9).

C. Large Tank Studies

1. Purpose

The purposes of the experimental work described herein were to observe the characteristics of diffracted waves throughout a large area in the lee of offshore structures, and to compare the observations with theory,

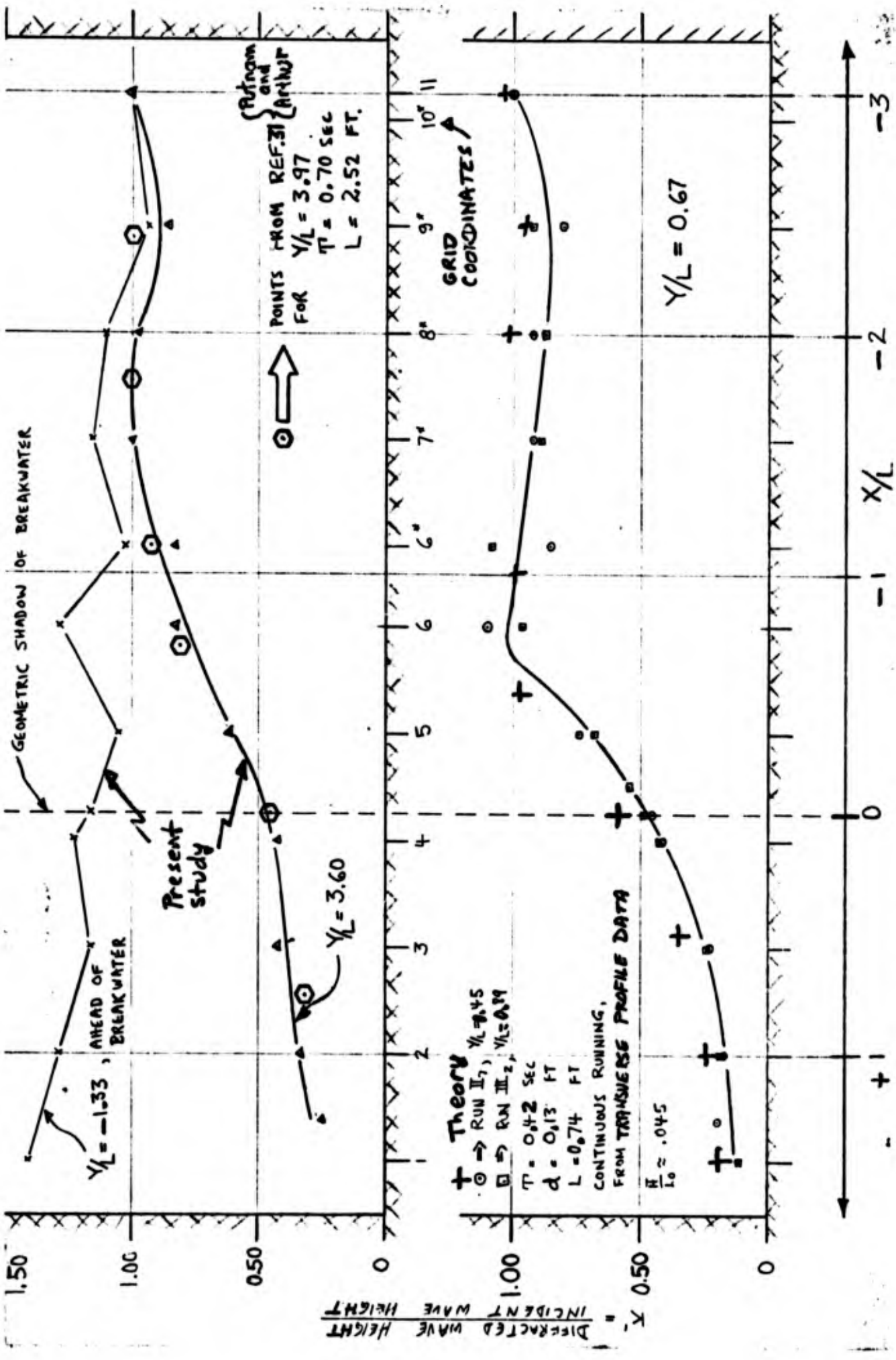

Fig. 15. Wave diffraction coefficient profile across the ripple tank. Comparison of ripple tank data with data of Putnam and Arthur, and with theory.

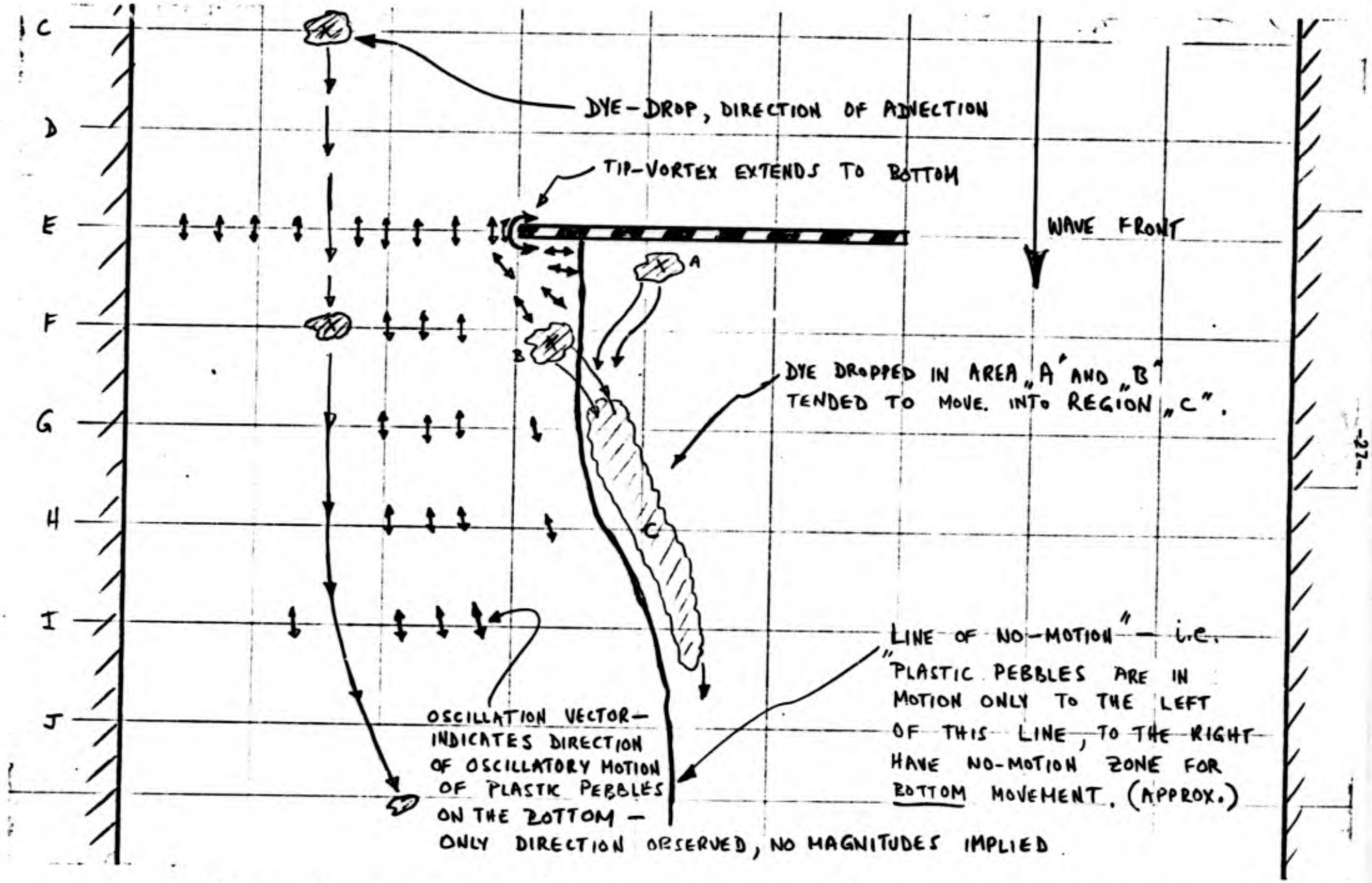

Fig. 16. Visual observations of water particle motions for the case of detached breakwater, ripple tank test. d = 0.13 ft, T = 0.39 sec, λ = 1.25 ft.

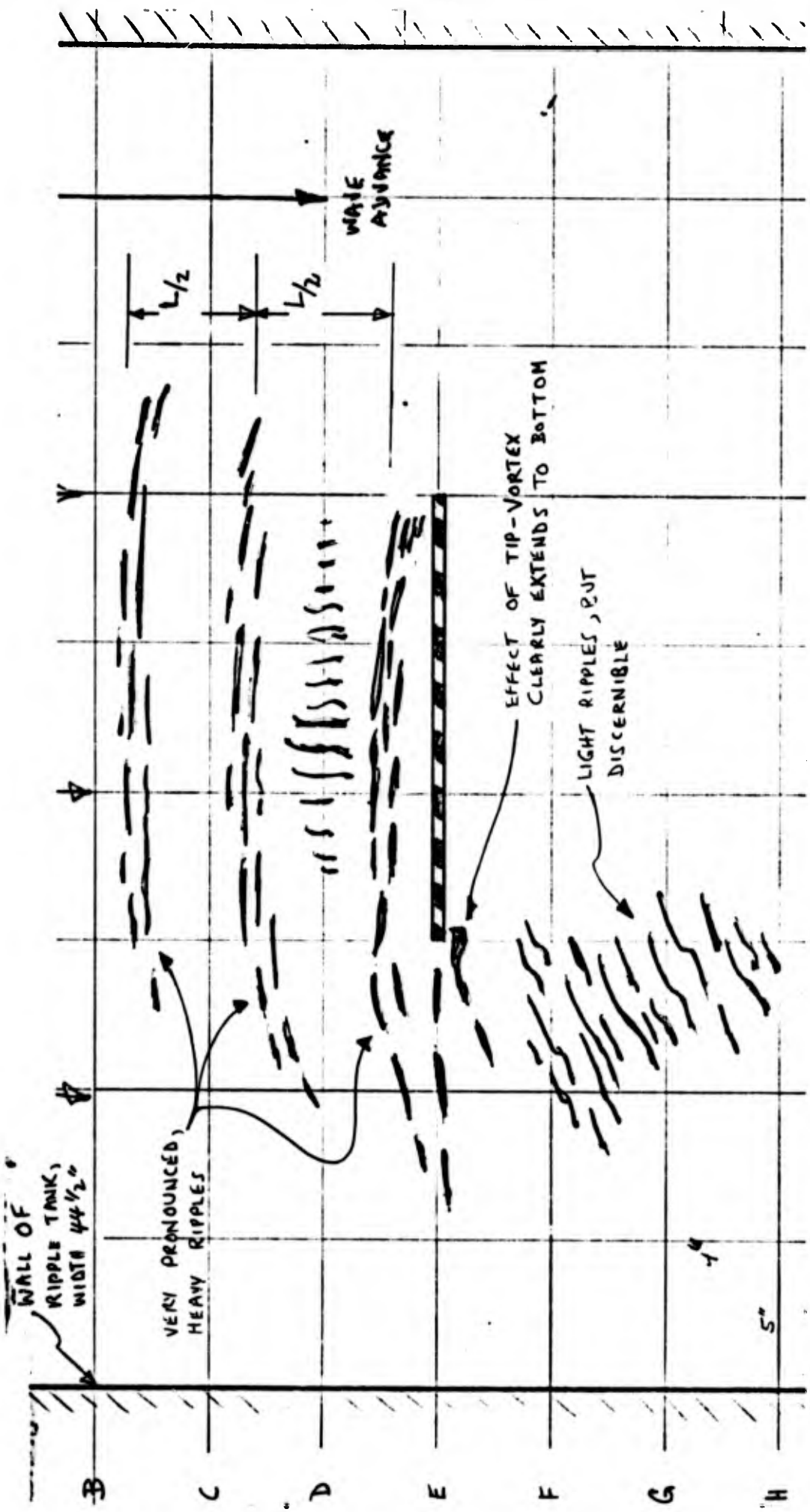

Fig. 17. Accretion of very fine sand particles in the form of "bottom ripples," detached breakwater, ripple tank test. d = 0.13 ft, T = 0.39 sec, λ = 1.25 ft.

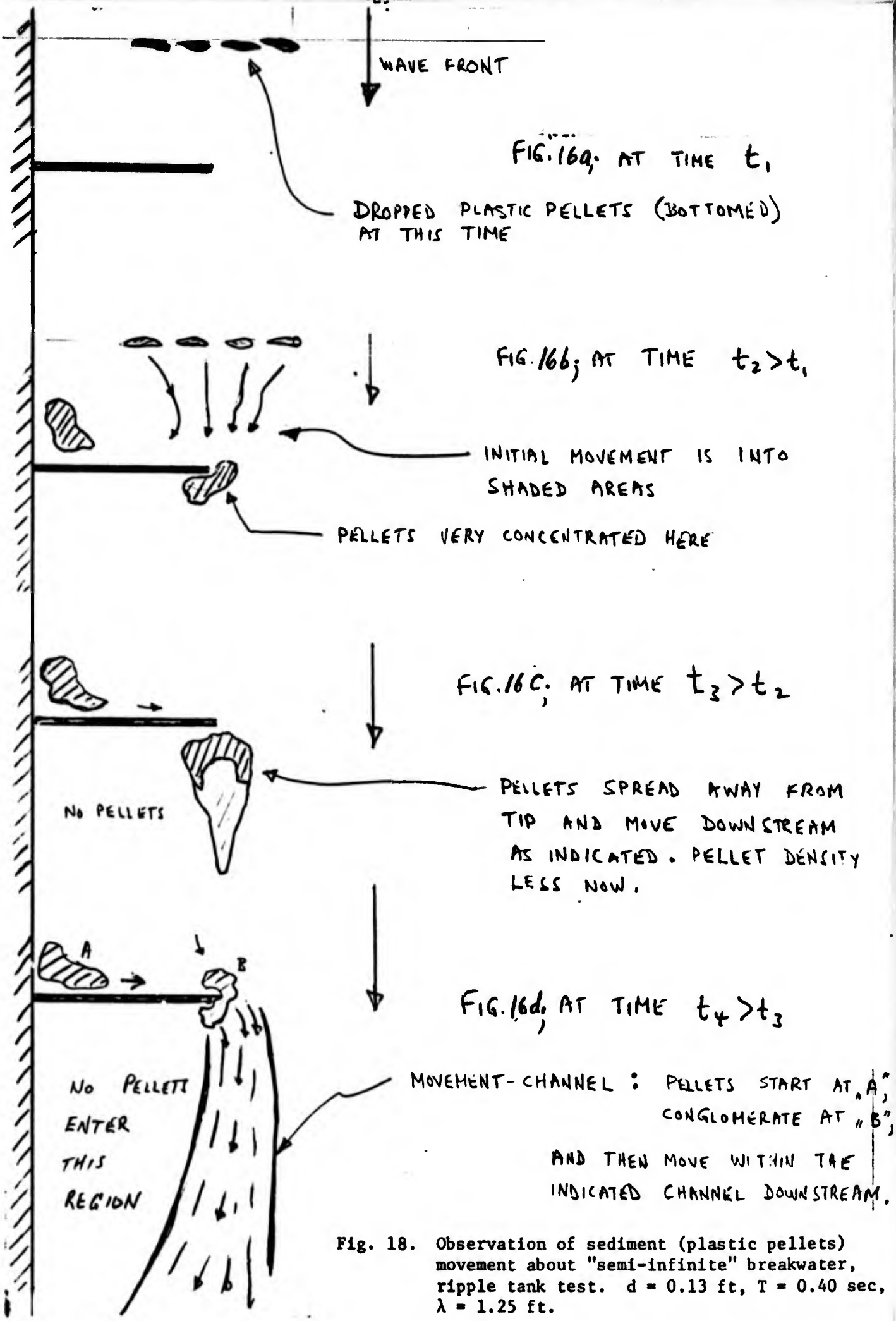

Fig. 18. Observation of sediment (plastic pellets) movement about "semi-infinite" breakwater, ripple tank test. d = 0.13 ft, T = 0.40 sec, λ = 1.25 ft.

and to determine the effect on the diffracted waves of several different shapes of offshore structures together with their wave energy absorbing characteristics.

2. Experimental Arrangements

The main portion of the experimental studies was conducted in the Model Basin of the Hydraulic Engineering Laboratory of the University of California at its Richmond Field Station. The experimental arrangements are shown in Figs. 19 and 20. The model basin is 148 ft long, 64 ft wide and 2-1/2 ft deep, with wave energy absorbers placed along the side walls. A 1:17 slope beach made of sand fill topped with a layer of cement (about 1/4 inch thick) with a layer of 2-1/2 inch thick horsehair matting placed on top of the cement is located at a distance of 107 feet from the wave generator. A carriage 70 feet long with 14 wave gages 5 feet apart is free to move along the stationary truss. This permits a coverage of an area of more than 4000 sq.ft. At the end of the carriage a wave gage is attached which, in turn, is free to move along the carriage. An additional wave gage is mounted on a cantilever beam near the wave generator face and is free to move longitudinally in the direction of wave advance.

The wave gages are of the parallel wire resistance type. The locations of the wave gages are shown in Fig. 19. The output of the gages were recorded on multi-channel rectilinear oscillographs. Up to 16 channels were used to record the waves simultaneously.

Models of different sizes and geometry were tested. Either a beach or rolls of "horsehair" was placed in front of the model to reduce wave reflection from the rigid impervious vertical wall structures.

3. Modifications to Facilities

Considerable work was necessary to be able to perform the tests in the model basin. A beach had to be constructed, a movable truss designed,

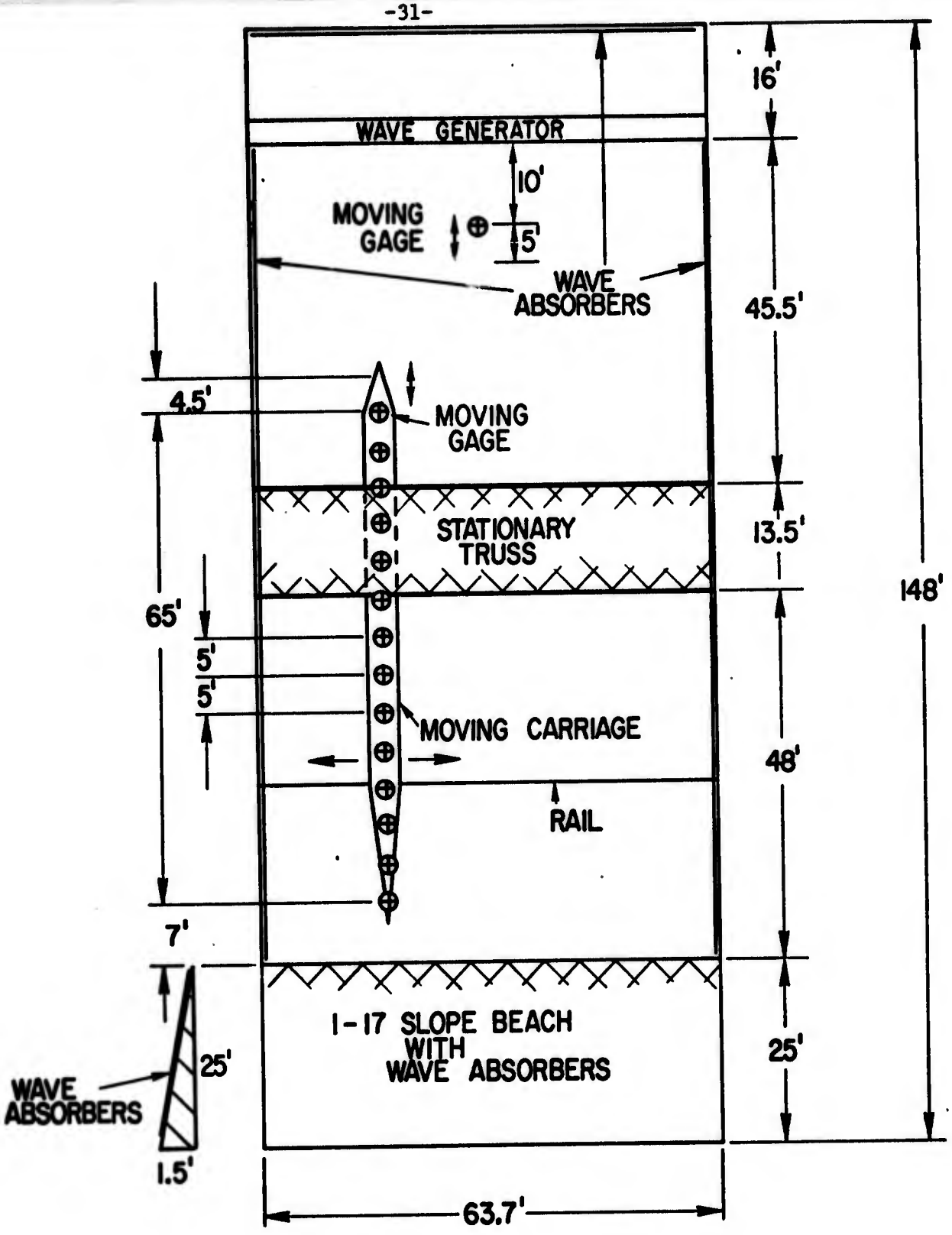

⊕ LOCATION OF WAVE GAGE

FIG. 19 GENERAL LAYOUT OF EXPERIMENT (TOP VIEW)

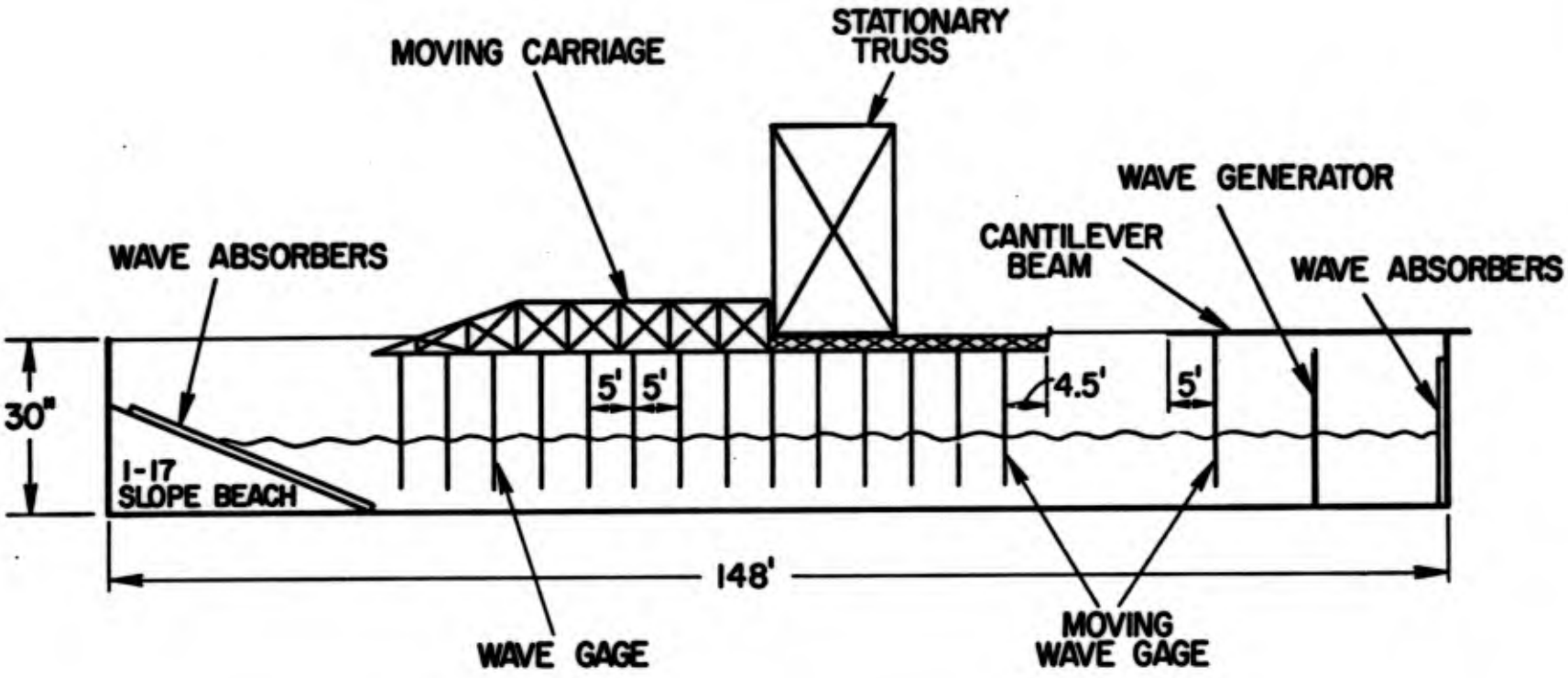

FIG. 20 GENERAL LAYOUT OF EXPERIMENT (VERTICALLY EXAGGERATED)
(SIDE VIEW)

constructed, and installed, new wave recorders fabricated, a special boom designed and built, and the wave generator stiffened. In addition a number of modifications had to be made during the course of the experiments.

It was found that the wave generator did not have uniform motion owing to three factors which were changed. The bearing in the center drive arm was repaired, and the entire "piston" portion stiffened. This was not found to be adequate, so the center drive arm was disconnected from the piston and the piston was then driven only by the drive arms near the left and right ends of the piston. Measurements were made of the piston stroke at a number of locations along the piston for three cases: original condition, bearing repaired and piston stiffened, and center drive arm disconnected. The results for two different wave periods are shown in Table 1. It can be seen that there was a considerable improvement in regard to the uniform stroke of the piston after the piston had been stiffened and the center drive disconnected.

4. Experimental Technique

The procedure for each run was as follows:

(1) The water in the basin was set to the required depth.

(2) Recorders connected to the wave gages were balanced and calibrated.

(3) The wave generator, set at the desired frequency and stroke, was started and allowed to reach equilibrium.

(4) To obtain the reflection coefficient, one of the moving gages was moved longitudinally in the direction of wave progress.

(5) To obtain wave height records on a grid base, the 70 ft carriage was moved to the desired location, held there for about 10 seconds, and then moved onto the next position.

(6) Each position was repeated several times.

Table 1. MEASUREMENT OF WAVE GENERATOR PISTON STROKE

(Note: Two values given for piston stroke, for example, 31/60. The first number is the stroke for a wave period of 0.69 sec, and the second number is for a wave period of 0.82 sec.

Station	Position from ℄ feet	Piston Stroke, mm		
		(1) Original Condition	(2) Center Bearing Fixed and Piston Stiffened	(3) Center Drive Arm Disconnected in addition to (2)
1	-32	31/60	37/61	37½/56
2	-28	27/57	35/59	36½/57
3	-15		33/57	34½/56
4	-6	24/56	30/55	36½/57½
5	+6	24/55	30/55½	37/56½
6	+15	27½/56	32/59	34/56
7	+28		34½/60	35/57
8	+32	30½/60	35/60½	36½/57

(7) The model to be tested was then placed in the basin. Repeat 4, 5, 6.

(8) When enough data had been obtained, the wave generator was turned off, and the recorder was calibrated again to see if there was any change.

5. Wave Characteristics in Model Basin Without Structure Installed

An extensive effort was made to measure and understand the wave characteristics in the model basin, as the wave heights were not uniform along the wave crest (transverse direction) or along the direction of wave advance (longitudinal direction). An example of the results of a study that was made for one of the better conditions is shown in Table 2. Wave heights are tabulated for 528 points in the basin for a wave period of 0.67 seconds and an overall mean wave height of 0.090 foot. The wave heights along a crest line lie within ± 15% of the mean value of all the measurements made along that crest line. The mean height of the waves along any particular crest line (transverse direction) varies by less than ± 5% of the overall mean wave height. The standard deviation is 7.9% of the overall mean wave height.

Over a longitudinal distance of 60 feet (the first transverse measurements were made 35.5 feet from the wave generator and the last were made 95.5 feet from the generator) there is no sign of wave attenuation with longitudinal distance traveled. The height variation along a crest line is not dependent on the distance from the wave generator.

The wave height at any point is uniform with respect to time. The basin reflections were small, as indicated by a reflection coefficient measured approximately 10 feet from the generator plate, which was of the order of 5%.

TABLE 2. WAVE HEIGHT IN BASIN WITHOUT STRUCTURE INSTALLED. T = 0.67 SECOND; H_{mean} = 0.090 FEET

GAGE NO / LOCATION	#15	#14	#12	#11	#2	#4	#6	#8
-20 ft	0.103 FT	0.114 FT	0.113 FT	0.112 FT	0.095 FT	0.092 FT	0.089 FT	0.096 FT
	.100	.114	.113	.107	.101	.096	.089	.094
-18¾ ft	.086	.099	.107	.112	.099	.100	.089	.092
	.081	.094	.109	.098	.103	.108	.094	.087
-17½ ft	.081	.086	.076	.102	.099	.100	.096	.085
	.086	.089	.093	.098	.103	.096	.096	.085
-16¼ ft	.092	.089	.078	.105	.103	.096	.094	.089
	.095	.089	.080	.091	.103	.102	.094	.085
-15 ft	.092	.089	.087	.086	.099	.108	.094	.089
	.089	.089	.087	.083	.098	.112	.089	.082
-13¾ ft	.086	.096	.087	.085	.083	.108	.094	.085
	.076	.091	.087	.092	.077	.092	.098	.078
-12½ ft	.076	.089	.083	.095	.084	.088	.098	.085
	.078	.089	.087	.088	.077	.085	.094	.087
-11¼ ft	.092	.089	.091	.088	.077	.088	.094	.089
	.092	.089	.091	.095	.077	.083	.089	.094
-10 ft	.086	.089	.087	.095	.077	.087	.096	.099
	.081	.086	.078	.088	.079	.093	.091	.094
-8¾ ft	.081	.089	.080	.092	.088	.077	.089	.094
	.076	.086	.083	.078	.095	.088	.083	.087
-7½ ft	.086	.091	.087	.078	.075	.088	.083	.085
	.086	.089	.091	.078	.088	.104	.088	.085
-6¼ ft	.092	.079	.085	.085	.081	.104	.081	.089
	.092	.089	.087	.095	.081	.106	.089	.085
-5 ft	.081	.089	.081	.105	.089	.100	.089	.087
	.081	.091	.089	.102	.090	.094	.102	.089
-3¾ ft	.081	.094	.091	.092	.088	.088	.104	.092
	.086	.089	.093	.081	.095	.088	.106	.096
-2½ ft	.092	.089	.087	.085	.092	.091	.098	.081
	.092	.089	.089	.093	.092	.096	.089	.089
-1¼ ft	.089	.091	.091	.098	.088	.096	.085	.089
	.081	.101	.096	.098	.081	.096	.081	.087
CENTER LINE OF TANK	.086	.101	.093	.091	.091	.092	.087	.089
	.086	.089	.091	.095	.088	.096	.087	.087

	#15	#14	#12	#11	#2	#4	#6	#8
+1¼ ft	.092	.084	.089	.092	.088	.092	.081	.087
	.086	.084	.089	.088	.095	.081	.094	.087
+2½ ft	.084	.091	.087	.088	.095	.088	.094	.085
	.076	.099	.091	.092	.088	.088	.098	.085
+3¾ ft	.081	.099	.096	.102	.088	.088	.094	.085
	.086	.086	.087	.102	.081	.092	.094	.089
+5 ft	.092	.079	.087	.095	.081	.094	.085	.082
	.086	.077	.089	.085	.084	.102	.085	.085
+6¼ ft	.086	.084	.091	.078	.088	.104	.083	.089
	.086	.089	.083	.075	.094	.096	.085	.089
+7½ ft	.086	.094	.078	.088	.095	.088	.088	.094
	.076	.094	.074	.092	.092	.077	.094	.085
+8¾ ft	.086	.089	.078	.098	.088	.077	.094	.091
	.086	.084	.091	.094	.081	.085	.094	.094
+10 ft	.086	.079	.098	.090	.077	.096	.102	.099
	.076	.069	.098	.086	.075	.092	.089	.104
+11¼ ft	.076	.081	.096	.092	.084	.092	.094	.094
	.076	.089	.081	.092	.088	.092	.089	.089
+12½ ft	.081	.099	.087	.088	.095	.096	.094	.087
	.086	.094	.078	.085	.092	.092	.098	.082
+13¾ ft	.089	.089	.083	.085	.092	.092	.094	.085
	.092	.084	.083	.085	.088	.100	.087	.085
+15 ft	.092	.079	.087	.097	.092	.101	.089	.088
	.086	.079	.087	.097	.097	.100	.085	.094
+16¼ ft	.086	.084	.093	.102	.095	.092	.081	.089
	.081	.084	.100	.102	.088	.092	.094	.089
+17½ ft	.081	.094	.100	.098	.092	.087	.098	.087
	.086	.097	.100	.102	.094	.088	.102	.087
+18¾ ft	.092	.104	.104	.105	.098	.092	.091	.088
	.092	.099	.109	.103	.101	.100	.094	.089
+20 ft	.097	.109	.111	.105	.095	.100	.085	.092
MEAN	.086	.090	.090	.093	.089	.093	.091	.089

Note: All gages used were mounted on the carriage which could be moved along the wave crest. Gages #15, #14, #12, #11, #2, #4, #6 and #8 were 35.5 ft, 40.5 ft, 50.5 ft, 55.5 ft, 65.5 ft, 75.5 ft 85.5 ft and 95.5 ft away from the generator, respectively.

For this specific wave generator setting, the overall mean wave height of 0.090 foot is assumed to be the representative wave height in the basin. Incident wave heights and diffracted wave heights could be obtained simultaneously by placing the structure model within the path of the movable array of gages. Normally the gage farthest away from the model in the seaward direction (towards the generator) was used to measure the incident wave (#15). The mean of wave gage #15 was found to be less than ± 5% of the representative wave height. A good correlation between the mean wave height as measured by gage #15 and the representative wave heights (i.e., "no model in the basin" overall wave height) is thus evident, and #15 can be used for the incident wave height.

The example described above is for one of the better conditions. Some others were nearly as good, while still others were more variable. It was decided to study the diffraction of waves by model structures at this time using only the more uniform incident wave conditions.

Studies of this sort were necessary as there is a growing body of evidence on the difficulty of generating a uniform stable wave field in a wide long model basin. Cross waves form under some circumstances, transverse waves under other circumstances, and waves that become progressively more irregular as they move down the basin under other conditions. This problem was discussed briefly in the Third Quarterly Progress Report (21 March-20 June 1973); references are given herein.

6. Results

A large number of tests were run for a variety of conditions. Many of the figures showing experimental results are given in an appendix to this report. Examples of the original oscillograph records of the tests are shown in Figs 21 and 22. In Fig. 21 are shown traces for the case of the oscillograph being run at a slow speed, which was adequate from the standpoint

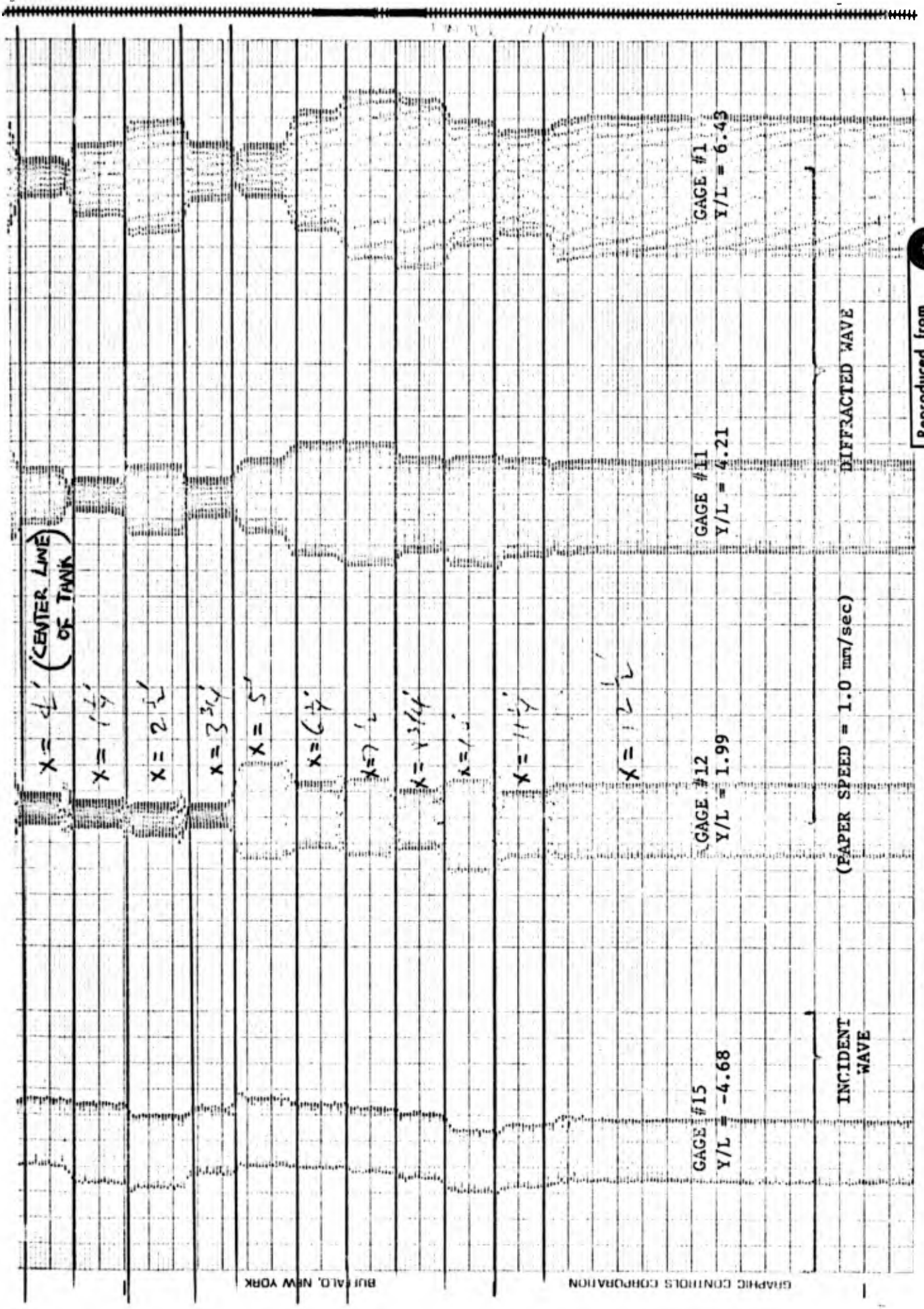

FIG. 21 SAMPLE OF DATA TRACE.

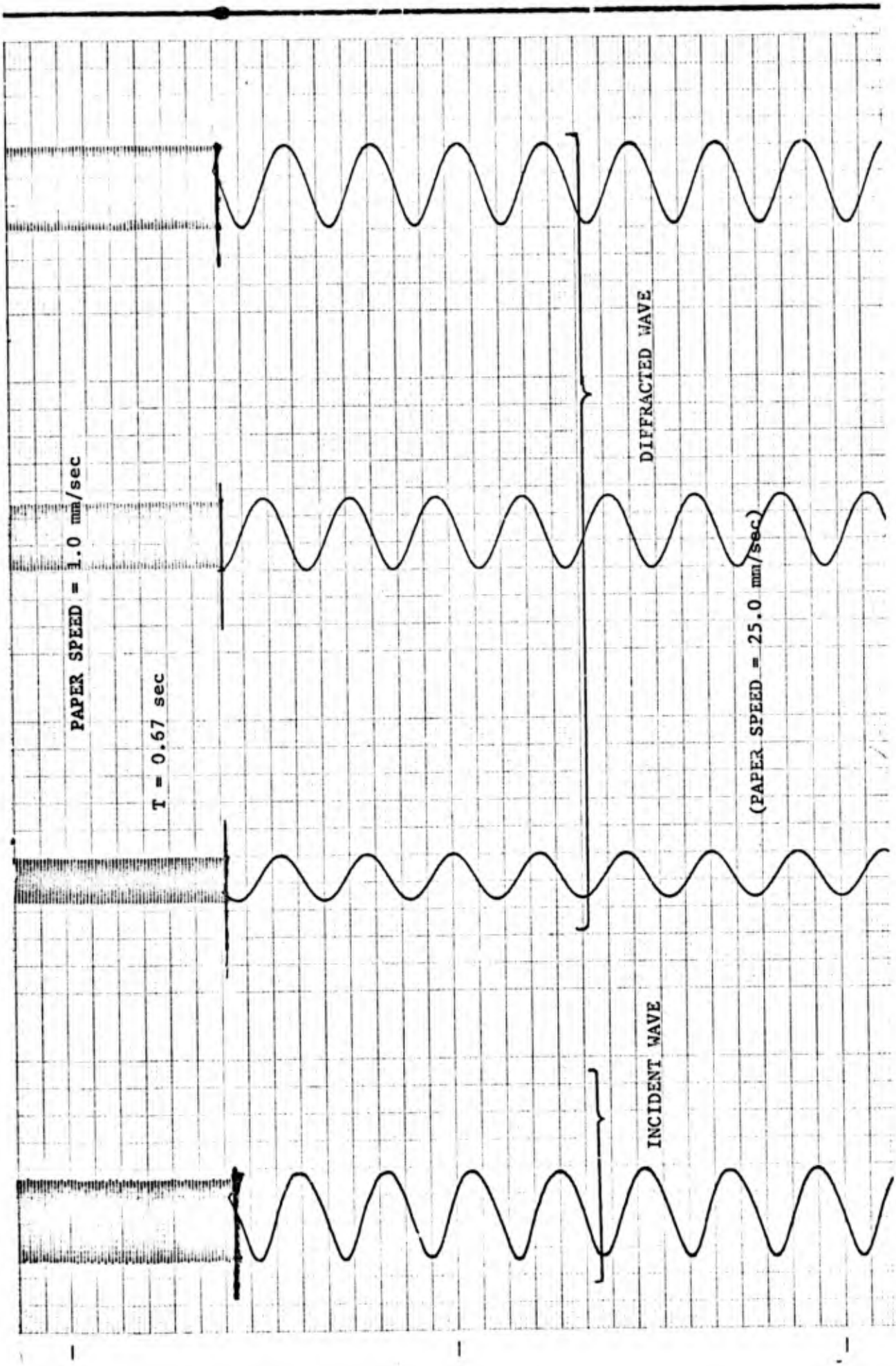

FIG. 22 SAMPLE OF DATA TRACE INDICATING WAVE SHAPE.

of measuring the wave heights. In Fig. 22 are shown examples of traces for the case of the oscillograph being run at a higher speed, to show the wave form.

a. Incident Wave and Wave Characteristics Without Model Installed.

Without a model in the basin one would hope to generate regular waves (no secondary peaks, signs of instability) that are of uniform height along the crestline. It was acertained that we could generate waves that were of a stable profile (2 dimensional, vertical plane, see Fig. 22) and that this wave shape did not change significantly as the wave progressed from the generator toward the beach over a distance of over 100 ft. The disintegration of the wave train could be avoided by adjusting the pertinent parameters (d/L, H/L, T) appropriately. A more persistent problem involves the 3-dimensional character of the waves - i.e. along a crestline it was found that the wave amplitude varies significantly, even though point for point the wave is regular (that is sinusoidal) and stable. This situation is thought to be due to some type of standing waves that are generated with their crestlines at right angle to the wave generator. One might attribute the phenomenon to so called cross waves, but this is not tenable since it was observed both at wave generator frequencies that would set up resonant cross waves and at those frequencies that should prevent their existence, that the wave height distribution along a crestline was not significantly altered. By trial and error the optimum conditions were found; they resulted in a height variation at any lateral section (crest-wise) of about ±15% about the mean, with a standard deviation of about 9% of the mean. The 2-dimensional wave profile (actually, the surface time history) for incident and diffracted wave is shown in

Fig. 22. The way in which wave amplitudes were obtained for incident and diffracted wave is shown in Fig. 21. The parameter shown in this figure is measured from the wave-tank centerline along the wave crestline. (In all other work in this report, x is a horizontal coordinate associated with a breakwater). The lateral variation of wave heights is typically as shown in Figs. A1, A7, and A13 in the appendix.

The data were obtained while the wave generator was running continuously which was often for the entire day. It was acertained that such a running mode was valid as long as the sources of reflection within the basin were minimal. Comparison of results obtained by this method (continuous-running) and by the stop-start method (intermittent-running) led to this conclusion. The reflection coefficient as meausred about 10 feet away from the wave generator was typically 0.05 (i.e., 5%) for the basin without model, with wave energy absorbers on the beach face and along the tank walls. With the insertion of the model, this value increased to 0.10, rarely to 0.15. It was found that a wave height measurement made at any location x, y, within the testing grid could be relied upon to be time-invariant for most of the tests performed. Exceptions to this were encountered at times in the lee of the structures, thus a time-wise instability of the diffraction profiles was occasionally observed and monitored.

b. General Characteristics of the Diffracted Waves

The continuous running testing procedure was used to acquire most of the reported herein data. To justify its use comparisons were made of the diffracted wave height as determined by this method and those obtained by the "intermittent running" procedure. The results of this are shown in Figs. A1-A3. Clearly, there is no consistent significant difference. It

appears that the diffraction profiles determined by the "continuous-running" procedure do not incorporate standing wave effects. The "intermittent-running"procedure does not allow sufficient time for these to be set up.

During most the tests performed, it was found that the incident and diffracted waves were stable with respect to time. This was always a prime criterion for aquiring reliable data. At times it was discovered that the diffraction profiles were shifting even though the incident wave profile (height distribution along the crest line) was steady with respect to time. This can be seen in Figs. A1 to A10. In Fig. A7 the incident wave profile is shown for two different times, and in Figs. A8 to A10 the corresponding diffraction profiles are shown for 3 different sections in the lee of the structure.

Since the incident wave is not of uniform height it must be anticipated that the diffracted waves will be detrimentally affected. To what extent the diffraction patterns will be upset by this had to be determined. It is possible to do this by comparing two diffraction profiles obtained for the same location, running condition and model with the only difference being that the incident waves are purposely different. In one case the incident wave may have a large wave height just at the tip of the model, whereas in the second case, it might be relatively small. If this is so, then different amounts of energy will be diffracted into the lee (see Fig.2a), and this should have an effect on the diffracted profile. In actual practice it is not the incident wave that was altered (it is steady with respect to time and repeatable) but rather the location of the model that was changed inorder to obtain the desired modification of the incident wave. In Figs. A4-A6 results of such tests are displayed. It may be

concluded that the lateral wave height variations for the incident wave, as encounted during these tests, are small enough to ensure reasonably reliable data in and near the shadow zone of the model.

c. Semi-infinite Breakwater

The superposition method predicts the wave heights in the lee of a detached breakwater based upon the diffraction behavior about a semi-infinite breakwater. In order to interpret discrepancies between this theory and experimental results it was necessary to have a good knowledge of the diffraction behavior of waves in the vicinity of a semi-infinite breakwater. Figs. A11, A14, A17 show the diffraction profiles at y/l=2.0, 8.6, and 21.9, and are typical for our findings (additional data are shown in Figs. A11-A17). The essentials of the test arrangements are shown in Fig. A11. The test was separated into two parts, one with a tip splitter plate and one without. Data were obtained for each case both by running continuously and by running intermittently. The number of points obtianed by the "intermittent-running" procedure was sufficient to ensure the validity of the main body of data that was obtained by running continuously. From our data we cannot detect a significant effect of the splitter plate. Concentrating for now principally on the region $-4 \leq x/L \leq 7$ one can observe the following:

1) For $y/L<6$, say, the theory if quite exact in the lee and its prediction too low for $x<0$ (open sea)

2) For $y/L>8$, say, the theory predicts wave heights that are conservative for $x<0$ but that are too low for the shadow zone $x>0$.

3) At $y/L=21.9$ we may note that the energy seems to be transferred into the lee to a much greater extent than predicted by theory. From this we can anticipate that the Superposition Method will similarly

result in a discrepancy between its predictions and the experimentally determined values.

d. Thin Detached Breakwater

The diffraction profiles were obtained for a series of values of λ/L and y/L. The data given in the Appendix generally consist of 3 profiles for each particular model configuration, corresponding to $y/L=2.0, 8.6$, and 21.9. In Figs. A18-A34 these profiles are shown for the case of normal incidence ($\theta_o=90$) and $\lambda/L=0.9$, 1.7, 3.5, 5.2, and 7.0, in that order. On each plot both the experimentally determined curve and theoretically predicted one (according to Superposition Method) have been drawn.

As a general observation it has been noted that the effect of the structure is strongly felt even at a distance of 22L behind a structure only $\lambda=0.9L$ wide (see Fig. A20)

In Fig. A24 the profile is shown for $\lambda/L=1.69$. It can be seen that directly in the lee the wave diffraction coefficient varies from 0.3 to 1.0 rather drastically. The profiles typically show a number of crests and troughs that vary in number and location, depending upon λ/L and y/L. The troughs have been named "interference channels" since they were first observed as channels of relatively calm water extending into the lee of the structure and can be predicted from simple wave interference considerations. Tests were performed to determine the effect of splitter plates on the detached breakwater $\lambda=1.63L$ wide. With wave energy absorbing material on the seaward side of the breakwater, it was found that with or without splitter plates the results were essentially the same. The influence of the splitter plates is thus of the order of the experimental variations that occur when testing the same model at the same conditions

a number of times.

Two cases of oblique wave incidence (θ_o=45) are given in Figs. A35-A40. These correspond to λ/L=2.3 and 5.1. A peculiar peak in diffraction coefficient was found near the right tip of the wider breakwater, as indicated in Fig. A38.

e. Significance of Projected Width, λp

A series of tests was performed in which the projected width of the structure (projected normally to the wave) was kept constant, as shown in Fig. A41. The results as shown in Figs. A14-A44 of the Appendix indicate that λp is the governing parameter for the structures. There are variations but these would appear even if the same model was tested repeatedly. It is felt that the agreement is quite good for engineering purposes for the whole range of values of y/L. The agreement between Run I and Run II (see Fig. A41) is particularly striking. It is believed that it is now possible to simplify many diffraction problems and to develope a better feeling for the diffraction behavior.

f. Three Dimensional Structures

A semi-circular structure was tested, with its curved surface facing seaward, and with an incident wave angle θ_o=90°. The pertinent conditions and results are shown in Figs. A45-A47 of the Appendix. Two separate tests were performed, with and without wave energy absorbing material on the seaward face of the structure. The points corresponding to the case with an absorber have been connected by a line. Note that the incident wave is also plotted in Fig. A45. The incident wave profiles are misleading here since they incorporate the pronounced standing waves set up near this model. The incident wave is measured at a section only about 7 ft from the model and is thus very sensitive to the reflective properties of the structure. A significant portion of the reflected energy does not reach the generator,

but is dissipated by the wall wave energy absorbers. The incident wave profiles, in this case, are not an indication of the energy distribution in the incident wave train. The good agreement between the results for the fully reflecting and the partially reflecting structure is thus believed to be reasonable.

A rectangular structure was also tested, but only with wave energy absorbing material on the seaward face. The results are shown in Figs. A48-A50. Curves were drawn to compare the behavior of a thin detached breakwater, the semicircular structure and the rectangular structure for incident waves at $\theta_o=90°$, and with the structures having approximately the same width. These plots are shown in Figs. A51-A53, and are interesting since they indicate that the behavior is, for many practical purposes, the same. The manner in which the waves separate from the structure (towards the lee) is the same in all cases. This seems to be the governing feature, with the seaward geometry of less significance.

IV. ANALYSIS OF TEST RESULTS

A. Superposition Method

The authors decided to explore a Superposition Method (i.e., using only the "non-interaction term") as a result of their laboratory observations rather than from mathematical considerations. It was observed in the Model Basin ("Large Tank") tests that in the lee of a detached breakwater there exist peculiar areas of low wave heights. These areas were termed "interference channels" after it was discovered that the existence of these channels could be predicted by treating each tip of the breakwater as a source of circular waves and then noting the interference pattern set up thereby (Fig. 23).

Assume that each tip of the detached breakwater behaves as though it was a portion of a semi-infinite breakwater. At any point in the lee of the breakwater two wave-trains coming around the tips can be superimposed, and so determine the wave amplitude at that location. This sequence is shown in Figs. 24, 25, and 26. For simplicity consider, as an example, a point located two wavelengths in the lee of the breakwater and one-half wavelength to the inside of the right tip, with the incident waves moving in a direction normal (θ_o = 90 degrees) to the breakwater of length $\lambda = 2L$, as shown in Fig. 27. The superposition method assumes that this isolated breakwater can be separated into the two semi-infinite breakwater as indicated in Figs. 28 and 29. From each of the component breakwaters (Figs. 28 and 29) it is possible to determine the diffraction coefficient, K', and phase angle, α, according to the well established semi-infinite theory.

From Penney and Price (1952) one can obtain a clearer physical understanding of the semi-infinite diffraction behavior by again separating

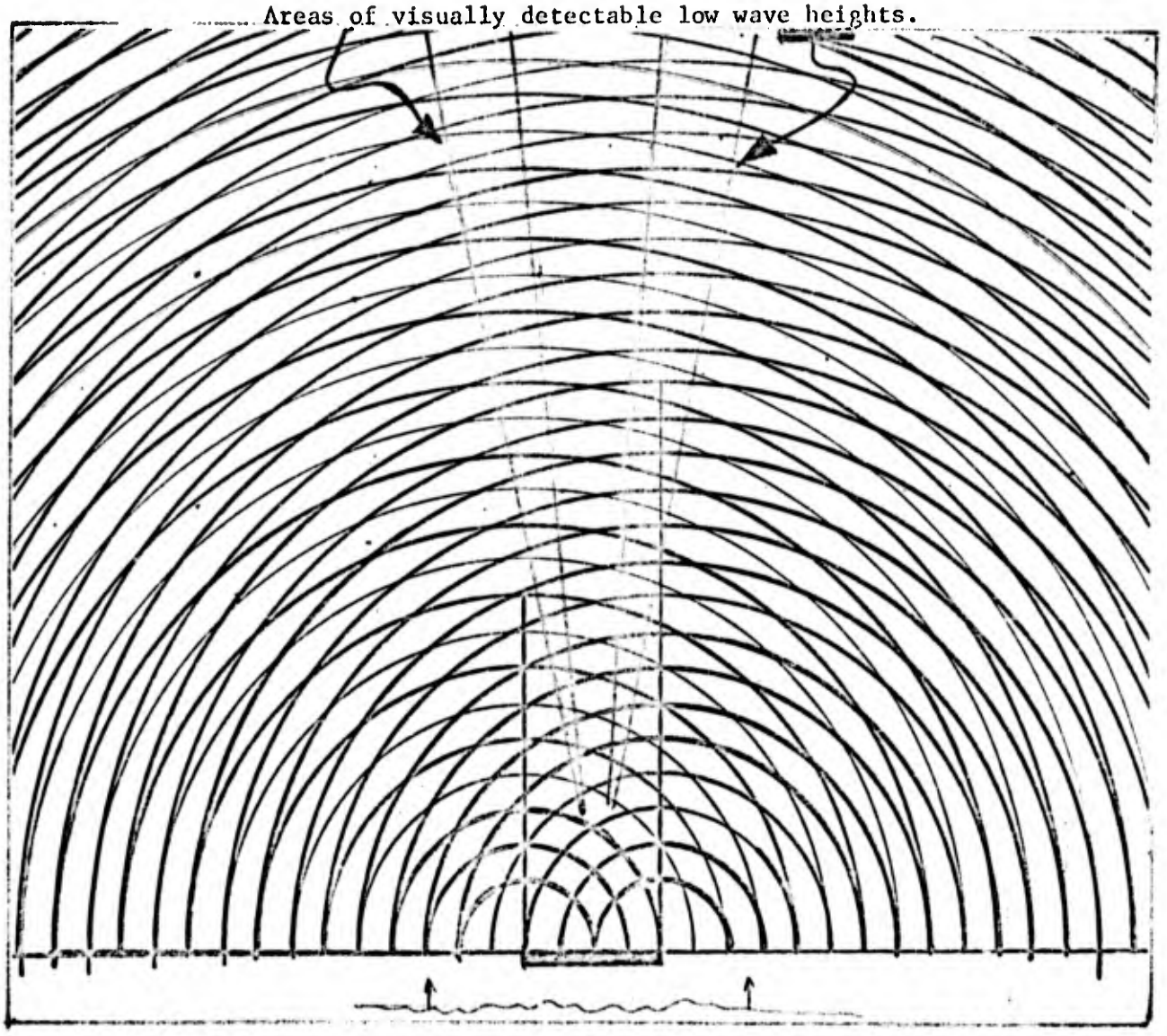

Fig. 23. Superposition of waves from two tips showing "interference channels."

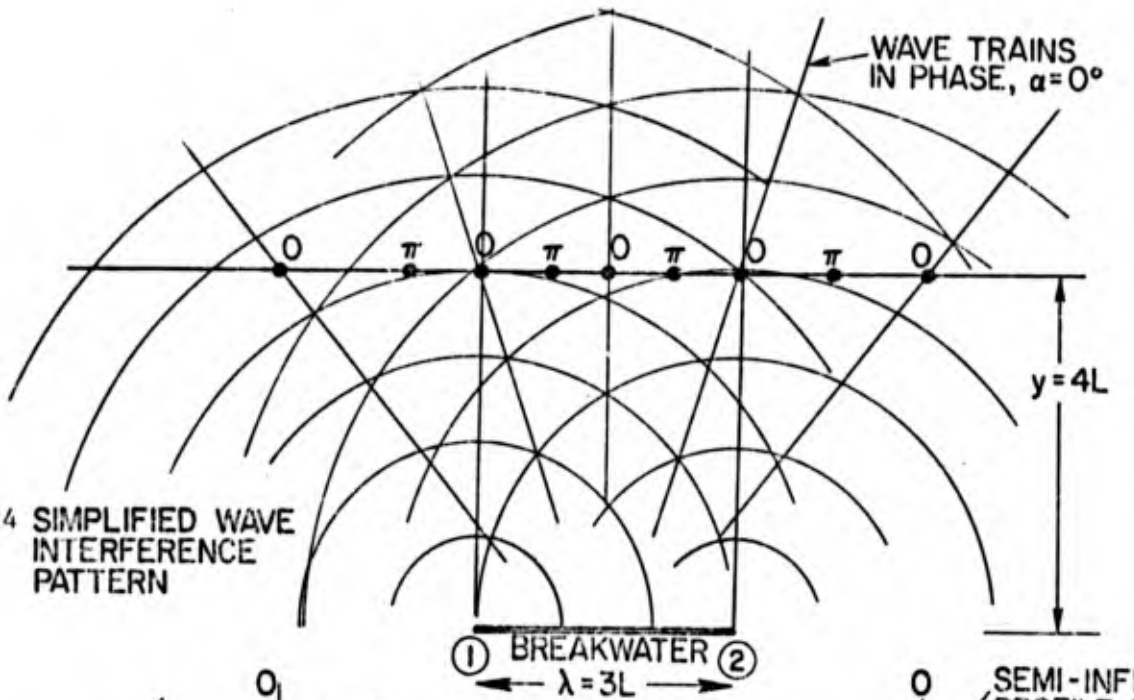

FIG. 24 SIMPLIFIED WAVE INTERFERENCE PATTERN

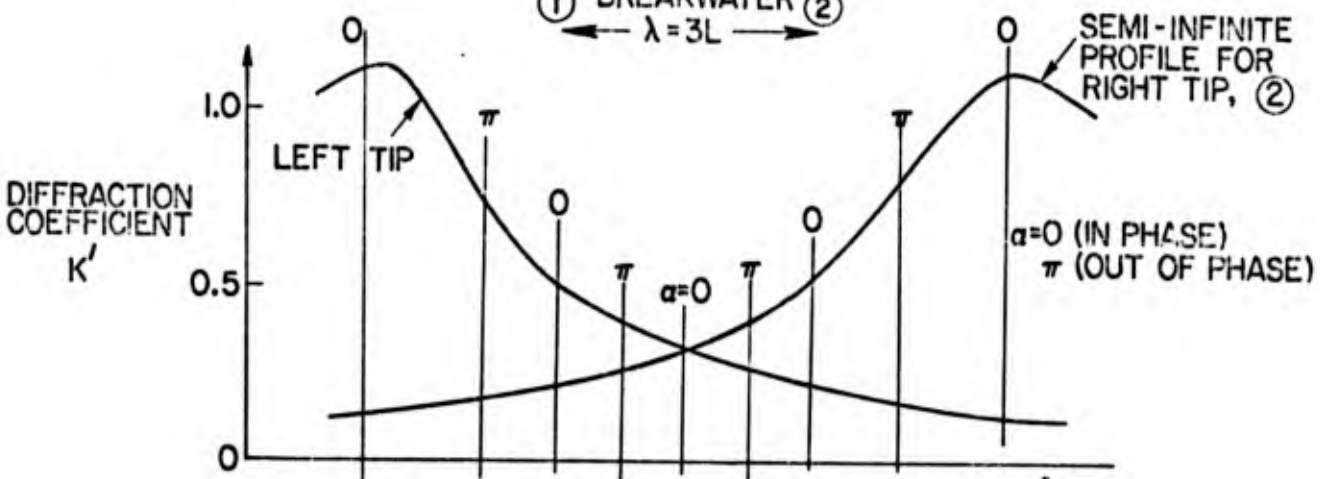

FIG. 25 SEMI-INFINITE DIFFRACTION PROFILES FOR y=4L, PHASE ANGLE FROM ABOVE FIGURE

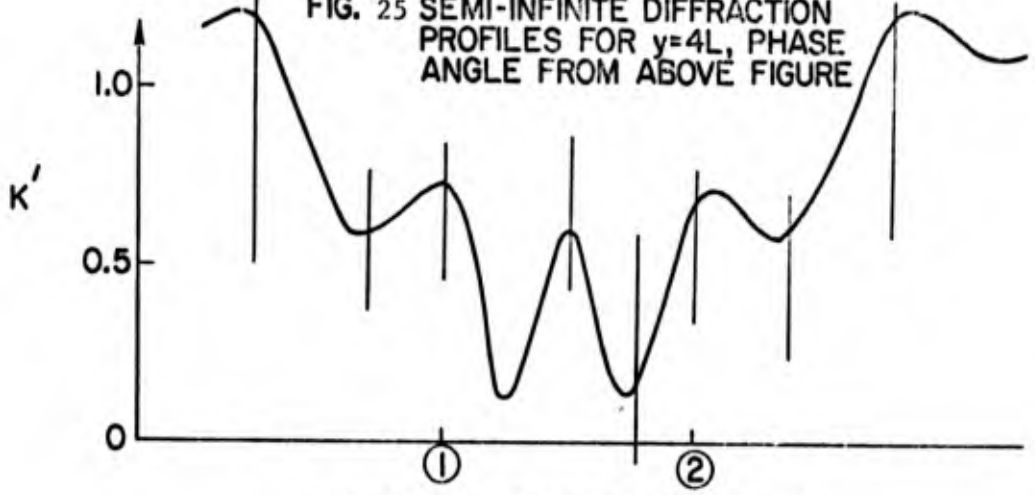

FIG. 26 SUM OF ABOVE PROFILES TAKING ACCOUNT OF PHASE ANGLE

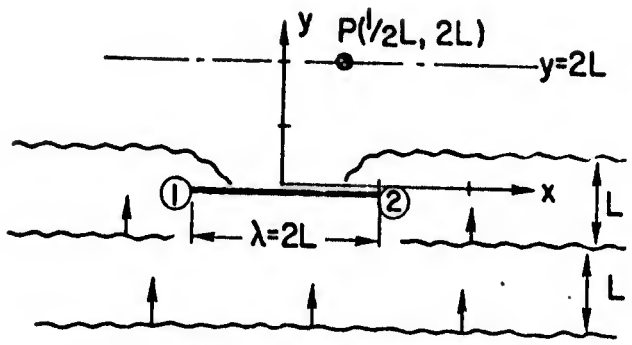

FIG. 27 SKETCH SHOWING DIFFRACTION

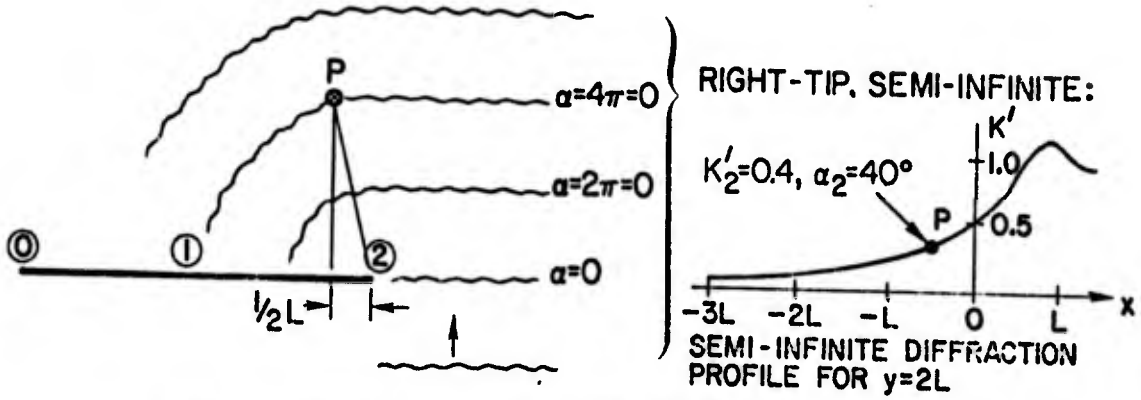

FIG. 28 DIFFRACTION AROUND RIGHT HAND TIP

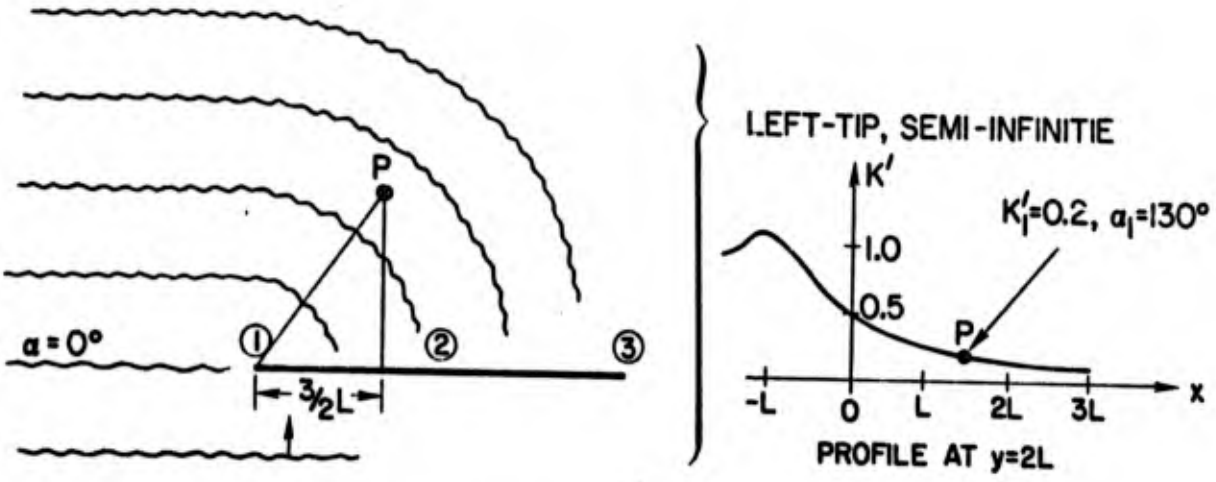

FIG. 29 DIFFRACTION AROUND LEFT HAND TIP

the solution into an incident wave (geometrical optics) and a diffracted wave, as shown in Figs. 30a and 30b. The superposition of these two waves results in Figs. 31 and 32. Note that the width of the shaded wave crests is a measure of the wave height. In Fig. 34 the added solutions are shown (as Fig. 31) for an incident wave angle of 90°. There, only wave fronts and contours of equal diffraction coefficient are shown. In Fig. 33 diffraction profiles are drawn, corresponding to the case of Fig. 34. This separation into incident and diffracted waves is helpful, but in our superposition method only the complete exact solution of the semi-infinite diffraction problem, as it is available in the form of a computer program, has been used. Our further concern is thus only with the situation shown in Figs. 34 and 31 and 32.

We now return to the situation shown in Fig. 27, and the point in the lee of the breakwater at which we are going to determine the wave height. Considering the right tip, tip 2 in Fig. 28, one might find that $K'_2 = 0.45$ and $\alpha_1 = 10^o$, say; similarly for the left tip, Fig. 29: $K'_1 = 0.20$ and $\alpha = 190^o$. Since the phase angles in each case are for the same incident wave it follows that their phase relationship with respect to one another is given by $\alpha = \alpha_1 - \alpha_2$. We add the waves as follows: $K'^2 = K'^2_1 + K'^2_2 + 2K'_1 K'_2 \cos\alpha$ and obtain $K' = 0.25$ at that location.

A computer program was written to perform these calculations for any angle of incidence and breakwater length. The source of our semi-infinite data was the report by Fan, Cumming and Wiegel (1967), "Computer Solution of Wave Diffraction by Semi-infinite Breakwater." This computer program is valid for any distance away from or near the tip.

The superposition method as outlined above is inherently only valid in the lee of the breakwater. This can be deduced from the component

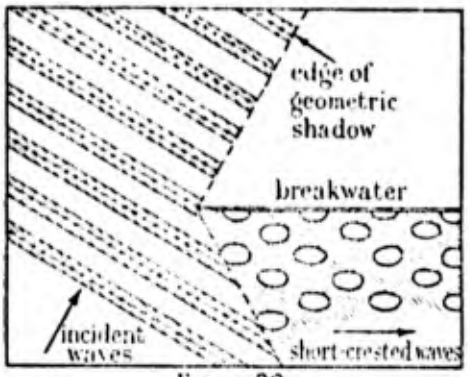

FIGURE 30a

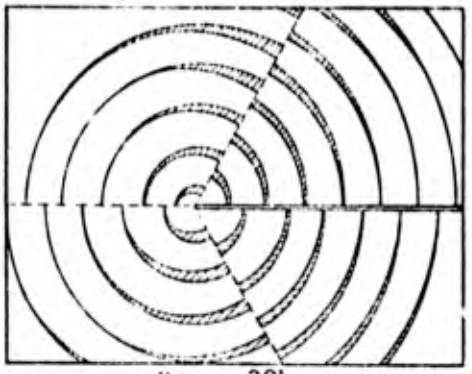

FIGURE 30b

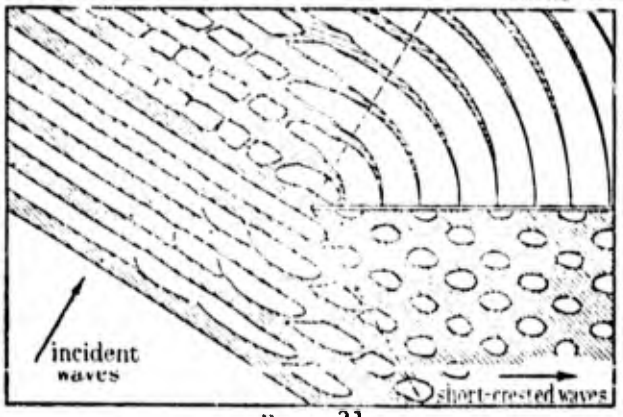

FIGURE 31

FIGURES 30*a*, *b*. Wave patterns for waves incident at 60° to a rigid breakwater. Figure *a* shows the pattern according to geometrical optics. Figure *b* shows the diffraction waves.

FIGURE 31 The wave pattern for waves incident at 60° to a rigid breakwater. The pattern shown is the superposition of the geometrical optics waves of figure *a* and the diffraction waves of figure *b*. The width of the shaded areas representing the waves gives an idea of their height.

(From Penney and Price, 1952)

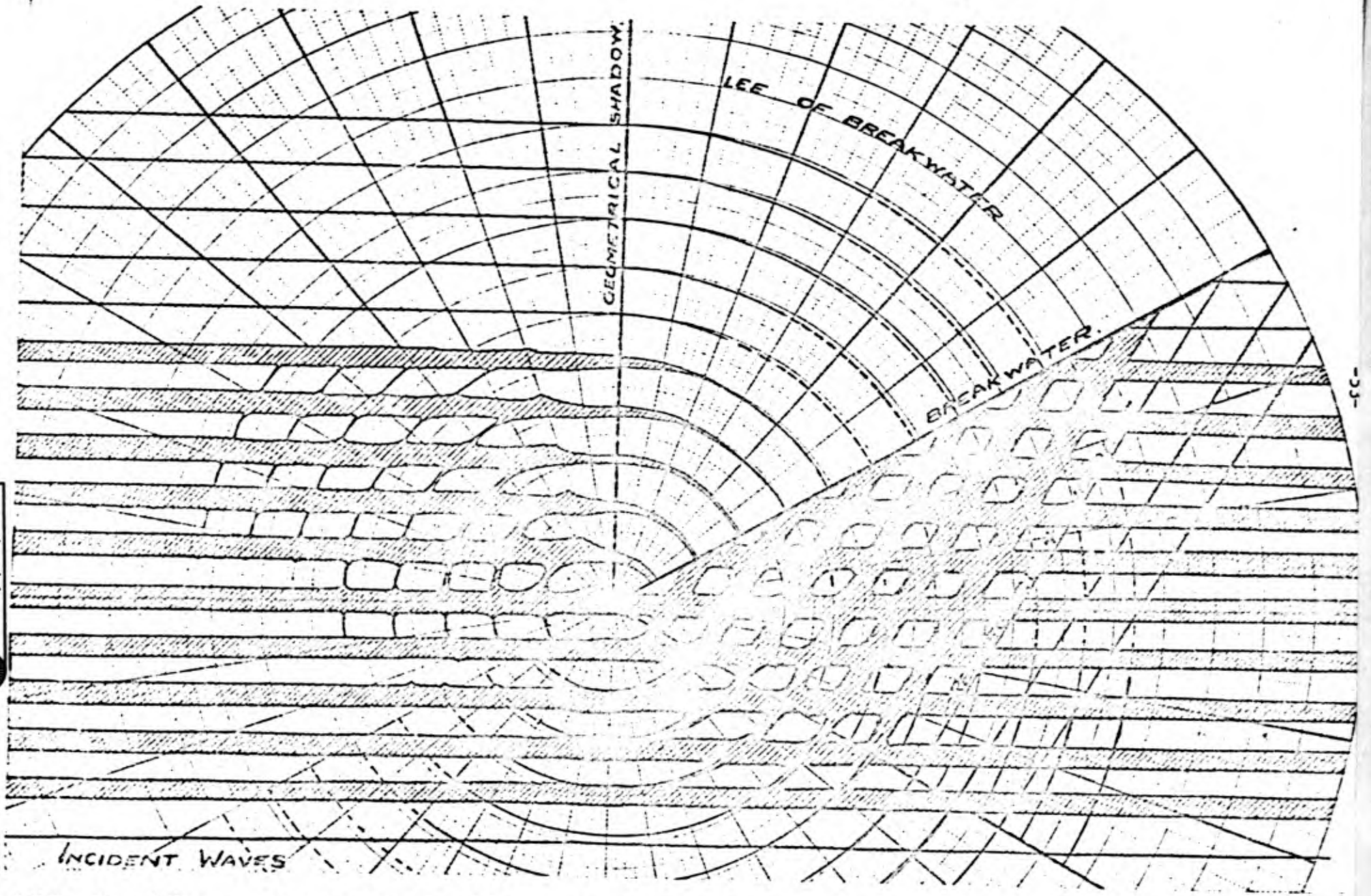

FIG. 32 WAVES INCIDENT AT 60° TO A SEMI INFINITE RIGID BREAKWATER.

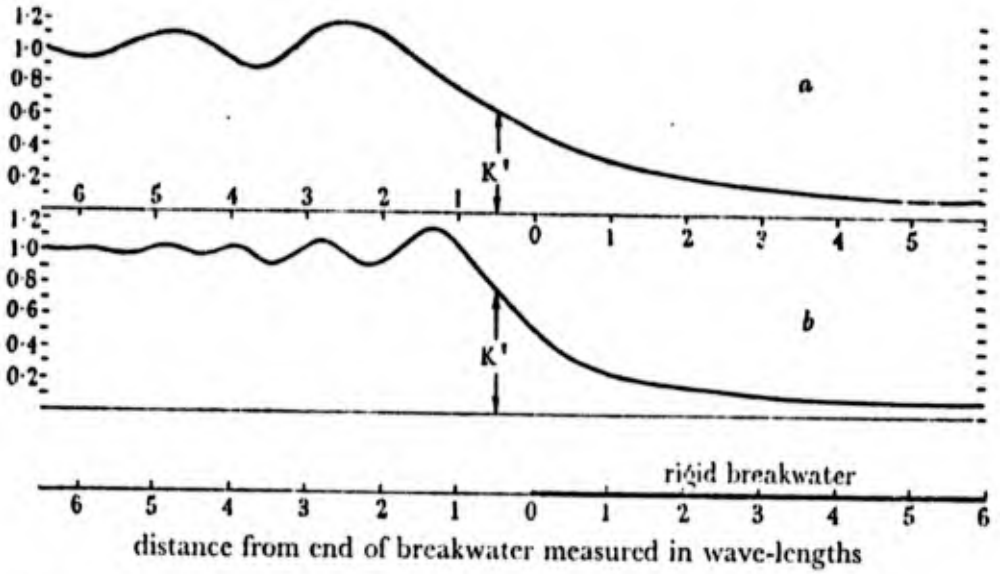

FIGURE 33 The maximum height of waves at normal incidence on a rigid breakwater, at distances $2\,L(b)$ and $8L(a)$ behind the breakwater. To obtain the wave heights at any distance $y = nL$ (where $n > 4$) behind the breakwater, multiply the values at $y = 8L$ by the factor $\sqrt{(\frac{1}{8}n)}$.

(From Penney and Price, 1952, Ref. 29)

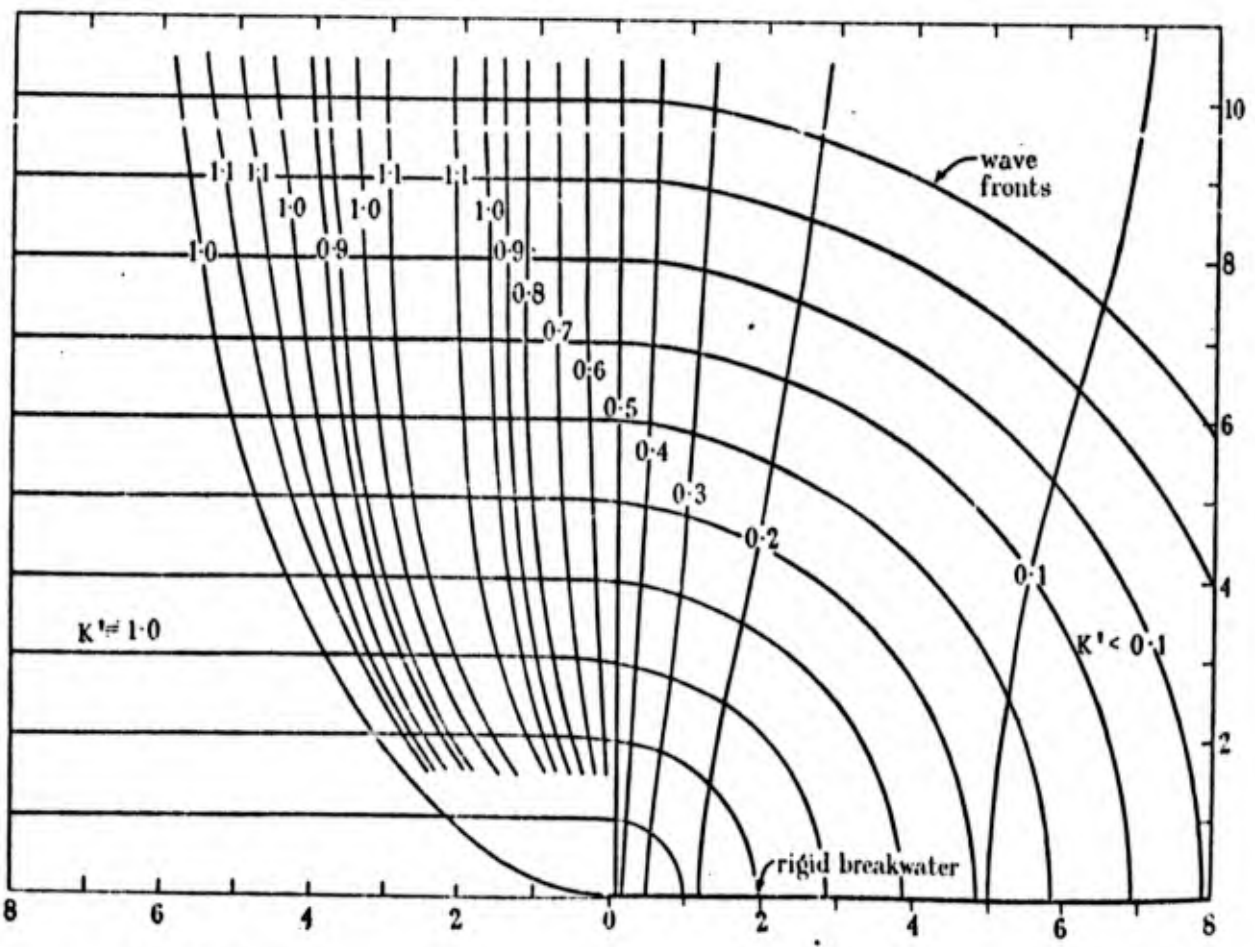

FIGURE 34 Wave fronts and contour lines of maximum wave heights in the lee of a rigid breakwater, the waves being incident normally.

(From Penney and Price, 1952, Ref. 29)

breakwaters, Figs. 28 and 29, which clearly have a solid wall boundary (Sections $\overline{01}$ and $\overline{23}$) where there should be no boundary. Adding the solutions seaward of the breakwater would thus generate standing waves that cannot exist in reality. To what extent these non-existent walls will influence the solution can be deduced in a qualitative sense from the following:

(1) The semi-infinite solution indicates that along the extension of the breakwater, $\theta = \pi$ in Fig. 35, the value of the diffraction coefficient is always unity.

(2) The rigorous solution for the case of a detached breakwater (see Montefusco, 1968) indicates that here also $K' = 1.0$ along the extension of the breakwater as shown in Fig. 36. This is a consequence of rigorously satisfying the real boundary conditions for the isolated breakwater.

Now it is necessary to look at the superposition method and see how close it comes to producing a physically real situation along the extension of the breakwater. The physically real condition is given by (2) above, i.e., $K' = 1.0$, since in this exact solution the physically real boundary conditions are completely satisfied. We might consider "$K' = 1.0$ along the breakwater extension" a "secondary boundary condition." Now, apply the superposition method along the breakwater and its extension as is indicated in Figs. 36 and 37. In Fig. 37 the semi-infinite diffraction profiles have been sketched for the case $y = 0+$; i.e., at the shoreward face of the breakwater. In Fig. 38 the profiles shown in Fig. 37 have been added in the region of interest, taking account of the phase relationships as displayed in Fig. 36. The undulation about $K' = 1.0$ can now be used as a measure of inaccuracy for the superposition method. For a short breakwater (in Fig. 38, the distance $\overline{12}$ would be small) one can see that the amplitude

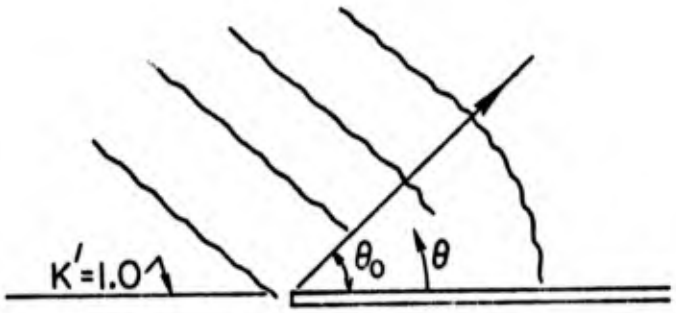

FIG. 35 DEFINITION SKETCH

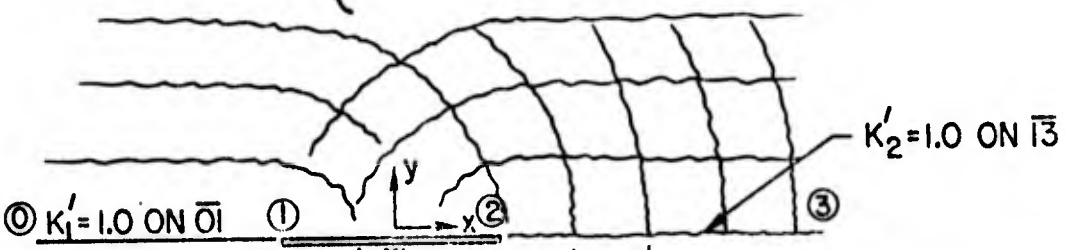

FIG. 36 DETACHED BREAKWATER WITH K' EQUAL UNITY ALONG "EXTENSION OF BREAKWATER"

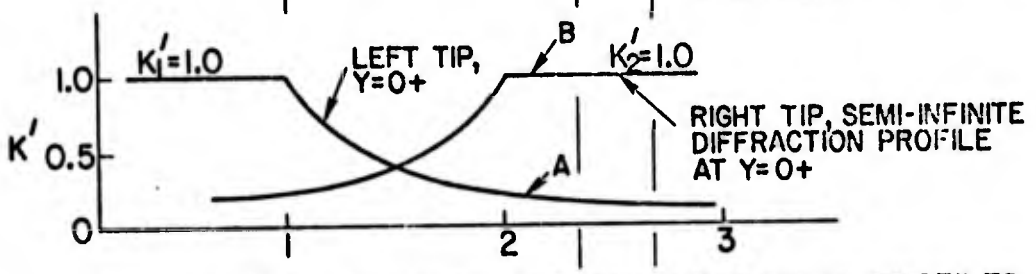

FIG. 37 LEFT AND RIGHT HAND TIPS DIFFRACTION PROFILES AT THE SHOREWARD FACE OF THE BREAKWATER, Y=0+

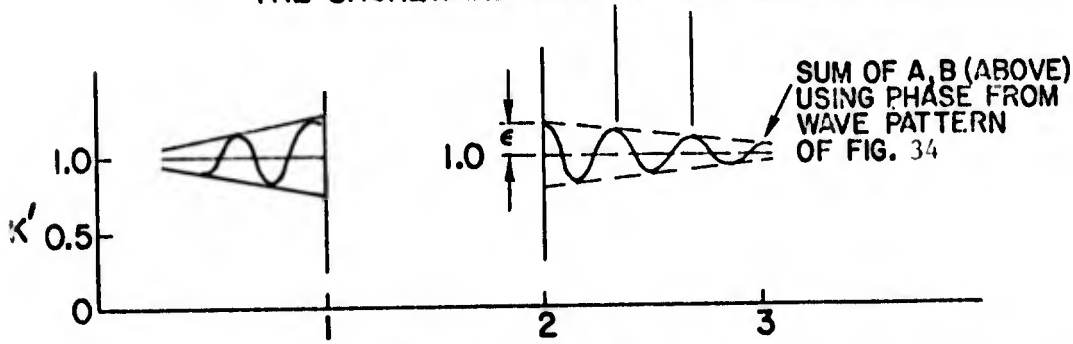

FIG. 38 PREDICTED VARIATION OF K' ACCORDING TO THE SUPERPOSITION METHOD, ALONG THE "BREAKWATER EXTENSION," LEE SIDE

ϵ in Fig. 38 will be relatively large; as the breakwater length increases, the magnitude of ϵ continually decreases. Describing the diffraction coefficient at the tip as $K'_T = 1.0 \pm \epsilon$, one would obtain, for a fairly long breakwater with $\lambda/L = 5.0$: $K'_{T5} = 1.0 \pm 0.10$ as a measure of error. According to Wada (1965) this breakwater is sufficiently long to allow deletion of the "interaction term"; i.e., here, the superposition method should compare well with the exact solution. Reducing the breakwater length to $\lambda/L = 1.5$ we find that the maximum oscillation has increased to $K'_{T1.5} = 1.0 \pm 0.18$. Thus, ϵ has only increased from 0.10 to 0.18 while the breakwater length was reduced from 5L to 1.5L. From this one might anticipate that the superposition method is usable, for engineering purposes, down to a value of λ/L of about 1.5. Thus, it should be useful for a range of breakwater dimensions that is quite real in application.

The Superposition Method applies equally well for angles of incidence other than 90 degrees. In this case the phase difference between the waves leaving each tip must be accounted for. This phase difference can be deduced from the geometry, as shown in Fig. 39.

B. Modified Superposition Theory

The Superposition Method uses as its building-blocks the semi-infinite theory. The results of the Superposition Method will thus directly reflect the validity of the semi-infinite theory. If the semi-infinite theory does not agree with the experimental data then the Suerpposition Method will also indicate a similar discrepancy. A modified Superposition Method (also called the "mixed" approximate theory) was tried in which the phase relationship between the two wave trains ("RPH" in the computer program) is obtained from the semi-infinite theory, but the amplitude of the wave trains is

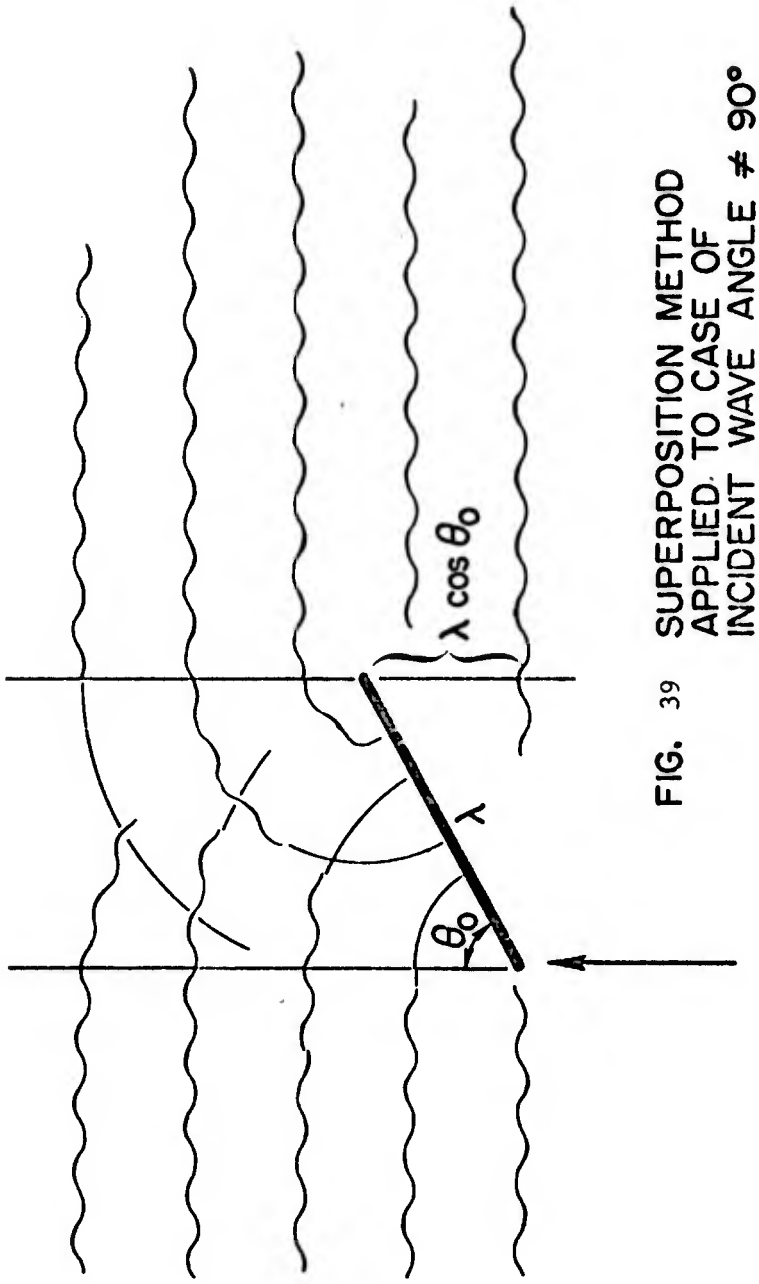

FIG. 39 SUPERPOSITION METHOD APPLIED TO CASE OF INCIDENT WAVE ANGLE ≠ 90°

obtained from the experimentally obtained semi-infinite diffraction profile, Figs. A11-A18. This was considered to be reasonable, since the circular wave fronts predicted by the theory seemed to be very predominant and persistent. The results of this modified Superposition Method are shown in Figs. A29, A34 in the Appendix.

C. Comparison of Laboratory Results with Theory

It has been pointed out that the Superposition Method should become more accurate as λ/L increases. Looking at the experimental results for waves of normal incidence (θ_o = 90 degrees) and y/L - 2.0, though, it is discovered that the agreement between theory and experiment is quite good, even if λ/L be 0.9. Near the breakwater, y/L of the order of 2, the theory thus describes the diffraction behavior adequately for engineering purposes. The results shown in Fig. A18, A26, for λ/L = 0.9 and 3.5, respectively, demonstrate this. As one proceeds further into the lee of the breakwater, the significance of the λ/L parameter becomes noticeable. To note the trend, one can compare Fig. A23 with Fig. A31, which are the diffraction profiles for y/L = 8.6 for λ/L = 1.7 and 5.2, respectively. The theoretical and experimental curves are clearly in better agreement for the wider breakwater. As one proceeds to y/L = 21.9 the agreement is poor, regardless of the width of the breakwater. It should be noted that a similar trend was observed for the semi-infinite breakwater; i.e., close to the breakwater there was good agreement between theory and experiment, while further in the lee there was increasingly poor agreement. At y/L = 21.9 there was a significant discrepancy between theory and experiment. This certainly accounts for some of the disagreement between the profiles according to the Superposition Method and those of experiment.

For the case of oblique wave incidence the Superposition Method exhibits the same characteristics as for waves of normal incidence. From Fig. A35 and A38 the comparison between $\lambda/L = 2.3$ and 5.1 can be made for $y/L = 2$ and $\theta_o = 45$. The significance of the projected width λ_p is predicted by the Superposition Method. This is indicated in Fig. A44 for the case of $\lambda_p = 1.63$.

V. DISCUSSION

One of the most important problems that had to be resolved for these studies was concerned with the fact that there were a limited number of combinations of wave heights, wave periods and water depths for which the incident waves were reasonably uniform in three dimensions. An extensive and very time consuming survey of combinations of these variables was performed, and a number of "good" combinations of the variables were found. These conditions were used in the tests reported herein.

One important study made was to determine the effect of placing wave energy absorbing material in front of the model breakwater and wave splitters at each breakwater end. This was done to minimize the complications that would be introduced by waves reflecting from the breakwater, back to the wave generator, reflecting from the wave generator, etc. Tests were run for intervals of time sufficiently short that the reflection problem could be neglected. It was found that the diffracted waves were the same for both cases. These results permitted the use of wave energy absorbing material so that runs of long duration could then be made with a resulting saving of considerable time.

Specific results have been discussed in detail in the section on results, and are given again in the conclusion, so they will not be rewritten here.

Two examples will be given below on the use of the work developed on this project.

1. Calculate and plot diffraction coefficients in the lee of an offshore breakwater, in water of constant depth for the case in which the length of the breakwater is 1.75 times as long as the

wave length ($\lambda/L = 1.75$). Use the superposition approximate theory.

Make use of Program FINBW (Fig. 40). The source of the semi-infinite data called for in the program is obtained by use of Subroutine WDIFFR which is given in Appendix B1. WDIFFR, in turn requires the use of Subroutine FRSNL, which is given in Appendix B2. An example of 3 pages of the data printout is given in Fig. 41.

Use is then made of Program FBWC (Fig. 43) to plot lines of equal diffraction coefficient K'. These values have been plotted in a reasonably large scale in Fig. 44 for the lee area of Y/L and X/L both between 0 and 4, in order to compare the results with the theoretical results of Montefusco (Fig. 45). They compare rather favorably. The results are plotted in Fig. 46 for the range of Y/L between 0 and 22.250 and X/L between 0 and 4.

2. A semi-circular offshore island, with the semi-circular front facing the incoming incident waves, with $\lambda/L = 1.75$ as in example 1. What is the diffraction coefficient at several distances in its lee. The values of K' calculated in example 1 can be used. The results shown in Fig. A21 show the superpsoition theory to be useful close to a thin vertical rigid breakwater (Y/L = 1.98), and the results shown in Fig. A45 indicate that these same calculations would be reasonably valid for the semi-circular island. However, it can be seen from Fig. A24 that the approximate theory does not predict the diffraction coefficient reliability at a larger distance, in

FIG. 40PROGRAM FINBW, APPROXIMATE ("SUPERPOSITION") THEORY SOLUTION WITH THE AID OF SUBROUTINE WDIFFR

```
      PROGRAM FINBW (INPUT,OUTPUT)
C     DIFFR. OF GRAVITY WAVES BY FINITE BW BASED ON HEL 1-8
      READ  11, (B,WLX,ANG,N1,N2)
   11 FORMAT (3F10.4,2I10)
      BL=B/WLX
      PRINT  17,(BL,WLX,ANG)
   17 FORMAT (1H1,20X,*WAVE DIFFRACTION-FINITE BREAKWATER      B/L= *F9.3
     1,10X,*WAVELENGTHUNIT*,F6.3,10X,*ANGLE*,F6.3)
      PRINT 19
   19 FORMAT (1H0,14X,*Y/L*,7X,*DK1*,7X,*PH1*,7X,*DK2*,7X,*PH2*,7X,
     2*RPH*,7X,*DKSUM*,7X,*X/L*,7X,*X1/L*,7X,*Y1/L*)
      CTZ=COS(ANG*3.1415926/180.)
      STZ=SIN(ANG*3.1415926/180.)
      DPH=360.*BL*CTZ
C     COORD SYSTEMS ARE  X,Y = WAVE FIXED  AND  X1,Y1 = BW FIXED
C     DO-LOOPS PROCEED ALONG WAVE DIR., SUBRN. WDIFF WANTS BW-FIXED SYSTEM
      Y=-1.
      DO 41 I=1,N1
      Y=Y+1.
      X= -1.0
      DO 41 J=1,N2
      X=X+1.
      CANG=180.-ANG
      X1= X*STZ + Y*CTZ
      Y1= -X*CTZ + Y*STZ
      XX1=B/2.0+X1
      XX2=B/2.0-X1
C     LEFT TIP
      CALL WDIFFR  (WLX,ANG,XX1,Y1,R,AA,BB,WA,PH,RG)
C     RIGHT TIP
      CALL WDIFFR  (WLX,CANG,XX2,Y1,R,AA2,BB2,WA2,PH2,RG2)
C     APPROX. THEORY - SEMI-INFINITE SUPERPOSITIONING
      RPH=PH+DPH-PH2
      C=COS (RPH*3.1415926/180. )
      DKSUM=SQRT(WA**2+WA2**2+2.0*WA*WA2*C)
      XL=X/WLX
      YL= Y/WLX
      X1L= X1/WLX
      Y1L = Y1/WLX
      PRINT 32,  (YL,WA,PH,WA2,PH2,RPH,DKSUM,XL,X1L,Y1L)
   32 FORMAT (1H ,10X,10F10.3)
   41 CONTINUE
      STOP
      END
```

FIG. 41 EXAMPLE OF OUTPUT DATA FROM PROGRAM FJNBW.

WAVE DIFFRACTION-FJ ITE BREAKWATER λ/L= 1.750 WAVELENGTH UNIT 4.000 ANGLE 90.000

Y/L	DK1	PH1	DK2	PH2	RPH	DKSUM	X/L	X1/L	Y1/L
.250	.238	-7.496	.238	-7.496	.000	.476	0.	.000	.250
.250	.211	-95.876	.279	79.693	-175.568	.071	.250	.250	.250
.250	.191	175.173	.350	163.796	11.377	.539	.500	.500	.250
.250	.176	85.907	.493	-123.067	208.974	.356	.750	.750	.250
.250	.164	-3.552	.792	-86.373	82.821	.819	1.000	1.000	.250
.250	.154	-93.138	1.006	-84.770	-8.367	1.159	1.250	1.250	.250
.250	.146	177.191	1.050	-89.954	267.145	1.053	1.500	1.500	.250
.250	.139	87.456	1.001	-91.419	179.275	.863	1.750	1.750	.250
.250	.133	-2.323	.978	-90.032	87.709	.992	2.000	2.000	.250
.250	.127	-92.138	1.000	-89.335	-3.103	1.127	2.250	2.250	.250
.250	.122	178.020	1.013	-89.985	268.005	1.016	2.500	2.500	.250
.250	.118	88.156	1.000	-90.615	178.772	.882	2.750	2.750	.250
.250	.114	-1.725	.991	-90.009	88.285	1.001	3.000	3.000	.250
.250	.111	-91.620	1.000	-89.565	-2.055	1.111	3.250	3.250	.250
.250	.108	178.477	1.007	-89.995	268.467	1.009	3.500	3.500	.250
.250	.105	88.555	1.000	-90.328	178.883	.895	3.750	3.750	.250
.250	.102	-1.371	.995	-90.004	88.632	1.003	4.000	4.000	.250
.500	.243	-41.953	.243	-41.953	.000	.485	0.	.000	.500
.500	.214	-123.777	.286	35.305	-159.082	.115	.250	.250	.500
.500	.193	151.832	.359	103.883	47.949	.509	.500	.500	.500
.500	.177	65.888	.491	155.991	-90.103	.521	.750	.750	.500
.500	.165	-21.956	.705	-176.729	155.673	.559	1.000	1.000	.500
.500	.155	-108.675	.938	-171.476	62.801	1.018	1.250	1.250	.500
.500	.146	163.231	1.066	-176.408	339.639	1.205	1.500	1.500	.500
.500	.139	74.787	1.052	178.167	-103.380	1.029	1.750	1.750	.500
.500	.133	-13.920	.981	177.708	-191.628	.851	2.000	2.000	.500
.500	.128	-102.826	.969	-179.262	76.436	1.007	2.250	2.250	.500
.500	.123	168.109	1.009	-178.591	346.700	1.129	2.500	2.500	.500
.500	.118	78.918	1.020	179.662	-100.744	1.005	2.750	2.750	.500
.500	.114	-10.375	.996	179.009	-189.385	.883	3.000	3.000	.500
.500	.111	-98.753	.995	-179.902	80.049	1.010	3.250	3.250	.500
.500	.108	170.799	1.013	-179.270	350.069	1.109	3.500	3.500	.500
.500	.105	81.292	1.011	179.379	-98.546	1.001	3.750	3.750	.500
.500	.102	-8.263	.998	179.430	-187.693	.897	4.000	4.000	.500
.750	.248	-93.016	.248	-93.016	.000	.497	0.	.000	.750
.750	.218	-166.712	.294	-26.315	-140.396	.188	.250	.250	.750
.750	.196	115.084	.368	29.631	85.453	.430	.500	.500	.750
.750	.179	33.910	.498	70.284	-36.374	.642	.750	.750	.750
.750	.166	-49.286	.668	92.937	-142.223	.546	1.000	1.000	.750
.750	.156	-133.904	.880	99.763	-233.667	.797	1.250	1.250	.750
.750	.147	140.447	1.043	96.744	43.703	1.154	1.500	1.500	.750
.750	.140	54.034	1.087	90.433	-36.399	1.203	1.750	1.750	.750
.750	.134	-32.966	1.024	86.654	-119.620	.965	2.000	2.000	.750
.750	.128	-120.421	.959	88.494	-208.914	.849	2.250	2.250	.750
.750	.123	151.766	.976	91.762	60.004	1.043	2.500	2.500	.750
.750	.119	63.663	1.022	91.261	-27.597	1.129	2.750	2.750	.750
.750	.115	-24.674	1.020	89.050	-113.726	.980	3.000	3.000	.750
.750	.111	-113.210	.987	88.941	-202.151	.885	3.250	3.250	.750
.750	.109	158.092	.994	90.610	67.482	1.030	3.500	3.500	.750
.750	.105	69.259	1.009	90.939	-21.680	1.107	3.750	3.750	.750
.750	.102	-19.693	1.013	89.606	-109.299	.984	4.000	4.000	.750
1.000	.255	-155.370	.255	-155.370	.000	.510	0.	.000	1.000
1.000	.223	138.902	.303	-97.715	236.617	.259	.250	.250	1.000

EXPLANATION OF TABLE OF OUTPUTS

X,Y	Horizontal coordinates - wave fixed, see Fig. 42
X1, Y1	Horizontal coordinates - breakwater fixed, see Fig. 42
DK1	Diffraction coefficient component - left tip
DK2	Diffraction coefficient component - right tip
PH1	Phase angle, left tip
PH2	Phase angle, right tip
RPH	Relative phase angle between the two wave trains
DKSUM	Vectorial sum of DK1 and DK2
L	Wave length

FIG. 41, CONT.- EXAMPLE OF OUTPUT DATA FROM PROGRAM FINBW.

10.750	.165	-163.344	1.007	102.170	-265.514	1.098	2.750	2.750	10.750
10.750	.157	166.392	1.065	100.139	66.253	1.137	3.000	3.000	10.750
10.750	.150	134.472	1.110	97.526	36.946	1.233	3.250	3.250	10.750
10.750	.143	100.922	1.138	94.500	6.422	1.281	3.500	3.500	10.750
10.750	.137	65.771	1.146	91.283	-25.511	1.272	3.750	3.750	10.750
10.750	.132	29.050	1.133	88.166	-59.115	1.206	4.000	4.000	10.750
11.000	.368	-31.474	.368	-31.474	-.000	.736	0.	.000	11.000
11.000	.335	-43.157	.405	-21.269	-21.889	.727	.250	.250	11.000
11.000	.308	-56.365	.446	-12.489	-43.876	.701	.500	.500	11.000
11.000	.283	-71.140	.492	-5.090	-66.050	.660	.750	.750	11.000
11.000	.261	-87.518	.544	1.015	-88.533	.609	1.000	1.000	11.000
11.000	.242	-105.527	.600	5.859	-111.386	.550	1.250	1.250	11.000
11.000	.225	-125.191	.662	9.511	-134.702	.529	1.500	1.500	11.000
11.000	.210	-146.524	.728	12.038	-158.562	.538	1.750	1.750	11.000
11.000	.197	-169.533	.797	13.507	-183.040	.600	2.000	2.000	11.000
11.000	.186	165.779	.867	13.990	151.790	.709	2.250	2.250	11.000
11.000	.175	139.418	.937	13.556	125.852	.846	2.500	2.500	11.000
11.000	.166	111.394	1.002	12.326	99.068	.989	2.750	2.750	11.000
11.000	.158	81.722	1.060	10.374	71.348	1.120	3.000	3.000	11.000
11.000	.151	50.421	1.106	7.938	42.584	1.221	3.250	3.250	11.000
11.000	.144	17.516	1.136	4.877	12.639	1.277	3.500	3.500	11.000
11.000	.139	-16.967	1.147	1.700	-18.667	1.279	3.750	3.750	11.000
11.000	.133	-52.909	1.136	-1.421	-51.578	1.223	4.000	4.000	11.000
11.250	.369	-121.030	.369	-121.030	-.000	.738	0.	.000	11.250
11.250	.337	-132.519	.405	-110.985	-21.532	.730	.250	.250	11.250
11.250	.309	-145.495	.446	-102.334	-43.161	.704	.500	.500	11.250
11.250	.284	-160.004	.492	-95.023	-64.981	.664	.750	.750	11.250
11.250	.262	-176.079	.543	-88.995	-87.084	.615	1.000	1.000	11.250
11.250	.243	166.257	.599	-84.192	250.444	.566	1.250	1.250	11.250
11.250	.226	146.964	.660	-80.555	227.519	.534	1.500	1.500	11.250
11.250	.212	126.043	.725	-78.021	204.064	.539	1.750	1.750	11.250
11.250	.199	103.480	.793	-76.524	180.004	.595	2.000	2.000	11.250
11.250	.187	79.272	.863	-75.995	155.267	.698	2.250	2.250	11.250
11.250	.177	53.422	.932	-76.359	129.781	.830	2.500	2.500	11.250
11.250	.167	25.940	.997	-77.528	103.468	.972	2.750	2.750	11.250
11.250	.159	-3.162	1.055	-79.404	76.242	1.104	3.000	3.000	11.250
11.250	.152	-33.866	1.102	-81.865	47.999	1.209	3.250	3.250	11.250
11.250	.145	-66.149	1.134	-84.759	18.610	1.272	3.500	3.500	11.250
11.250	.139	-99.588	1.147	-87.894	-12.094	1.283	3.750	3.750	11.250
11.250	.134	-135.356	1.139	-91.013	-44.343	1.238	4.000	4.000	11.250
11.500	.370	149.398	.370	149.398	-.000	.740	0.	.000	11.500
11.500	.339	139.097	.406	159.287	-21.190	.732	.250	.250	11.500
11.500	.310	125.340	.447	167.815	-42.475	.701	.500	.500	11.500
11.500	.286	111.088	.492	175.333	-63.945	.669	.750	.750	11.500
11.500	.264	95.304	.543	-179.005	274.308	.621	1.000	1.000	11.500
11.500	.245	77.959	.598	-174.242	252.201	.573	1.250	1.250	11.500
11.500	.228	59.033	.658	-170.620	229.652	.540	1.500	1.500	11.500
11.500	.213	38.507	.723	-168.079	206.586	.541	1.750	1.750	11.500
11.500	.200	16.372	.790	-166.556	182.928	.591	2.000	2.000	11.500
11.500	.188	-7.375	.859	-165.984	158.609	.687	2.250	2.250	11.500
11.500	.178	-32.733	.927	-166.290	133.557	.815	2.500	2.500	11.500
11.500	.169	-59.694	.992	-167.391	107.697	.954	2.750	2.750	11.500
11.500	.160	-88.247	1.050	-169.193	80.946	1.087	3.000	3.000	11.500
11.500	.153	-118.375	1.098	-171.580	53.205	1.195	3.250	3.250	11.500
11.500	.146	-150.060	1.131	-174.410	24.350	1.266	3.500	3.500	11.500
11.500	.140	176.723	1.147	-177.500	354.223	1.286	3.750	3.750	11.500

EXPLANATION OF TABLE OF OUTPUTS

X,Y	Horizontal coordinates - wave fixed, see Fig. 42
X1, Y1	Horizontal coordinates - breakwater fixed, see Fig. 42
DK1	Diffraction coefficient component - left tip
DK2	Diffraction coefficient component - right tip
PH1	Phase angle, left tip
PH2	Phase angle, right tip
RPH	Relative phase angle between the two wave trains
DKSUM	Vectorial sum of DK1 and DK2
L	Wave length

FIG. 41, CONT. - EXAMPLE OF OUTPUT DATA FROM PROGRAM FINBW.

21.500	.240	79.612	.706	-168.052	247.664	.654	2.000	2.000	21.500
21.500	.227	65.908	.756	-166.701	232.608	.644	2.250	2.250	21.500
21.500	.216	51.325	.807	-165.880	217.205	.648	2.500	2.500	21.500
21.500	.205	35.854	.858	-165.566	201.420	.671	2.750	2.750	21.500
21.500	.195	19.488	.909	-165.728	185.216	.715	3.000	3.000	21.500
21.500	.186	2.220	.959	-166.338	168.558	.777	3.250	3.250	21.500
21.500	.178	-15.953	1.006	-167.361	151.407	.854	3.500	3.500	21.500
21.500	.171	-35.035	1.050	-168.758	133.723	.940	3.750	3.750	21.500
21.500	.164	-55.028	1.087	-170.496	115.458	1.028	4.000	4.000	21.500
21.750	.399	69.324	.399	69.324	-.000	.798	0.	.000	21.750
21.750	.372	62.207	.428	75.715	-13.508	.795	.250	.250	21.750
21.750	.348	54.345	.460	81.401	-27.056	.806	.500	.500	21.750
21.750	.326	45.717	.494	86.403	-40.686	.771	.750	.750	21.750
21.750	.305	36.305	.531	90.742	-54.437	.751	1.000	1.000	21.750
21.750	.287	26.092	.571	94.441	-68.348	.727	1.250	1.250	21.750
21.750	.270	15.062	.613	97.520	-82.458	.702	1.500	1.500	21.750
21.750	.255	3.200	.658	100.004	-96.804	.677	1.750	1.750	21.750
21.750	.241	-9.509	.705	101.913	-111.422	.657	2.000	2.000	21.750
21.750	.229	-23.076	.754	103.272	-126.348	.646	2.250	2.250	21.750
21.750	.216	-37.511	.805	104.105	-141.616	.649	2.500	2.500	21.750
21.750	.206	-52.823	.856	104.437	-157.261	.671	2.750	2.750	21.750
21.750	.196	-69.021	.907	104.297	-173.317	.712	3.000	3.000	21.750
21.750	.187	-86.109	.956	103.712	-189.822	.773	3.250	3.250	21.750
21.750	.179	-104.094	1.003	102.717	-206.811	.848	3.500	3.500	21.750
21.750	.171	-122.976	1.047	101.349	-224.326	.932	3.750	3.750	21.750
21.750	.164	-142.760	1.085	99.692	-242.412	1.019	4.000	4.000	21.750
22.000	.399	-20.534	.399	-20.534	-.000	.799	0.	.000	22.000
22.000	.373	-27.594	.428	-14.192	-13.402	.796	.250	.250	22.000
22.000	.349	-35.391	.460	-8.546	-26.845	.787	.500	.500	22.000
22.000	.326	-43.944	.494	-3.576	-40.367	.772	.750	.750	22.000
22.000	.306	-53.271	.531	.738	-54.009	.753	1.000	1.000	22.000
22.000	.288	-63.389	.570	4.419	-67.809	.729	1.250	1.250	22.000
22.000	.271	-74.316	.612	7.488	-81.804	.704	1.500	1.500	22.000
22.000	.255	-86.064	.657	9.967	-96.031	.680	1.750	1.750	22.000
22.000	.241	-98.648	.704	11.878	-110.527	.659	2.000	2.000	22.000
22.000	.229	-112.081	.753	13.245	-125.325	.648	2.250	2.250	22.000
22.000	.217	-126.371	.803	14.090	-140.461	.650	2.500	2.500	22.000
22.000	.206	-141.529	.853	14.440	-155.968	.670	2.750	2.750	22.000
22.000	.197	-157.561	.904	14.320	-171.881	.710	3.000	3.000	22.000
22.000	.188	-174.475	.954	13.760	-188.235	.768	3.250	3.250	22.000
22.000	.180	167.726	1.001	12.793	154.934	.842	3.500	3.500	22.000
22.000	.172	149.038	1.044	11.454	137.585	.925	3.750	3.750	22.000
22.000	.165	129.460	1.083	9.786	119.674	1.011	4.000	4.000	22.000
22.250	.401	-110.396	.400	-110.395	-.000	.800	0.	.000	22.250
22.250	.373	-117.399	.429	-104.100	-13.299	.797	.250	.250	22.250
22.250	.349	-125.132	.460	-98.494	-26.638	.788	.500	.500	22.250
22.250	.327	-133.611	.494	-93.556	-40.055	.774	.750	.750	22.250
22.250	.307	-142.855	.531	-89.266	-53.590	.754	1.000	1.000	22.250
22.250	.288	-152.882	.570	-85.602	-67.280	.731	1.250	1.250	22.250
22.250	.272	-163.706	.612	-82.543	-81.163	.706	1.500	1.500	22.250
22.250	.256	-175.343	.656	-80.069	-95.274	.682	1.750	1.750	22.250
22.250	.242	172.194	.703	-78.156	250.350	.662	2.000	2.000	22.250
22.250	.229	158.894	.751	-76.783	235.676	.650	2.250	2.250	22.250
22.250	.218	144.745	.801	-75.925	220.670	.651	2.500	2.500	22.250
22.250	.207	129.739	.851	-75.559	205.297	.670	2.750	2.750	22.250
22.250	.197	113.867	.902	-75.658	189.525	.708	3.000	3.000	22.250

EXPLANATION OF TABLE OF OUTPUTS

X,Y	Horizontal coordinates - wave fixed, see Fig. 42
X1, Y1	Horizontal coordinates - breakwater fixed, see Fig. 42
DK1	Diffraction coefficient component - left tip
DK2	Diffraction coefficient component - right tip
PH1	Phase angle, left tip
PH2	Phase angle, right tip
RPH	Relative phase angle between the two wave trains
DKSUM	Vectorial sum of DK1 and DK2
L	Wave length

X,Y : WAVE-ALIGNED COORDINATE SYSTEM

X',Y': BREAKWATER-FIXED COORDINATE SYSTEM

λ_p : PROJECTED WIDTH OF BREAKWATER

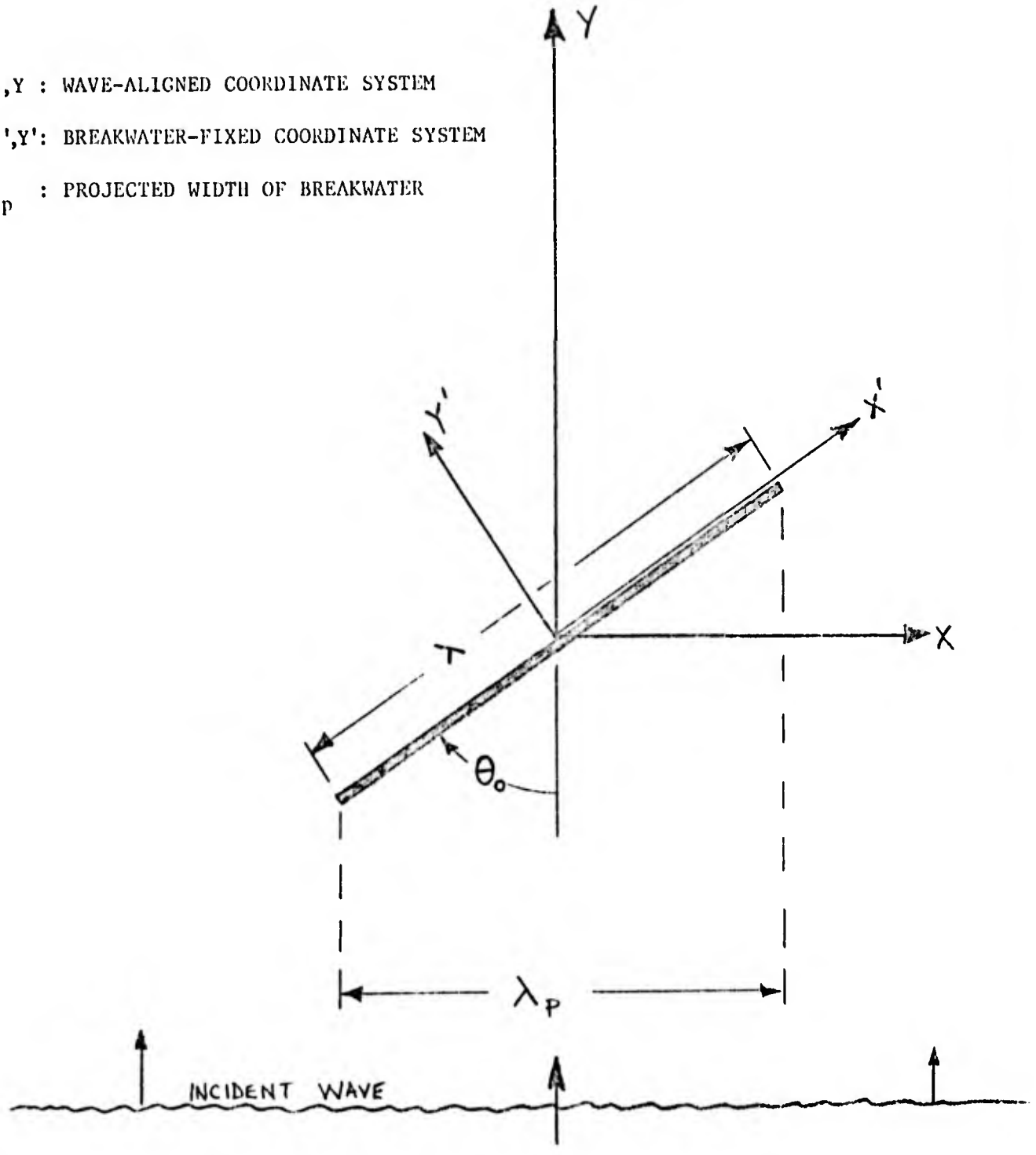

FIG.42 DEFINITION SKETCH

FIG.43PROGRAM FBWC, USING GRAPHICAL DISPLAY SYSTEM TO PLOT THE WAVE DIFFRACTION COEFFICIENT CONTOUR USING DATA GENERATED FROM PROGRAM FINBW.

```
      PROGRAM FBWC(INPUT,OUTPUT,TAPE99,TAPE97)
C
      DIMENSION X(100),Y(100),Z(33,33),ZLEVEL(20)
      DIMENSION  BUFXYZ(2000),SPECS(35)
C        SPECIAL TOOL
      SPECS(11)=1.0
C        SPECIFY INTERMEDIATE TAPE NUMBER
      SPECS(12)=99.
C        SPECFY XDIST,YDIST,XLENGTH,YLNGTH
      SPECS(1)=1.5
      SPECS(2)=2.0
      SPECS(7)=5.0
      SPECS(8)=5.0
C        SPECIFY  XDIV,YDIV
      SPECS(9)=16.0
      SPECS(10)=16.0
      CALL AXLILI(SPECS)
C        AXLILI DRAW THE X-Y AXIS WITH UNIFORM TICK MARKS
C
C        PREPARE FOR CONTOUR PLOTTING
C
C        SPECIFY XRIGHT,XLEFT,YTOP,YBOT
      SPECS(3)=4.0
      SPECS(4)=0.0
      SPECS(5)=4.0
      SPECS(6)=0.0
C        SPECFY STAPE,XCILNS,YROWS,ZLENVLS
      SPECS(30)=97.
      SPECS(31)=33.
      SPECS(32)=33.
      SPECS(33)=5.
C
      LENGTH=1000.
C
C        READ IN DATA- ZLEVEL
      NZL=SPECS(33)
      READ 50,(ZLEVEL(I),I=1,NZL)
   50 FORMAT  (5F10.1)
C
C        READ IN COORDINATE DATA
      NX=SPECS(31)
      NY=SPECS(32)
C
C
      DO 30  J=1,NY
      DO 25  I=1,NX
   25 READ 60,X(I),Y(J),Z(I,J)
   30 CONTINUE
   60 FORMAT(3F10.3)
C        CONLI CONSTRUCTS CONTOUR LINES USING LINERA INTERPOLATION
      CALL CONLI(X,Y,Z,ZLEVEL,BUFXYZ,LENGTH,SPECS)
C
C        TERMINATE  PLOTTING


      CALL GDSEND(SPECS)
C
      STOP
      END
```

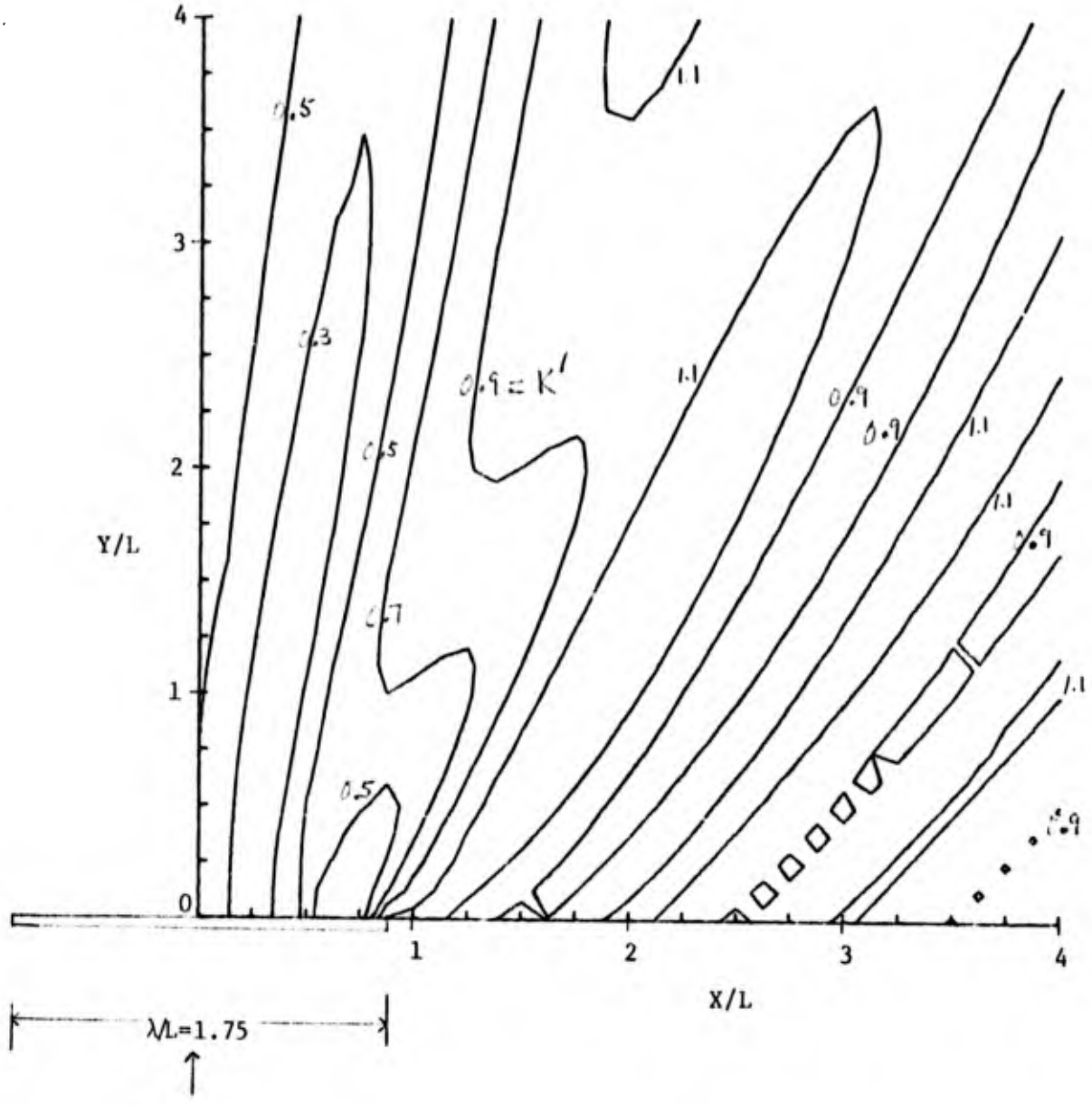

FIG. 44 WAVE DIFFRACTION CONTOURS, DETACHED BREAKWATER, APPROXIMATE ("SUPERPOSITION") THEORY

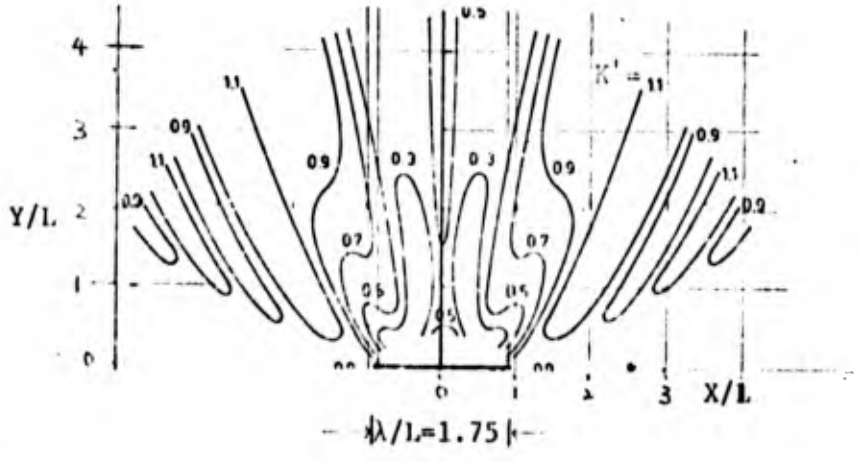

FIG. 45 WAVE DIFFRACTION CONTOURS, DETACHED BREAKWATER, ANALYTICAL SOLUTION BY MONTEFUSCO (1968)

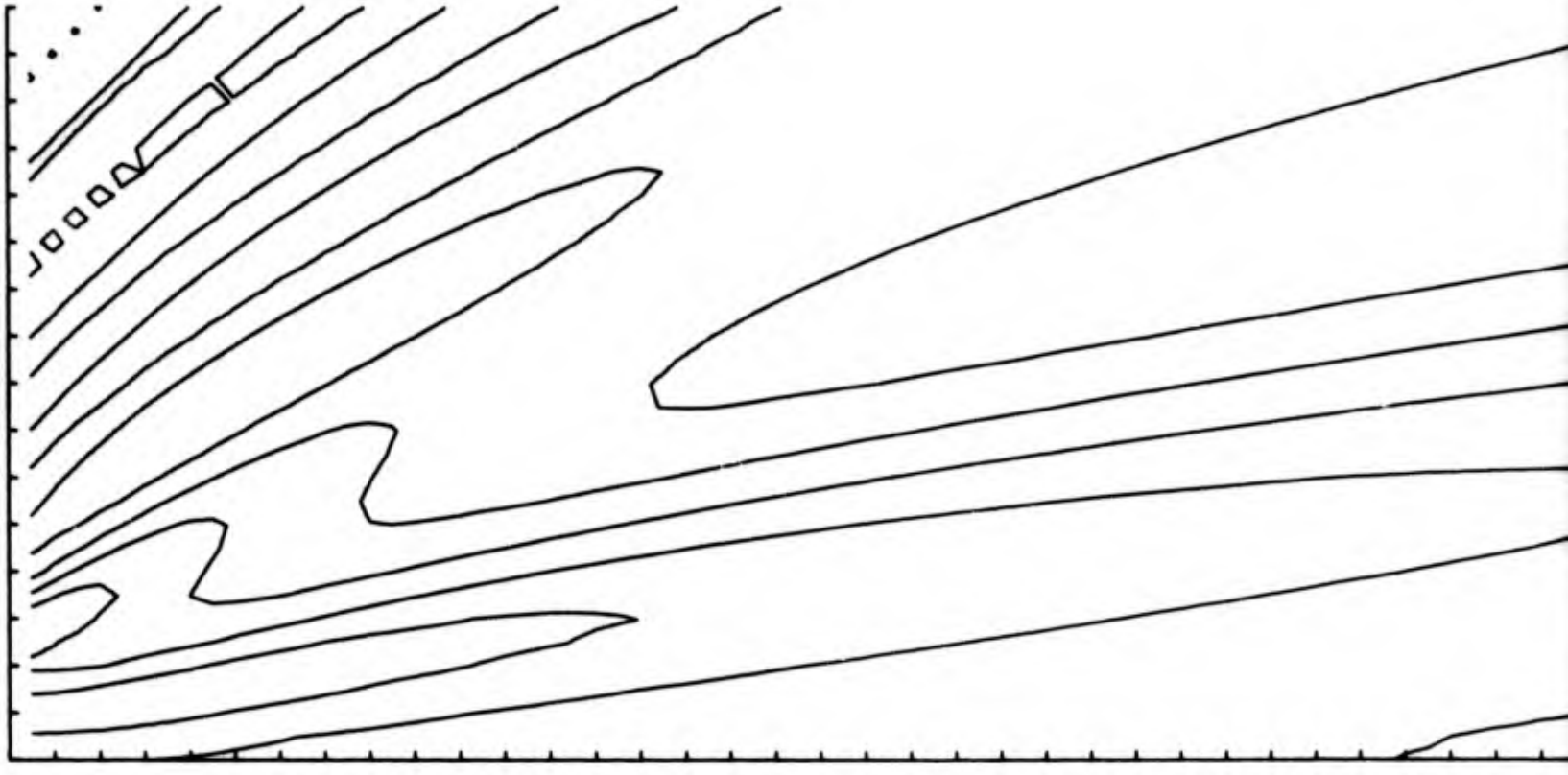

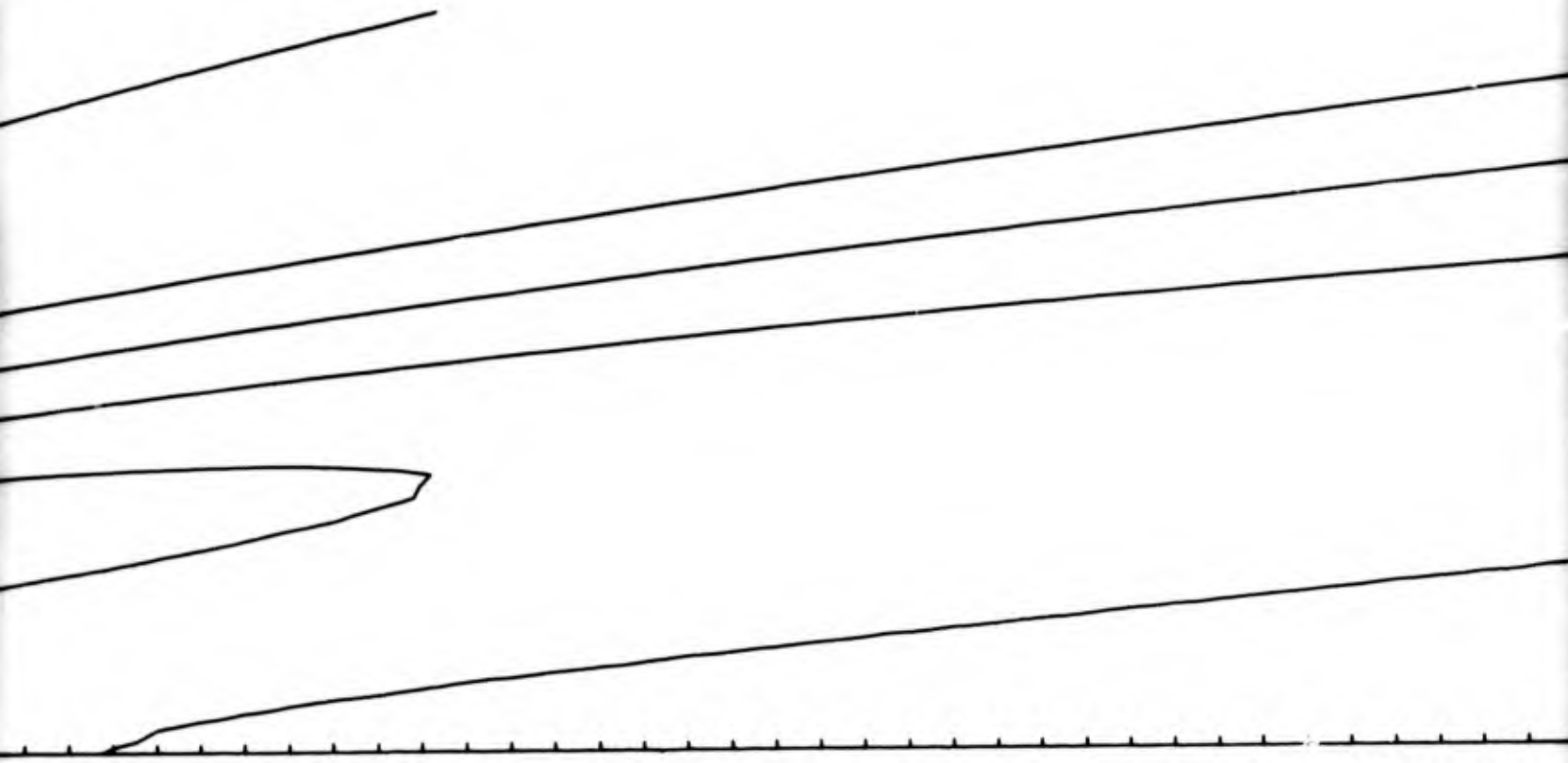

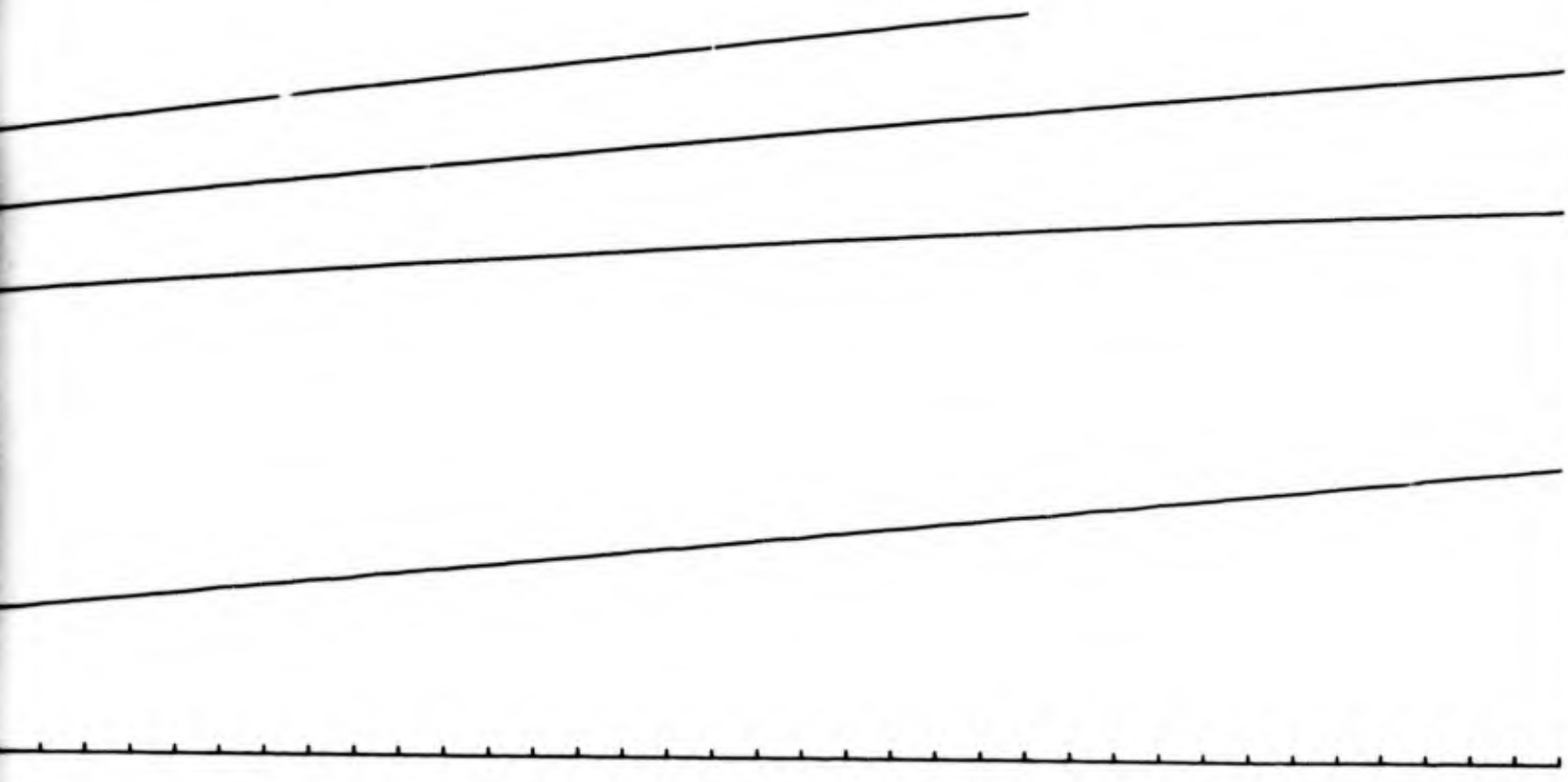

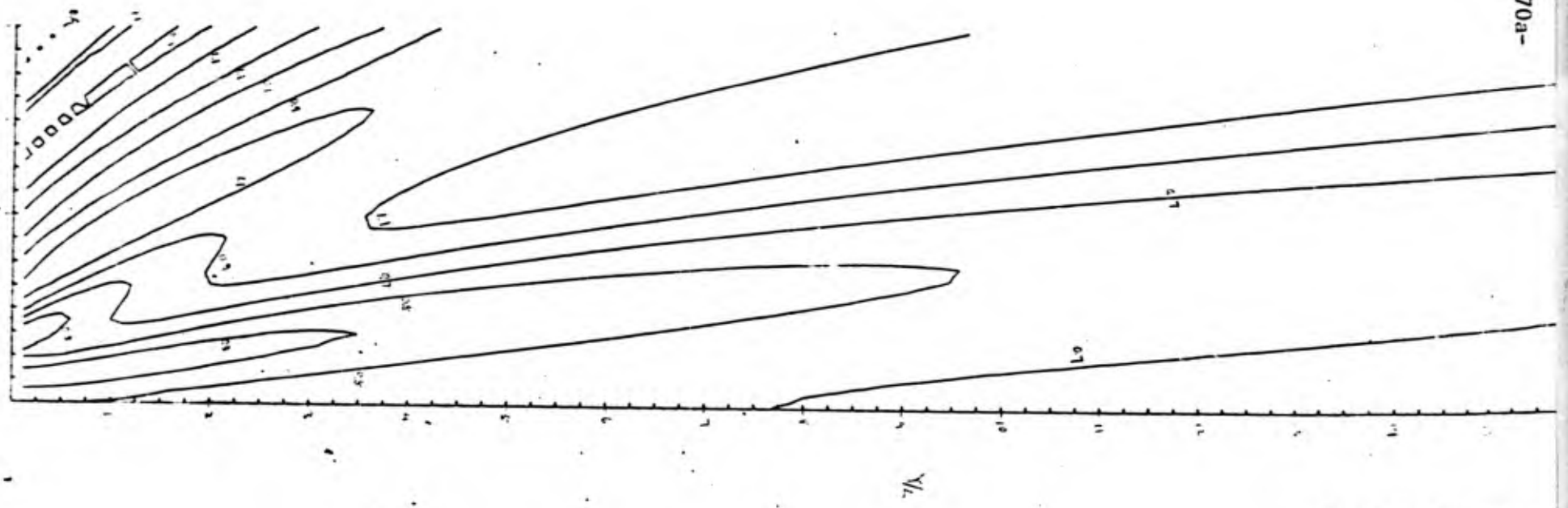

FIG. 46 Wave Diffraction Contours, Detached Breakwater, Approximate ("Superposition") Theory, for Y/L ≤ 0.250 ≤ 22.250

this case for Y/L = 21.9, for a thin rigid vertical breakwater. The experimental data shown in Fig. A51 reveal that the measured diffraction coefficient at Y/L = 21.9 is nearly the same for both types of offshore structures.

The conclusion is that reasonably reliable diffraction coefficients can be calculated for the lee of a semi-circular offshore island for small values of Y/L, but that a hydraulic model study would be needed to predict values of K' for large values of Y/L in its lee.

VI. SUMMARY AND CONCLUSIONS

The report presents the first phase of a laboratory study, combined with existing diffraction theory which has been extended together with a computer program which has been modified, of the diffraction of "uniform" periodic waves by rigid impervious vertical wall offshore structures. The difficulties encountered in trying to obtain uniform waves in a wide hydraulic model basin are described, together with modifications to the equipment to improve the wave characteristics. An approximate method is described which was developed to permit the use of the theory of wave diffraction by a semi-infinite breakwater oriented at any angle with the incident waves. This theory is compared (favorably) with measured data obtained in the hydraulic model study. Numerous laboratory results are presented for a variety of cases.

In general, it was found for the semi-infinite breakwater that for small values of y/L (e.g., near the breakwater in its lee) the diffraction theory predicted the measured values reasonably well. For large values of y/L (say, for $y/L > 10$) the theoretical diffraction coefficients were larger than the measured values in the region of $-1 < x/L < -4$, and smaller than the measured values in the lee (shadow region) of the breakwater. The difference between theory and measurements increased with increasing distrance from the breakwater (increasing y/L).

Specific conclusions reached as a result of the work described herein are:

1. Physical arrangements and wave measuring equipment were designed and constructed which permitted the reasonably rapid measurement of wave characteristics at a large number of locations in the large tank (Model

Basin). This was necessary as a great number of measurements have to be obtained for an adequate study of waves that are scattered by a structure such as an offshore island or detached breakwater.

2. There is a growing body of evidence that it is rather difficult to obtain a uniform stable wave field in a wide long model basin. As a result of equipment modifications and tests with a large number of combinations that were reasonably uniform in three dimensions. These have been used for the tests reported herein.

3. It was found to be necessary to place wave energy absorbing material in front of the model structures to prevent reflection of waves from it, owing to the fact that these waves would re-reflect from walls of the basin and the wave generator. Tests were made with a small number of waves both with and without the wave energy absorbing material. It was found that the diffracted waves in the lee of the structure were essentially the same for both cases. Use of the wave energy absorbing material permitted the use of a continuous wave generating program which, in turn, permitted much more effective and rapid testing to be done than was the case when the generator was run for a short time to generate a few waves which were measured prior to stopping the wave generator to allow the basin to become calm before it was started again with a few more measurements being made.

4. Experiments conducted in a small "ripple tank" were found to be quite useful in planning the larger scale studies to be made in the Model Basin.

5. Almost no hydraulic model studies of the diffraction of waves by structures have been reported in the technical literature. Owing to this, some experiments were made for the case of a semi-infinite breakwater

(rigid impervious vertical wall). It was found that for small values of y/L (near the breakwater, in its lee) the diffraction theory predicted the measured values reasonably well. For larger values of y/L (say, y/L>10) the theoretical diffraction coefficients, K', were larger than the measured values in the region of $-1 < x/L < -4$, and smaller than the measured values in the lee (shadow region) of the breakwater. The difference between theory and measurements increased with increasing distance from the breakwater (increasing y/L). The reason for this has not been determined.

6. An approximate ("superposition") diffraction theory for detached breakwater was developed, and its reliability tested in the Model Basin. The comparison was quite good for small values of y/L in the lee of the breakwater. The comparisons became progressively poorer with increasing y/L, similar to the discrepancy between theory and measurements for a semi-infinite breakwater.

7. The findings in #6 above, together with the findings in #5 above, led to the development of a "semi-theoretical" approach. The experimental values of K' obtained for a semi-infinite breakwater were combined with the theoretical values of the phase of the diffracted waves about each tip of the breakwater to calculate values of K' in the lee of a detached breakwater. The agreement between the "semi-theory" and the measurements were good for rather large values of y/L.

8. A computer program was developed to extend the program of Fan, Cumming and Wiegel for the approximate ("superposition") theory. This permits the rapid calculation of values of K' in the lee of a detached breakwater. Another computer program was developed, and used, to permit the computer plotting of the results.

9. It was found that the diffraction coefficients in the lee of sharp corner structures (rectangular island, semi-circular island with the straight section on the lee side, and thin detached breakwater) are very similar. The seaward geometry and reflective characteristics of these structures did not effect the diffraction profiles significantly.

10. For waves obliquely incident upon a thin detached breakwater it was found that the parameter $\lambda\rho$, of the width of the structure as projected normally into the wave crest-line, is the governing parameter. This experimental finding is verified by the theoretical superposition method and should allow the simplification of many diffraction problems.

VII. ACKNOWLEDGMENTS

The work reported herein was done under Contract DACW72-72-C-0030 between the Coastal Engineering Research Center (U.S. Army, Corps of Engineers) and the University of California.

VIII. REFERENCES

1. Anonymous, "Aquaports: Is the Convenience Worth the Complexity?" Astronautics and Aeronautics, Vol. 7, No. 4, April 1969, pp. 24-25.

2. Anonymous, "Bahia, Brazil" (note on a proposed artificial island to be used as a bulk terminal for salt), The Dock & Harbour Authority, Vol. 51, No. 600, October 1960, p. 268.

3. Anonymous, "Floating Nuclear Power Plants Near Reality," Ocean Industry, Vol. 6, No. 9, September 1971, p. 60.

4. Anonymous, "Offshore Nuclear Plants are Being Considered by a New Jersey Utility," Civil Engineering, Vol. 41, No. 9, September 1971, p. 27.

5. Anonymous, "Building a Multipurpose Island in the Sea," Ocean Industry, Vol. 8, No. 4, April 1973, pp. 187-194.

6. Ashworth, Joseph A., "Site Related Design for the Atlantic Generating Station," Nuclear Engineering International, Vol. 18, No. 205, June 1973, pp. 483-486.

7. Baker, Bevan B., and E. T. Copson, "Sommerfeld's Theory of Diffraction," Ch. 4, The Mathematical Theory of Huygens' Principle, Claredon Press, Oxford, England, 2nd ed., 1950, pp. 124-189.

8. Barnard, B.J.S. and W. G. Pritchard, "Cross-waves, Part 2. Experiments," Jour. Fluid Mechanics, Vol. 55, Part 2, 1972, pp. 245-255.

9. Benjamin, T. Brooke and J. E. Feir, "The Disintegration of Wave Trains on Deep Water," Jour. of Fluid Mechanics, Vol. 27, Part 3, 24 February 1967, pp. 417-430.

10. Berkhoff, J.C.W., "Computation of Combined Refraction-Diffraction," Ch. 24, Proceedings of the Thirteenth Coastal Engineering Conference, July 10-14, 1972, Vancouver, B.C., Canada, ASCE, 1972, pp. 471-490.

11. Biesel, Francis, "Refraction de la Houle Avec Diffraction Moderee," Proceedings of the Thirteenth Coastal Engineering Conference, July 10-14, 1972, Vancouver, B.C., Canada, Vol. 1, Ch. 25, ASCE 1972, pp. 491-501.

12. Blume, John A., and James M. Keith, "Rincon Offshore Island and Open Causeway," Jour. of the Waterways and Harbors Division, Proc. ASCE, Vol. 85, No. WW3, September 1959, pp. 61-92.

13. Blue, Frank Lee, Jr., and J. W. Johnson, "Diffraction of Water Waves Passing Through a Breakwater Gap," Trans. Amer. Geophys. Union, Vol. 30, No. 5, October 1949, pp. 705-718.

14. Bowen, A. J., "Rip Currents, 1, Theoretical Investigations," Jour. Geophys. Res., Vol. 74, No. 23, 1969, pp. 5467-5479.

15. Bowen, A. J. and D. L. Inman, "Rip Currents, 2, Laboratory and Field Observations," Jour. Geophys. Res., Vol. 74, No. 23, 1969, pp. 5479-5491.

16. Bragg, Dan M., and James R. Bradley, "Work Plan for a Study of the Feasibility of an Offshore Terminal in the Texas Gulf Coast Region," Texas A&M University, TAMU-56-71-212, June 1971, 29 pp.

17. Carr, J. H., and M. E. Stelzriede, "Diffraction of Water Waves by Breakwaters," Ch. 14 in Gravity Waves, U.S. National Bureau of Standards Circular No. 521, November 1952, pp. 109-125.

18. Chakrabarti, Subrata K., "Nonlinear Wave Forces on Vertical Cylinder," Journal of the Hydraulics Division, Proc. ASCE, Vol. 98, No. HY11, November 1972, pp. 1895-1909.

19. Einstein, H. A., and R. L. Wiegel, "A Literature Review on Erosion and Deposition of Sediment Near Structures in the Ocean," University of California, Berkeley, California, Hydraulic Engineering Laboratory, Tech. Rept. No. HEL 21-6, February 1970, 198 pp.

20. Fairchild, J. C., "Laboratory Test of Longshore Transport," Proc. Tenth Conf. Coastal Engineering, ASCE, Vol. 2, 1970, pp. 867-891.

21. Fan, Shou-Shan, J. D. Cumming and R. L. Wiegel, "Computer Solution of Wave Diffraction by Semi-infinite Breakwater," University of California, Berkeley, California, College of Engineering, Tech. Rept. No. HEL 1-8, October 1967, 376 pp.

22. Garcia, William J., Jr., "Literature Survey and Bibliography of Engineering Properties of Marine Sediments," University of California, Berkeley, California, College of Engineering, Tech. Rept. No. HEL 2-27, February 1971, 31 pp.

23. Garrett, C.J.R., "On Cross-waves," Jour. of Fluid Mechanics, Vol. 41, Part 4, 1970, pp. 837-849.

24. Gibson, Ray, "Hugh Submerged Tank Will Store Crude Off Dubai," World Petroleum, Vol. 39, No. 8, 1 August 1968, pp. 27-29.

25. Gilbert, G., D. M. Thompson and A. J. Brewer, "Design Curves for Regular and Random Wave Generators," Jour. Hydraulic Research, IAHR, Vol. 9, No. 2, 1971, pp. 163-196.

26. Goda, Yoshimi and Tomotsuka Yushimura, "Discussion of Wave Diffraction by Detached Breakwater," Jour. Waterways, Harbors and Coastal Engineering Division, Proc. ASCE, Vol. 99, No. WW2, May 1973, pp. 285-288.

27. Harza, Richard D., "Trends in Offshore Airports," Transportation Engineering Jour., Proc. ASCE, Vol. 98, No. TE4, November 1972, pp. 985-1003.

28. Hoffman, John F., "Man-Made Islands Can Solve Many of Our Problems," Ocean Industry, Vol. 5, No. 2, February 1970, pp. 48-51.

29. Hönl, H., A. W. Maue, and K. Westpfahl, "Theorie der Beugung," Handbuch der Physik, Berlin: Springer-Verlag, Vol. XXV/1, 1961, pp. 218-544.

30. Ito, Yoshiyuki, and Katsutoshi Tanimoto, "A Method of Numerical Analysis of Wave Propagation--Application to Wave Diffraction and Refraction," Proceedings of the Thirteenth Conference on Coastal Engineering, July 10-14, 1972, Vancouver, B.C., Canada, Vol. 1, Ch. 26, ASCE, 1972, pp. 503-522.

31. Johnson, J. W., "Engineering Aspects of Diffraction and Refraction," Trans. ASCE, Paper No. 2556, Vol. 118, 1953.

32. Johnson, J. W., "The Littoral Drift Problem at Shoreline Harbors," Jour. of the Waterways and Harbors Division, Proc. ASCE, Vol. 83, No. WW1, Paper No. 1211, April 1957.

33. Lacombe, H., "The Diffraction of a Swell. A Practical Approximate Solution and Its Justification," Ch. 16 in Gravity Waves, U.S. National Bureau of Standards Circular No. 521, November 1952, pp. 129-140.

34. Larras, Jean, "Diffraction de la Houle par une Jeteé," Bulletin of the Permanent International Association of Navigation Congresses, No. 13, 1972, pp. 41-52.

35. Lin, J. D. and L. N. Howard, Non-linear Standing Waves in a Rectangular Tank Due to Forced Oscillation, Massachusetts Institute of Technology, Hydrodynamics Laboratory, Tech. Rept. No. 44, October 1960, 108 pp.

36. Longuet-Higgins, M. S., "Resonant Interactions Between Two Trains of Gravity Waves," Jour. Fluid Mechanics, Vol. 12, Part 3, 1962, pp. 321-332.

37. MacCamy, R. C. and R. A. Fuchs, Wave Forces on a Pile: A Diffraction Theory, U.S. Army Corps of Engineers, Beach Erosion Board, Tech. Memo No. 69, December 1954.

38. Macomber, Frank, "FAA Seeks Offshore Airport Aid," San Diego Union, 8 December 1968.

39. Madsen, O. S., "Waves Generated by a Piston-type Wave Maker," Proc. Tenth Conf. Coastal Engineering, ASCE, Vol. 1, 1970, pp. 589-609.

40. Mahoney, J. J., "Cross Waves, Part 1, Theory," Jour. Fluid Mechanics, Vol. 55, Part 2, 1972, pp. 229-245.

41. Migliardi, Tasco, Aldo and Vincenzo Pezza, "Rapport, Sujet 1," XXII International Navigation Congress, Ottawa 1973, Section II, Subject 1, pp. 117-131.

42. Miles, John and Freeman Gilbert, "Scattering of Gravity Waves by a Circular Dock," Jour. Fluid Mechanics, Vol. 34, Part 4, 23 December 1968, pp. 783-793.

43. Montefusco, Luigi, "The Diffraction of a Plane Wave by an Isolated Breakwater," Meccanica, September 1968, pp. 156-166.

44. Morse, P. M., and P. J. Rubinstein, "The Diffraction of Waves by Ribbons and Slits," Physical Review, Vol. 54, December 1938, pp. 895-898.

45. Nawy, Edward G., and Fred C. Koletty, "Offshore Jetport for New York-New Jersey Megalopolis," Transportation Engineering Jour., Proc. ASCE, Vol. 98, No. TE2, pp. 243-262.

46. Penney, W. G., and A. T. Price, "The Diffraction Theory of Sea Waves by Breakwaters, and the Shelter Afforded by Breakwaters," Phil. Trans., Roy. Soc. (London), Ser. A., Vol. 244, March 1952, pp. 236-253.

47. Posey, Chesley J., "Protection of Offshore Structures Against Underscour," Jour. of the Hydraulics Division, Proc. ASCE, Vol. 97, No. HY7, July 1971, pp. 1011-1016.

48. Putnam, J. A., and R. S. Arthur, "Diffraction of Water Waves by Breakwaters," Trans. Amer. Geophys. Union, Vol. 29, No. 4, August 1948, pp. 481-490.

49. Shepard, Tim, "Air Terminal Off the Coast Suggested Here," San Diego Union, 10 December 1968.

50. Shirdan, Leon, "Island Harbours and Their Influence on Adjacent Shores," Proceedings of the Seventh Conference on Coastal Engineering, Council on Wave Research, The Engineering Foundation, 1961, pp. 808-816.

51. Silvester, R., and T. Lim, "Application of Wave Diffraction Data," Proceedings of the Eleventh Conference on Coastal Engineering, London, September 1968, pp. 248-270.

52. Sommerfeld, A., "Mathematische Theorie der Diffraction," Math. Ann. Vol. 47, 1896, pp. 317-374.

53. Stiassnie, Michael, and Geodeon Dagan, "Wave Diffraction by Detached Breakwater," Jour. of the Waterways, Harbors and Coastal Engineering Division, Proc. ASCE, Vol. 98, No. WW2, May 1972, pp. 209-224.

54. U.S. Army Coastal Engineering Research Center, "Shore Protection Planning and Design," U.S. Army Corps of Engineers, Technical Report No. 4, 3rd edition, 1966.

55. Wada, Akira, "On a Method of Solution of Diffraction Problems," Coastal Engineering of Japan, Vol. 8, 1965.

56. Watson, Kenneth M., Bruce J. West and J. Alex Thomson, Energy Spectra of the Ocean Surface: An Eigenmode Approach, Rome Air Development Center, Griffiss Air Force Base, New York, Technical Report, RADC-TR-73-74, February 1973, 65 pp.

57. Weidlinger, Paul, "Floating Airport," Ocean Industry, Vol. 5, No. 5, May 1970, pp. 47-49.

58. West, Richard, "Long Beach Considering Airport in Sea," Los Angeles Times, 26 January 1969, p. B1.

59. Wiegel, R. L., "Diffraction of Waves by Semi-infinite Breakwater," Jour. of the Hydraulics Division, Proc. ASCE, Vol. 88, No. HY1, January 1962, pp. 27-44.

60. Wiegel, Robert L., Oceanographical Engineering, Prentice-Hall, Inc. 1964, 532 pp.

61. Wiegel, Robert L., "Quarterly Progress Reports: Effect of Large Nearshore Structures on Wave Motion in Vicinity of Structure and Adjacent Coast," University of California, Berkeley, California, 1972-73.

62. Xercavins, M., "Offshore Oil Storage in the North Sea--Ekofisk Reservoir," Proc. of the FIP Symposium: Concrete Sea Structures Tbilisi, September 1972, Federation Internationale de la Precontrainte, pp. 105-108.

APPENDIX A

MODEL BASIN DATA

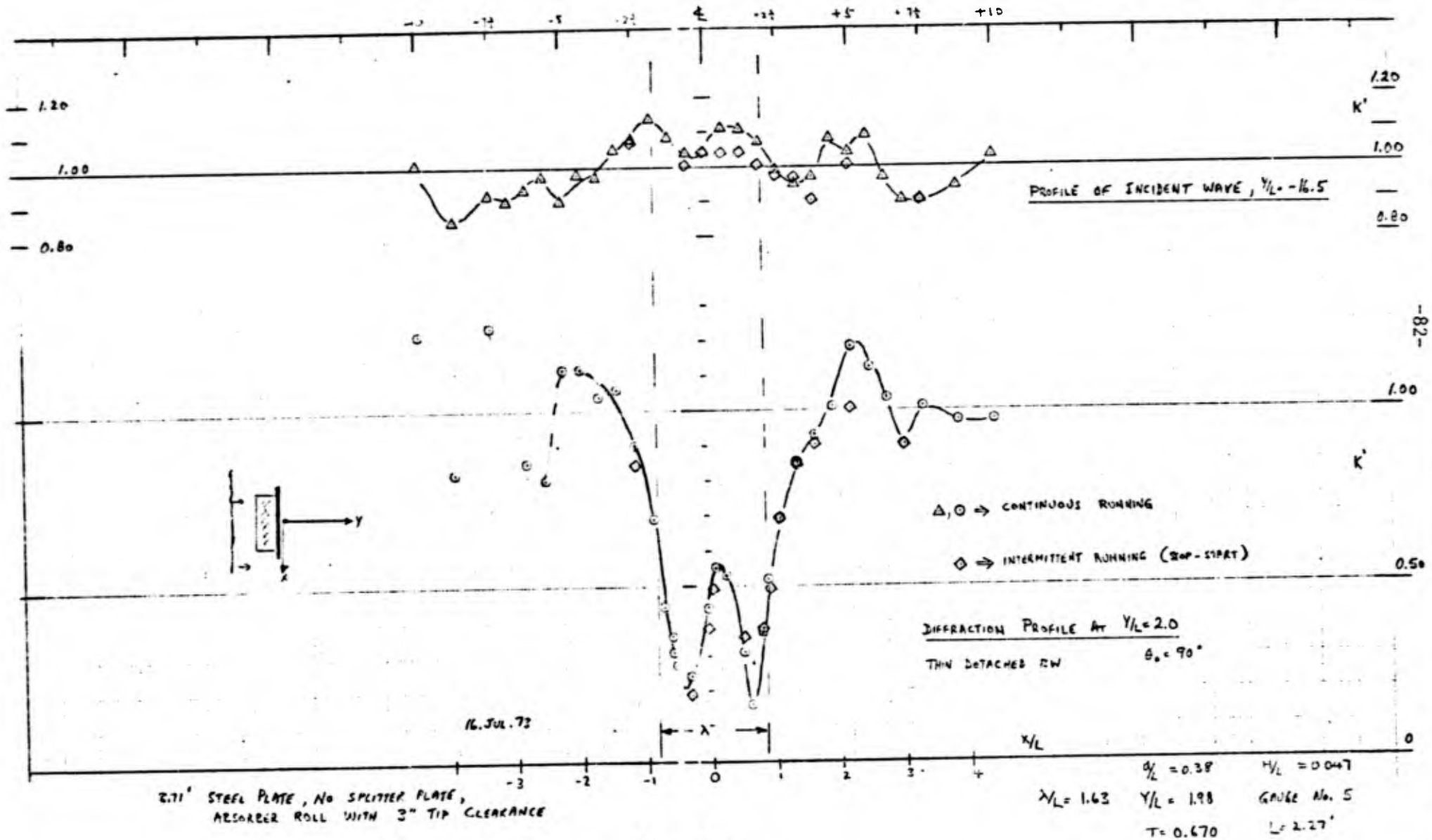

FIG A.1

16 JULY 1973

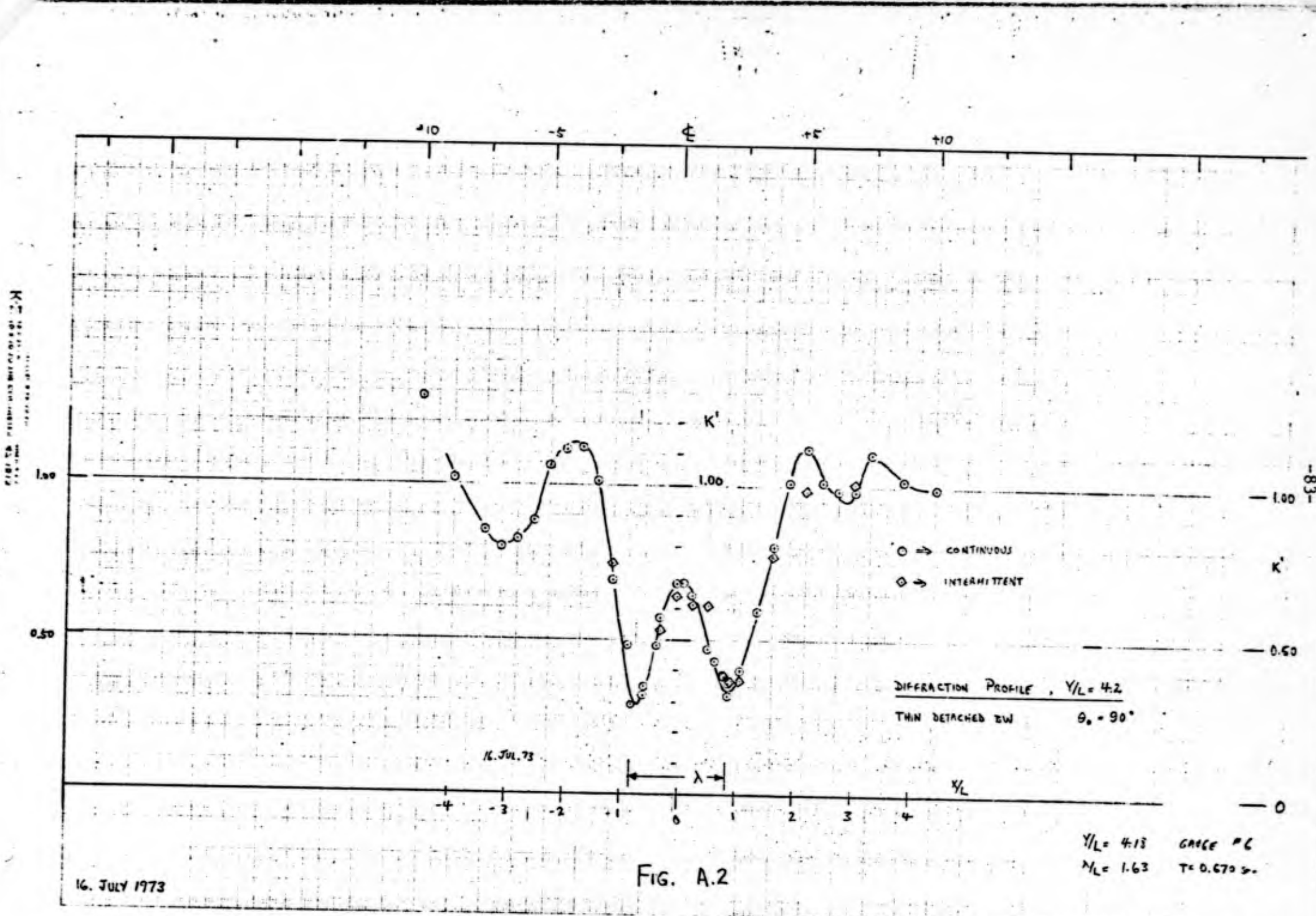
-10
-5
ξ
+5
+10
K'
1.00
0.50
1.00
0.50
0
K'
○ ⇒ CONTINUOUS
◇ ⇒ INTERMITTENT
DIFFRACTION PROFILE , Y/L = 4.2
THIN DETACHED EW θ₀ = 90°
16. JUL. 73
λ
X/L
-4
-3
-2
+1
0
1
2
3
4
Y/L = 4.13 GAGE #C
X/L = 1.63 T = 0.670 s.
16. JULY 1973

FIG. A.2

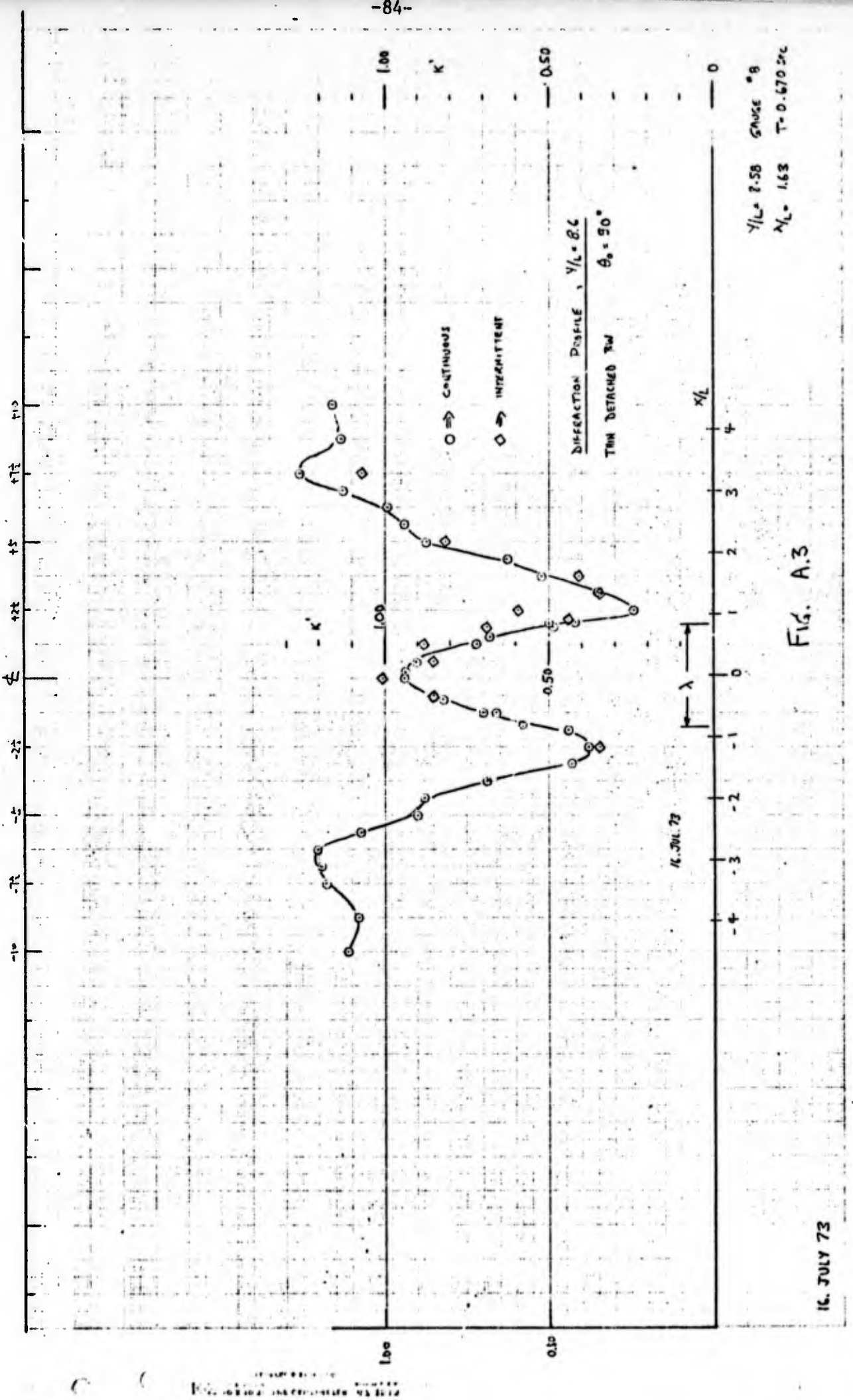
K'
1.00
0.50
0
O ⇒ CONTINUOUS
◇ ⇒ INTERMITTENT
DIFFRACTION PROFILE, Y/L = 8.6
THIN DETACHED RIM
θ₀ = 90°
Y/L = 8.58 GAUGE #8
X/L = 1.63 T = 0.670 sec
X/L
λ
16 JUL 73
16. JULY 73

FIG. A.3

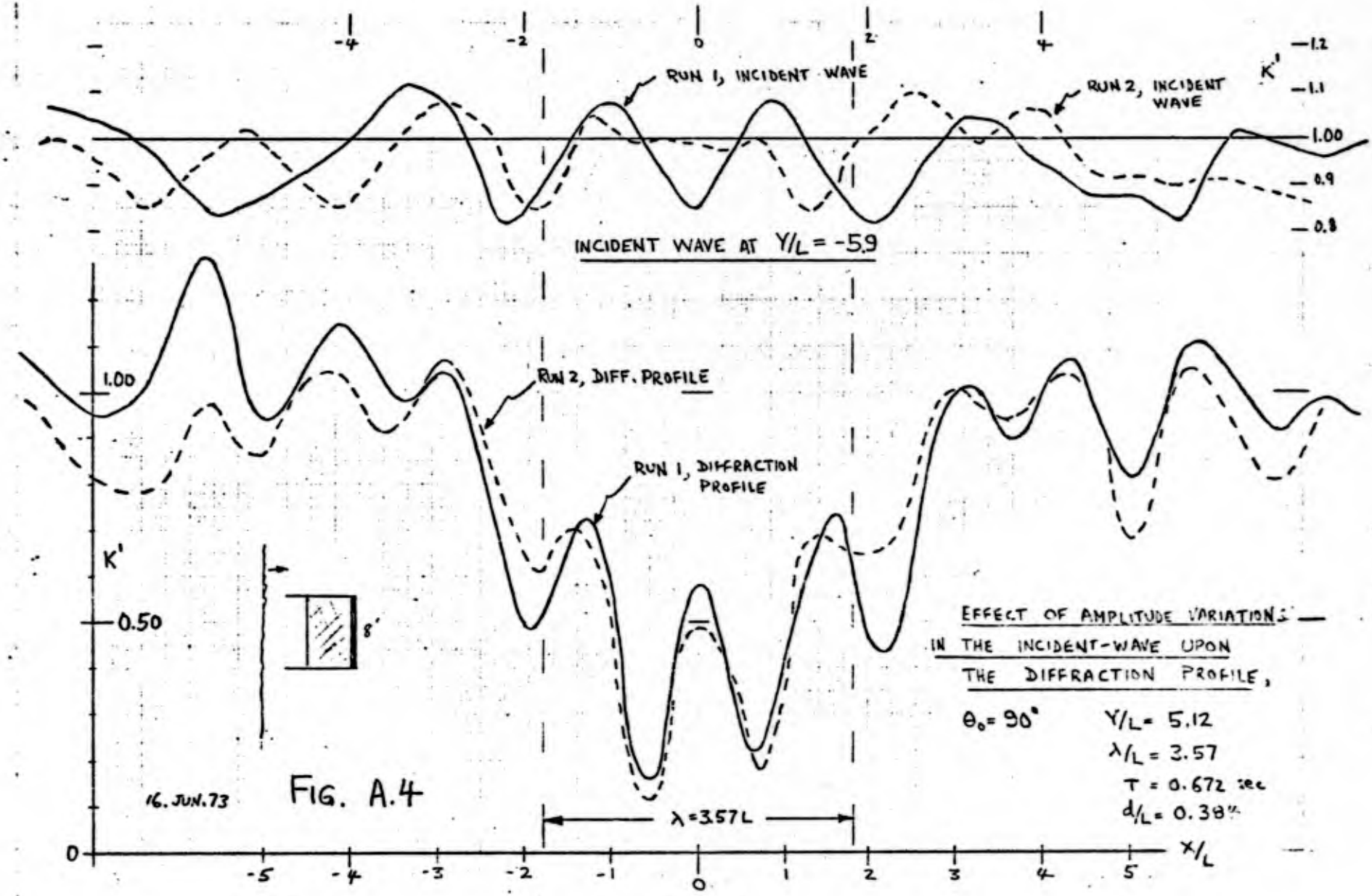
RUN 1, INCIDENT WAVE
RUN 2, INCIDENT WAVE
K'
INCIDENT WAVE AT Y/L = -5.9
RUN 2, DIFF. PROFILE
RUN 1, DIFFRACTION PROFILE
8"
λ=3.57L
X/L
EFFECT OF AMPLITUDE VARIATIONS IN THE INCIDENT-WAVE UPON THE DIFFRACTION PROFILE,
θ₀= 90°
Y/L= 5.12
λ/L= 3.57
T = 0.672 sec
d/L= 0.38"
16. JUN. 73

FIG. A.4

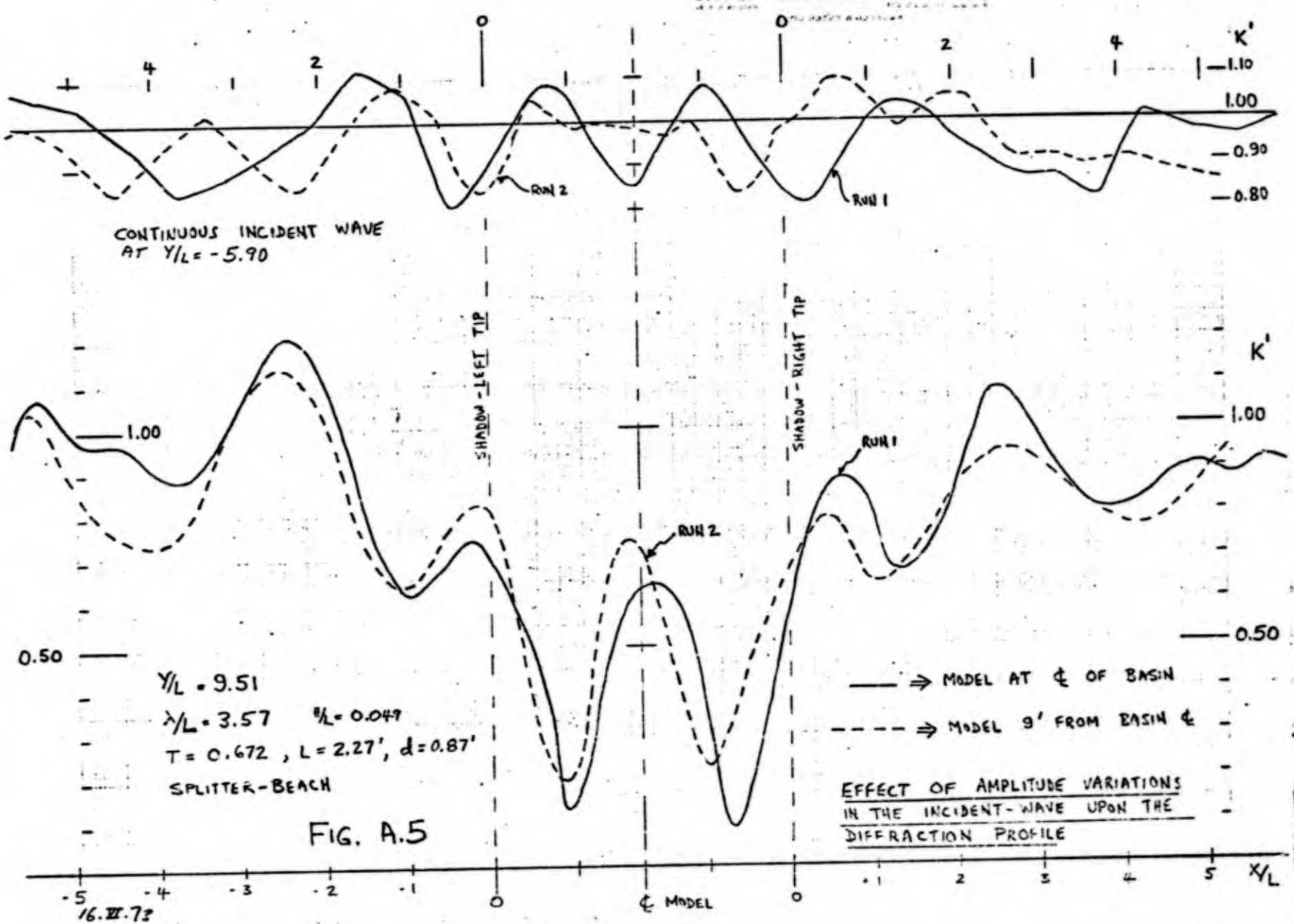
K'
1.10
1.00
0.90
0.80
RUN 2
RUN 1
CONTINUOUS INCIDENT WAVE
AT Y/L = -5.90
SHADOW - LEFT TIP
SHADOW - RIGHT TIP
K'
1.00
0.50
RUN 1
RUN 2
Y/L = 9.51
λ/L = 3.57
B/L = 0.049
T = 0.672 , L = 2.27', d = 0.87'
SPLITTER-BEACH
⇒ MODEL AT ℄ OF BASIN
⇒ MODEL 9' FROM BASIN ℄
EFFECT OF AMPLITUDE VARIATIONS
IN THE INCIDENT-WAVE UPON THE
DIFFRACTION PROFILE
-5
-4
-3
-2
-1
0
℄ MODEL
0
1
2
3
4
5
X/L
16.XII.73

FIG. A.5

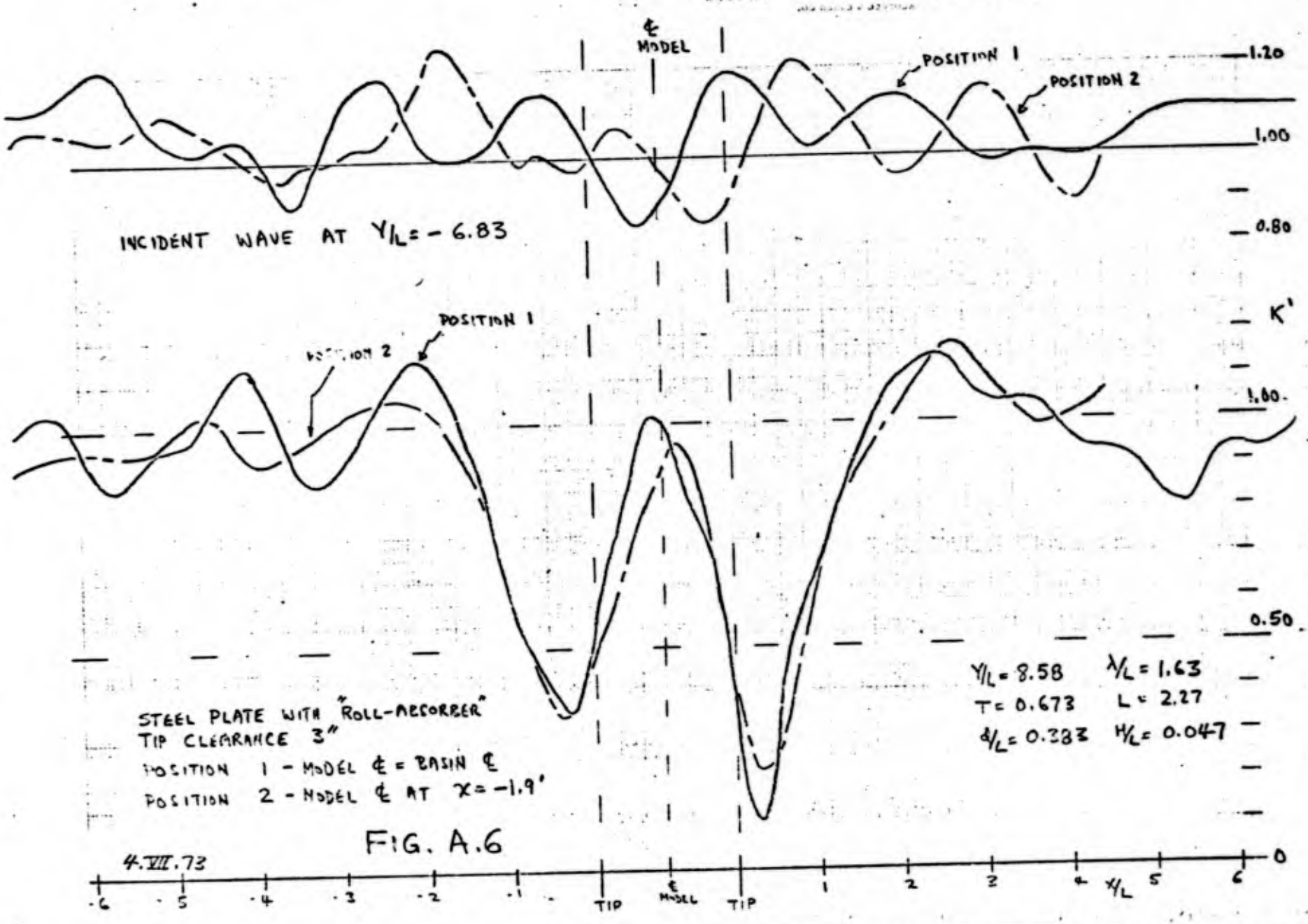
℄ MODEL
POSITION 1
POSITION 2
1.20
1.00
0.80
K'
1.00
0.50
INCIDENT WAVE AT Y/L = - 6.83
POSITION 1
POSITION 2
STEEL PLATE WITH "ROLL-ABSORBER"
TIP CLEARANCE 3"
POSITION 1 - MODEL ℄ = BASIN ℄
POSITION 2 - MODEL ℄ AT X = -1.9'
Y/L = 8.58 λ/L = 1.63
T = 0.673 L = 2.27
d/L = 0.383 H/L = 0.047
4.VII.73
-6 -5 -4 -3 -2 -1 TIP ℄ MODEL TIP 1 2 3 4 Y/L 5 6
0

FIG. A.6

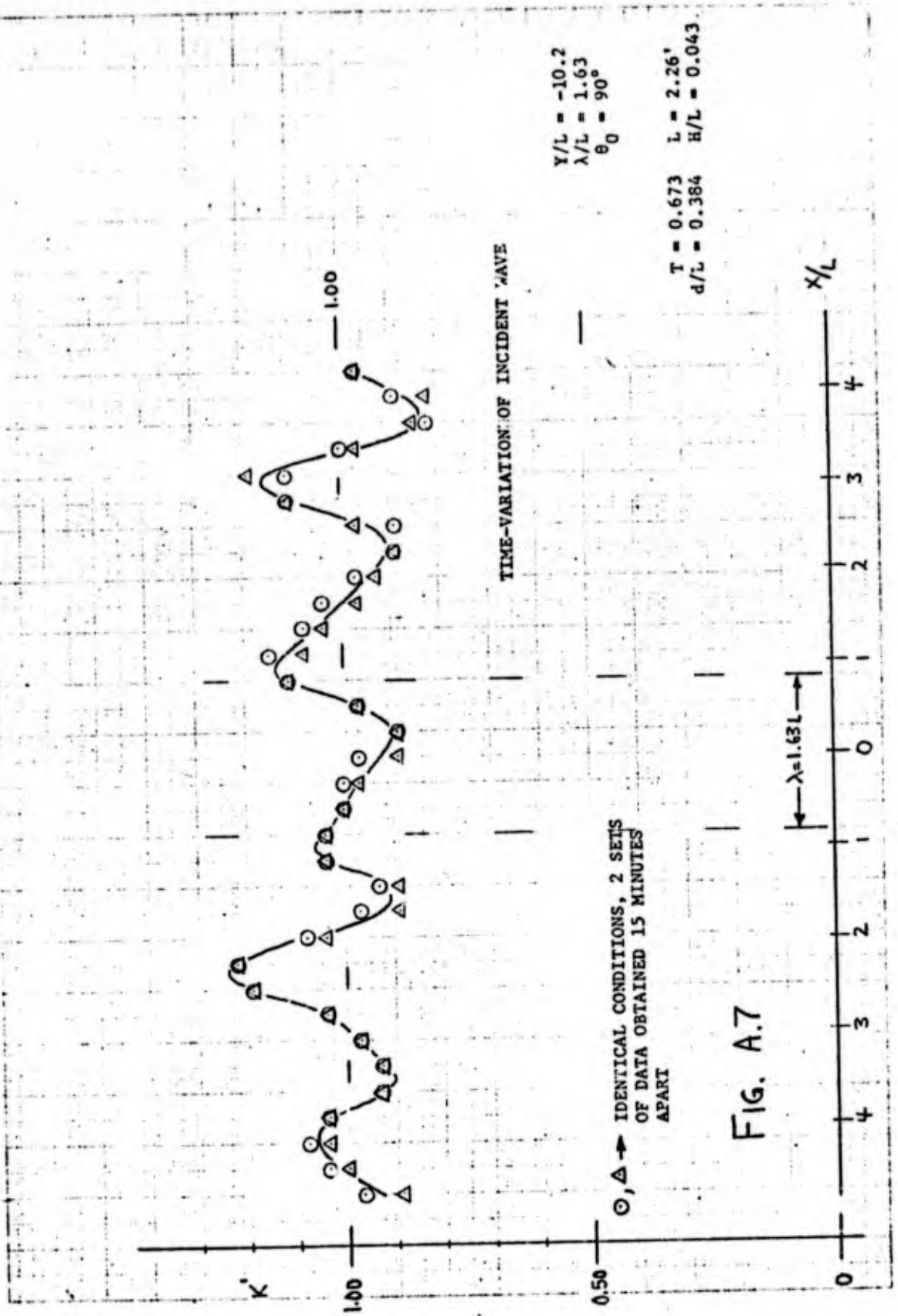
TIME-VARIATION OF INCIDENT WAVE
Y/L = -10.2
λ/L = 1.63
θ0 = 90°
T = 0.673 L = 2.26'
d/L = 0.384 H/L = 0.043
1.00
0.50
K'
X/L
λ=1.63L
0, Δ → IDENTICAL CONDITIONS, 2 SETS OF DATA OBTAINED 15 MINUTES APART

FIG. A.7

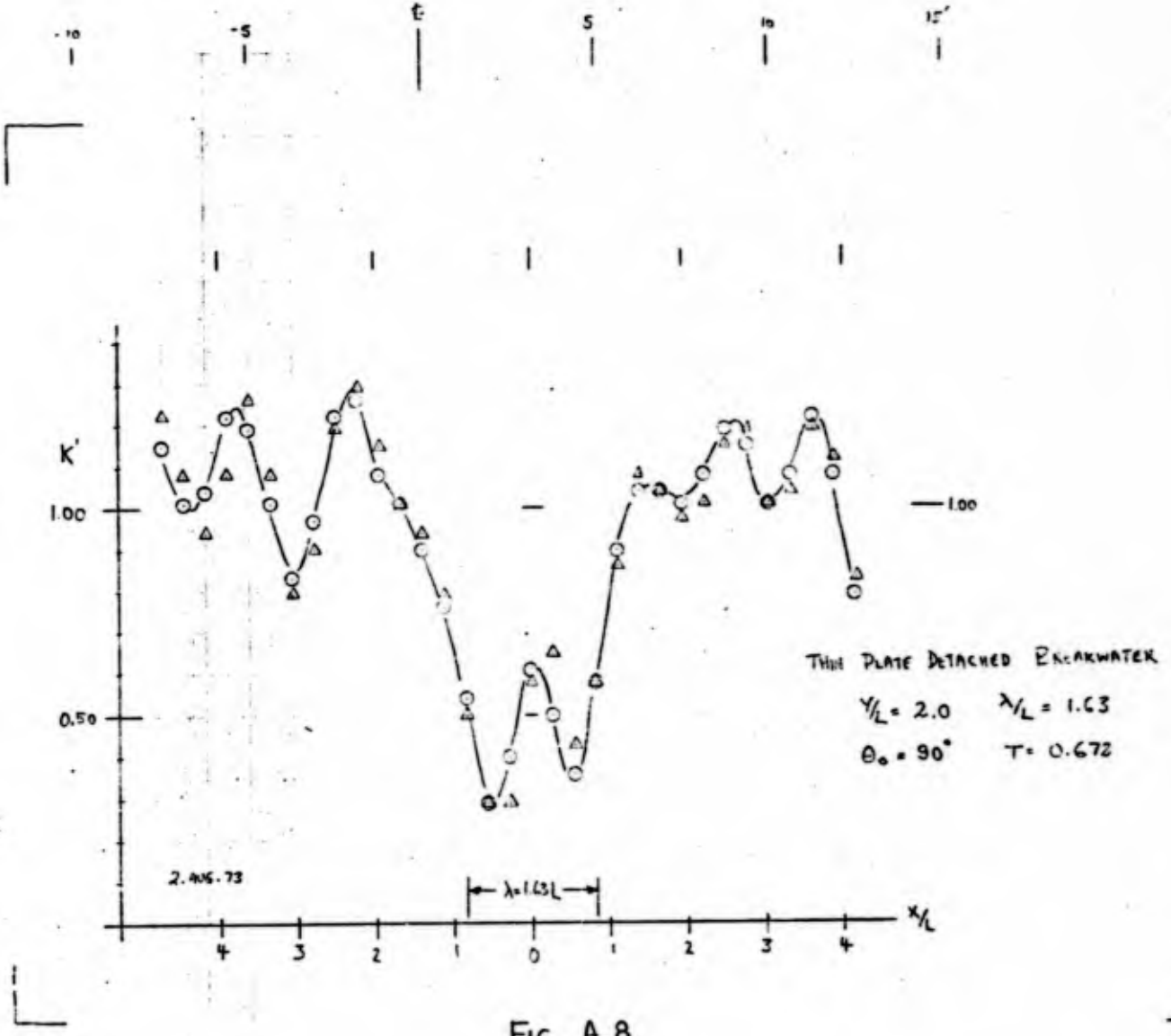

FIG. A.8

- 2. AUG. 73 , Y/L = 1.99 - GAUGE # 2

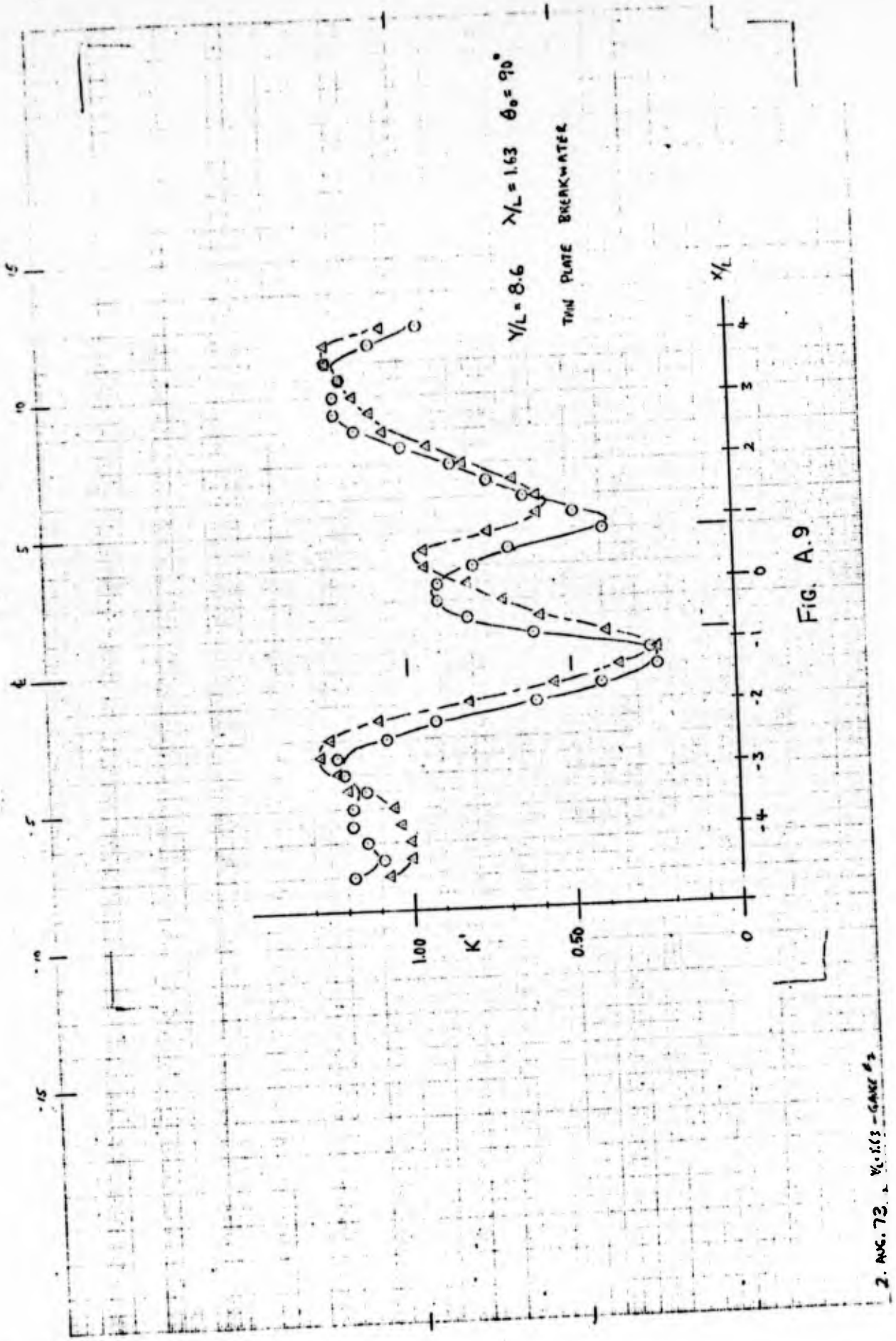
Y/L = 8.6 λ/L = 1.63 θ₀ = 90°
THIN PLATE BREAKWATER
K'
1.00
0.50
0
X/L
4
3
2
0
-1
-2
-3
-4
.15
.10
.05
.05
.10
.15

Fig. A.9

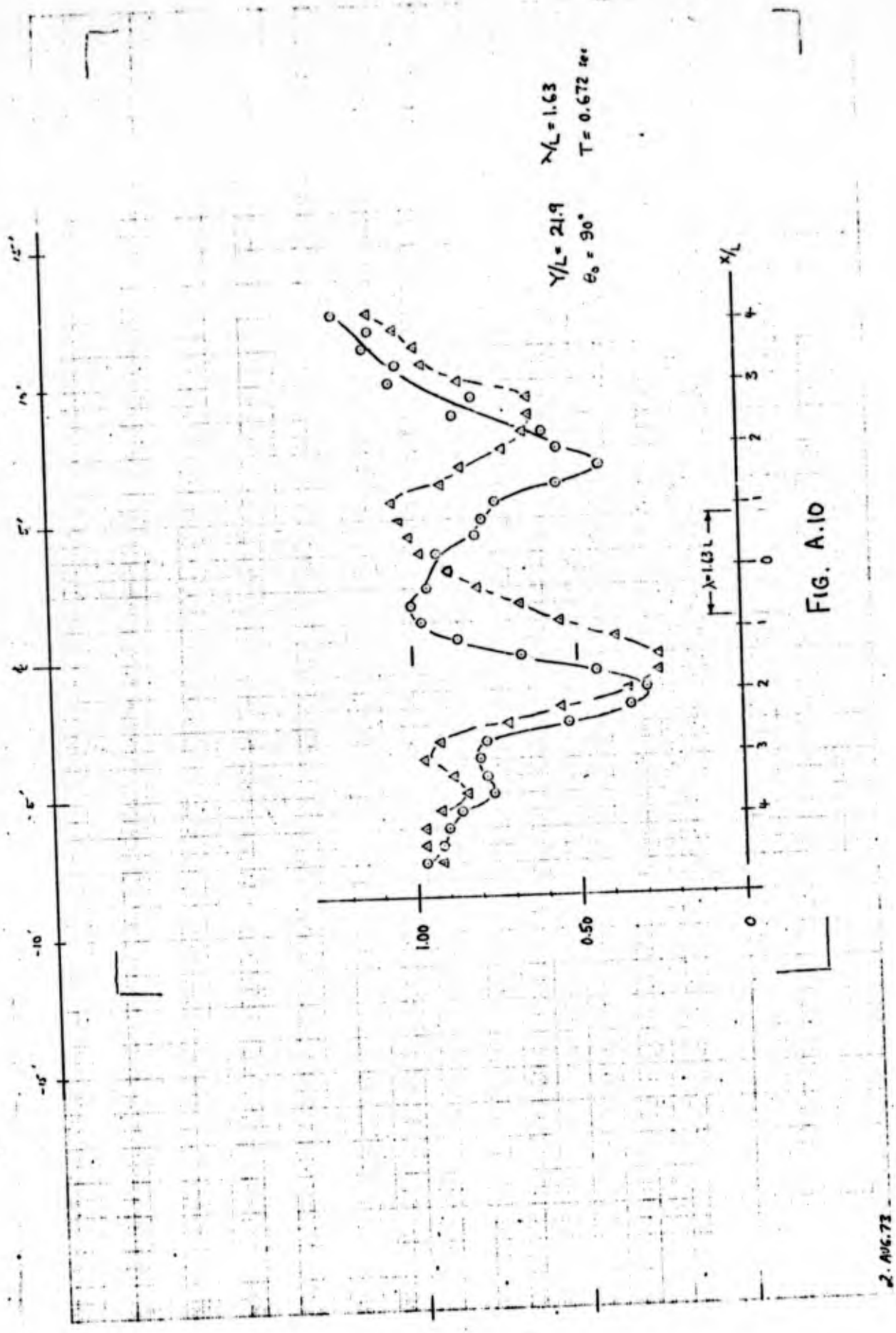
Y/L = 21.9
θ₀ = 90°
X/L = 1.63
T = 0.672 sec
X/L
λ = 1.63L
1.00
0.50
0
-15'
-10'
-5'
0
5'
10'
15'
2 AUG 73

FIG. A.10

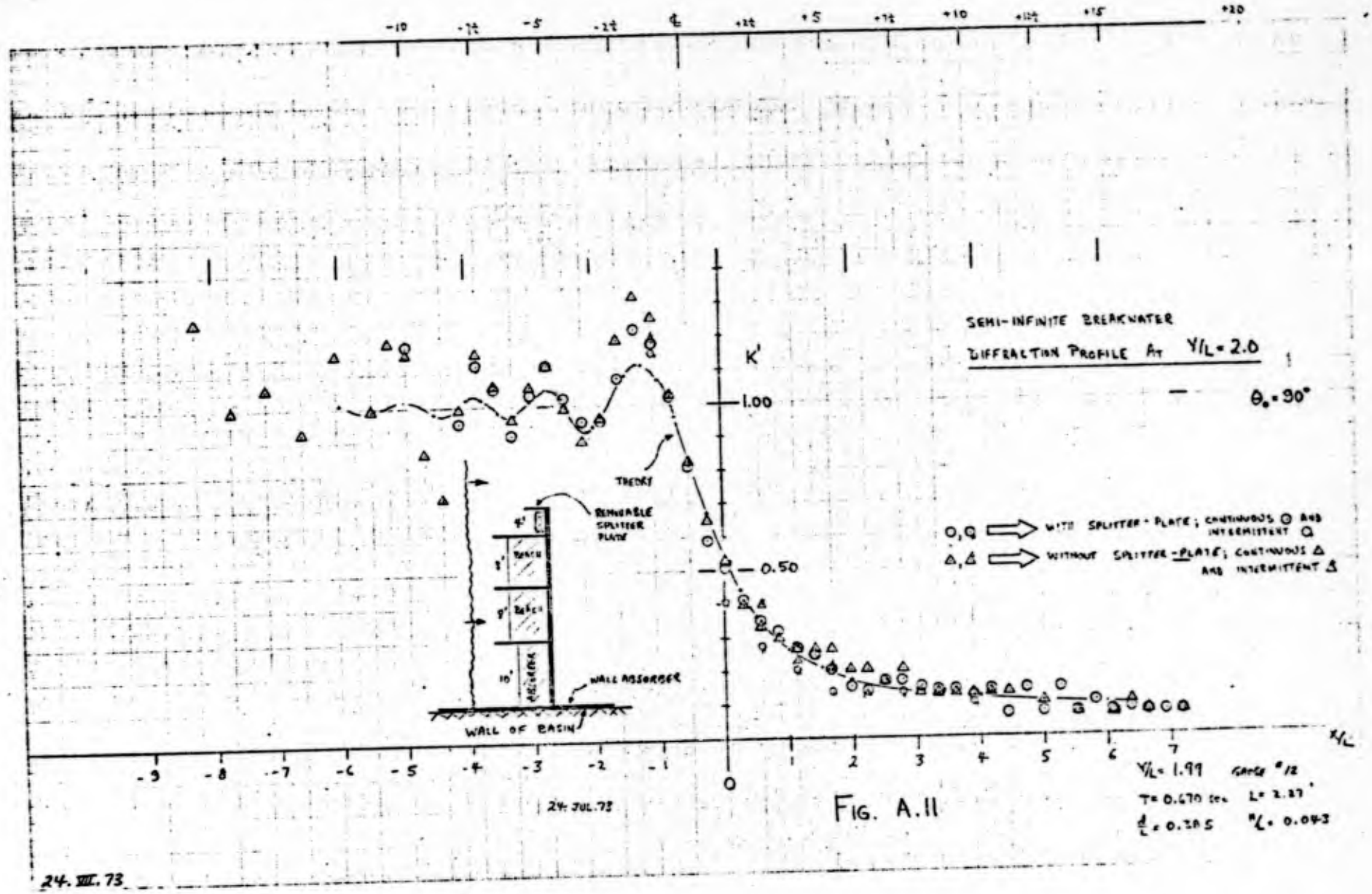
SEMI-INFINITE BREAKWATER
DIFFRACTION PROFILE AT Y/L = 2.0
θ₀ = 90°
K'
1.00
0.50
0
TREDS
REMOVABLE SPLITTER PLATE
WALL ABSORBER
WALL OF BASIN
X/L
-9 -8 -7 -6 -5 -4 -3 -2 -1 0 1 2 3 4 5 6 7
-10 -7½ -5 -2½ ℄ +2½ +5 +7½ +10 +12½ +15 +20
○,● WITH SPLITTER-PLATE; CONTINUOUS ○ AND INTERMITTENT ●
△,▲ WITHOUT SPLITTER-PLATE; CONTINUOUS △ AND INTERMITTENT ▲
Y/L = 1.99 GAGE #12
T = 0.670 sec L = 2.27'
d/L = 0.205 H/L = 0.043
24 JUL 73
24. VII. 73

FIG. A.11

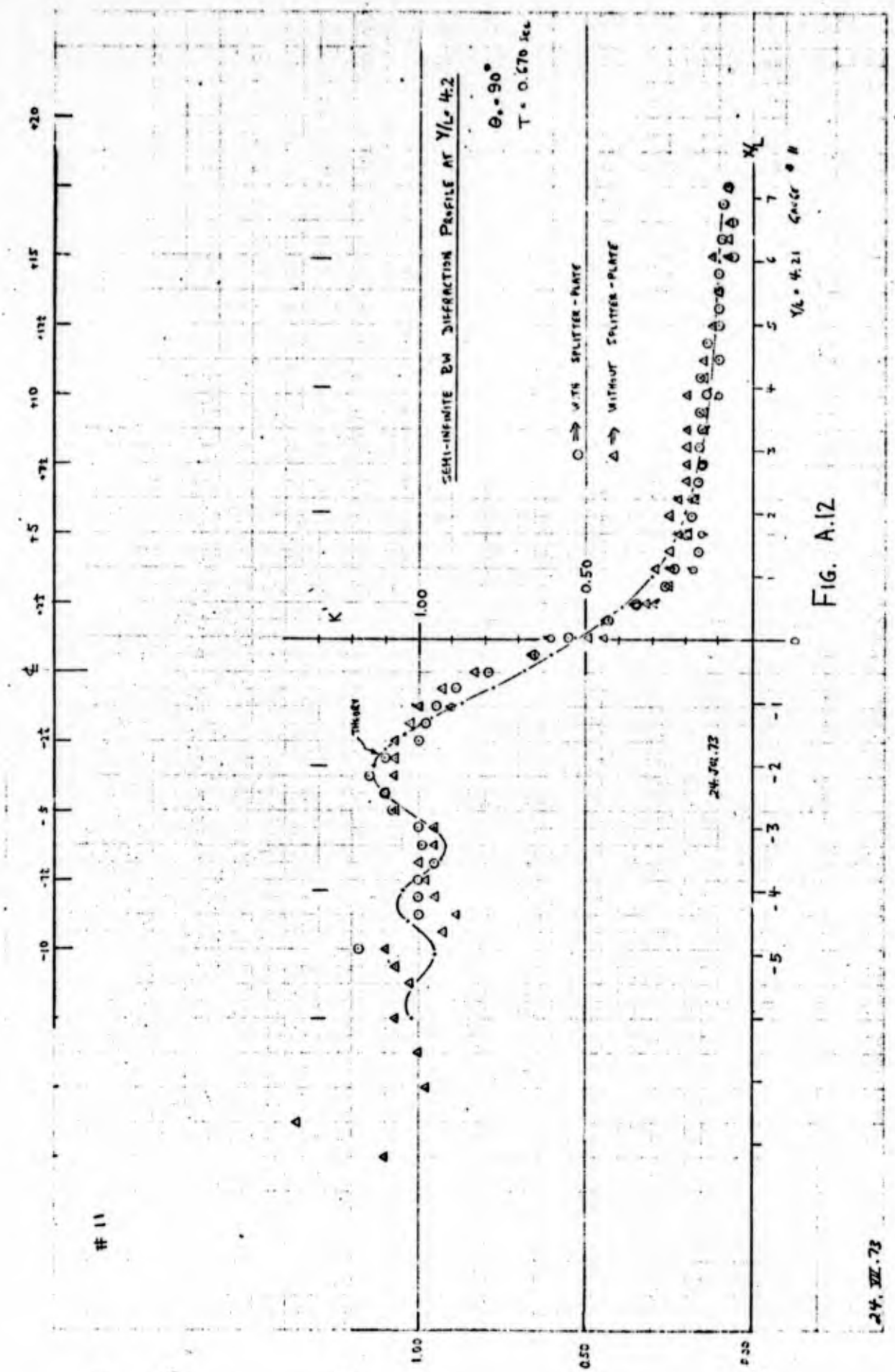
SEMI-INFINITE BW DIFFRACTION PROFILE AT Y/L = 4.2
θ = 90°
T = 0.670 sec
○ ⇒ WITH SPLITTER-PLATE
△ ⇒ WITHOUT SPLITTER-PLATE
Y/L = 4.21
K'
X/L
THEORY
24.VII.73
#11
24. VII. 73

FIG. A.12

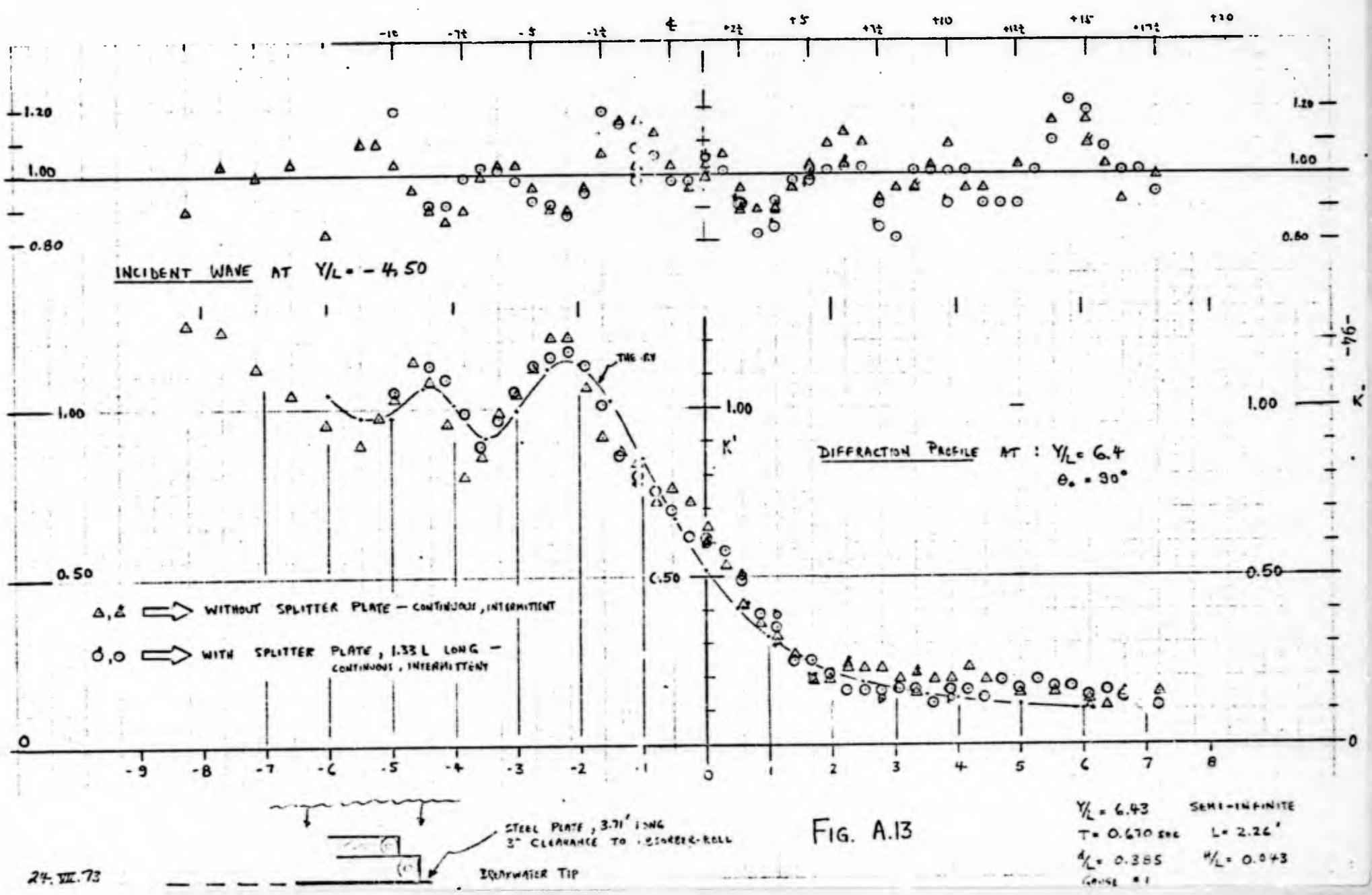
INCIDENT WAVE AT Y/L = -4.50
DIFFRACTION PROFILE AT : Y/L = 6.4
θ₀ = 30°
K'
1.20
1.00
0.80
0.50
0
-10 -7½ -5 -2½ 0 +2½ +5 +7½ +10 +12½ +15 +17½ +20
-9 -8 -7 -6 -5 -4 -3 -2 -1 0 1 2 3 4 5 6 7 8
Δ,▲ ⇨ WITHOUT SPLITTER PLATE — CONTINUOUS, INTERMITTENT
O,● ⇨ WITH SPLITTER PLATE, 1.33 L LONG — CONTINUOUS, INTERMITTENT
STEEL PLATE, 3.71' LONG
3" CLEARANCE TO SCREEN-ROLL
SQUARE WATER TIP
Y/L = 6.43
T = 0.670 SEC
d/L = 0.385
GAUGE #1
SEMI-INFINITE
L = 2.26'
H/L = 0.043
24. VII. 73

FIG. A.13

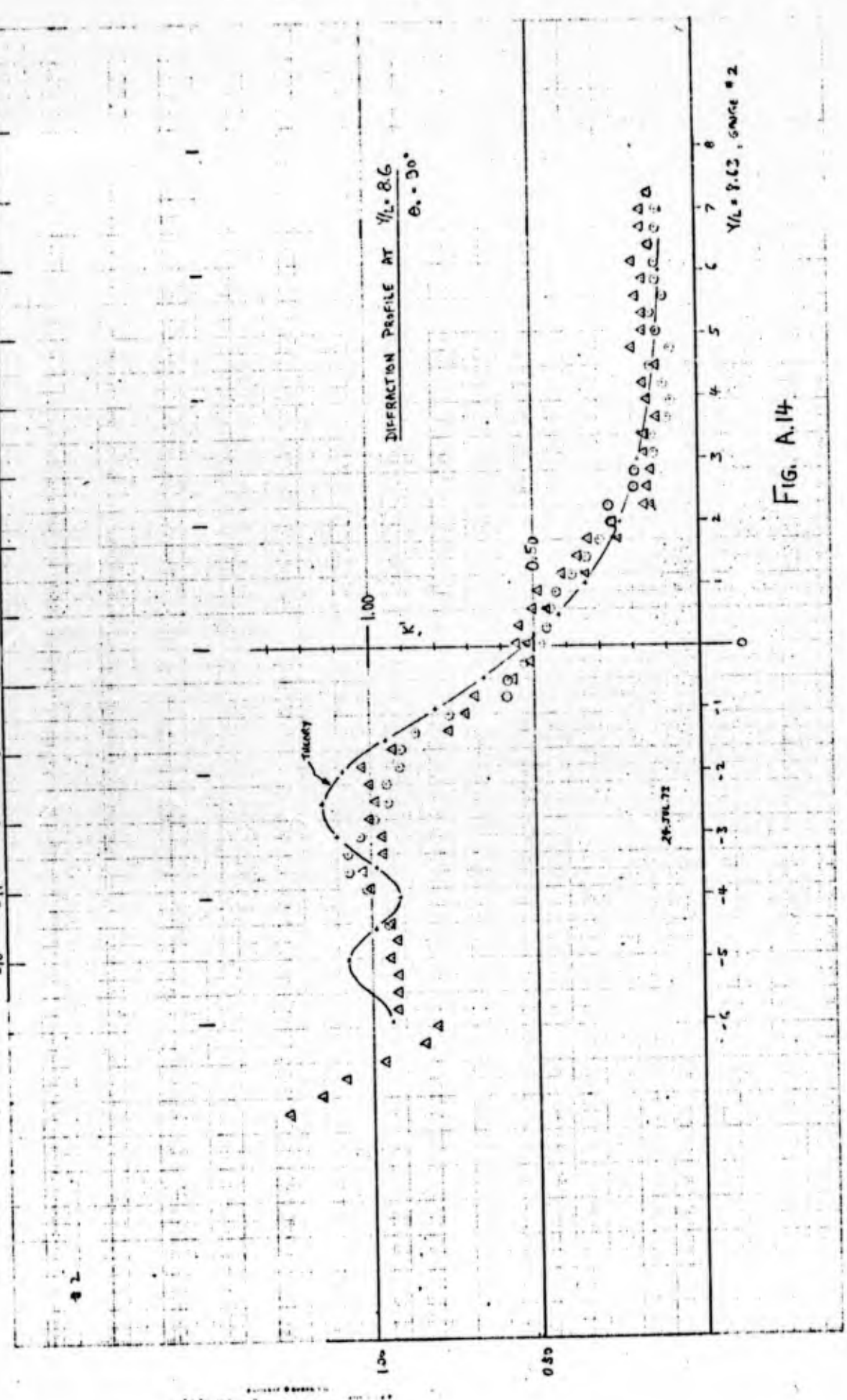
DIFFRACTION PROFILE AT Y/L = 8.6
θ = 30°
Y/L = 8.62, GAGE #2
TURNEY
1.00
0.50
K'
24 JULY 73

FIG. A.14

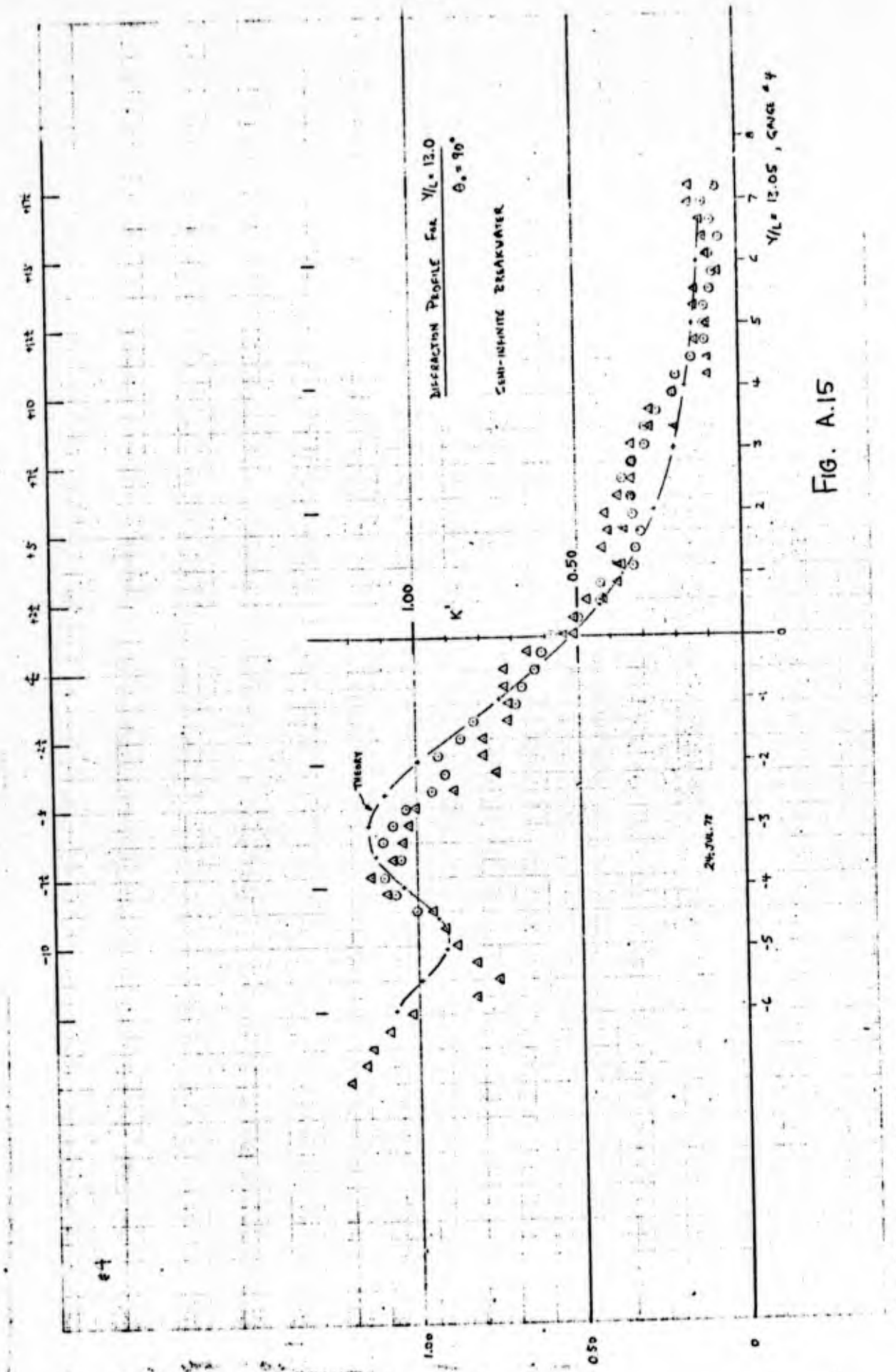
DIFFRACTION PROFILE FOR Y/L = 12.0
θ = 90°
SEMI-INFINITE BREAKWATER
K'
1.00
0.50
0
Y/L = 12.05, GAGE # 4
THEORY
24 JUL 73

FIG. A.15

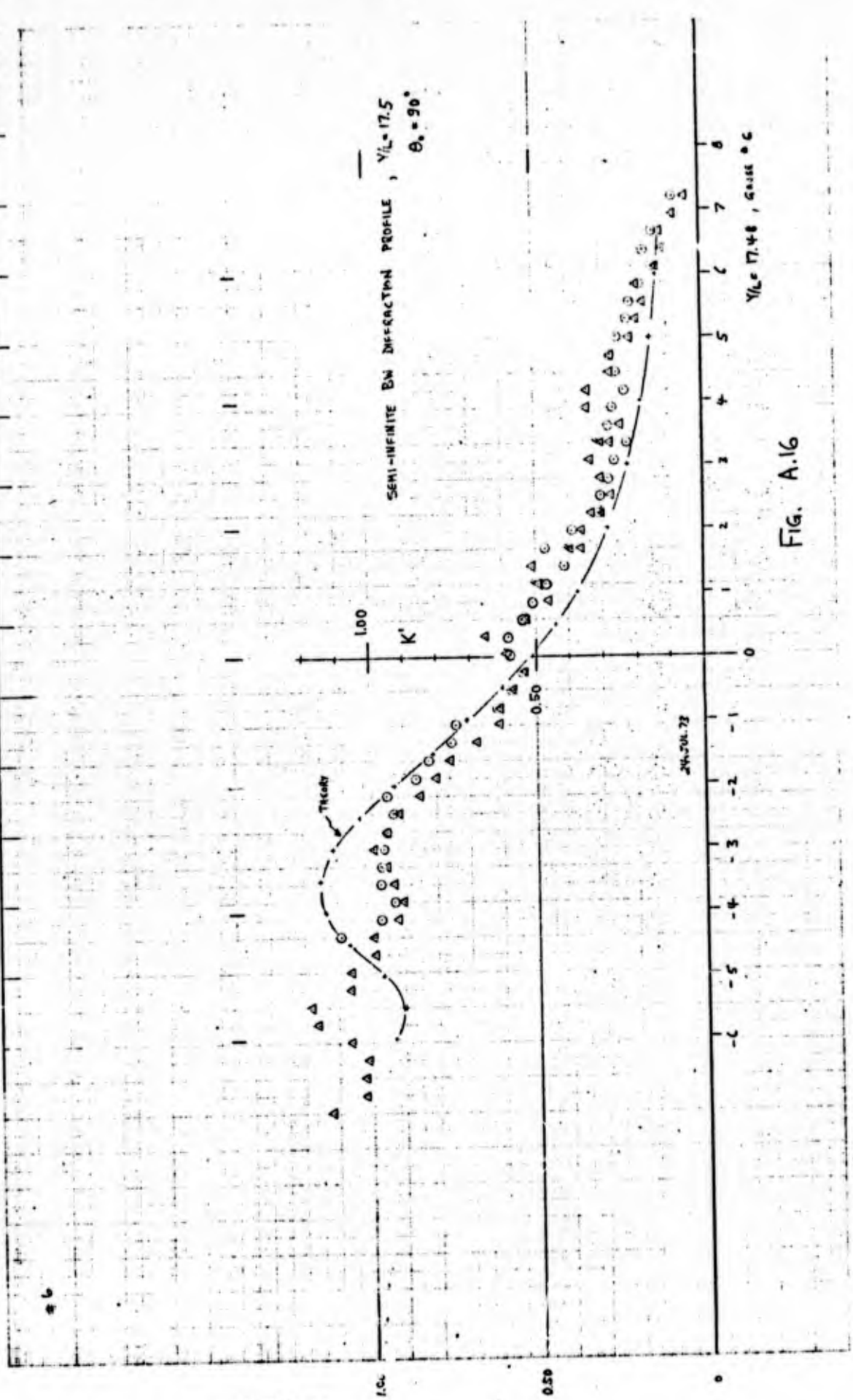
SEMI-INFINITE BW DIFFRACTION PROFILE , Y/L = 17.5
θ₀ = 90°
Y/L = 17.48 , GAUGE °C
K'
1.00
0.50
0
THEORY
24 JULY 73

FIG. A.16

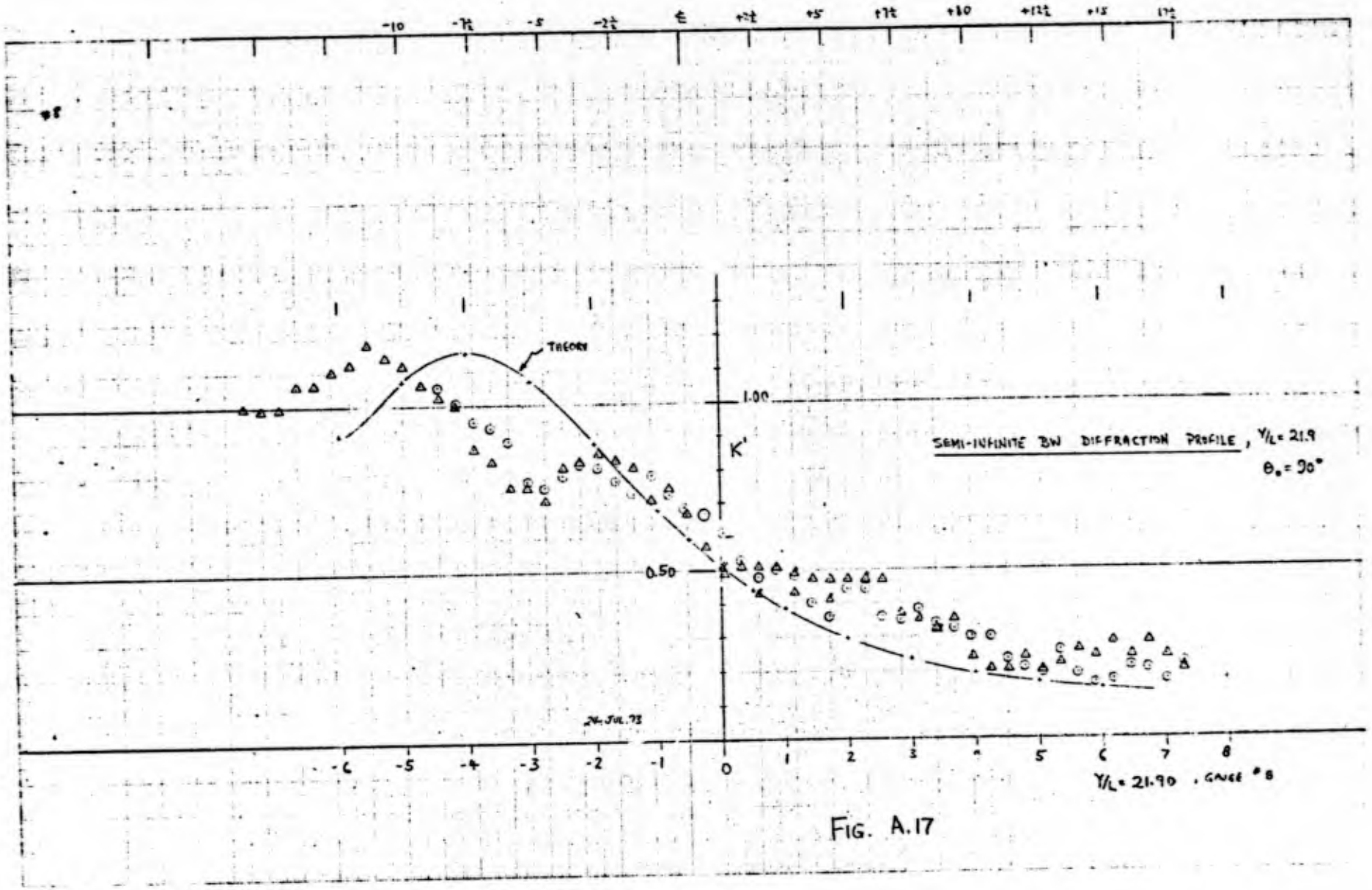
THEORY
1.00
K'
0.50
SEMI-INFINITE BW DIFFRACTION PROFILE, Y/L = 21.9
θ₀ = 90°
Y/L = 21.90 . GAGE #8
24 JUL. 73
24 July 73

FIG. A.17

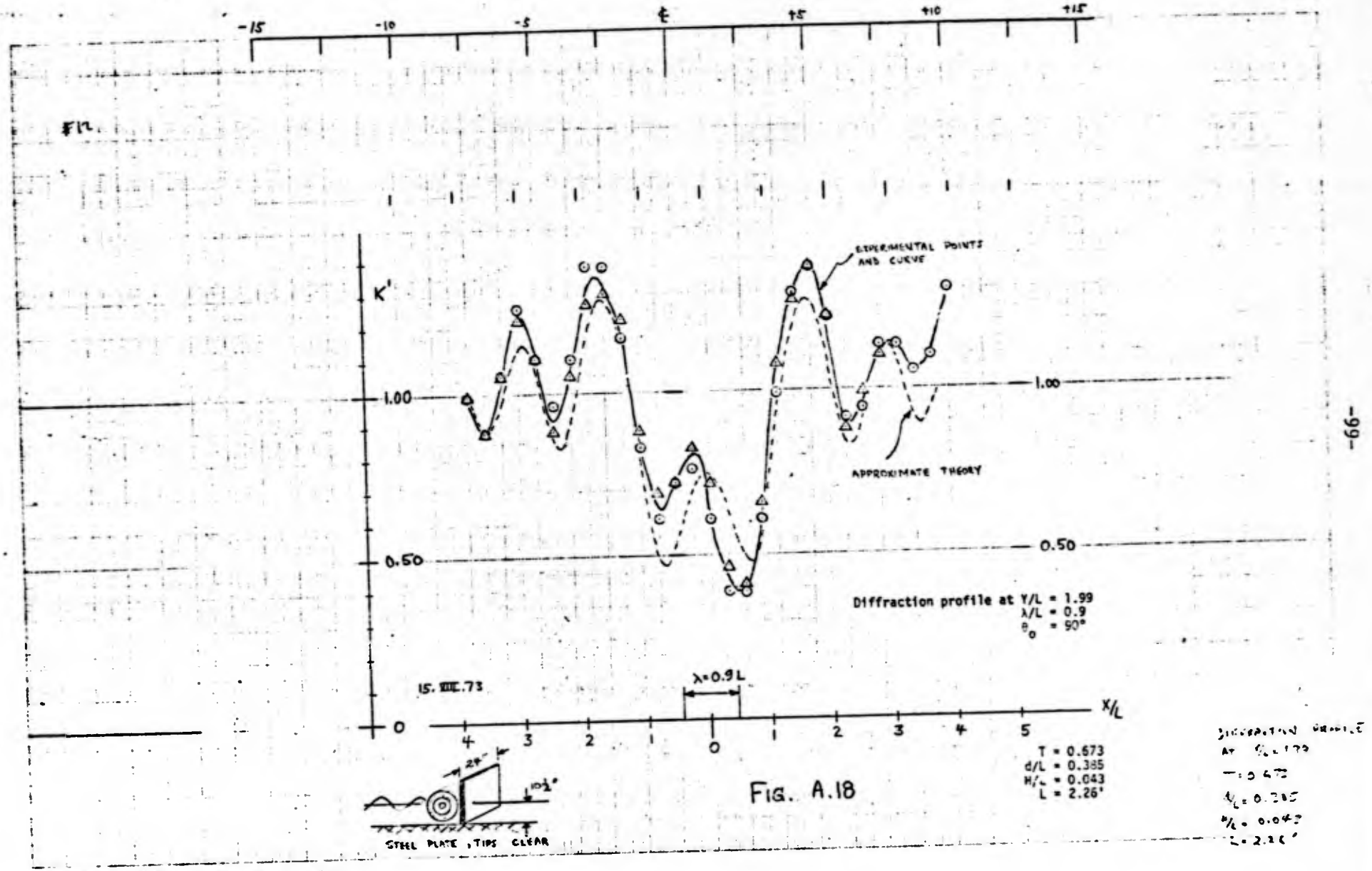
-15
-10
-5
0
+5
+10
+15
#12
K'
1.00
0.50
0
EXPERIMENTAL POINTS AND CURVE
APPROXIMATE THEORY
1.00
0.50
Diffraction profile at Y/L = 1.99
λ/L = 0.9
θ0 = 90°
15. VIII. 73
λ=0.9L
X/L
4
3
2
1
0
1
2
3
4
5
T = 0.673
d/L = 0.385
H/L = 0.043
L = 2.26'
24"
10½"
STEEL PLATE, TIPS CLEAR
15 AUG 73 RUN II #12

FIG. A.18

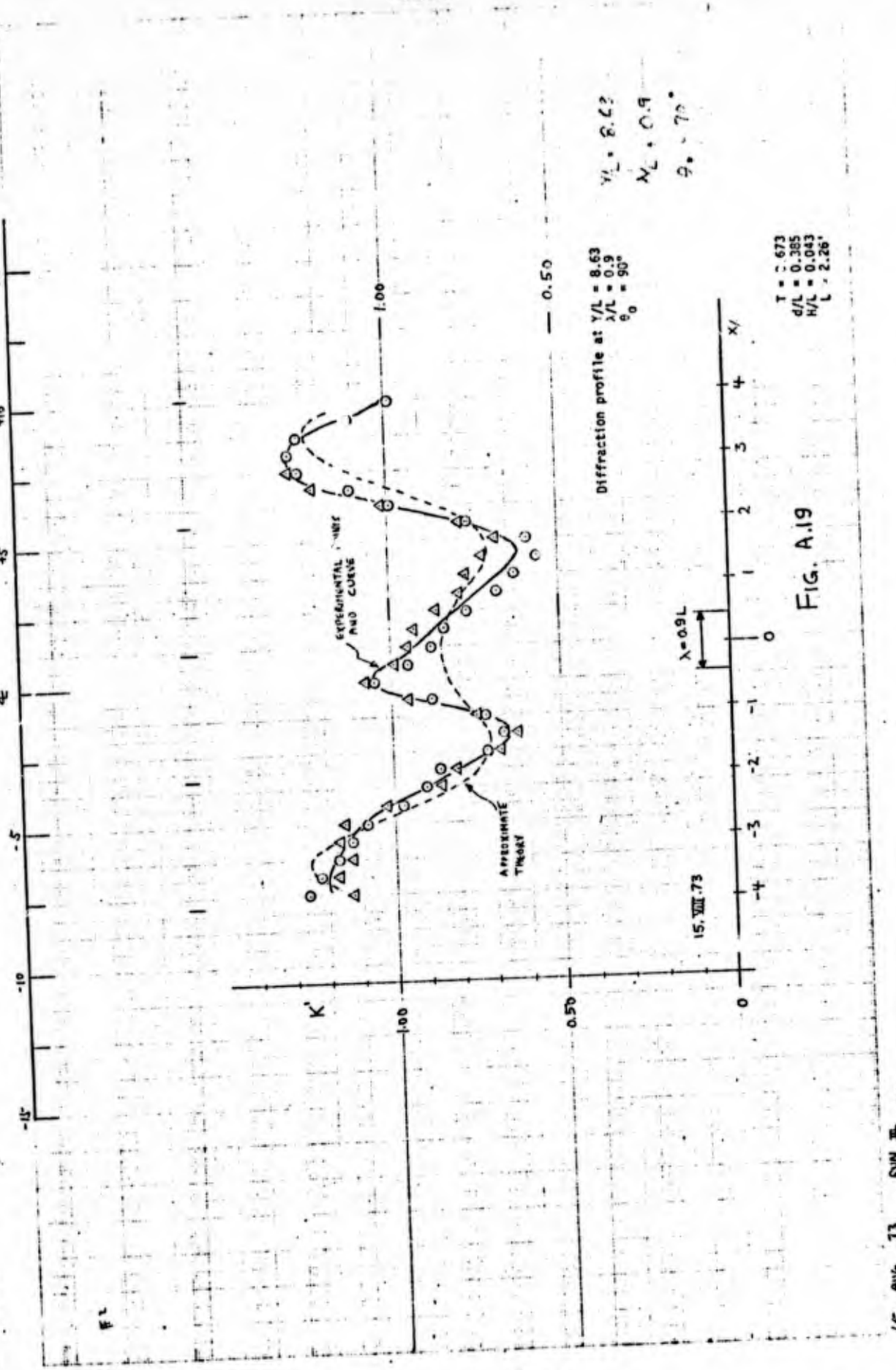
Diffraction profile at Y/L = 8.63
λ/L = 0.9
θ0 = 90°
Y/L = 8.63
λ/L = 0.9
θ0 = 70°
T = 0.673
d/L = 0.385
H/L = 0.043
L = 2.26'
EXPERIMENTAL AND CURVE
APPROXIMATE THEORY
K'
1.00
0.50
X/
λ=0.9L
15. VIII. 73
16 Aug 73 DVM III #2

FIG. A.19

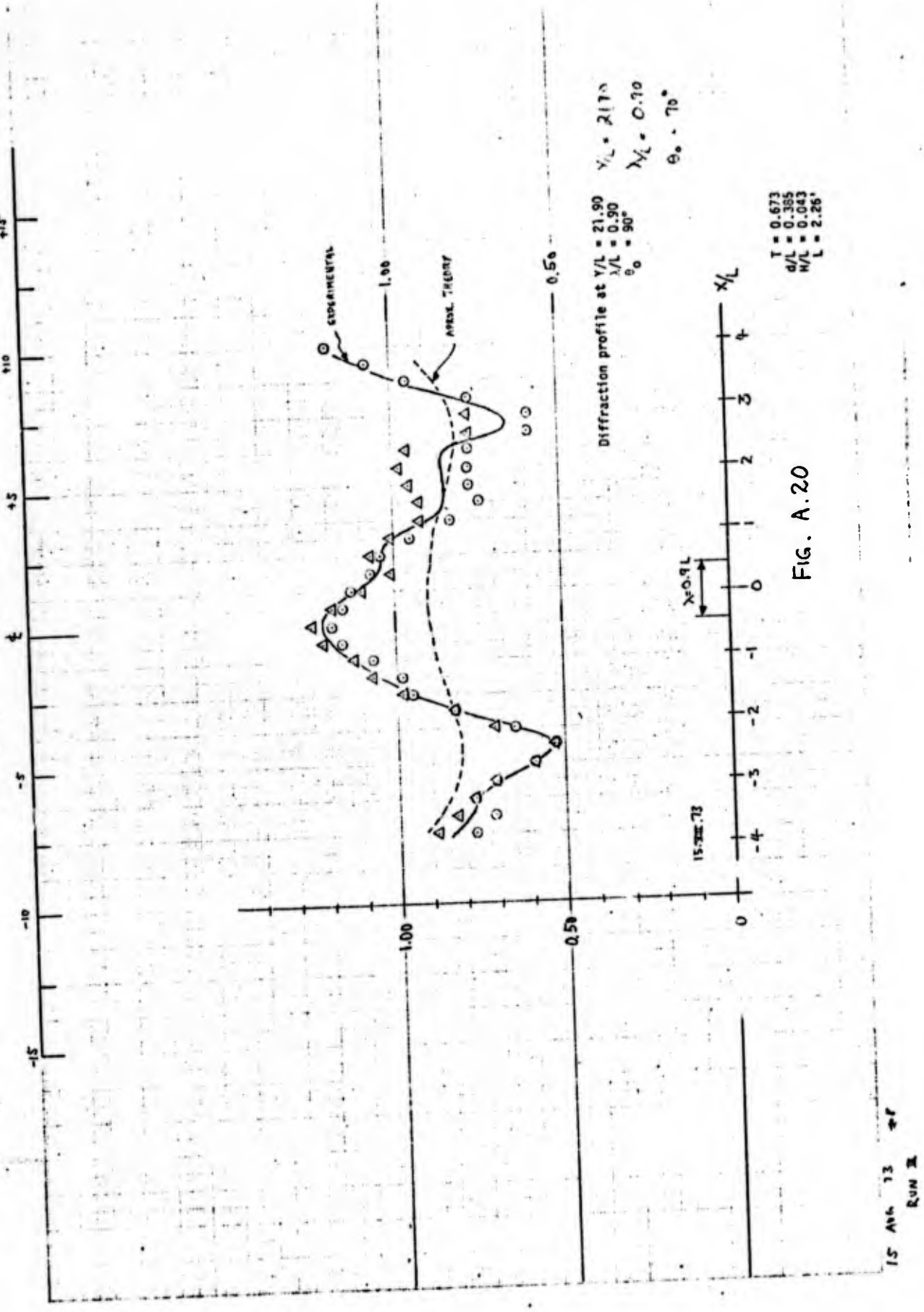
EXPERIMENTAL
ANAL. THEORY
1.00
0.50
Diffraction profile at Y/L = 21.90
X/L = 0.90
θ₀ = 90°
T = 0.673
d/L = 0.385
H/L = 0.043
L = 2.26'
X/L
λ=0.9L
15 Aug 73
RUN 11

FIG. A.20

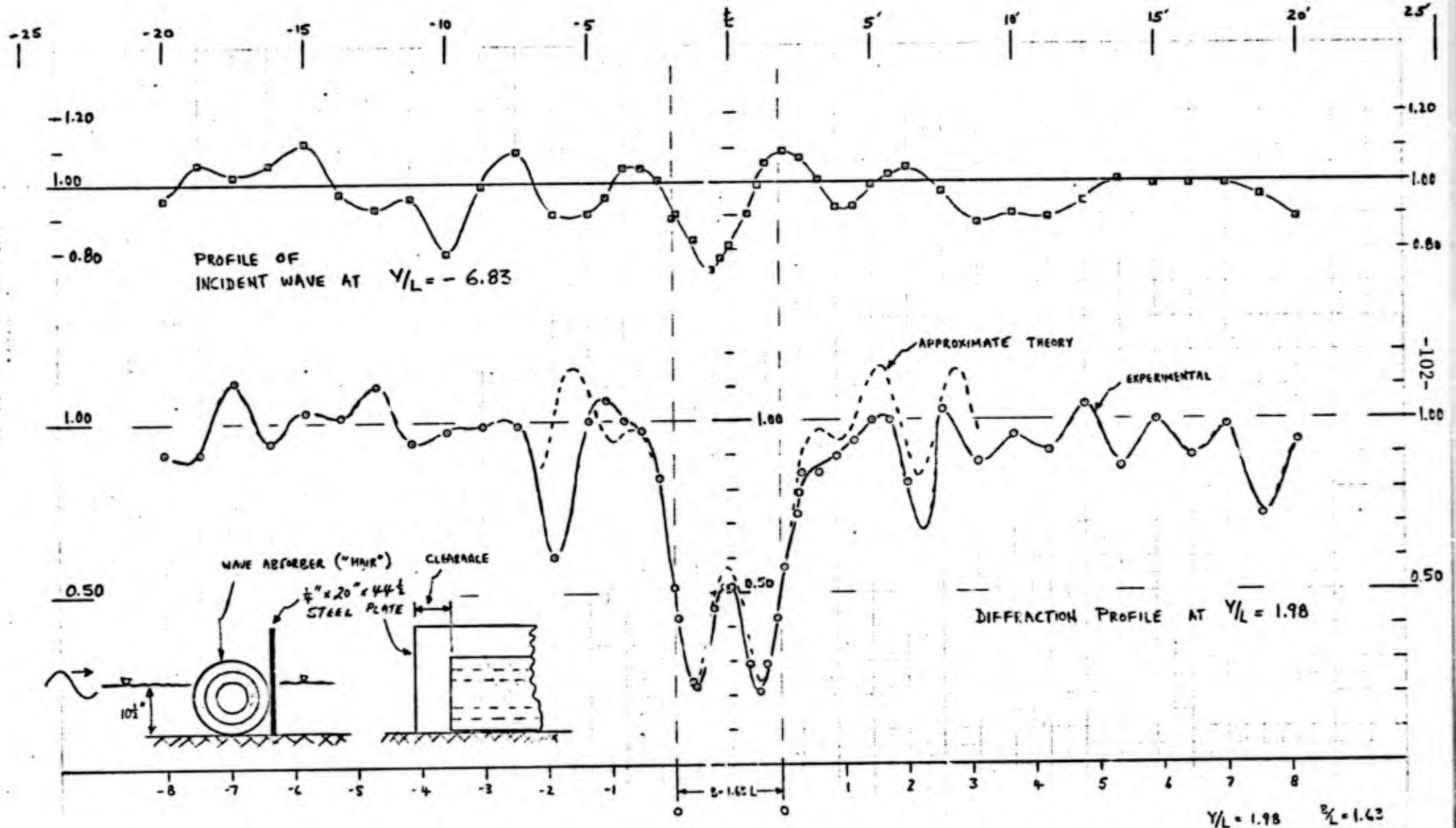

FIG. A.21

Y/L = 1.98 B/L = 1.63
T = 0.673 L = 2.27'
d/L = 0.382 H/L = 0.047

4. XII. 73

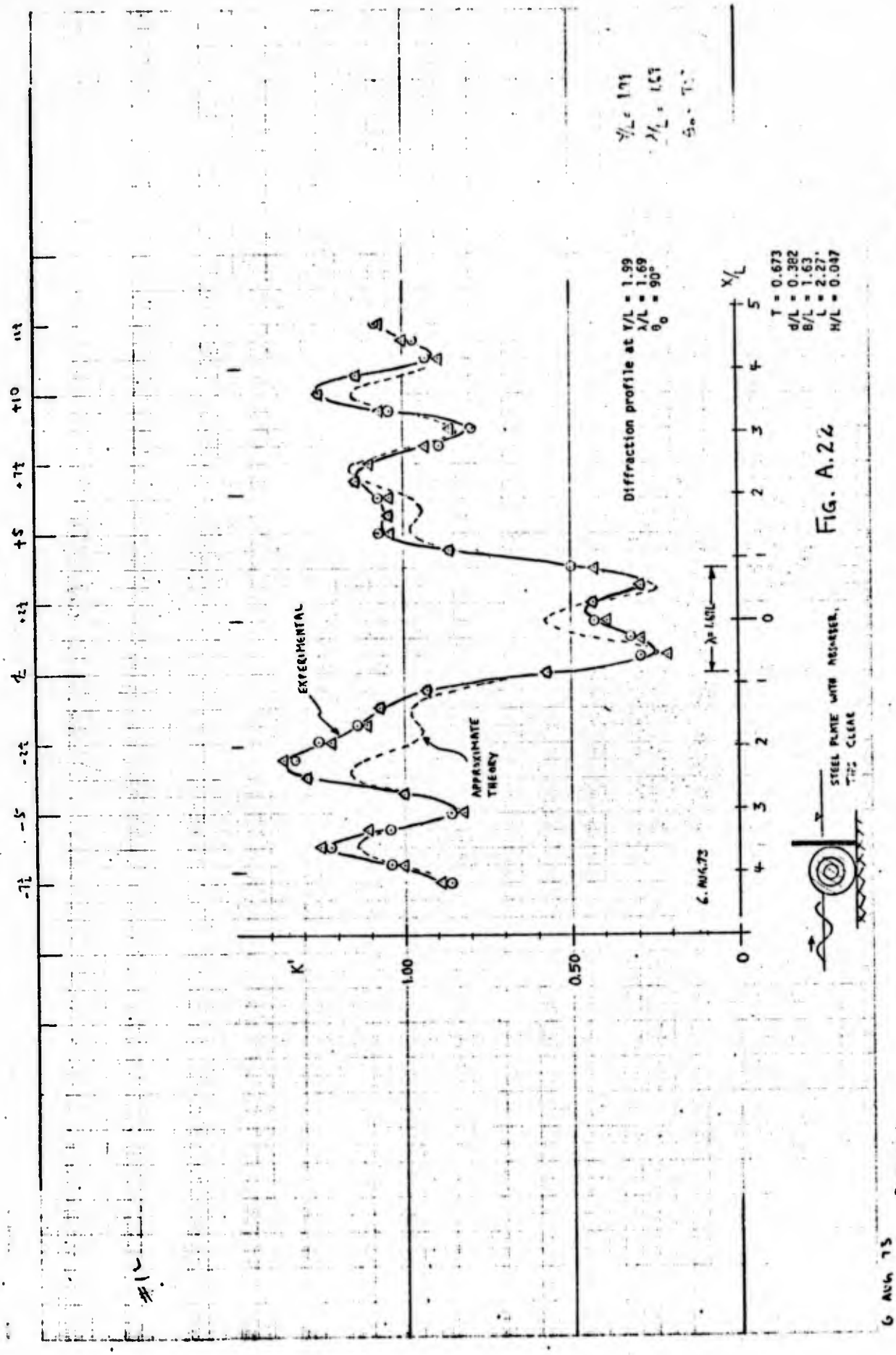

FIG. A.22

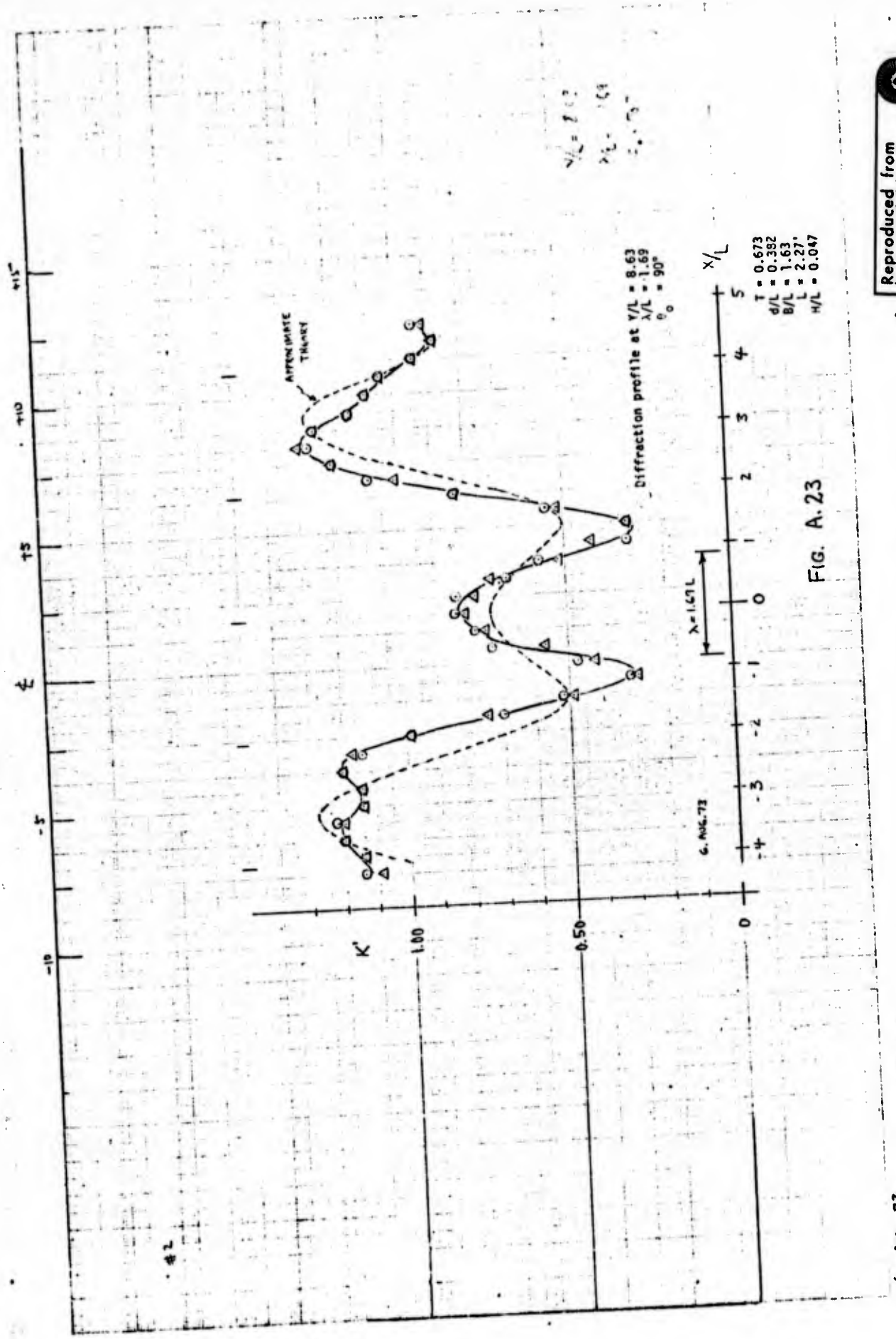

FIG. A.23

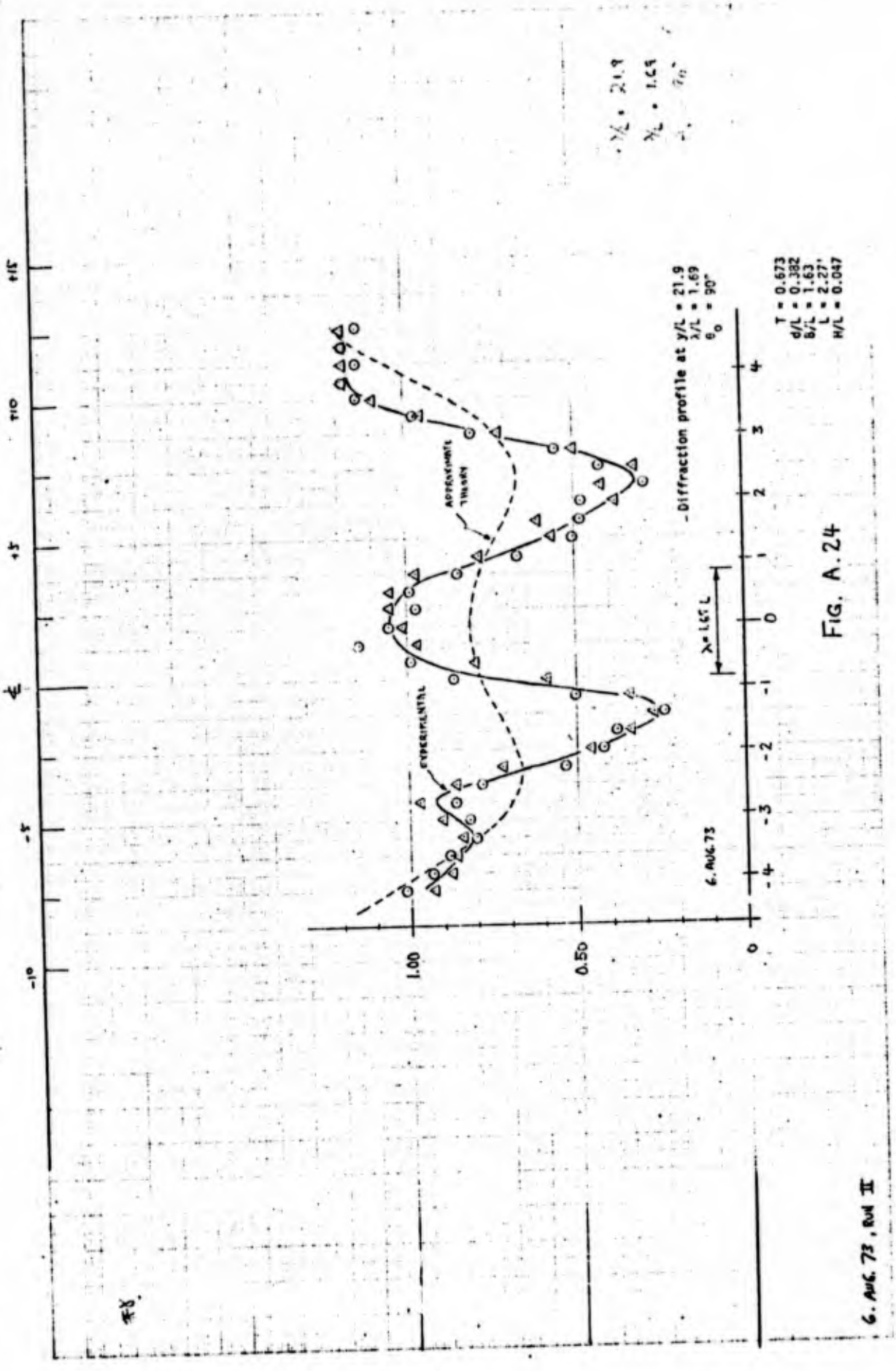
Diffraction profile at y/L = 21.9
λ/L = 1.69
θ₀ = 90°
T = 0.673
d/L = 0.382
B/L = 1.63
L = 2.27'
H/L = 0.047
λ= 1.69 L
6. AUG. 73
1.00
0.50
0
+15
+10
+5
-5
-10
EXPERIMENTAL
APPROXIMATE THEORY
6. Aug. 73, Run II

FIG. A.24

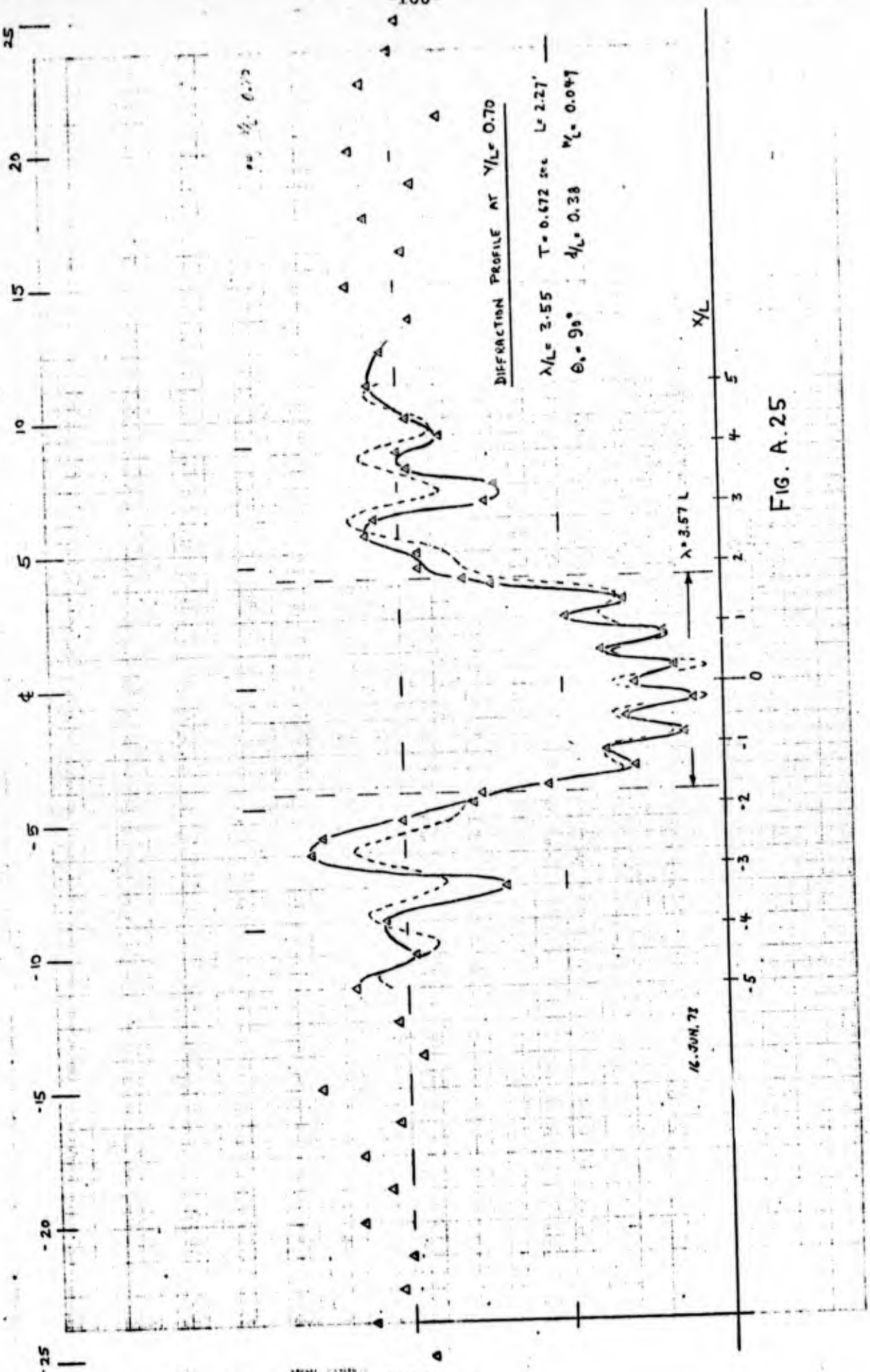
DIFFRACTION PROFILE AT Y/L= 0.70
λ/L= 3.55 T= 0.672 sec L= 2.27'
θ₀= 90° d/L= 0.38 Y/L= 0.049
λ= 3.57 L
X/L
16 JUN. 71

FIG. A.25

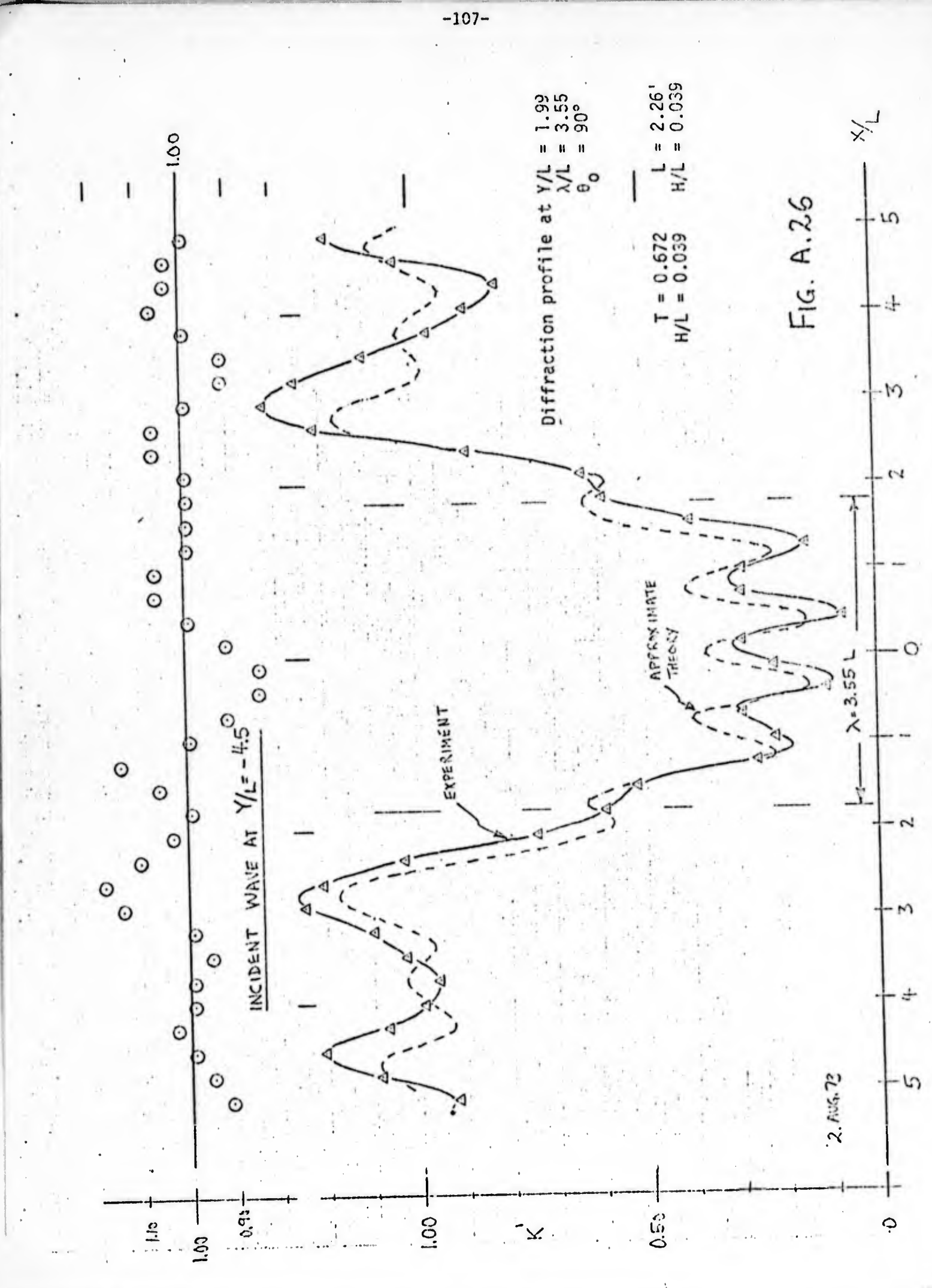
Diffraction profile at Y/L = 1.99
λ/L = 3.55
θo = 90°
T = 0.672
H/L = 0.039
L = 2.26'
H/L = 0.039
EXPERIMENT
APPROXIMATE THEORY
INCIDENT WAVE AT Y/L = -4.5
λ = 3.55 L
K'
X/L
2 AUG. 72

FIG. A.26

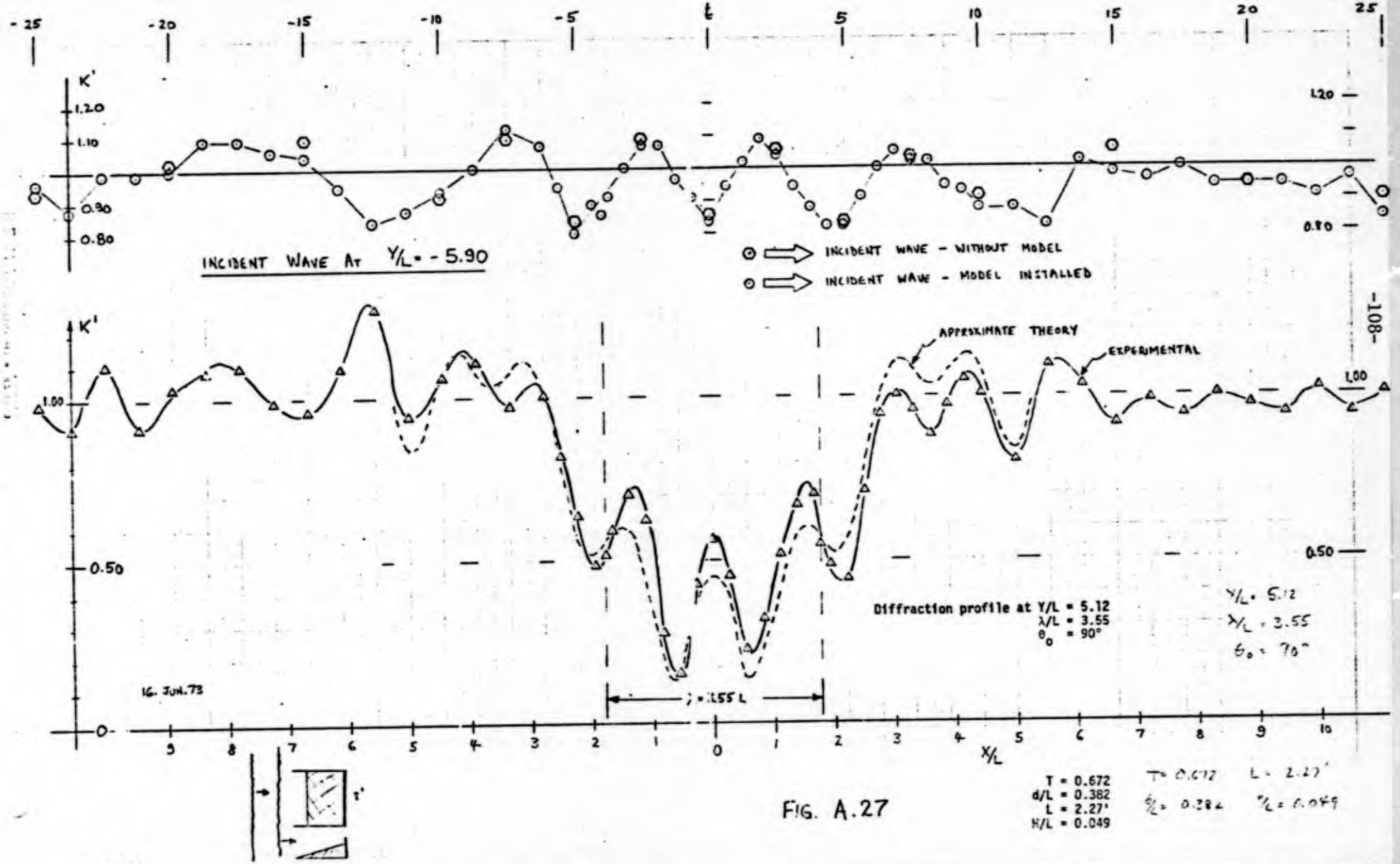
-25
-20
-15
-10
-5
0
5
10
15
20
25
K'
1.20
1.10
0.90
0.80
INCIDENT WAVE AT Y/L = -5.90
INCIDENT WAVE - WITHOUT MODEL
INCIDENT WAVE - MODEL INSTALLED
APPROXIMATE THEORY
EXPERIMENTAL
1.00
0.50
0
Diffraction profile at Y/L = 5.12
λ/L = 3.55
θ0 = 90°
Y/L = 5.12
λ/L = 3.55
θ0 = 70°
16. JUN. 73
λ = 3.55 L
X/L
T = 0.672
d/L = 0.382
L = 2.27'
H/L = 0.049
T = 0.672 L = 2.27'
d/L = 0.382 H/L = 0.049
16. II. 73

FIG. A.27

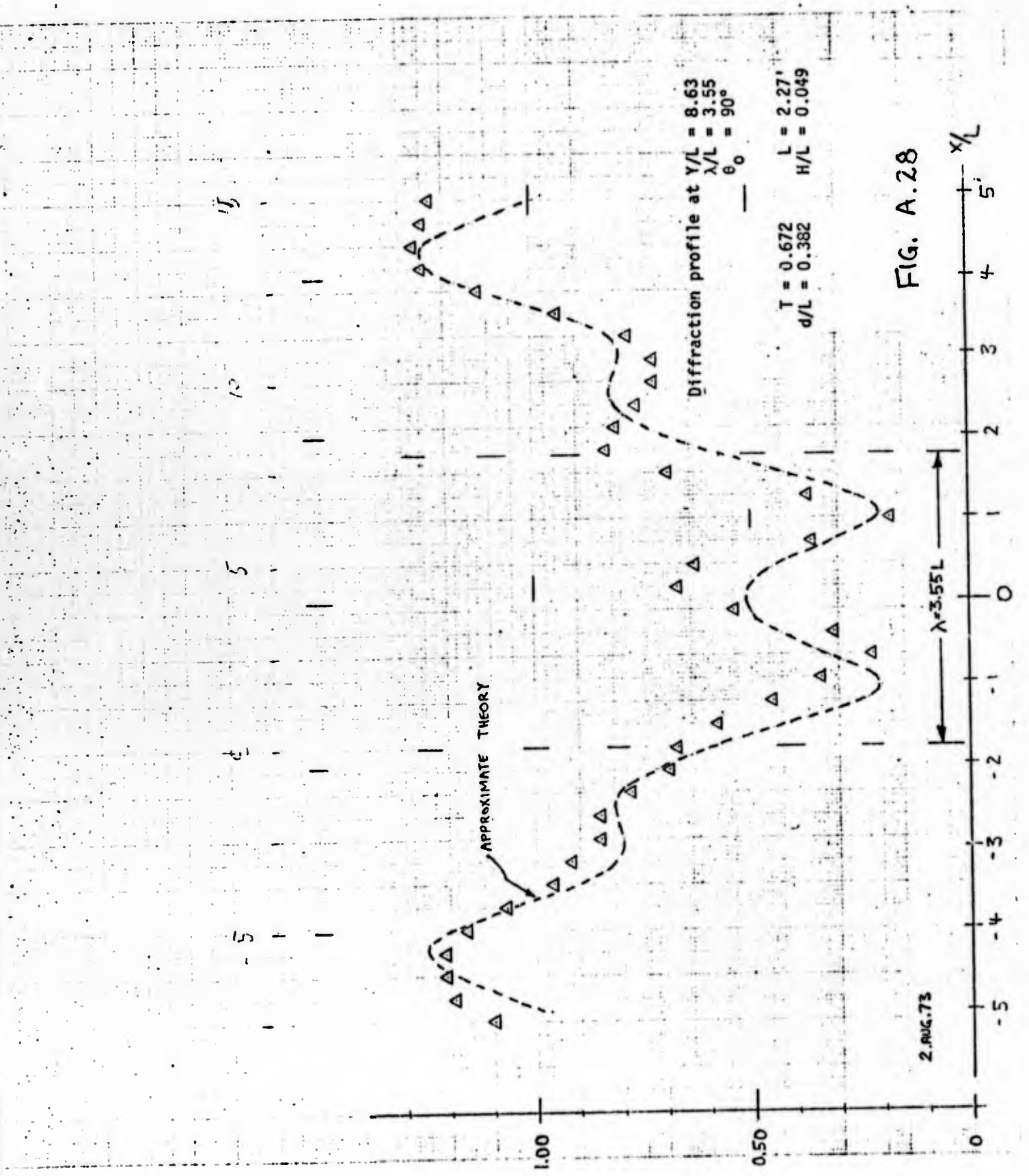
Diffraction profile at Y/L = 8.63
λ/L = 3.55
θo = 90°
T = 0.672
d/L = 0.382
L = 2.27'
H/L = 0.049
APPROXIMATE THEORY
λ=3.55L
X/L
1.00
0.50
0
2.AUG.73

FIG. A.28

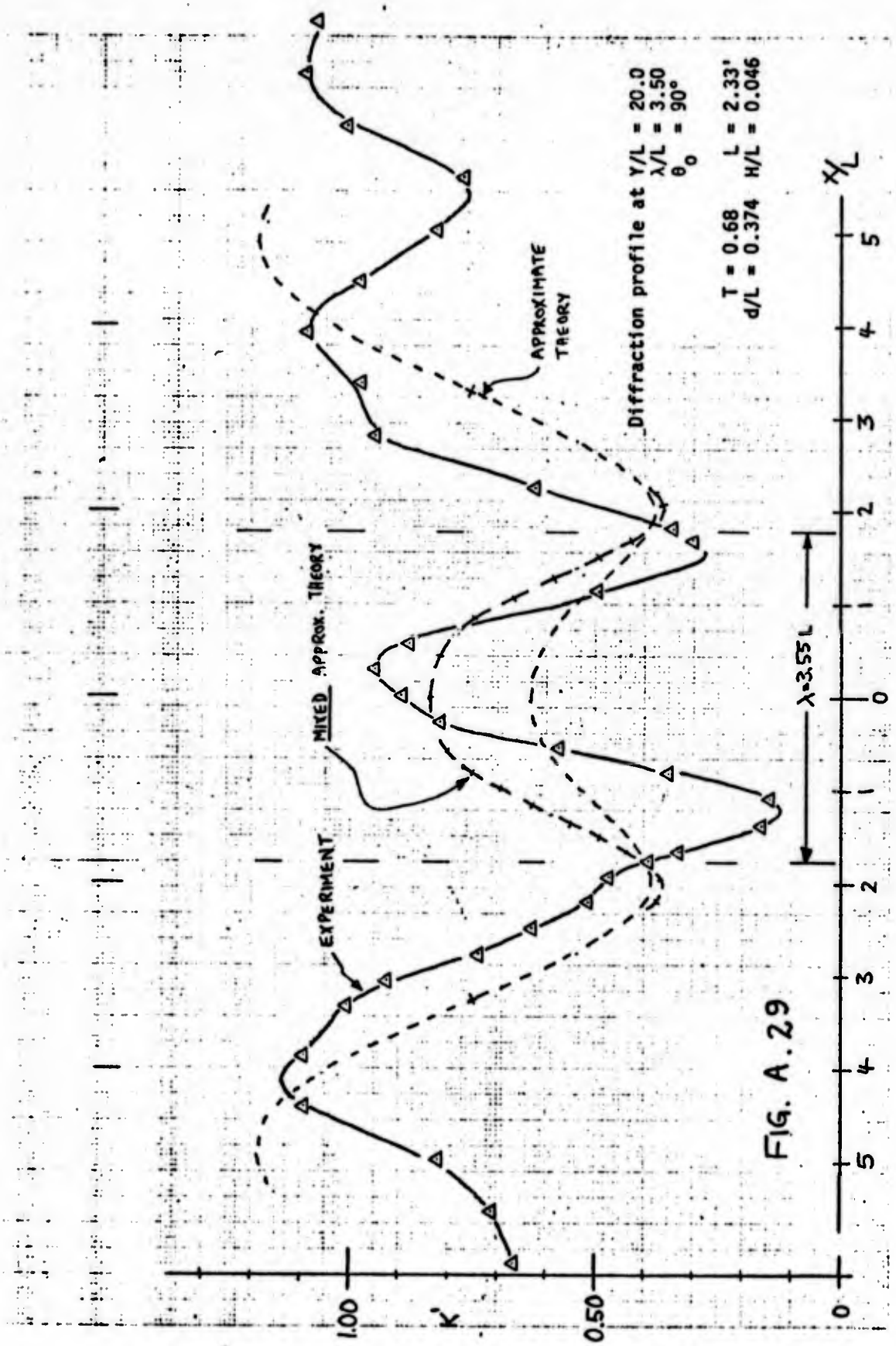
Diffraction profile at Y/L = 20.0
λ/L = 3.50
θo = 90°
T = 0.68 L = 2.33'
d/L = 0.374 H/L = 0.046
APPROXIMATE THEORY
MIXED APPROX. THEORY
EXPERIMENT
λ=3.55L
X/L
K'
1.00
0.50
0
1
2
3
4
5

FIG. A.29

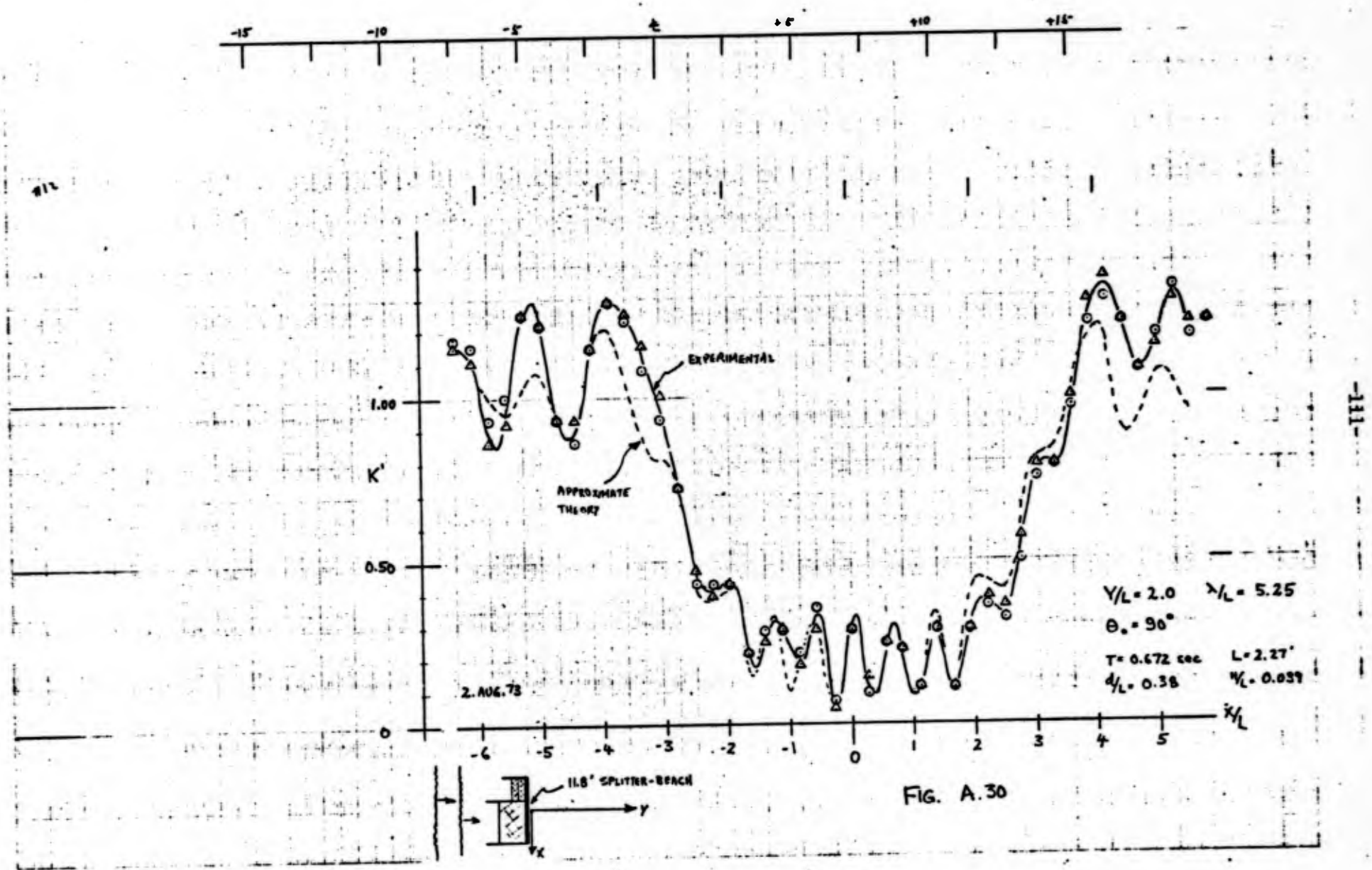
-15°
-10°
-5°
0°
+5°
+10°
+15°
EXPERIMENTAL
APPROXIMATE THEORY
1.00
0.50
0
K'
2. AUG. 73
Y/L = 2.0
λ/L = 5.25
θ₀ = 90°
T = 0.672 sec
L = 2.27'
d/L = 0.38
H/L = 0.039
-6
-5
-4
-3
-2
-1
0
1
2
3
4
5
X/L
11.8' SPLITTER-BEACH
Y
X

FIG. A.30

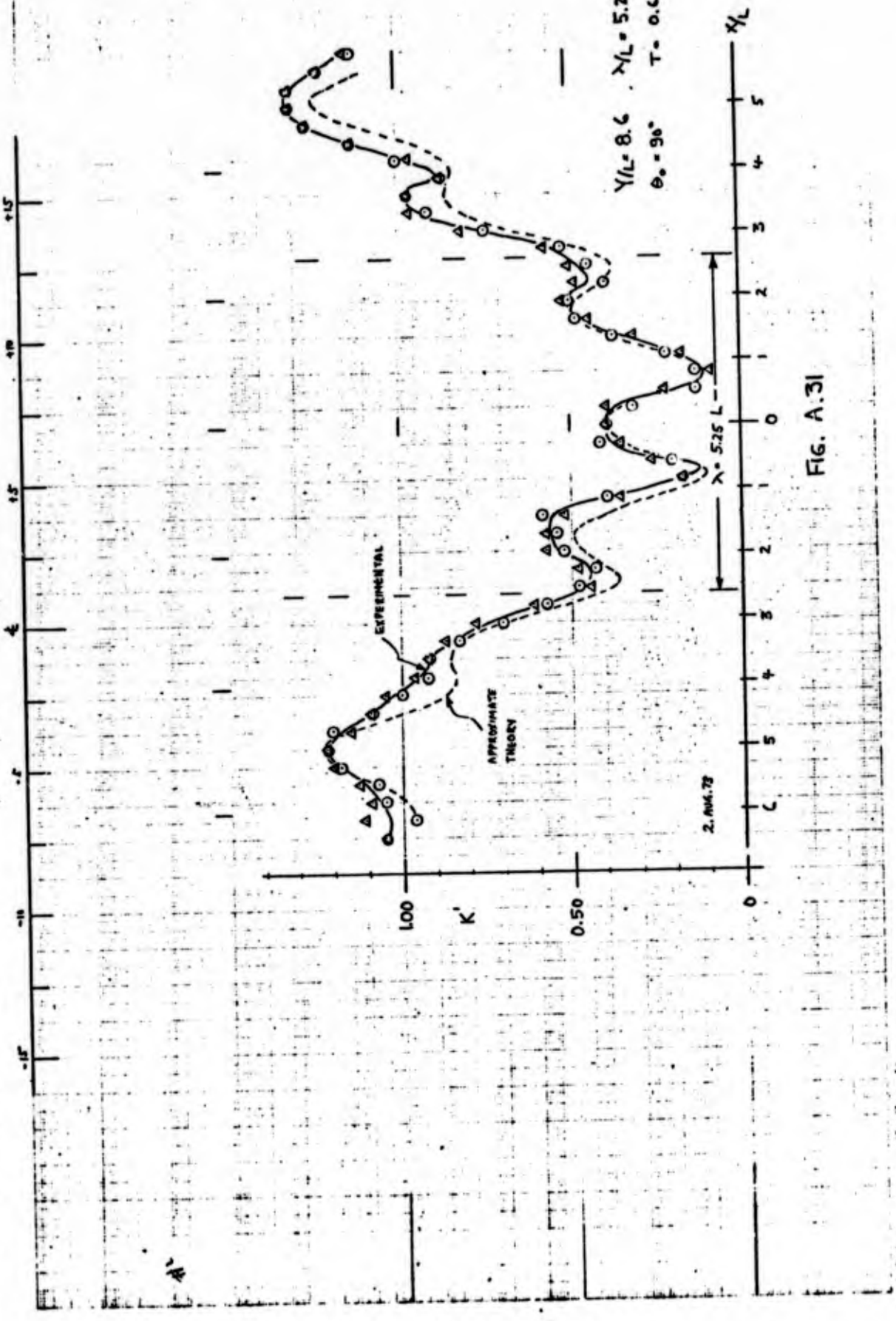
Y/L = 8.6
X/L = 5.25
θ = 90°
T = 0.672 sec
EXPERIMENTAL
APPROXIMATE THEORY
K'
1.00
0.50
X/L
X = 5.25 L
2 AUG 72

FIG. A.31

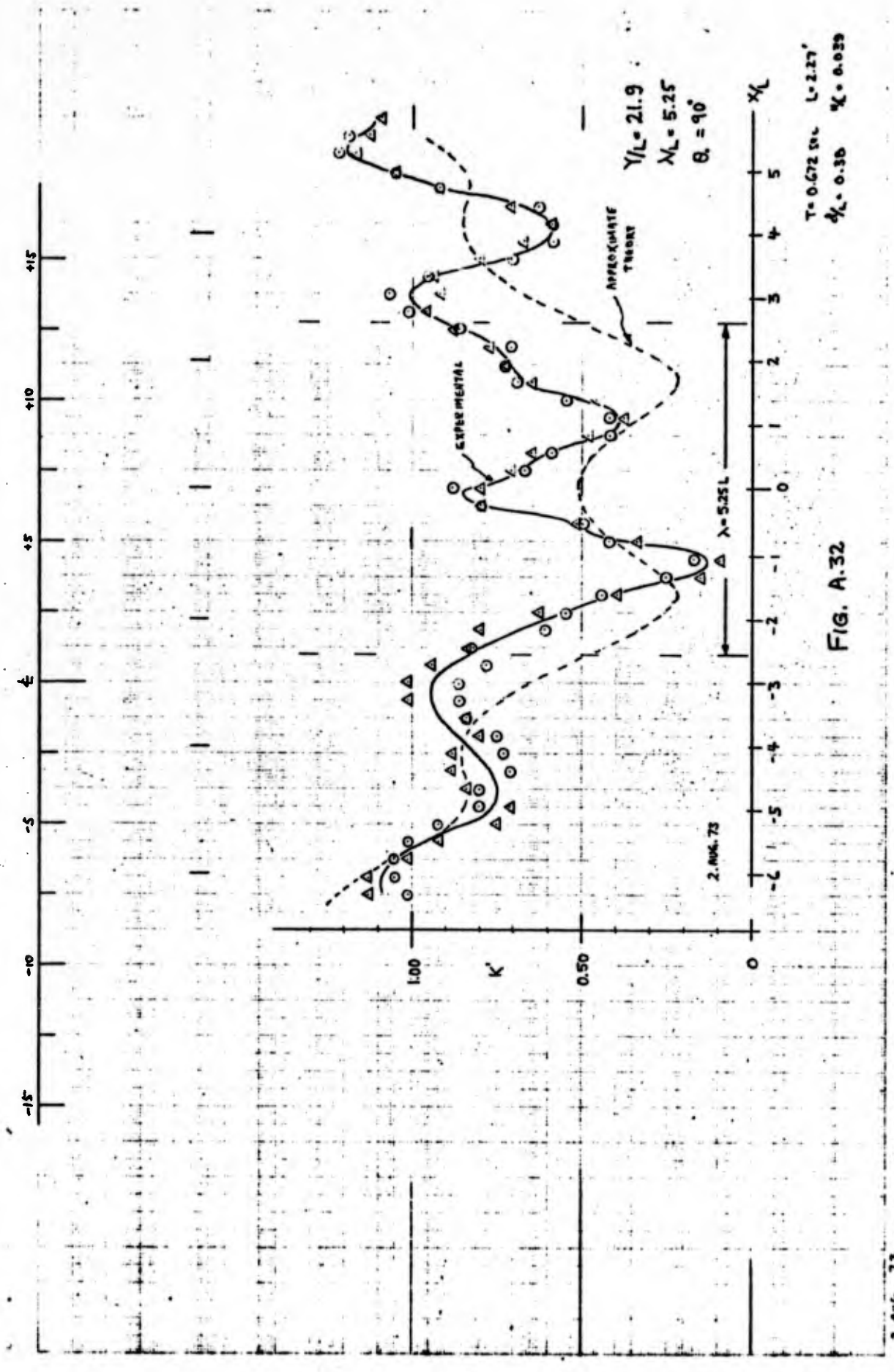
Y/L = 21.9
λ/L = 5.25
θ = 90°
T = 0.672 sec
L = 2.27'
k = 0.35
k = 0.039
EXPERIMENTAL
APPROXIMATE THEORY
λ = 5.25L
2 AUG. 73
K'
1.00
0.50
0
x/L
+15
+10
+5
0
-5
-10
-15
5
4
3
2
1
0
-1
-2
-3
-4
-5
-6

FIG. A.32

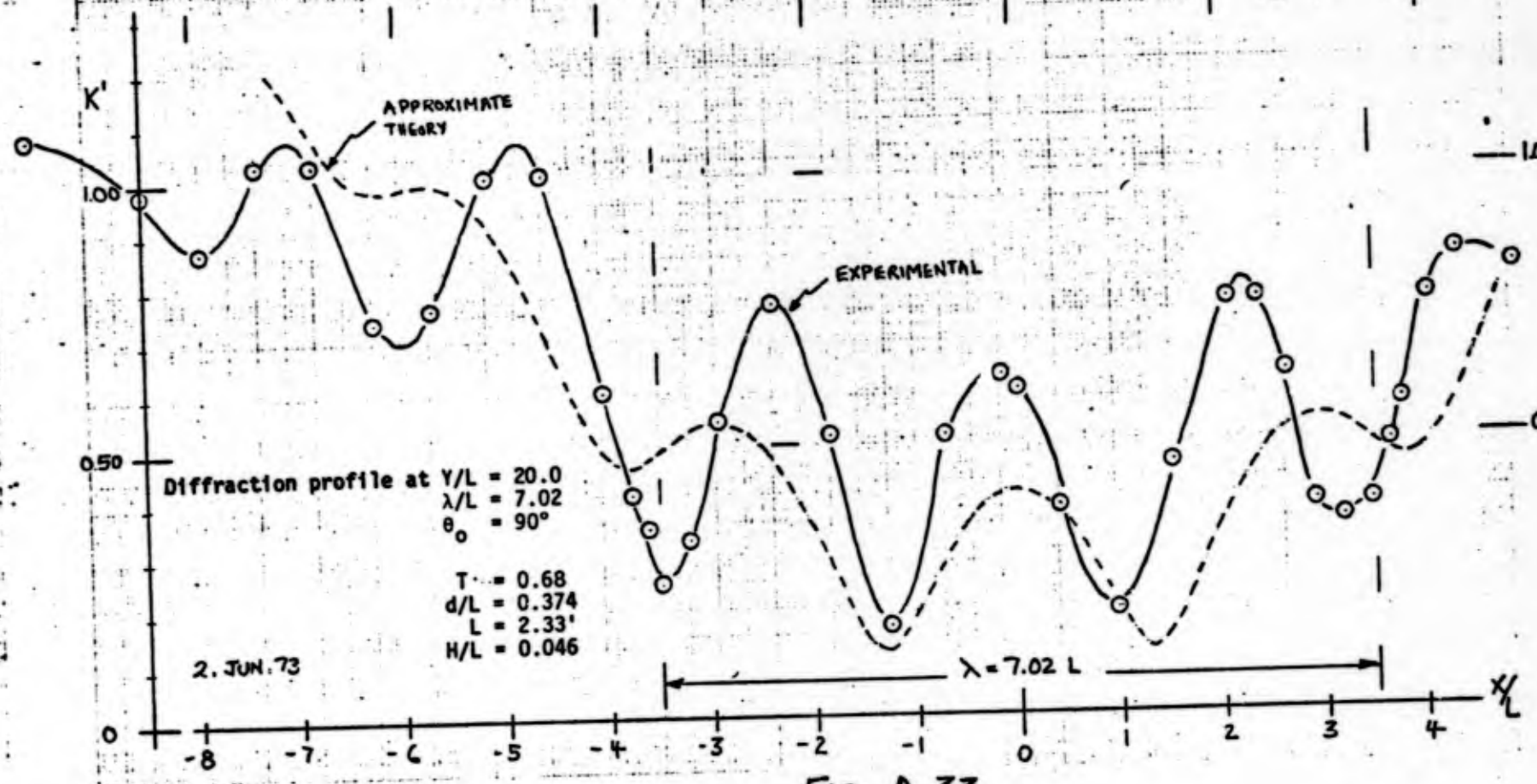
K'
APPROXIMATE THEORY
EXPERIMENTAL
1.00
0.50
0
Diffraction profile at Y/L = 20.0
λ/L = 7.02
θo = 90°
T = 0.68
d/L = 0.374
L = 2.33'
H/L = 0.046
2. JUN. 73
λ = 7.02 L
X/L
-8
-7
-6
-5
-4
-3
-2
-1
0
1
2
3
4

FIG. A.33

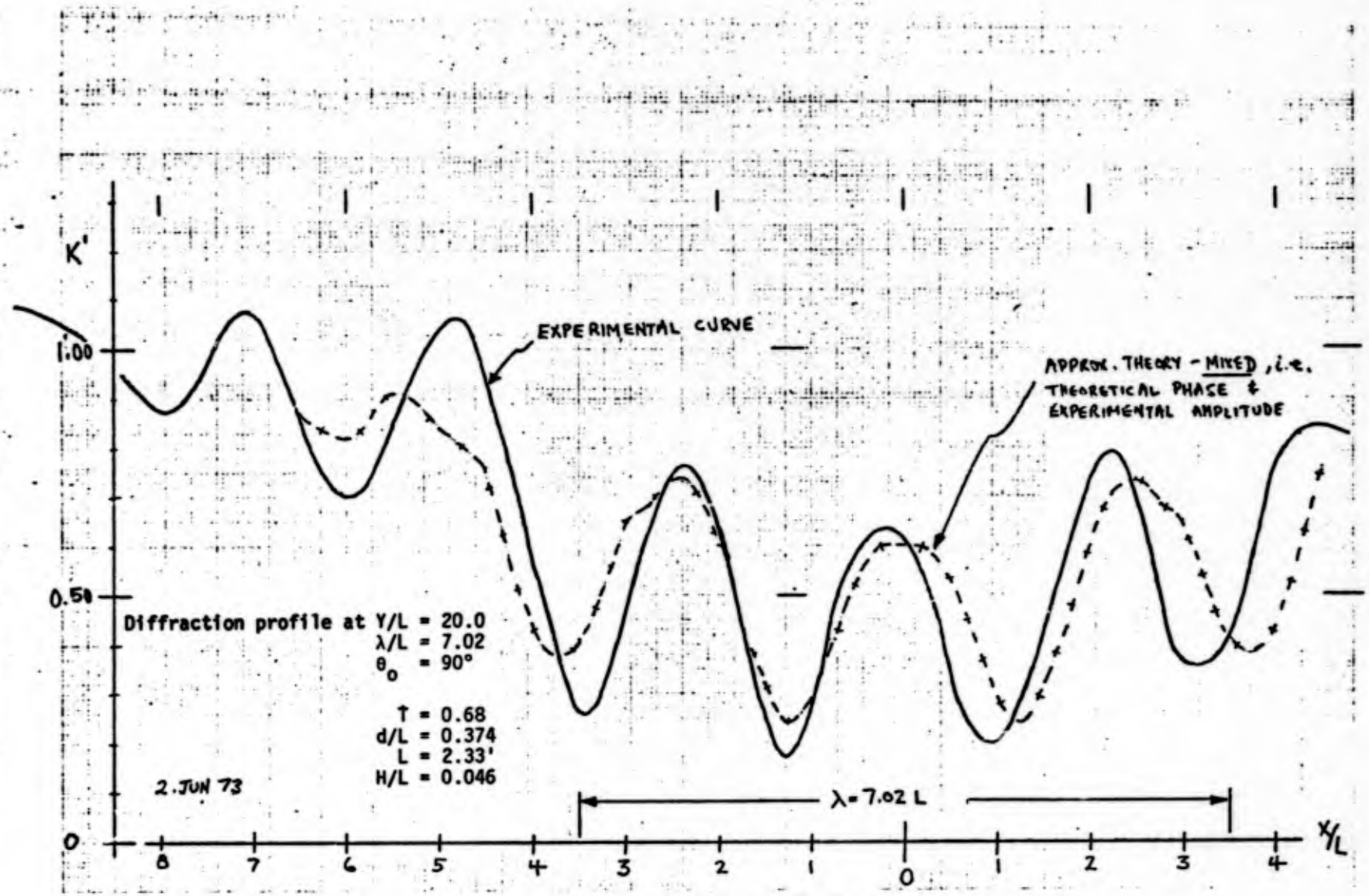
K'
1.00
0.50
0
EXPERIMENTAL CURVE
APPROX. THEORY - MIXED, i.e. THEORETICAL PHASE & EXPERIMENTAL AMPLITUDE
Diffraction profile at Y/L = 20.0
λ/L = 7.02
θo = 90°
T = 0.68
d/L = 0.374
L = 2.33'
H/L = 0.046
2 JUN 73
λ = 7.02 L
8 7 6 5 4 3 2 1 0 1 2 3 4
X/L

FIG. A.34

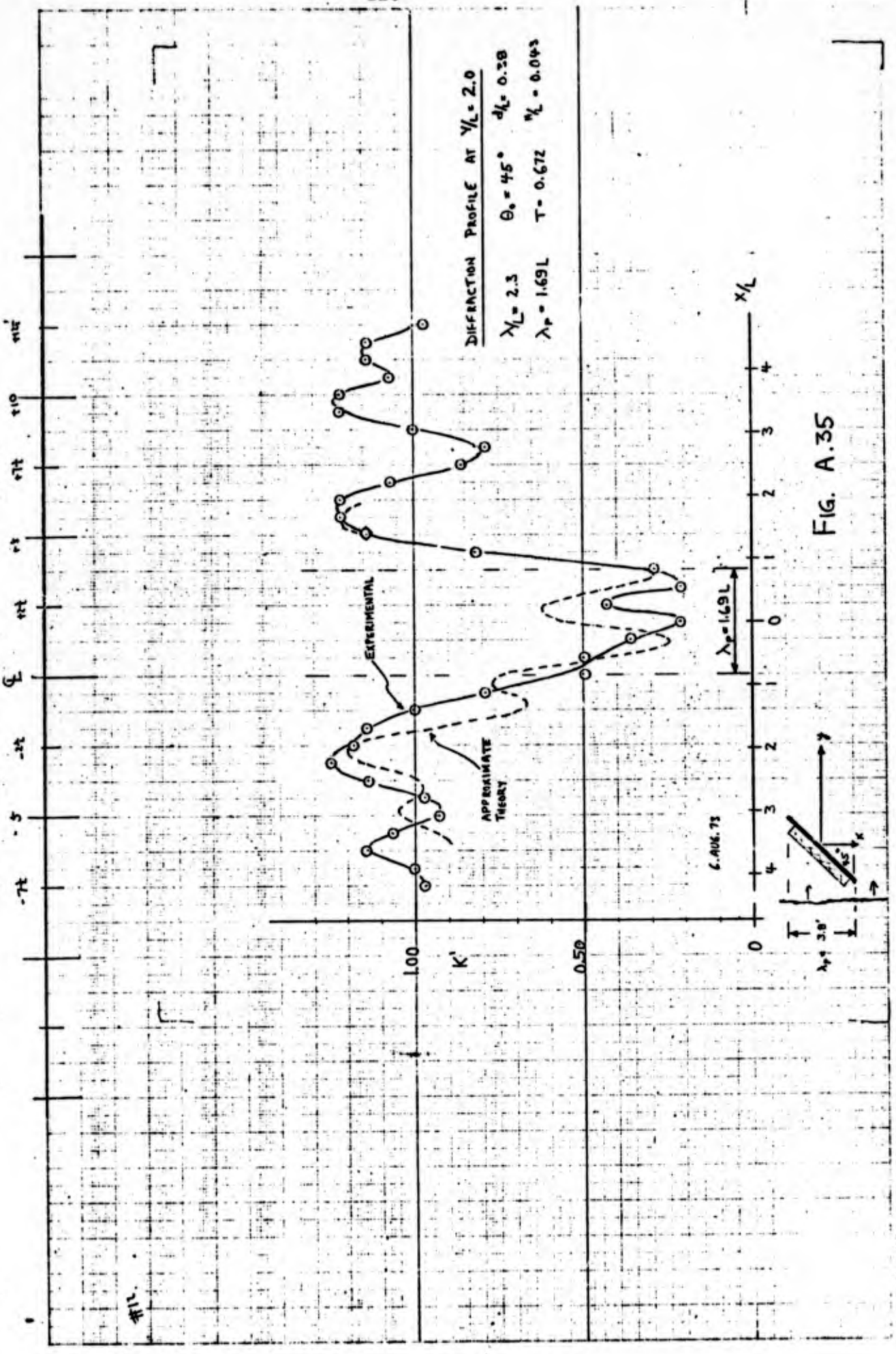
DIFFRACTION PROFILE AT Y/L = 2.0
λ/L = 2.3
θ₀ = 45°
d/L = 0.38
λp = 1.69L
T = 0.672
%L = 0.043
EXPERIMENTAL
APPROXIMATE THEORY
λp=1.69L
X/L
K'
1.00
0.50
6 AUG. 72
#12
RUN II
6 Aug 72 #12 Run 2 & 3 (arrays)

FIG. A.35

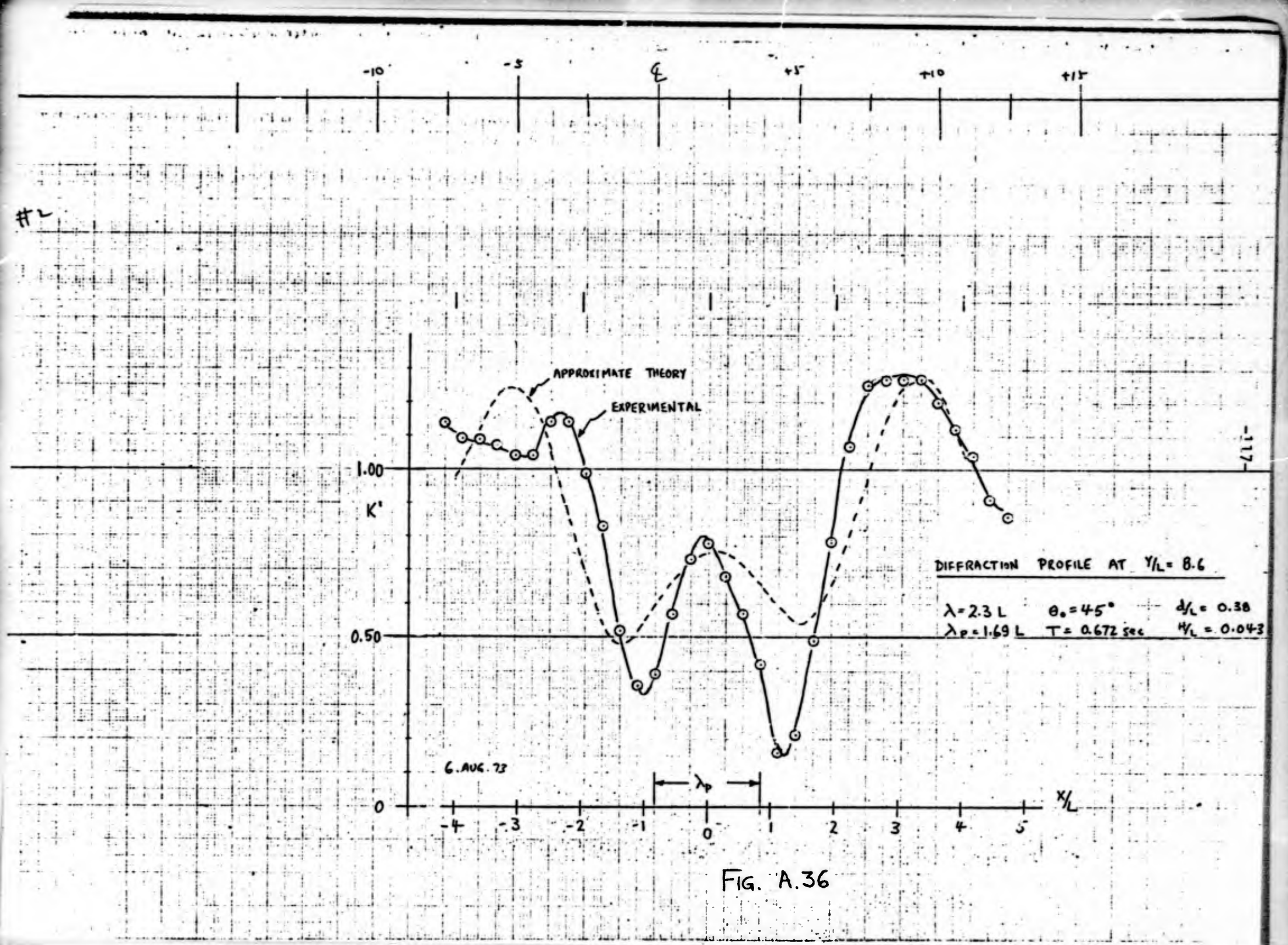
-10
-5
℄
+5
+10
+15
#2
APPROXIMATE THEORY
EXPERIMENTAL
1.00
K'
0.50
0
6. AUG. 73
λ_p
-4
-3
-2
-1
0
1
2
3
4
5
X/L
DIFFRACTION PROFILE AT Y/L = 8.6
λ = 2.3 L
θ₀ = 45°
d/L = 0.38
λp = 1.69 L
T = 0.672 sec
H/L = 0.043
-117-

FIG. A.36

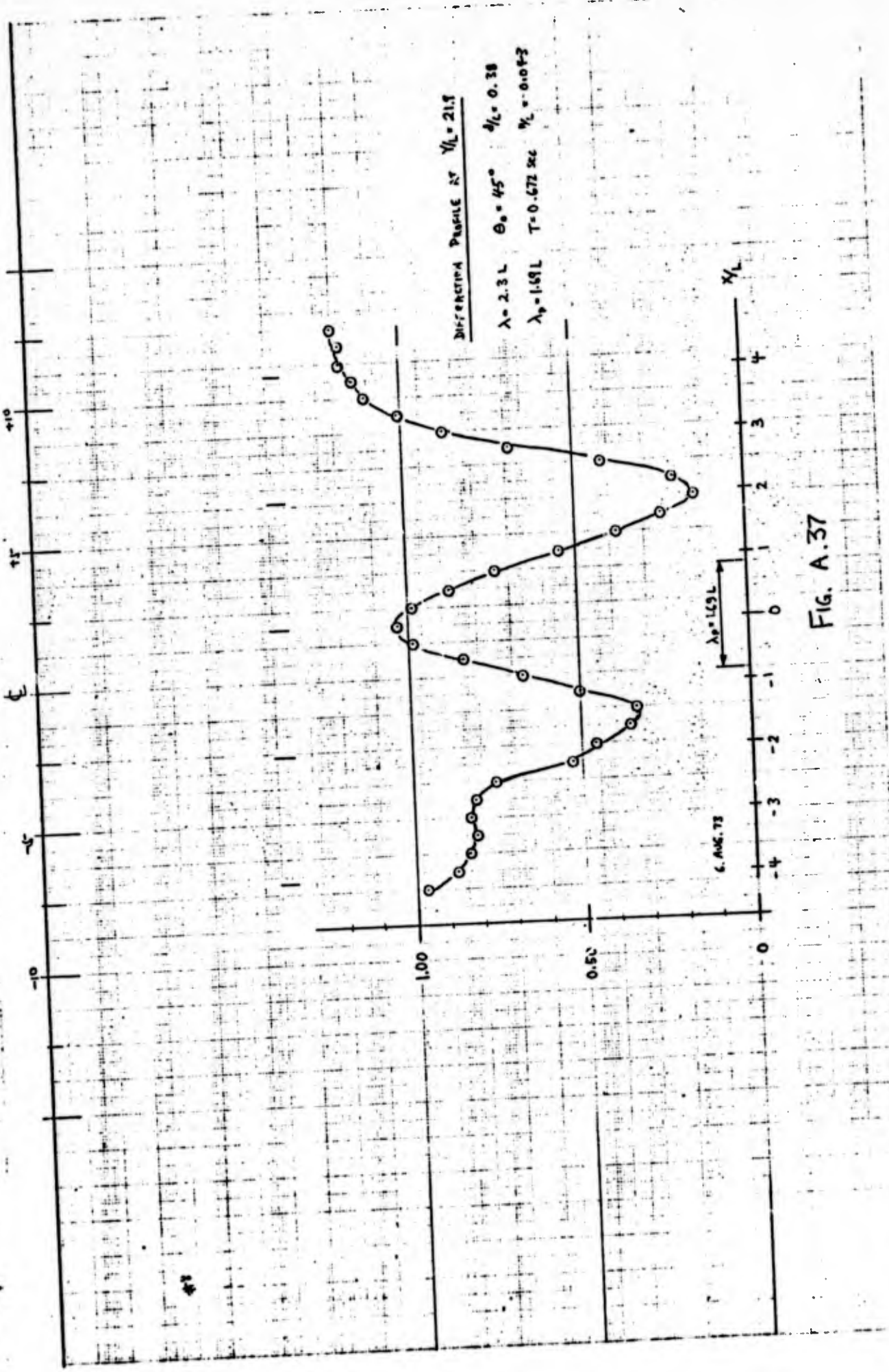
DIFFRACTION PROFILE AT Y/L = 21.5
λ = 2.3 L
θ₀ = 45°
d/L = 0.38
λ₀ = 1.69 L
T = 0.672 sec
ν/L = 0.043
X/L
λ₀ = 1.69 L
6 AUG. 73
1.00
0.50
0
+10
+5
-5
-10
6 AUG 73
RUN 11

FIG. A.37

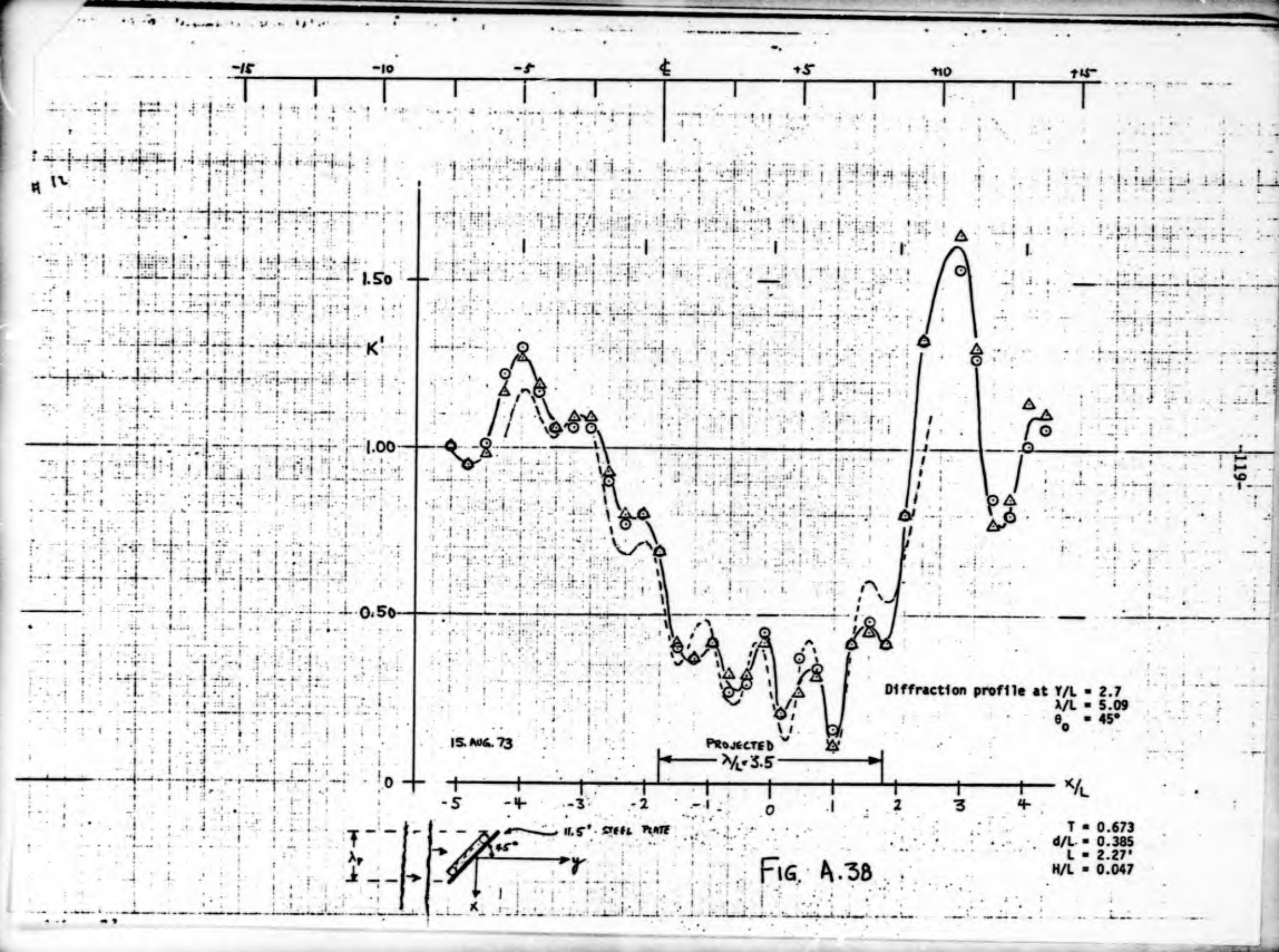
-15
-10
-5
℄
+5
+10
+15
1.50
K'
1.00
0.50
0
-5
-4
-3
-2
-1
0
1
2
3
4
X/L
15. AUG. 73
PROJECTED
λ/L=3.5
Diffraction profile at Y/L = 2.7
λ/L = 5.09
θo = 45°
T = 0.673
d/L = 0.385
L = 2.27'
H/L = 0.047
11.5° STEEL PLATE
45°
λp
y
x

FIG. A.38

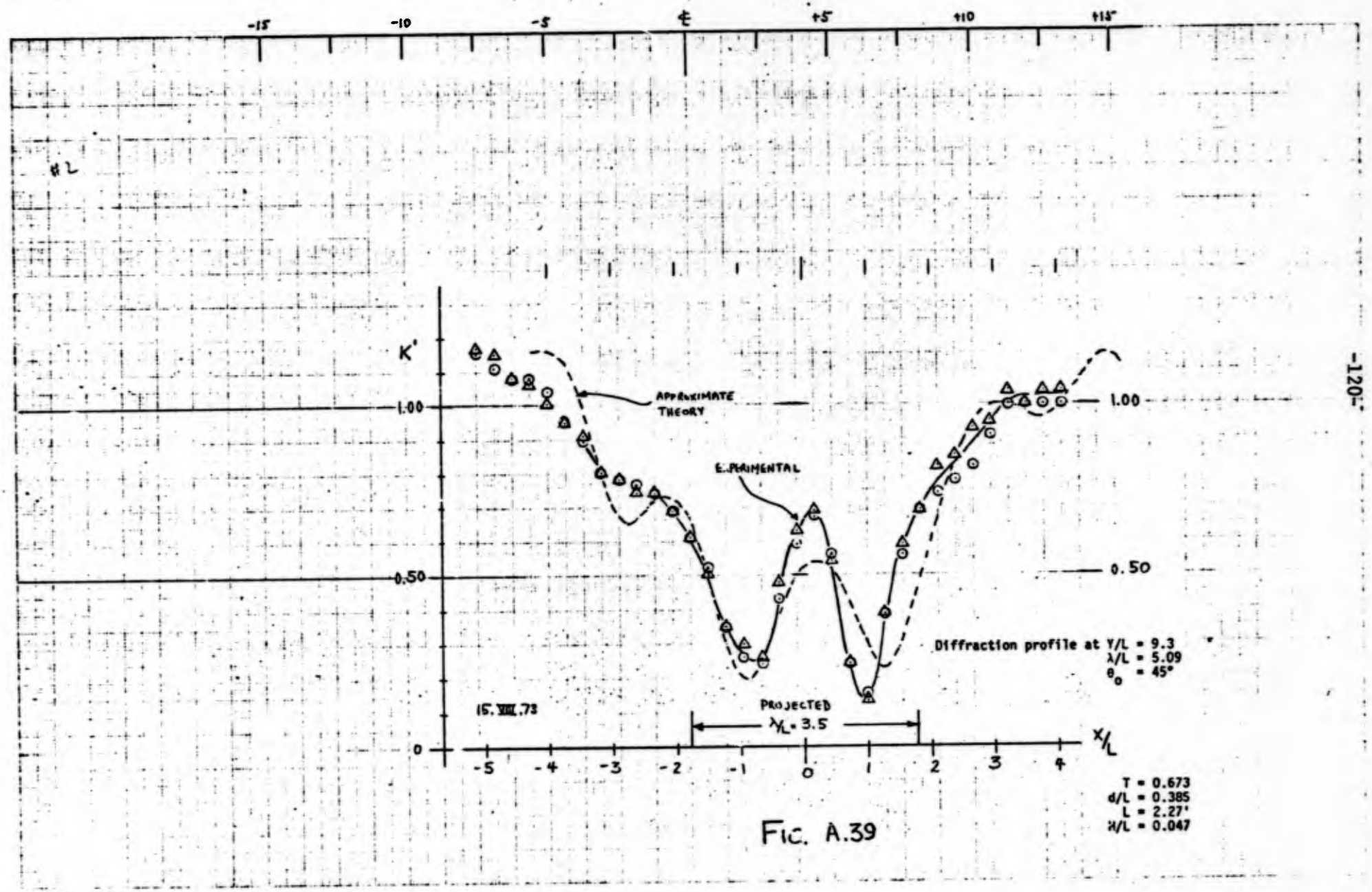
-15
-10
-5
ξ
+5
+10
+15
#2
K'
1.00
0.50
0
APPROXIMATE THEORY
EXPERIMENTAL
1.00
0.50
Diffraction profile at Y/L = 9.3
λ/L = 5.09
θo = 45°
15. VIII. 73
PROJECTED λ/L = 3.5
X/L
-5
-4
-3
-2
-1
0
1
2
3
4
T = 0.673
d/L = 0.385
L = 2.27'
H/L = 0.047
15 AUG RUN I #1

FIG. A.39

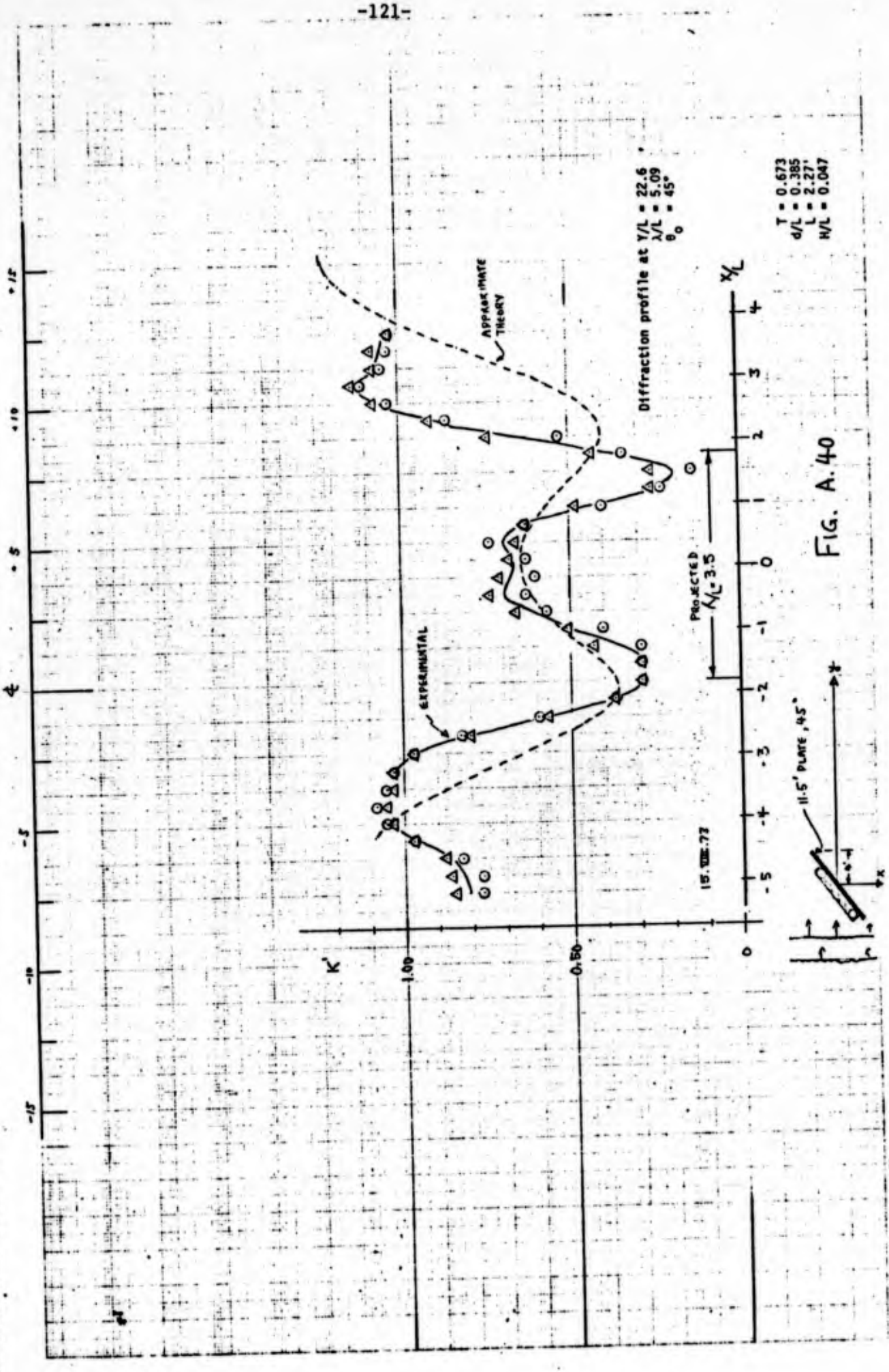
Diffraction profile at Y/L = 22.6
λ/L = 5.09
θ₀ = 45°
T = 0.673
d/L = 0.385
L = 2.27'
H/L = 0.047
APPROXIMATE THEORY
EXPERIMENTAL
PROJECTED
X/L = 3.5
X/L
K'
1.00
0.50
11.5' PLATE, 45°

FIG. A.40

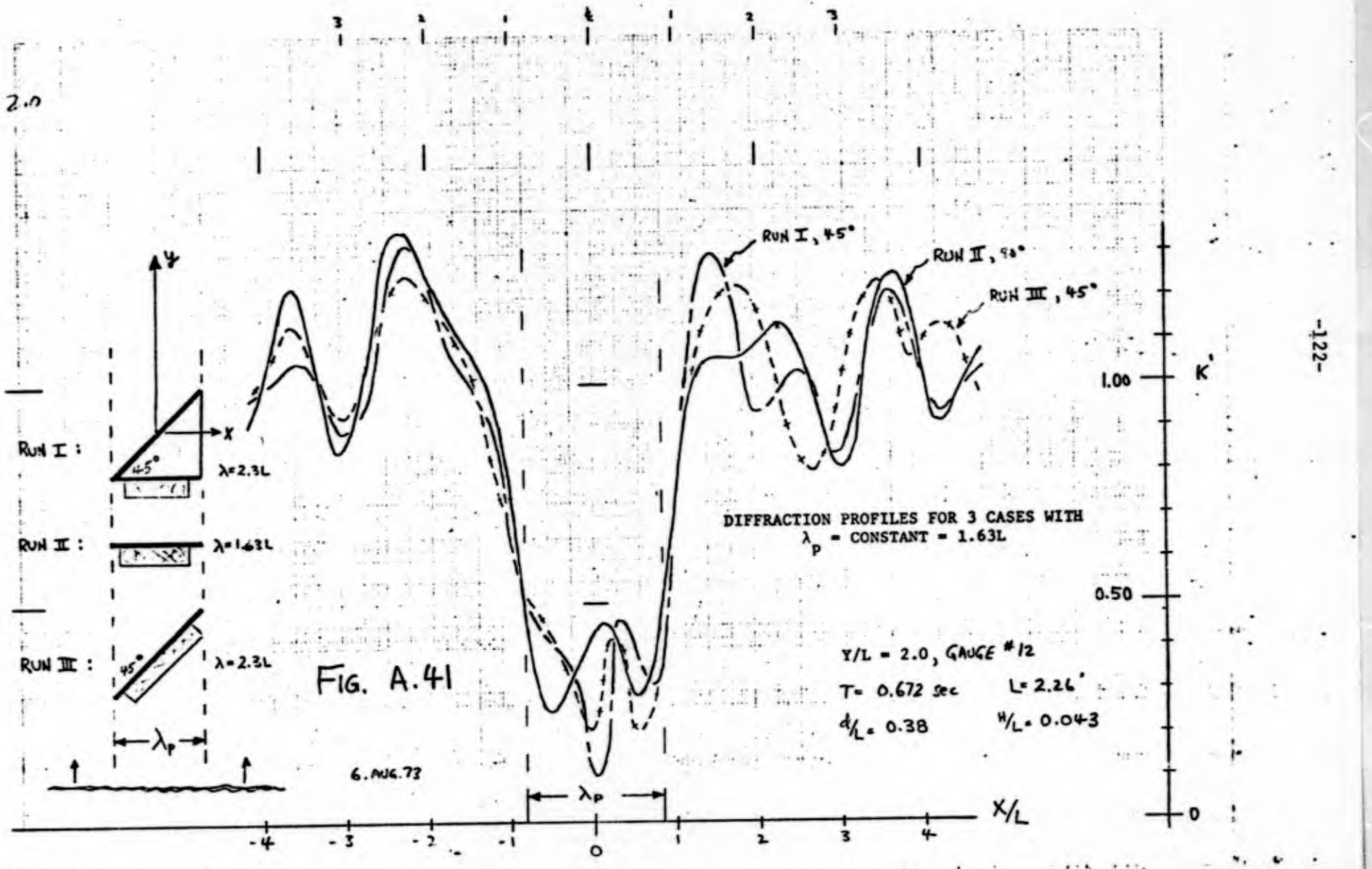
Y/L = 2.0
RUN I, 45°
RUN II, 90°
RUN III, 45°
RUN I :
45°
λ=2.3L
RUN II :
λ=1.63L
RUN III :
45°
λ=2.3L
ψ
X
λp
DIFFRACTION PROFILES FOR 3 CASES WITH
λp = CONSTANT = 1.63L
Y/L = 2.0, GAUGE #12
T= 0.672 sec
L= 2.26'
d/L = 0.38
H/L = 0.043
6. AUG. 73
X/L
K'
1.00
0.50
0
-4
-3
-2
-1
0
1
2
3
4

FIG. A.41

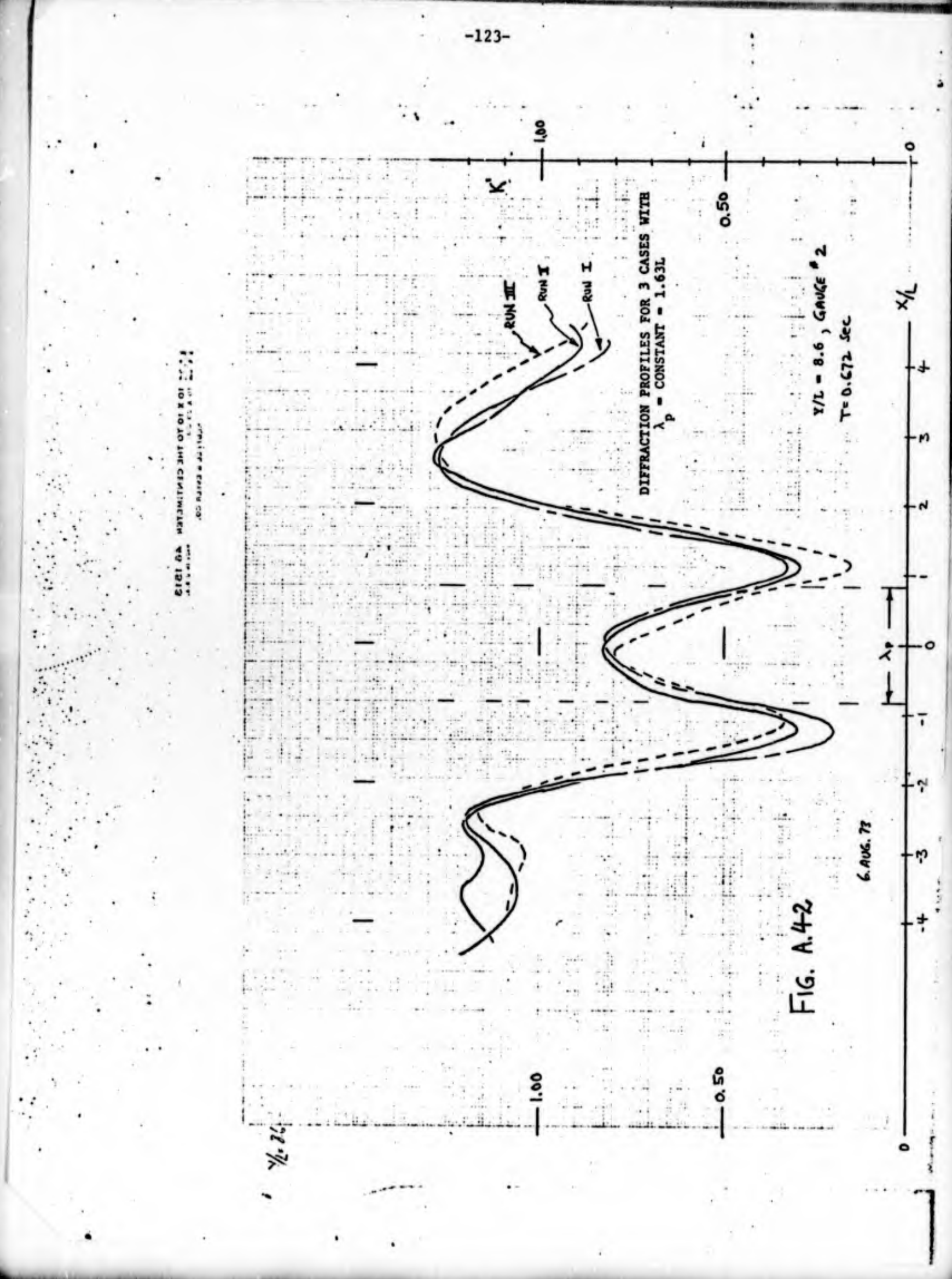
DIFFRACTION PROFILES FOR 3 CASES WITH
λ_p = CONSTANT = 1.63L
Y/L = 8.6 , GAUGE # 2
T= 0.672 Sec
RUN III
RUN II
RUN I
K'
X/L
1.00
0.50
0
1
2
3
4
-1
-2
-3
-4
λ_p
6 AUG. 71

FIG. A.42

1/L = 21.4

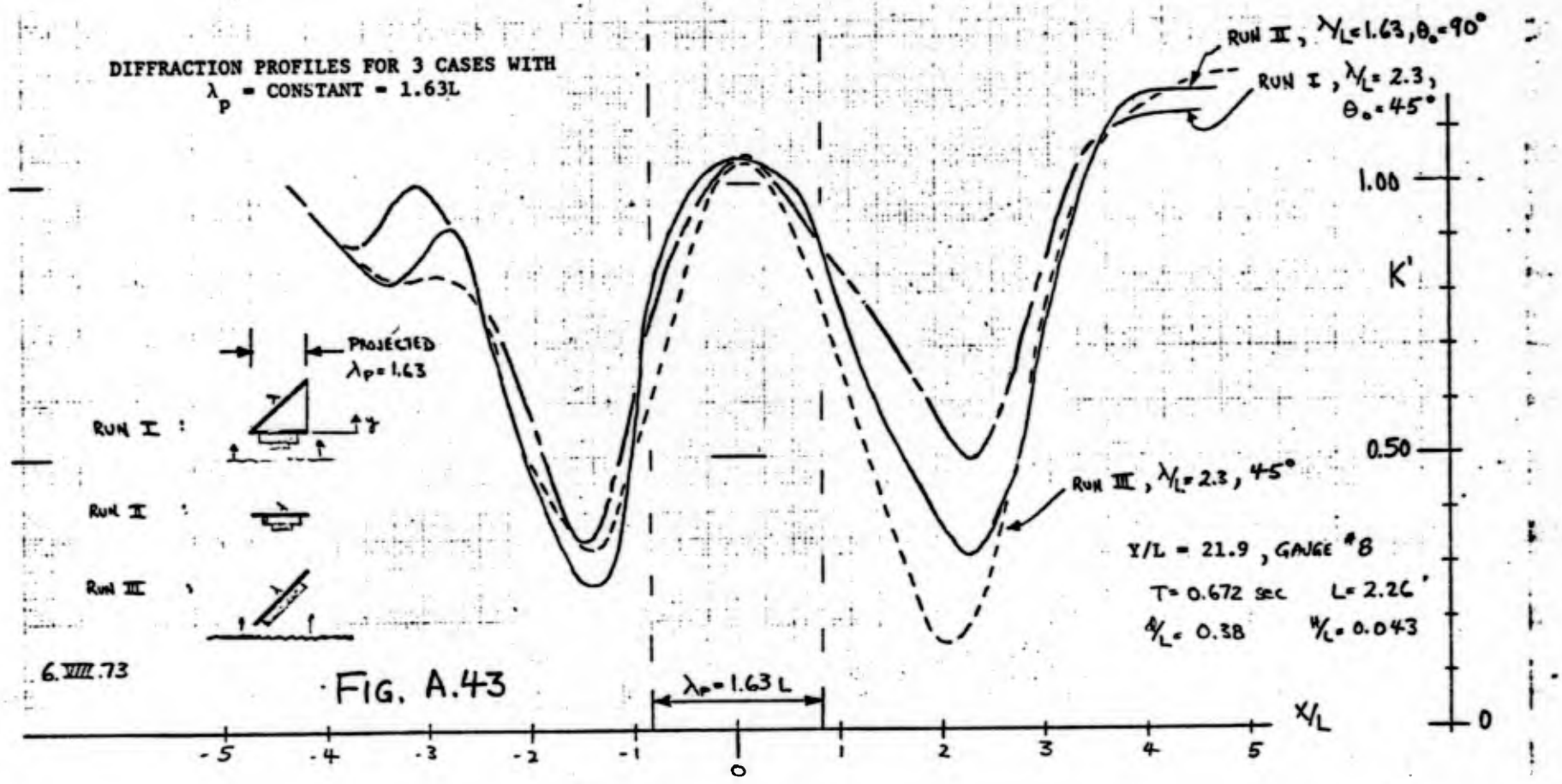
DIFFRACTION PROFILES FOR 3 CASES WITH
λ_p = CONSTANT = 1.63L
RUN II , λ/L=1.63, θ_o=90°
RUN I , λ/L= 2.3, θ_o=45°
RUN III , λ/L= 2.3, 45°
PROJECTED λ_p=1.63
RUN I :
RUN II :
RUN III :
Y/L = 21.9 , GAUGE #8
T= 0.672 sec L= 2.26'
d/L = 0.38 H/L = 0.043
6.VIII.73
FIG. A.43
λ_p=1.63 L
K'
1.00
0.50
0
X/L
-5 -4 -3 -2 -1 0 1 2 3 4 5

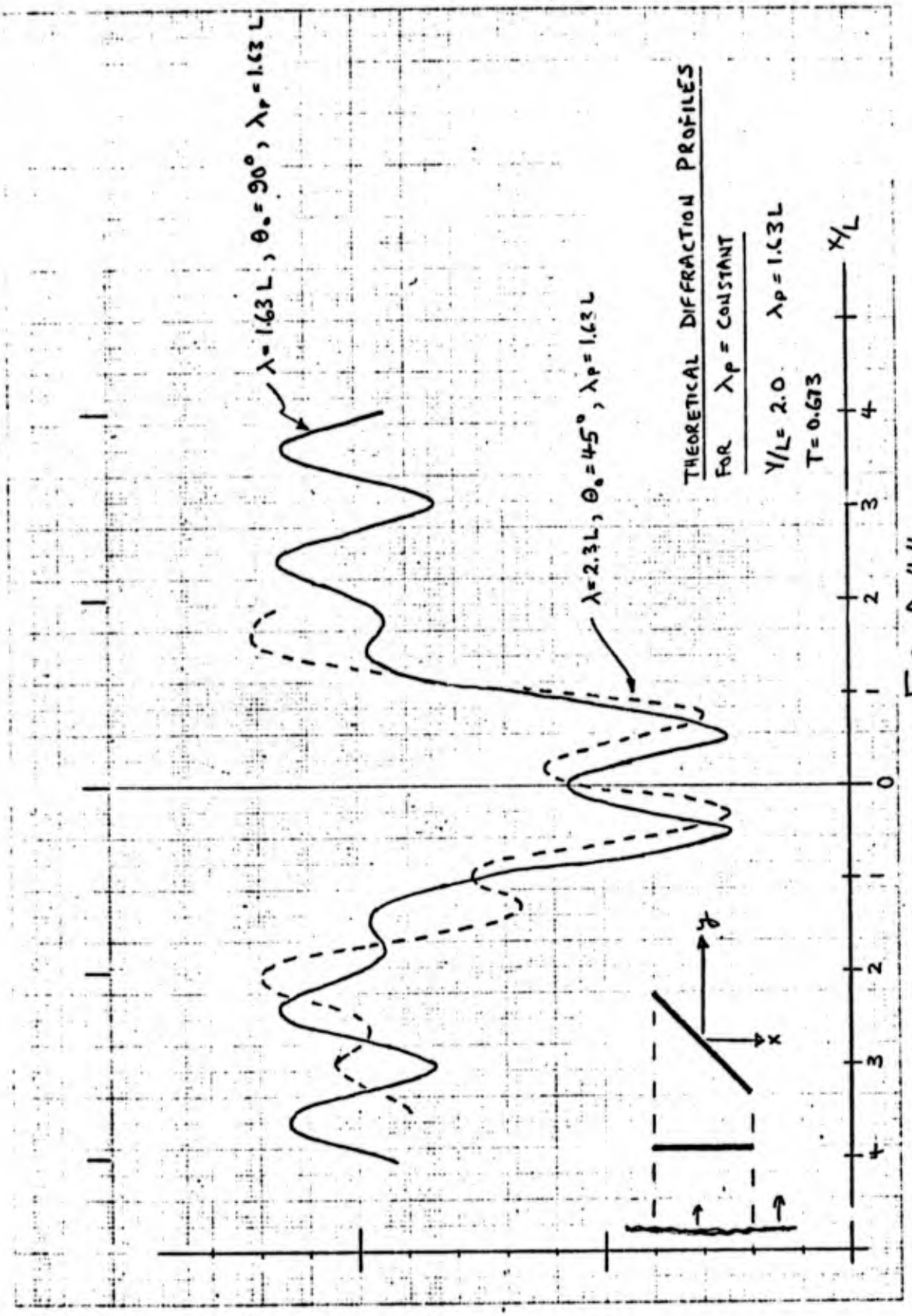
λ=1.63 L, θ₀=90°, λp=1.63 L
λ=2.3L, θ₀=45°, λp=1.63 L
THEORETICAL DIFFRACTION PROFILES
FOR λp = CONSTANT
Y/L= 2.0 λp=1.63L
T=0.673
X/L
0
1
2
3
4
y
x

FIG. A.44

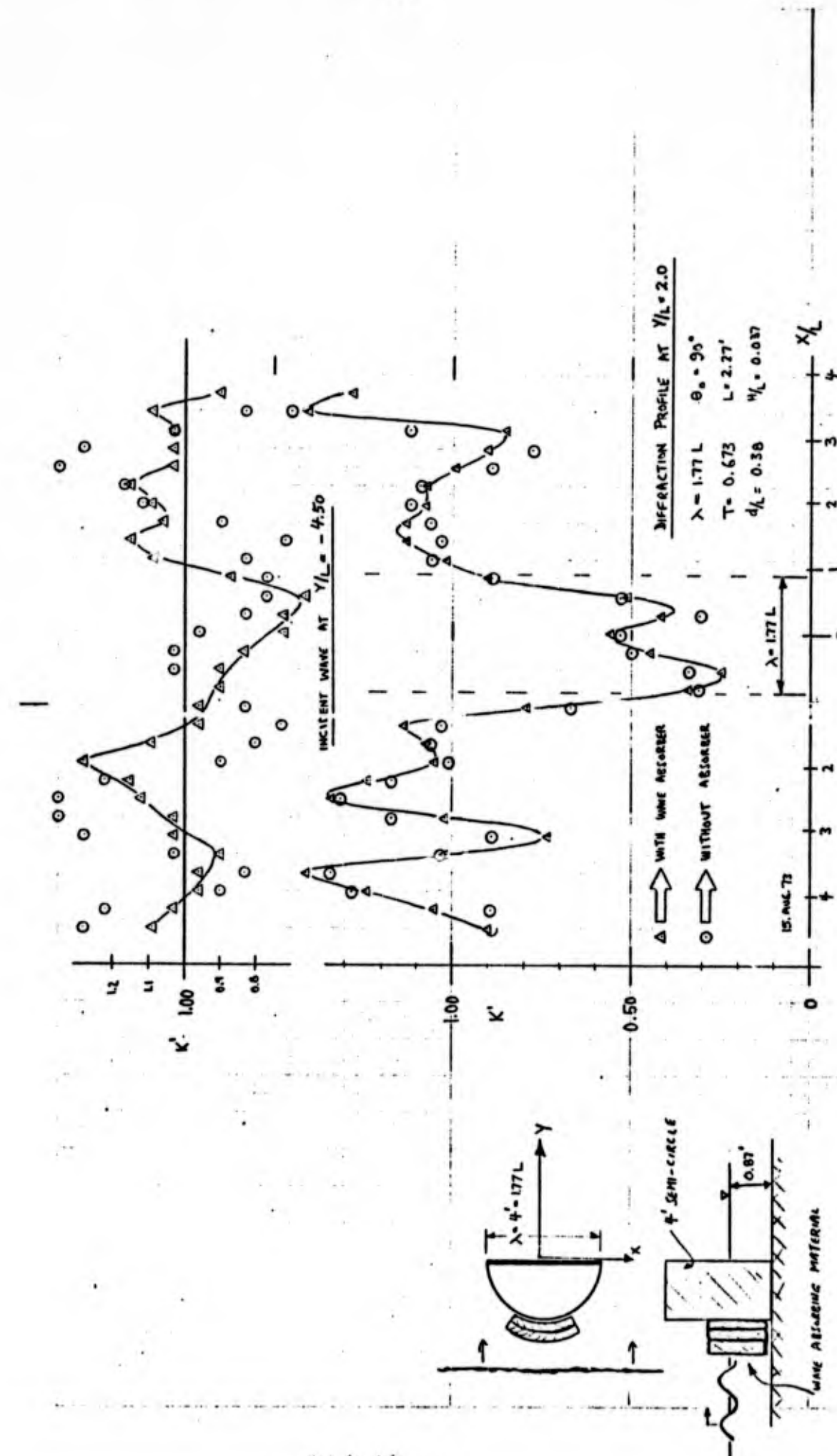
INCIDENT WAVE AT Y/L = -4.50
DIFFRACTION PROFILE AT Y/L = 2.0
λ = 1.77 L
T = 0.673
d/L = 0.38
θ₀ = 90°
L = 2.27'
H/L = 0.037
WITH WAVE ABSORBER
WITHOUT ABSORBER
15. AUG. 73
K'
X/L
λ = 1.77 L
λ = 4' = 1.77 L
4' SEMI-CIRCLE
0.83'
WAVE ABSORBING MATERIAL

FIG. A. 4-5

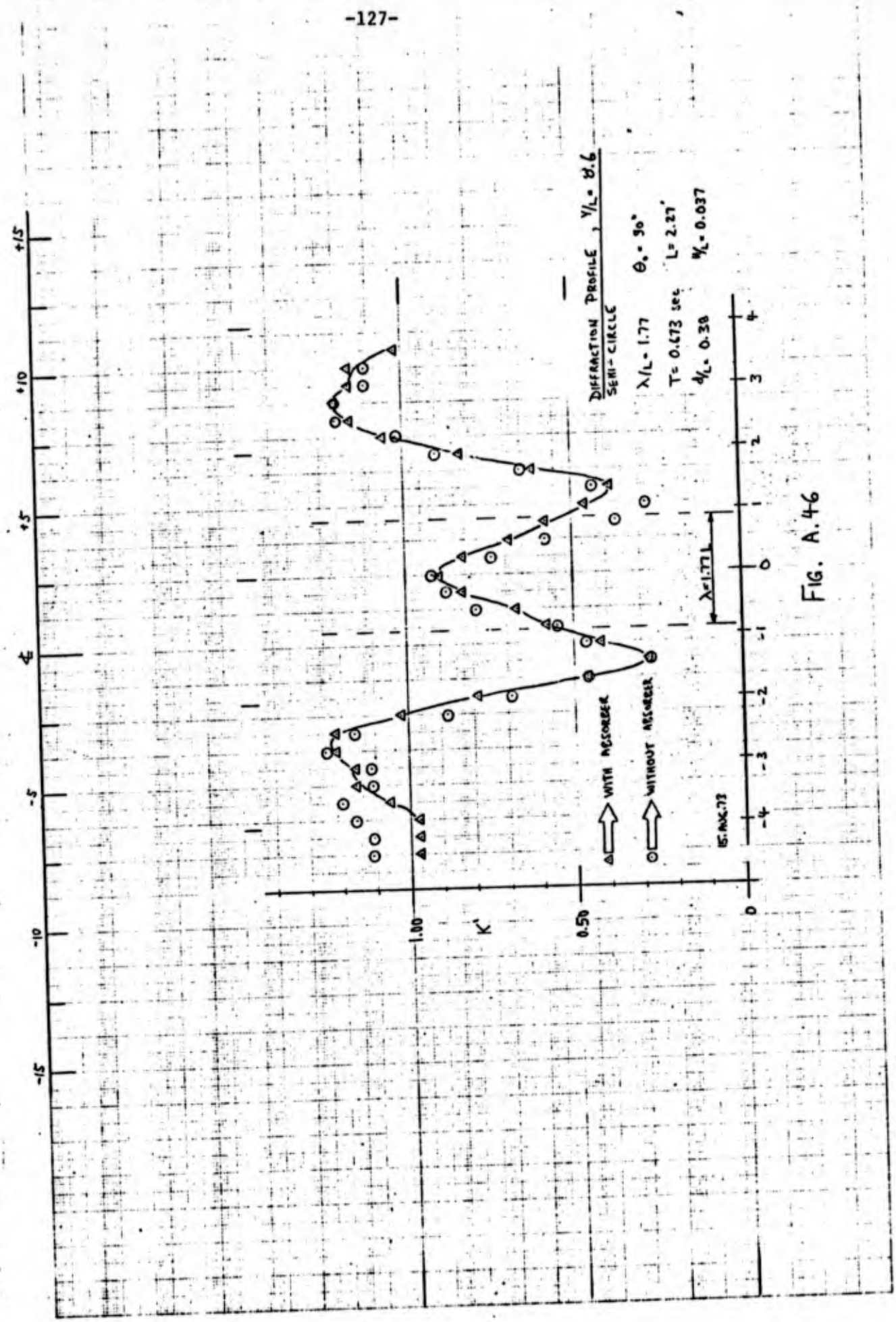

FIG. A.46

15 Aug 73 #2.
RUN II

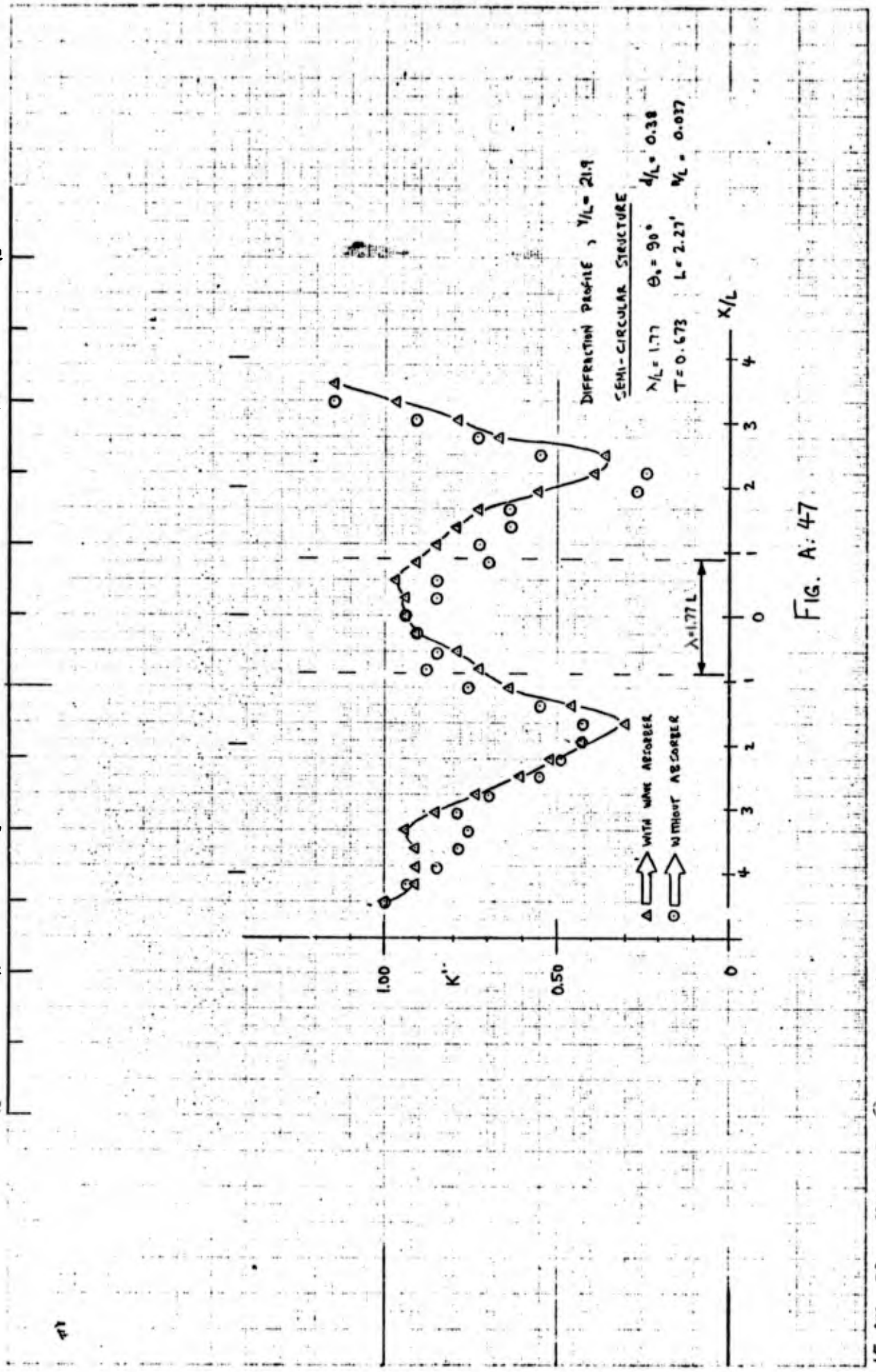
DIFFRACTION PROFILE , Y/L = 21.9
SEMI-CIRCULAR STRUCTURE
λ/L = 1.77
θ₀ = 90°
d/L = 0.38
T = 0.673
L = 2.27'
W/L = 0.017
WITH WAVE ABSORBER
WITHOUT ABSORBER
K'
1.00
0.50
X/L
λ=1.77 L
+15
+10
+5
0
-5
-10
-15
15 AUG 73
SEMI-CIRCLE
RUN IX

FIG. A: 47

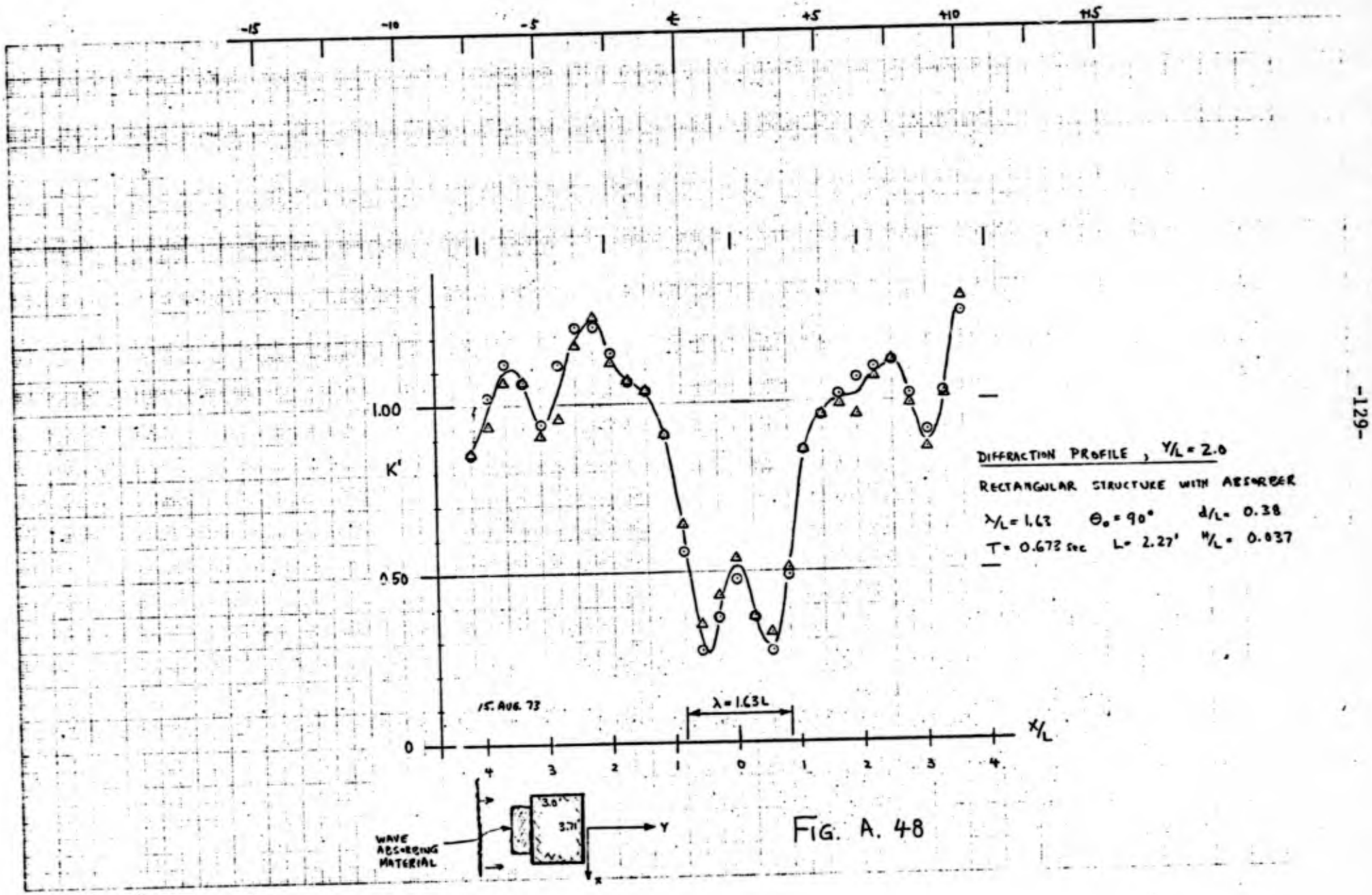
-15
-10
-5
+5
+10
+15
1.00
K'
.50
0
15 AUG 73
λ = 1.63L
X/L
4
3
2
1
0
1
2
3
4
3.0
3.71
Y
x
WAVE ABSORBING MATERIAL
DIFFRACTION PROFILE, Y/L = 2.0
RECTANGULAR STRUCTURE WITH ABSORBER
λ/L = 1.63 θ₀ = 90° d/L = 0.38
T = 0.673 sec L = 2.27' H/L = 0.037
15 AUG 73
#12 RUN 2

FIG. A. 48

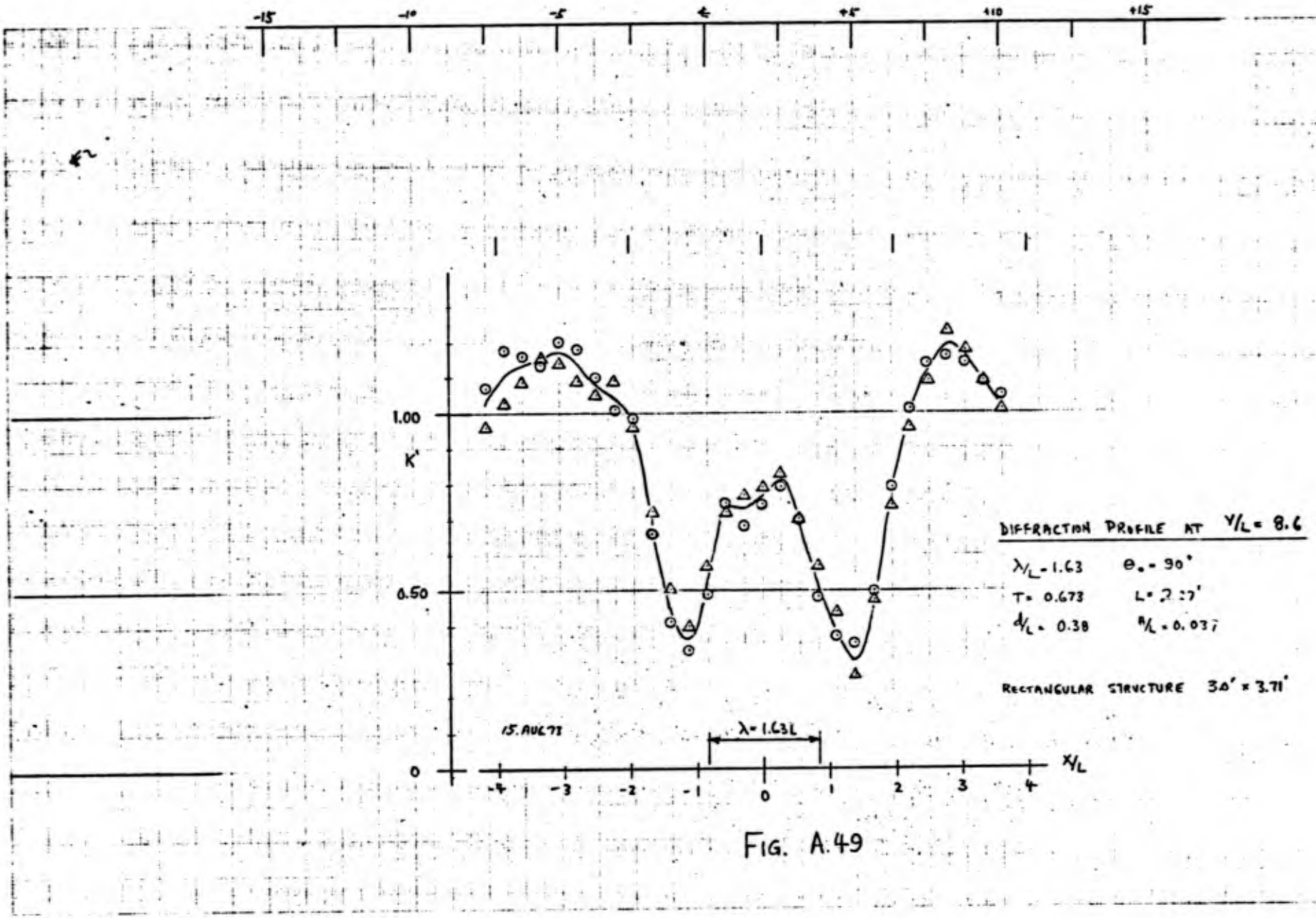
-15
-10
-5
0
+5
+10
+15
1.00
K'
0.50
0
-4
-3
-2
-1
0
1
2
3
4
X/L
15. AUG 73
λ = 1.63L
DIFFRACTION PROFILE AT Y/L = 8.6
λ/L = 1.63
θ = 90°
T = 0.673
L = 2.27'
d/L = 0.38
R/L = 0.037
RECTANGULAR STRUCTURE 30' × 3.71'
15 AUG 73 RUN II

FIG. A.49

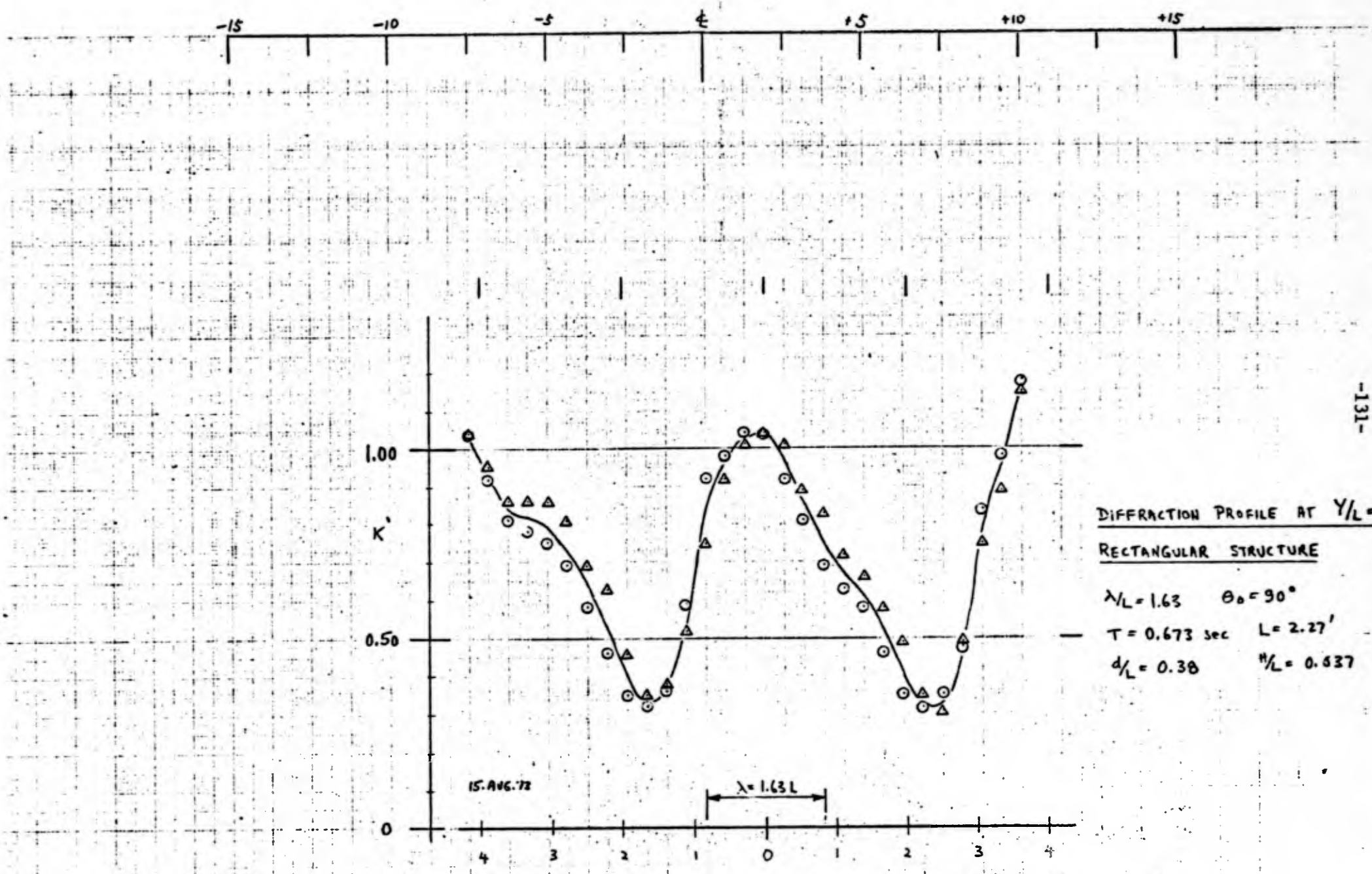

DIFFRACTION PROFILE AT $Y/L = 21.$

RECTANGULAR STRUCTURE

$\lambda/L = 1.63$ $\theta_0 = 90°$

$T = 0.673$ sec $L = 2.27'$

$d/L = 0.38$ $H/L = 0.637$

FIG. A.50

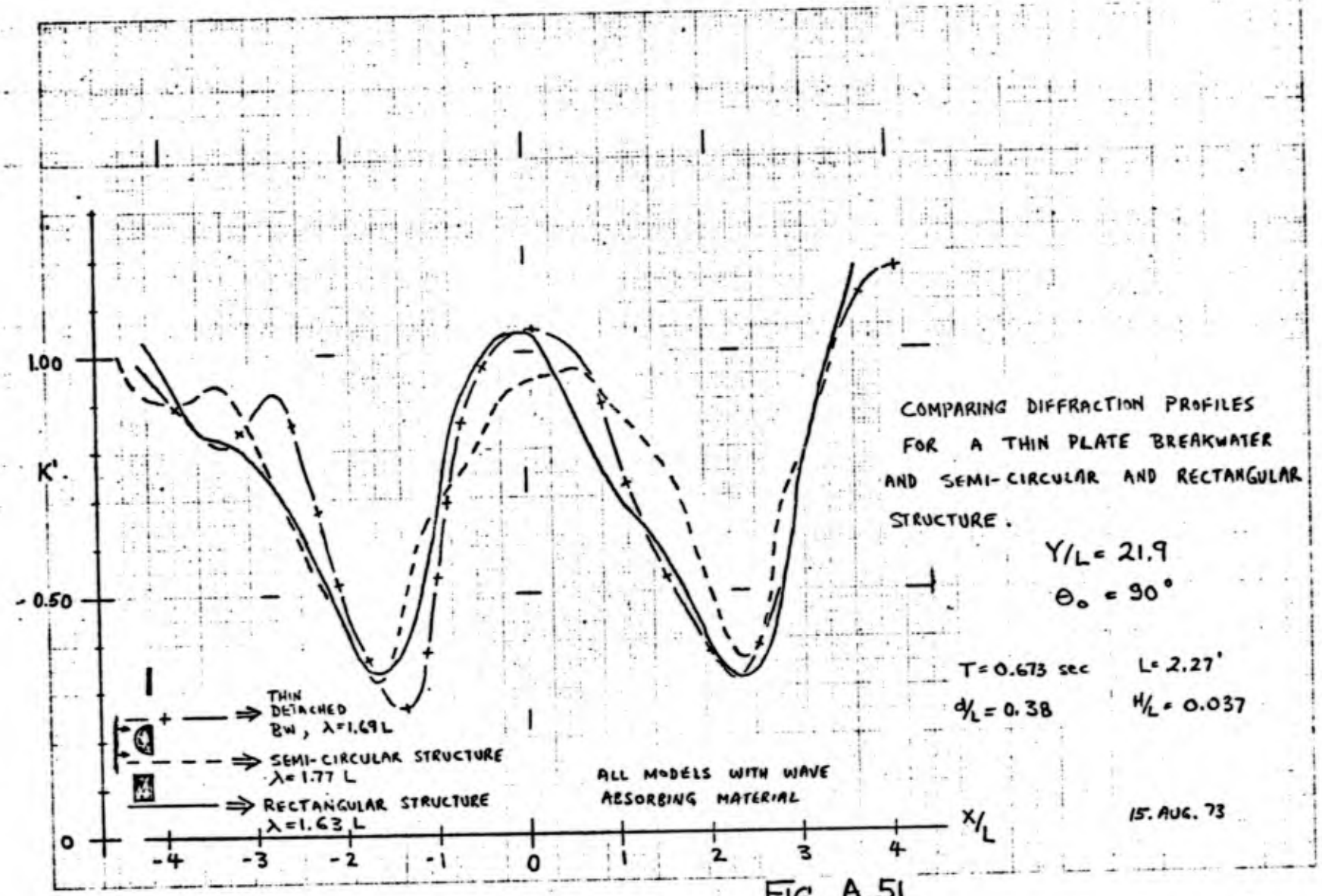
1.00
K'
0.50
0
-4
-3
-2
-1
0
1
2
3
4
X/L
THIN DETACHED BW, λ=1.69 L
SEMI-CIRCULAR STRUCTURE λ=1.77 L
RECTANGULAR STRUCTURE λ=1.63 L
ALL MODELS WITH WAVE ABSORBING MATERIAL
COMPARING DIFFRACTION PROFILES FOR A THIN PLATE BREAKWATER AND SEMI-CIRCULAR AND RECTANGULAR STRUCTURE.
Y/L = 21.9
θ₀ = 90°
T = 0.673 sec
L = 2.27'
d/L = 0.38
H/L = 0.037
15. AUG. 73

FIG. A.51

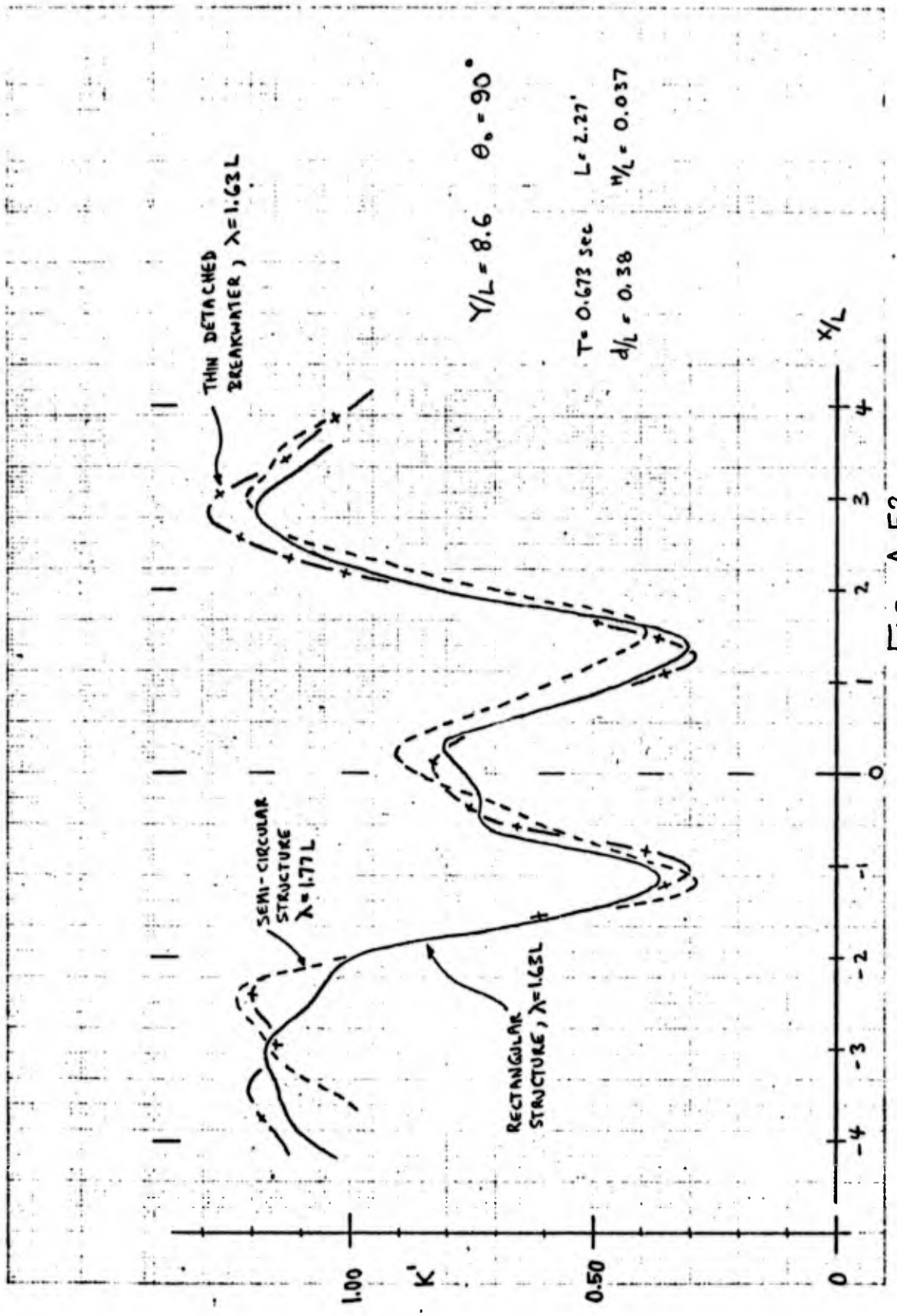
THIN DETACHED BREAKWATER, λ=1.63L
Y/L = 8.6
θ₀ = 90°
T = 0.673 sec
L = 2.27'
d/L = 0.38
H/L = 0.037
SEMI-CIRCULAR STRUCTURE λ=1.77L
RECTANGULAR STRUCTURE, λ=1.63L
K'
1.00
0.50
0
X/L
-4
-3
-2
-1
0
1
2
3
4

FIG. A.52

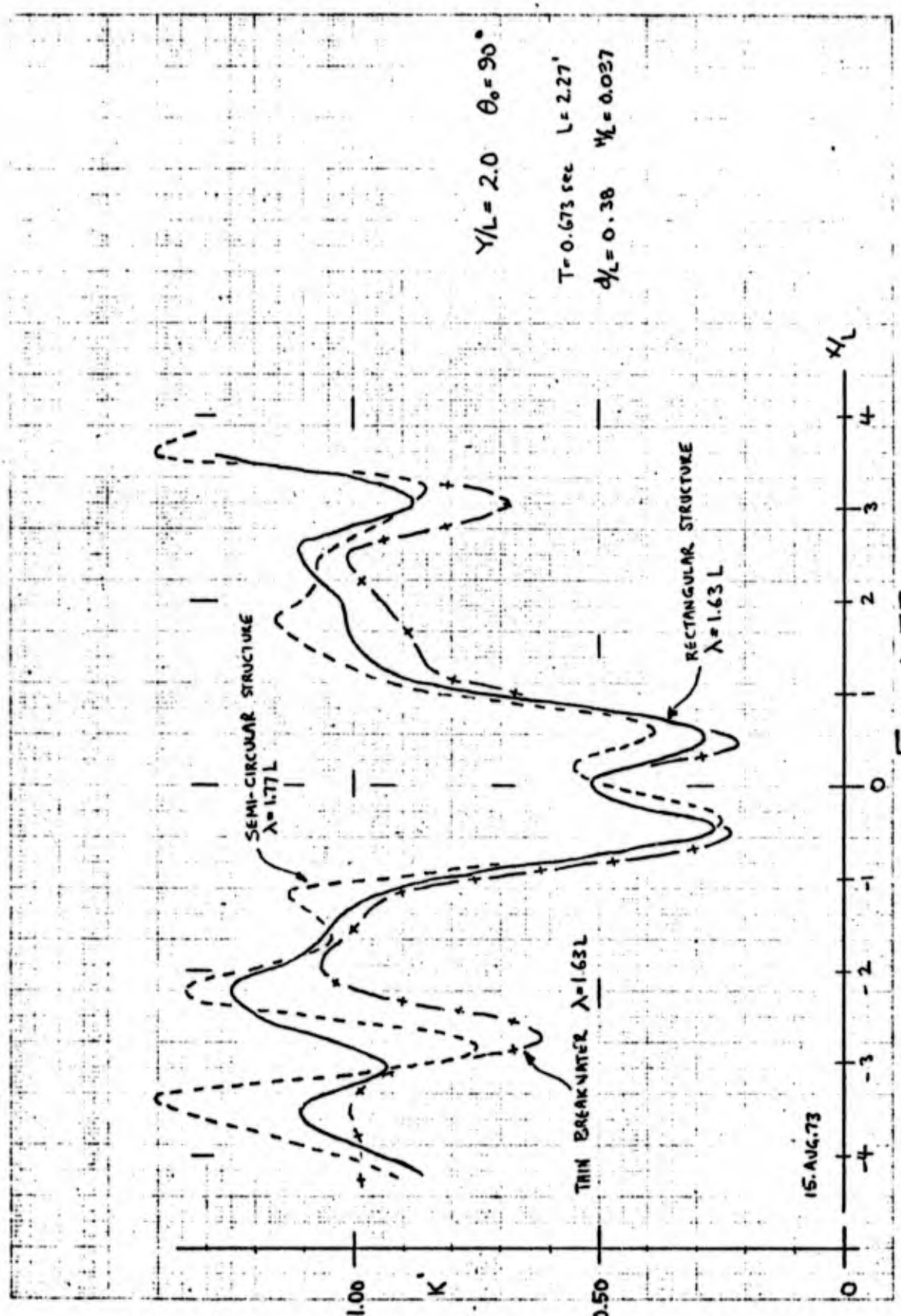
Y/L = 2.0 θ₀ = 90°
T = 0.673 sec L = 2.27'
d/L = 0.38 H/L = 0.037
SEMI-CIRCULAR STRUCTURE λ = 1.77 L
RECTANGULAR STRUCTURE λ = 1.63 L
THIN BREAKWATER λ = 1.63 L
15 AUG 73
K'
1.00
0.50
0
X/L
4
3
2
1
0
-1
-2
-3
-4

FIG. A.53

APPENDIX B

COMPUTER PROGRAMS WDIFFR AND FRSNL

FIG.B1 SUBROUTINE WDIFFR, TO CALCULATE WAVE DIFFRACTION BY SEMI-INFINITE BREAKWATER WITH THE AID OF SUBROUTINE FRSNL.

```
      SUBROUTINE WDIFFR ( WLX, ANG, X, Y, P , AA , BB , WA , PH , RG )
C     WAVE NUMBER = WK
      DATA RGQ/6H  Q    /,RGR/6H  R    /,RGS/6H  S    /
      COMPLEX  D(1), A(1) , F(1), U(1) ,W(1)
C     AG= ANGLE  IN RADIANS
      WK = 6.2831843 /WLX
      AG=ANG    * .0174532925
      CA = WK * COS ( AG)
      SA = WK * SIN ( AG )
C     R =  DISTANCE FROM THE ORIGIN
      R =       SQRT (X    ** 2 + Y     **2 )
      WR=R*WK
      P = X    * CA + Y     * SA
      Q=X    * CA-Y    * SA
      AY = ABS(Y    )
C     TT IS USED TO TEST FOR REGION OF DIFFRACTED WAVE
      TT=X    * SA - CA * AY
C     ZA IS ARGUMENT FOR FRESNEL INTEGRAL ( KR - XCOS A - Y SIN A )
      ZA =WR - P
      ZB =WR - Q
      CALL FRSNL (ZA, U)
      CALL FRSNL (ZB, W )
C     COMPUTATION OF EXP (-IKRCOS (O-O))
      D =  CMPLX (COS (P), - SIN (P) )
      F =  CMPLX (COS (Q), - SIN (Q) )
      U  =U  * (1. , 1. )
      W = W *  ( 1. , 1. )
      IF (TT) 1, 2, 2
2     IF (Y    ) 3, 4, 4
1     A  = (U  * D  + D  - W  * F  + F  )/2.
      RG = RGQ
      GO TO  5
3     A  = (U  * D  + D  + W  * F  + F  )/2.
      RG = RGR
      GO TO  5
4     A = (-U * D + D -W *F + F  ) /2.
      RG = RGS
5     WA = CABS (A )
      AA = REAL ( A)
      BB =    AIMAG ( A )
      PH = ( ATAN2 ( BB, AA ))* 180. / 3.1415926
200   CONTINUE
      RETURN
      END
```

FIG.B2 SUBROUTINE FRSNL, TO COMPUTE THE FRESNEL INTEGRAL (WRITTEN IN FAP LANGUAGE)

```
      SUBROUTINE FRSNL(XA,RESULT)
      DIMENSION COM(24)
      COMPLEX C(12), RESULT
      EQUIVALENCE (C,COM), (TEST,TEMP)
      DATA CLIMIT/0.00005/
      IF(XA) 10,5,10
5     RESULT=0.0
      RETURN
10    DO 12 I=1,12
      COM(I)=0.0
12    CONTINUE
      COM(9)=XA
      IF(COM(9)-8.)20, 30, 30
20    COM(3)=1.
      COM(5)=1.
      COM(11)=1.
21    COM(1)=COM(1)+1.
      COM(3)=COM(3)+2.
      C(3)= (C(3)/C(1))*C(5)*(0.,1.)
      C(6)=(C(3)/C(2))+ C(6)
      IF(COM(5))22,23,22
22    TEST= ABS(COM(5))-CLIMIT
      GO TO 24
23    TEST= ABS(COM(6))-CLIMIT
C     STOP LOOP WHEN A TERM IS LESS THAN CLIMIT
24    IF (TEST) 25,21,21
25    COM(9)= SQRT(COM(9))*.7978846
      COM(1) = COM(9)*COM(11)
      COM(2)=-COM(9)*COM(12)
26    RESULT =C(1)
C
      RETURN
C--------
30    COM(2)=COM(9)
      COM(9)=COM(9)*2.
      COM(3)=-1.
      COM(8)= 1.
      COM(12)= 1.
C     START OF ITERATIVE LOOP
C
31    COM(3)= COM(3)+2.
C
      C(3)=(C(4)*(0.,1.)/C(5))*C(2)
      IF(COM(5))33,32,33
32    COM(1)= ABS(COM(6))
      TEST = ABS(COM(7))-COM(6)
C
      GO TO 34
33    COM(1)= ABS(COM(5))
      TEST= ABS(COM(8))-COM(5)
C
34    IF(TEST) 40,35,35
35    IF(COM(1)-CLIMIT)37,36,36
```

```
36      COM(11)= COM(11) +COM(5)
C
        COM(12)= COM(12)+ COM(6)
        C(4)= C(3)
C
        GO TO 31
C
37      COM(11)= -COM(11)
C
        COM(9)= SQRT(COM(2))
        COM(1)= COS(COM(2))
        COM(2)= SIN(COM(2))
        COM(7)= .3989423
        COM(8)= 0.0
        C(1)= (.5,.5)-(C(1)*C(4)/C(5))*C(6)
        COM(2)= -COM(2)
        GO TO 26
C
40      TEMP=COM(2)
        COM(1)= (-COM(3)-2.)/COM(9)
        COM(2)= 1.
        COM(7)= -COM(1)/TEMP
        COM(8)= 0.
        COM(13)= (-COM(7)/TEMP)*2.
        COM(14)=0.
        DO 41 I= 1,3
        COM(2*I+13)=(-COM(2*I+11)/TEMP)*FLOAT(I+2)
        COM(2*I+14)=0.0
41      CONTINUE
        C(3)= C(3)/C(1)
        C(2)= C(1)*C(1)
        C(11)= (1.,0.)
        C(11)= C(4)/C(2)+ C(11)
        C(2)= C(2)*C(1)
        C(11)= -C(7)/C(2)+C(11)
        C(2)= C(2)*C(1)
        C(12)= C(4)*C(4)
        COM(9)= COM(23)*3.
        COM(10)= COM(24)*3.
        C(11)= (C(5)+C(8))/C(2)+C(11)
        C(2)= C(2)*C(1)
        C(5)= C(4)*C(7)
        COM(9)= COM(9)*10.
        COM(10)= COM(10)*10.
        C(11)=-((C(5)+C(9))/C(2))+C(11)
        C(2)= C(2)*C(1)
        C(1)= C(12)*C(4)
        COM(1)= COM(1)*15.
        COM(2)= COM(1)*15.
        C(7)= C(7)*C(7)
        COM(13)= COM(13)*10.
        COM(14)= COM(14)*10.
        C(5)= C(4)*C(8)
        COM(9)= COM(9)*15.
        COM(10)= COM(10)*15.
        C(6) = C(6) - ((C(5) + C(10) + C(1) + C(7))/ C(2) + C(11))*C(3)
        COM(2) = TEMP
        COM(10) = 0.
        GO TO 37
        RETURN
**********************
        STOP
**************************
```

APPENDIX C

DATA SAMPLE

DATA SAMPLE

	DIFFRACTED WAVE									INCIDENT WAVE		
	#8 at Y/L = 8.58			#6 at Y/L = 4.18			#5 at Y/L = 1.98			#15 at Y/L = −16.5		
	H (MM)	$\bar{H}$	K′	H(MM)	$\bar{H}$	K′	H (MM)	$\bar{H}$	K′	H(MM)	$\bar{H}_{(i)}$	$K_{(i)}$
−10 ft	18,18,17	17.6	1.11	25,25,22½	24	1.28	23,23,23	23	1.22	15,15,14	14.6	1.01
−8¾ ft	17½,17,17	17.2	1.08	20,19,19	19.2	1.02	16,14½,15½	15.5	.82	12½,12,12	12.2	.844
−7½ ft	19,19,18	18.8	1.18	16,16,16	16	.85	23,24,23	23.3	1.24	13,14,13	13.3	.92
	19,19	19	1.19	15,15	15	.80	21,21	21	1.12	13,13	13	.90
−6¼ ft	19,19,19½	19.1	1.20	15½,15,16	15.5	.82	16,16,16	16	.85	14,13½,13	13.5	.934
	17,17,17	17	1.07	17,16,16	16.3	.87	16,14½,15	15	.80	14,14,14,	14	.97
−5 ft	14,14,15	14.3	.90	20,21,18½	20	1.06	21½,21,20½	21	1.12	13,13,13	13	.90
	14,14,14,14	14	.88	20,21,21,21	20.8	1.11	21,22,21,21	21	1.12	14,14,14,15	14.2	.98
−3¾ ft	9½,12,11	11	.69	20,21,21½	21	1.12	18½,20½,20	19.5	1.04	14,14,14	14	.968
	6,7,7,7,	6.8	.43	19,19,19,19	19	1.01	20,20,20,20	20	1.06	15,16,15,15	15.2	1.05
−2½ ft	6½,5½,5½,	6	.38	12,13,14	13	.69	16,17,17½	17	.90	15,16,16	15.6	1.08
	7,6,½,7	7	.44	8½,9,9,9	9	.48	12½,13,13¼	13	.69	16½,17,16,16½	16.5	1.14
−1¼ ft	11½,11,11	11.2	.70	6½,6,6½	6	.32	5,6,6,	5.8	.31	16,16,15	15.7	1.086
	13,14,13,14,	13.5	.85	10½,10,11,11	10.7	.57	4,4,4.5	4.5	.24	15,15,15,15,	15	1.04
CENTER LINE OF TANK	15,14,15,16	15	.94	12,12½,13,13	12.7	.68	8.8 8½,8½	8.2	.44	15,15,15,15	15	1.04
	15,14,14,14½	14.3	.90	12,12,12,12	12	.64	9½,10,10,10½	10	.53	16,16,16,16	16	1.11
+1¼ ft	11,11½,12,	11.5	.72	8½,8½,9	8.8	.47	6,5½,6	5.8	.31	16,16,16	16	1.11
	8,7,8,8	7.8	.49	7½,7,7½,7	7.2	.38	6½,7,7,	6.9	.37	15,15,16,16	15.5	1.07
+2½ ft	3½,4,4.	3.8	.24	7,8,8,	7.6	.40	12,13,14	13.	.69	14,15,14	14.3	.99
	5,6,6,5½	5.6	.35	10½,11,11,11	11	.59	16,16,16,16½	16.1	.85	14,13,14,14	13.7	.95
+3¾ ft	8,8½,8	8.2	.52	15½,15,16	15	.80	18,17,17½	17.5	.93	14,14,14	14	.97
	10,10,10,9½	10	.63	19,19,19,19	19	1.01	19,18½,19,19	18.9	1.01	15,15½,16,16	15.7	1.08
+5 ft	13½,14,14,	13.8	.87	21,21,21	21	1.12	22,22½,22	22.1	1.18	15,15,15	15	1.04
	15,15,15,	15	.94	19,19,18½	19	1.01	21,21,21	21	1.12	16,15½,15½	15.8	1.09
+6¼ ft	15½,5½,16	15.7	.99	18½,18½,18	18.4	.98	19,20,19	19.3	1.03	14,14,14,	14	.97
	18,18	18	1.13	18½,18½	18.5	.98	17,17	17	.90	13½,13	13.2	.90
+7½ ft	20,20,19½	20	1.26	21,20,21	20.6	1.10	19,20,18	19	1.01	13,13,13	13	.90
+8¾ ft	18,18,18	18	1.13	19,20,19	19.2	1.02	18,18,19	18.2	.97	13½,13½,14	13.7	.947
+10 ft	19,18½,17½	18.5	1.16	18,19,18½	18.7	.99	18,18½,19	18.5	.98	15,15,14½	14.9	1.03